The effects of vibration as a mechanical stimulus on osteogenesis of mesenchymal progenitors

Jennifer Helen Edwards

Thesis submitted for the Degree of
Doctor of Philosophy
May 2013

Department of Materials Science and Engineering

Acknowledgements

First, I'd like to thank my supervisor, Dr Gwen Reilly, for all her input during my PhD, particularly her guidance, support and endless patience.

Thanks to everyone in Gwen's lab group for teaching me, especially A, Hayley and Robin. Also all of the people within the Kroto Research Institute who helped me in my time there. I'm particularly grateful to Katie, Celia, Carla and Anthony for keeping me going in roughly the right direction. It would have been a whole lot harder without you!

My parents for the love of science and a general curiosity in the first place.

And Rich, for putting up with the writing struggle and making the 6am coffee it involved.

(*Jennifer Helen Edwards*)

Abbreviations

α-gal α-Gal epitope (an α-linked galactose moeity)

αMEM Alpha minimum essential medium

β-GP β-glycerophosphate

μg Microgram

μl Microlitre

μm Micrometre

μM Micromolar

% Percentage

°C Degrees centigrade

2D Two dimensional

3D Three dimensional

AA2P ascorbic acid-2-phosphate

ALP Alkaline phosphatase

ANOVA Analysis of variance

ASC Adipose-derived stem cell

BMP Bone morphogenetic protein

Ca Calcium

CAB Cell assay buffer

CCA-SA Creative Commons Attribution-Share Alike (usage license)

CCPD Creative Commons Public Domain (usage license)

CDB Cell digestion buffer

cm Centimetre

cm^2 Square centimetre

cm^3 Centimetre cubed

CM Conditioned medium

CO_2 Carbon dioxide

Col Collagen

DAPI 4',6-diamidino-2-phenylindole

dex Dexamethasone

dH_2O Distilled water

DMEM Dulbecco's modified Eagle's medium

DMSO Dimethyl sulphoxide

DNA Deoxyribonucleic acid

ECM Extracellular matrix

ESC Embryonic stem cell

f Fungizone (amphotericin)

FBS Foetal bovine serum

FITC Fluorescein isothiocyanate

g Gram

gel Gelatin

Hz Hertz

KPa Kilopascal

L Litre

l-glut l-glutamine

LMHF Low magnitude, high frequency

M Molar

mg Milligram

min Minute

ml Millilitre

mm Millimetre

mM Millimolar

MPa Megapascal

MSC Mesenchymal stem cell

MTS 3-(4,5-dimethylthiazol-2-yl)-5-(3-carboxymethoxyphenyl)-2-(4-sulfophenyl)-2H-tetrazolium

MTT 3-(4,5-dimethylthiazol-2-yl)-2,5-diphenyltetrazolium bromide

n Number

nm Nanometre

nM Nanomolar

p/s Penicillin/streptomycin

Pa Pascal

PBS Phosphate-buffered saline

pg Picogram

PG PicoGreen

PGE_2 Prostaglandin E_2

pH Potential of hydrogen

PI Propidium iodide

PU Polyurethane

SD Standard deviation

TRITC Tetramethylrhodamine B isothiocyanate

V Vibrated

VEGF Vascular endothelial growth factor

Abstract

The use of mechanical stimulation during tissue engineering of bone is under much investigation. Stimulation of cells in constructs can lead to improved osteogenic differentiation and extracellular matrix production of mesenchymal stem cells. Low magnitude, high frequency (LMHF) vibration has been used *in vivo* to improve bone quality in patients with low bone mass and shows promise for improving the healing of large defects. As the mechanisms behind this stimulation are unknown, *in vitro* research has begun to investigate the response of different cell types found in bone to LMHF vibration. This research studies the osteogenic differentiation of a human mesenchymal progenitor cell line following this type of stimulation under a variety of conditions. Cell attachment to a 3D scaffold is demonstrated, before the use of LMHF vibration in 2D and later in 3D using mechanically different scaffolds. A possible signalling mechanism is also investigated. The research shows positive effects on both early cell differentiation and matrix mineralisation. Variability in the response of cells to loading regimens is found, suggesting that the responses to this type of loading are very sensitive to environmental conditions.

Contents

List of Figures

List of Tables

Chapter 1

Introduction

Cell culture is a technique allowing the expansion and study of a variety of cell types in an *in vitro* environment. This has applications for furthering our understanding of cellular function, as well as the creation of *in vitro* tissue models. Proper development of such models may allow their use as replacements for diseased or damaged tissue. The following chapter presents an overview of bone tissue *in vivo* as well as considerations for the creation of tissue engineered bone *in vitro*.

1.1 Bone - Structure and Function

In order to create successful tissue engineered bone replacements it is necessary to understand the complex structure of bone *in vivo*. The human skeleton is made up of 213 bones, providing structure, support and protection to the body. Bones also act as a repository for calcium and a variety of growth factors and cytokines. They consist of a mineralised collagen matrix, populated by various cell types (notably osteoblasts, osteocytes and osteoclasts), which are responsible for the maintenance and restructuring of the tissue. This tissue is highly dynamic,

responding to chemical and mechanical cues and altering the bone structure to meet the body's needs.

1.1.1 Macroscopic Structure

The bones which make up the human skeleton can be divided into two main types - long bones and flat bones. Long bones, such as the femur or radius, provide structural support for the body and act as levers for the muscles, allowing locomotion. Flat bones (for example the skull and ribs) provide protection for other internal organs which they surround. As well as providing structural support and protection, both types of bone serve additional functions. Flat bones, and the ends of long bones in the adult skeleton, contain red bone marrow. Red marrow is the site of haematopoiesis, containing haematopoietic stem cells and providing the body with red and white blood cells and platelets. The remainder of bone marrow is yellow, which consists mostly of fat cells and is found in the medullary cavity within the shafts of long bones (figure 1.1). The ratio of bone marrow changes from all red at birth to approximately 1:1 in an adult. Both types of marrow are infiltrated with blood vessels and capillaries. The mineralised matrix of the bone tissue acts as a calcium store and a source of growth factors and cytokines.

Long bones consist of a central hollow tube, known as the shaft or diaphysis. Towards the ends, these bones flare outwards to form the epiphyses and metaphyses (regions above and below the growth plate, respectively). During development of bones in youth or rapid growth after fracture, the bone tissue formed is known as woven bone. Woven bone is characterised by a haphazard arrangement of collagen fibres and is mechanically weak. The woven bone occurs as cells differentiate along a chondrogenic route and deposit hypertrophic cartilage, which is remodelled and mineralised by osteoblasts. This woven bone is gradually replaced, such that in

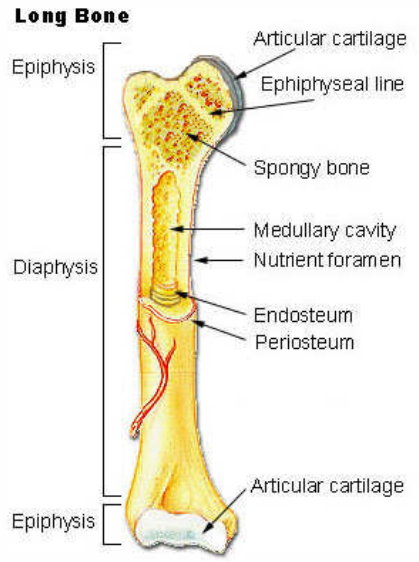

Figure 1.1: Macrostructure of long bones. Image taken from (PD-USGov 2012b), under the CCPD usage license, see (CC1 2012).

healthy adults almost all bone tissue is lamellar bone. Lamellar bone is much stronger than woven, as the collagen fibrils are arranged in aligned, overlapping parallel sheets or layers known as lamellae.

Within long bones, the diaphysis consists of a dense bone known as cortical bone, which comprises 80% of the adult skeleton. The remainder of long bones consists of a thin shell of cortical bone surrounding a core of cancellous bone. This cancellous bone is less dense than cortical (0.2 g.cm $^{-3}$ and 1.8 g.cm^{-3} respectively), being formed from a honeycomb-like network of trabecular struts surrounding bone marrow. The trabecular structure consists of a lattice of thin struts of lamellar matrix. Cancellous bone is highly porous (75-95% total volume of interconnected pores), with trabeculae 100-300 μm thick and spaced 300-1500 μm apart (Athanasiou et al. 2000). As well as acting as a container for the bone marrow, cancellous bone helps to reduce the overall weight of the skeleton while providing a large surface area at the joints. This large surface area is important to reduce pressure on the joints and ease movement. Flat bones also consist of a

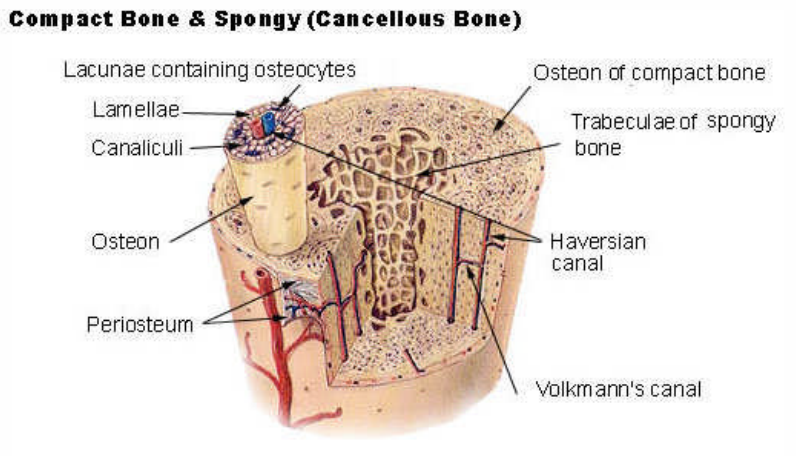

Figure 1.2: Structure of cortical and cancellous bone. Image taken from (PD-USGov 2012a), under the CCPD usage license, see (CC1 2012).

layer of cortical bone surrounding cancellous bone tissue and figure 1.2 shows the structure of cortical and cancellous bone.

The basic structural unit of cortical bone is known as an osteon or Haversian system (figure 1.3). These consist of a central Haversian canal surrounded by concentric layers of lamellar bone, approximately 200 μm wide and 10-20 mm long (Athanasiou et al. 2000). Embedded within these layers are osteocytes: bone cells responsible for mechanosensing which are encased within individual lacunae. Osteocytes are able to communicate with one another via cytoplasmic processes encased within narrow channels called canaliculi (figure 1.3). Transverse to the Haversian canals lie Volkman's canals, allowing the connection of individual Haversian systems. Both canals allow for the inclusion of blood vessels and nerves within the bone tissue.

The external surfaces of cortical bone are surrounded by membranous sheaths. On the outer surface of bones, this fibrous sheath is known as the periosteum and covers the surface except at the joints (which are instead covered by articular

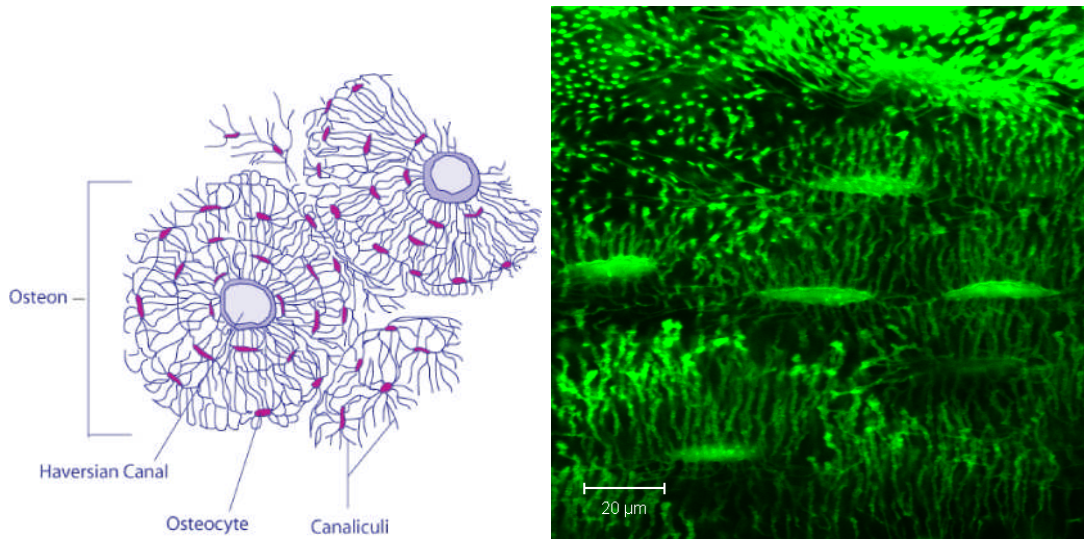

Figure 1.3: Left: Schematic of a transverse section through an osteon. Image taken from BDB (2012) (author BDB) under the Creative Commons Attribution-Share Alike 3.0 license, see (CC3 2012). Right: Osteocytes and canaliculi in bone matrix. Scale bar shows 20 μm. Confocal image included with permission of H. Morris.

cartilage). The outer layer of this membrane is dense fibrous connective tissue, anchored to the bone via Sharpey's fibres (strong collagen fibres which penetrate the bone tissue) and providing the anchor by which tendons attach to bone. The periosteum also contains blood vessels and nerve endings, as well as a supply of cells necessary for bone maintenance. The membrane lining the inner surface of cortical bone is the endosteum, which contains blood vessels, osteoblasts and osteoclasts (Stevens et al. 2005; Schwartz 2007; Sommerfeldt and Rubin 2001).

1.1.2 Mechanical Properties

In order to perform a structural support role within the body, bones must be able to withstand a variety of different forces. As such, not only is the quantity of bone important, but also the quality of the mineralised matrix microstructure. Small variations in this structure (in immature matrix, or due to tissue damage or aging) can have large effects on the strength and toughness of the skeleton. Bone can be considered a composite material, as it is constructed from an organic

phase (collagen fibrils) combined with an inorganic (mineral) phase. Collagen fibrils are arranged in lamellae, such that adjacent lamellae may be orientated differently by up to 90 degrees. This allows the structure to resist forces applied from different directions and also provides a resistance to tensional forces. The mineral element (carbonated hydroxyapatite, $Ca_{10}(PO_4)_6(OH)_2$) provides good resistance to compressive forces. Organisation of collagen fibrils into lamellae gives bone an anisotropic structure - its mechanical properties differ greatly in different directions. For example, cortical bone is stiffest longitudinally, and weakest under shear forces (Weiner and Wagner 1998; Weiner et al. 1999; Sommerfeldt and Rubin 2001).

The stress and strain response of bone to loading are used to define the material properties and allow comparison between bone from different sites or donors. Stress is a measure of the force applied per unit area of material ($\sigma = F/A$) and its unit is the Pascal (Pa). Applying a known force to different bone samples gives an indication of the varying stiffness. Strain (ε) is a measure of the deformation caused by an applied force relative to the original dimensions and is a dimensionless quantity. $\varepsilon = \Delta L/L$, where ΔL is the change in length and L is the original length. Both stress and strain may be caused by tensile (caused by extension), compressive (caused by a reduction in length) or shear forces (where opposing forces act in parallel to the material). The overall macrostructure (bone size, density, and curvature) is also important in the distribution of local strains. The site of harvest, developmental stage of bone and type of mechanical testing will affect the measured mechanical properties. A review by Yaszemski et al. (1996) compiled average values for the strength and modulus of human bone, collated in table 1.1.

Bone Type	Loading Type	Strength (MPa)	Young's Modulus (GPa)
Cortical (longitudinal)	Tension Compression	78.8-151 131-224	17-20
Cortical (transverse)	Tension Compression	51-56 106-133	6-13
Cortical	Torsion	53.1-70	3.3
Cancellous	*	5-10	0.05-0.1

Table 1.1: Approximate human bone strength and modulus. * Values for cancellous bone are midrange values, and both the strength and modulus depend on the density of bone at the site and the rate of loading. Compiled from review by (Yaszemski et al. 1996).

For bone tissue, the structure must provide a balance between toughness and stiffness. The overall structure of the organic matrix and presence of features such as lacunae help to limit the propagation of cracks in the matrix, while the mineral provides resistance to deformation (Hing 2004; Rubin et al. 2006). *In vivo*, bone structure is heavily influenced by the forces acting on the tissue. Changes in mechanical forces on the bone lead to many changes in the bone properties, such as density, structure, trabecular number and trabecular thickness. The normal mechanical environment of a region of bone will have an effect on the failure modes of the tissue under loading (Reilly and Currey 1999). The methods by which these forces may be detected by the cells within bone and used to direct remodelling are detailed further in section 1.2.

1.1.3 Bone Cells

While bones contain a variety of different cell and tissue types, including cartilage, nerves, blood vessels and stem cells, there are three cell types present in mature bone which are responsible for the maintenance of the bone matrix itself; osteoblasts, osteocytes and osteoclasts.

Osteoblasts are derived from osteoprogenitor cells of the mesenchymal stem cell (MSC) lineage, derived from the mesoderm (figure 1.4). Osteoblasts are cuboidal in shape, maintain many cell-cell and cell-matrix connections and are found on the bone surface. They are responsible for the deposition of the organic collagen matrix within mature bone, as well as its subsequent mineralisation. They are capable of producing 0.5-1.5 μm of matrix per day and have a lifespan of approximately 3 weeks (Sommerfeldt and Rubin 2001). These cells synthesise a variety of other molecules, such as cytokines and growth factors, which are incorporated into the bone matrix. Encapsulated attachment proteins (such as fibronectin) improve the attachment of cells to the matrix, which is necessary for cell recruitment in remodelling. Other molecules are present within the matrix, such as biglycan, osteonectin, osteopontin and osteocalcin, which are involved in matrix production, mineralisation and remodelling (Salgado et al. 2004). These growth factors and signalling molecules are released during bone remodelling. As the osteoblasts produce the bone matrix, they become encased within small chambers called lacunae and differentiate further into osteocytes.

Osteocytes are formed from osteoblasts fully embedded within the mineralised bone matrix, which have lost some of their cellular machinery. They are connected to each other via cytoplasmic processes in the canaliculi, as well as with osteoblasts on the bone surface through similar cytoplasmic processes. The osteocytes are thought to be responsible for the mechanosensitivity of bone tissue. However, it is not yet understood whether this mechanosensation is connected with the movement of fluid within the canaliculi, or deformation of the bone matrix itself (see section 1.2 for further discussion). Mechanosensation allows a response to external stimuli which may require changes to the bone matrix to maintain tissue function. Such stimuli can include changing levels of physical activity, the need

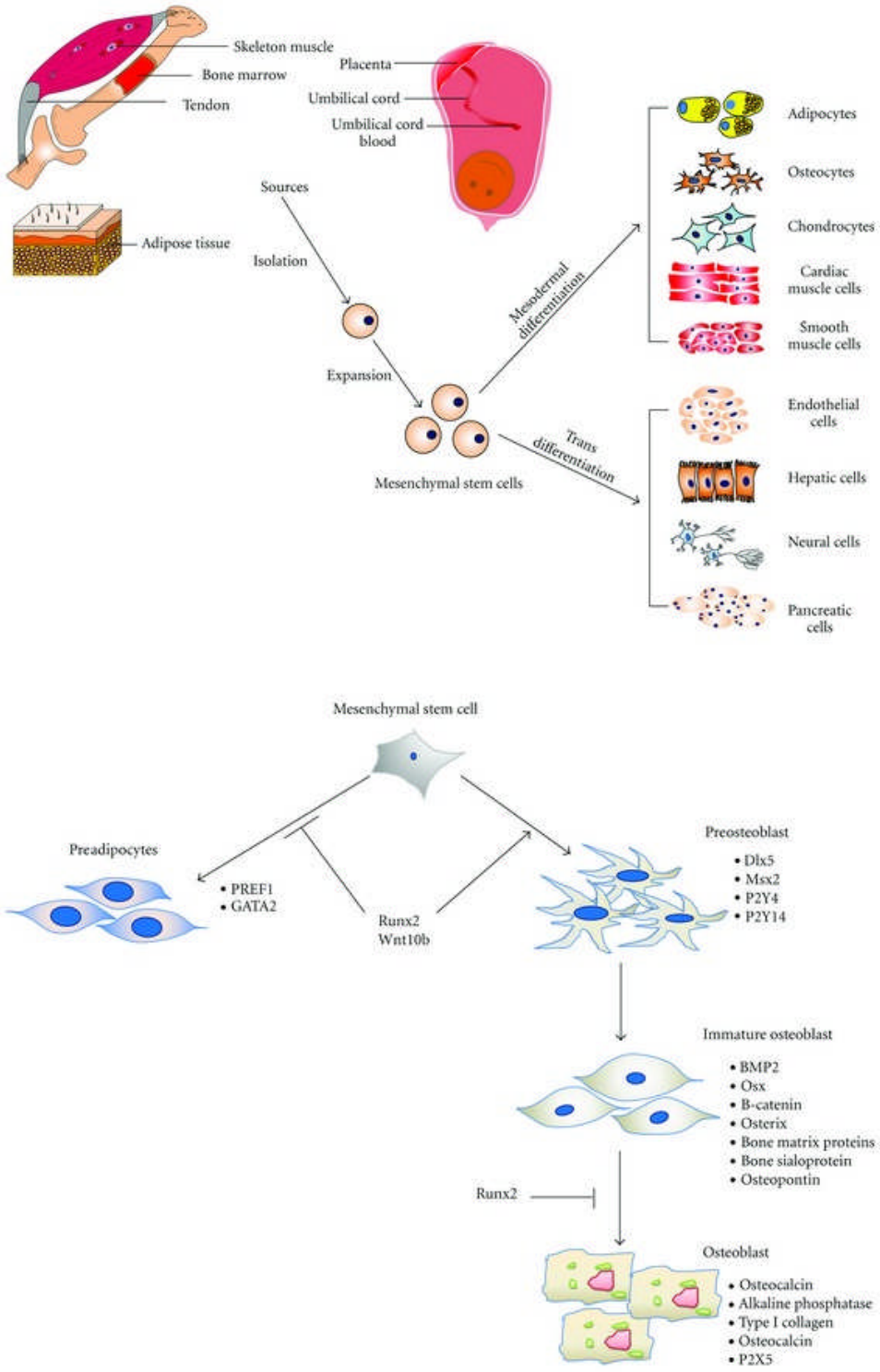

Figure 1.4: Differentiation pathways of mesenchymal stem cells (MSCs). Top image shows the multipotent MSCs, lower image shows osteogenic differentiation in more detail. Image copyright Yu Zhang et al. 2012, Zhang et al. (012a), an open access article distributed under the Creative Commons Attribution License (CC3 2012)

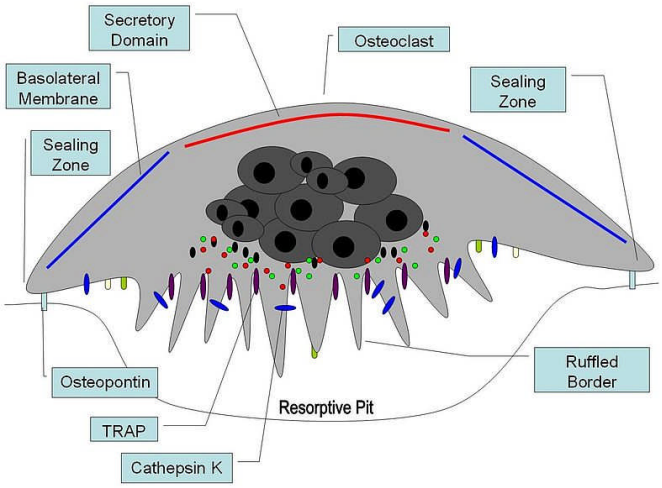

Figure 1.5: Schematic of an osteoclast attached to the bone surface. Author Cellpath, source (Cellpath), licensed under the CCA-SA 3.0 License, (CC3 2012).

to repair after a fracture or changing calcium requirements in the body. These stimuli are detected by the cells and can cause the release of soluble signalling factors, leading to the activation of a third cell type: osteoclasts.

Osteoclasts are responsible for the removal of bone matrix, allowing the tissue to remodel in response to external stimuli detected by osteocytes. Osteoclasts are large, multinucleated cells formed from the fusion of blood monocytes of the haematopoietic stem cell (HSC) lineage. They form a sealed pocket over the surface of bone, into which they secrete a cocktail of enzymes (figure 1.5). The pH in this area is lowered to between 2 and 4 and the cells are able to digest around 200,000 μm^3 of bone in one day (Sommerfeldt and Rubin 2001). These cells may be activated in the process of transforming immature woven bone into fully mature lamellar bone, as well as during later bone remodelling.

These three cell types act together to form a bone remodelling unit (BRU). Initially, mononucleated osteoclast precursor cells are recruited from the circulation, fusing together to form multinucleated osteoclasts. These cells attach to the bone

surface and begin the process of bone resorption. In the cavity created behind the osteoclast, osteoblasts from the bones surface, as well as osteocytes released from the matrix, attach to the exposed surface and begin matrix deposition and mineralisation. These osteoblasts are then encased in the deposited matrix, becoming osteocytes suitable for the detection of future remodelling requirements. A variety of stimulatory molecules, such as bone morphogenetic proteins (BMPs), transforming growth factor β (TGF-β) and fibroblast growth factors (FGFs) are involved in the development and maintenance of bone tissue (Hsiong and Mooney 2006). Some of these molecules are contained within the bone matrix and are released as the osteoclasts break down the mineralised matrix during remodelling.

During the healing of bone defects such as fractures, a cascade of events occurs. These can be divided into inflammation, repair and remodelling, followed by biomechanical adaptation. Ruptured blood vessels lead to the formation of a haemorrhage within the tissue and macrophages are recruited to remove dead cells and tissue. MSCs are recruited which form a callus around the fracture site, and begin to differentiate along osteogenic and chondrogenic lineages. Osteocytes form new bone in the outer regions of the callus, while chondrocytes create a hyaline cartilage template in the centre. Endochondral ossification, such as occurs in initial bone development, leads to the ossification of the cartilage template. This is then further remodelled as for normal bone remodelling (Doblar et al. 2004; Yaszemski et al. 1996; Fong et al. 2011). The density of osteocytes in areas of bone with different developmental histories varies, with higher numbers in callus or growth plate regions. Higher numbers of these cells may provide increased response to mechanical stimulus, increasing the rate of remodelling in immature or injured bone (Hernandez et al. 2004). Various molecules help to direct the healing process, such as bone morphogenic proteins (BMPs), platelet derived

growth factors (from the blood clot) and cytokines (such as interleukin-1 (IL-1) and IL-6). These factors help direct the healing response and are thought to be involved in the recruitment of cells to the wound as well as their proliferation and differentiation, but in many cases the mechanisms are not well understood (Mullender et al. 2004). It is important that the new bone formed during the repair is well vascularised to allow cell survival, requiring the presence of vacular endothelial growth factor (VEGF). VEGF encourages angiogenesis in the damaged bone, driving repair and osteogenesis (Hsiong and Mooney 2006). The more successful tissue repair strategies arising from tissue engineering may be those which attempt to recapitulate the natural tissue repair response.

1.2 Mechanosensitivity in Bone Tissue

Mechanical stimuli are important in bone tissue engineering protocols as bone cells are inherently mechanosensitive. Bone is a dynamic tissue, responding to a variety of mechanical and biological cues by resorbing and depositing bone. As bones act as a calcium (and, to a lesser extent, phosphate) store, some of these cues are molecular and are related to mineral homeostasis. For example, regulation of serum calcium levels is achieved by release of PTH, which leads to changes in the rate of bone remodelling (Stevens et al. 2005). As the major function of bones is to provide support for motion or protection of internal organs, the tissue structure must be maintained in order to provide suitable resistance to applied loads. The cues for this maintenance are provided by mechanical stimulation of the tissue.

As many bones are load bearing, changes in the loads which are applied should cause changes in the structure and quantity of bone tissue. It has been widely demonstrated that strenuous physical exercise can cause an increase in the amount

of bone tissue, the most widely recognised example that of the playing arm of tennis players. It has also been observed that there is a reduction in the bone mass of astronauts, who experience vastly reduced forces on their bones due to the weightlessness experienced in space (Rubin and Rubin 2006). This may be similar to the bone wastage seen in disuse, possibly due to reduction in bone cell mechanosensitivity (Klein-Nulend et al. 2003). It has also been proposed that the definition of disuse and overuse are dependant on normal physiological conditions for the particular person in question. Reducing activity in a weightlifter to levels found in people with less intensive exercise programs may result in a loss of bone due to effective disuse. Conversely, an increase in activity of someone previously bedridden to that of an same average person may involve a net increase in bone, due to effective overuse. There is also the suggestion that post menopausal bone loss in women may be due to a reduction in circulatory hormones, leading to a response similar to disuse (Skerry 2008). These are examples of the overall effects of changes in mechanical stimuli which affect bone structure and mass. For the cellular effects, there are several theories as to how the response to changes in mechanical conditions is brought about.

While the cells responsible for the mechanosensation properties of bone appear to be the osteocytes, it is not know whether the stimulus which they recognise is matrix deformation or fluid flow induced shear stresses. These cells are highly connected via cytoplasmic junctions in the canaliculi, allowing the formation of gap junctions with each other, cells on the bone surface and in the bone marrow. These gap junctions allow the direct transmission of mechanical signalling responses between connected cells (Donahue 2000; Batra et al. 2012; Yellowley et al. 2000). The cells can also release signalling molecules into the canaliculi which are transmitted via the intersitial fluid. Osteocytes are known to release nitric oxide

(NO), prostaglandins (e.g. PGE_2) and ATP shortly after they have been exposed to mechanical loading. They have also been shown to activate other anabolic pathways and support the formation and activation of osteoclasts (Bonewald 2006; Klein-Nulend et al. 2005; Papachroni et al. 2009; Jacobs et al. 2010; Liedert et al. 2006). It is likely that it is a combination of matrix deformation and fluid stresses which are important in the regulatory process.

Mechanical deformation of the bone matrix occurs as forces are applied to the bones. These can be normal activities such as walking, or higher impact such as contact sports. Forces applied to the bones cause the matrix to deform, which in turn will cause the cells residing within the matrix to undergo some motion. Cells are attached to the ECM by large numbers of integrins which will be affected by the application of mechanical loads. These signals can are transmitted through the cell via the actin cytoskeleton which can regulate their behaviour. Loading has been shown to affect osteocyte apoptosis, with increasing load decreasing apoptosis and *vice versa*. One problem with the study of the effects of direct mechanical loading on cells *in vitro* is that there is usually a fluid stress component generated as a side effect, making it difficult to separate the relative importance of the stimulation (Bonewald 2006; Baker and Zaman 2010; Klein-Nulend et al. 2005; Papachroni et al. 2009; Jacobs et al. 2010; Liedert et al. 2006)

In the case of a fluid flow stimulus, it is important to remember that osteocytes reside within lacunae, tightly encased in matrix. Cellular communication and nutrient transfer are achieved via the canaliculi, which contain interstitial fluid. Research has shown that the deformation of the bone matrix causes movement of the fluid within the canalicular network. While the application of loads causes low strain in the bone as a whole, the associated movement of fluid causes high strain

rates on the cells (Han et al. 2004; Burger and Klein-nulend 1999). There is much *in vitro* research suggesting that the fluid shear stress estimated to occur in the canalicular network is stimulatory to osteocytes (You et al. 2001; Owan et al. 1997; Mullender et al. 2004; Reilly et al. 2003; Gurkan and Akkus 2008). There is also evidence that osteocytes need only a low level of stimulation to prevent the loss of bone that occurs during prolonged disuse (Burger and Klein-nulend 1999). One problem with the use of *in vitro* studies to investigate osteocyte mechanosensitivity is the difference in the cell shape and orientation compared to the *in vivo* situation. (Bacabac et al. 2008) have shown that the morphology of osteoblast-like cells may have an effect on their ability to sense small strains *in vivo*. This is presumably due to the altered arrangement of cytoskeletal elements, which would affect the transmission of forces caused by external stimuli. Osteoblast-like cell lines have also been shown to respond to fluid forces, for example (Owan et al. 1997) and (Morris et al. 2010). Variations in the hydrostatic pressure, fluid flow and viscosity in the intramedullary cavity may also affect the differentiation of MSCs and the relative ratios of cell types within the marrow, which could affects the mechanosensitivity of bone tissue (Gurkan and Akkus 2008).

The ability of bone to adapt to changing demands is important for its continued function within the body. Research into the mechanisms of the remodelling response, cell recruitment and disease states may provide more information on the normal turnover of bone tissue and the mechanical cues which are required by the tissue. Tissue engineering could help us better understand the mechanisms involved in mechanosensation and apply these principles to provide better treatments for patients in the long term. More detail on the methods used *in vitro* to stimulate cells is provided later in section 1.8.

1.3 Clinical Need for Bone Replacement

There are many diseases which affect bone and can cause changes to its mechanical function. For some conditions, such as osteogenesis imperfecta or osteoporosis, there may not be a need for replacement of the tissue, rather an approach to address the low bone mass and skeletal fragility (Mauney et al. 2005). These conditions can however lead to an increase in fracture rate of the bones, which do not heal well afterwards.

While bone tissue has the capacity for self repair, there are many situations where there is a need for replacement bone tissue. Spinal fusion surgeries, revision surgery for total knee replacements, tumour resection and non-union fractures may all require replacement bone tissue in their treatment. Replacement bone tissue is desirable to allow the repair of damaged tissue and improvement in the quality of life of patients with bone damage. Between 1998 and 2005, there was an increase in total joint arthroplasties from 700,000 to 1,100,000. There are problems with non-union of bone and poor healing after such surgeries without the use of bone grafting, but bone grafting itself has a high complication rate. The cost of medical care for joint related replacements, fracture healing and reattachment was estimated as $20 billion USD in 2003, with a predicted rise to $74 billion by 2015. Traumatic fractures and spinal arthrodesis require hospitalisation in many cases, placing a burden on healthcare systems (statistics reported by Porter et al. (2009)). With an aging population remaining active later in life, there is a growing need for strategies to provide replacement bone tissue for treatment of critical sized defects and joint degeneration.

The current gold standard for the replacement of bone tissue is autograft, which uses the patients own tissue to repair the damage. While this technique means that the implanted tissue will not be rejected, there are several limitations. In patients where the tissue requires replacement due to disease, tissue from another location within the patient will have the same structural problems. The initial removal of the donor tissue also requires extra surgery and in many cases leads to donor site morbidity. This can cause pain, immobility and loss of function and the extra surgery required carries inherent risks, such as increased possibility of infection. Also, the bone is usually taken from the iliac crest and the amount of tissue which may be used is severely limited. For patients with large gaps to fill, the amount of material required cannot be obtained from their own healthy tissue (Porter et al. 2009; Hing 2004).

Another option is the use of allograft, tissue obtained from another human. As allograft bone is usually obtained from cadavers, it does not have the same limitations in the amount of tissue which can be harvested. This means allograft tissue can provide enough material to fill large gaps, although this may require multiple samples (Hing 2004). Allograft does introduce the possibility of tissue rejection or disease transmission, problems which are not encountered with autograft tissue. Rejection occurs due to the presence of unrecognised cell markers, causing the patient's immune system to attack the implanted tissues as a foreign object. The inflammatory response which occurs during tissue rejection can be very severe, leading to graft rejection and the need for further surgery. There is also the possibility that the donor may have a viral infection (such as HIV or hepatitis) which would be passed to the patient via the donated tissue. Donor screening is used to reduce the likelihood of disease transmission and tissue typing reduces the chances of acute rejection. While there are drugs available to help prevent tissue

rejection, this is not an ideal or perfect solution, as the patient will have an immune system with reduced efficiency. Freezing of samples and the use of irradiation can limit the number of pathological organisms within the tissue, as well as killing donor cells (although cell fragments still remain within the tissue). However, the techniques used to process tissue in this way are likely to alter the tissue structure and it may not have the required mechanical properties after treatment. One example is the use of ionising radiation to destroy inactivate bacteria within bone samples. This treatment is effective, but is known to affect both the mechanical and biological properties of the tissue (Nguyen et al. 2007; Currey et al. 1997).

Another possibility for tissue transplants is the use of xenograft tissue, which is taken from suitable animal donors. Xenograft material carries similar risks of rejection and disease transmission as with allograft tissue, but there may be a more readily available supply. In addition to viruses present within the donor animal, there may be endogenous retroviruses present within the cellular DNA which could cause problems after implantation within a human patient (van der Laan et al. 2000) and care must be taken to limit this risk, such as by removal of the animal cells prior to implantation. There are also problems with acute rejection of xenogenic tissues due to the presence of the α-galactose (α-gal) epitope. This epitope is expressed in the tissues of most animals, with the exception of humans and old world primates, as well as the cell walls of some bacteria. The human immune system attacks the epitope as foreign, leading to the acute rejection without immuno-supressants (Galili 1993; Badylak 2004). Decellularised heart valves, taken from porcine tissue, are already used in heart valve replacement surgeries. There are a variety of other tissues commercially available for use in soft tissue repair, consisting of both human and animal decellularised tissues (Hodde 2002; Gilbert et al. 2006; Crapo et al. 2011).

Bone graft substitutes are another class of materials used in the repair of damaged bone tissue. These materials are used as filler material in large gaps to promote regrowth and union of the fracture. Examples of bone graft substitutes include demineralised bone matrix (allograft or xenograft), hydroxyapatite powders or blocks, injectable cements (such as calcium phosphate) and bioactive glasses or polymers (Bauer 2007; Heest and Swiontkowski 1999). The materials may also contain proteins or growth factors to promote healing and integration, such as fibroblast growth factors or bone morphogenic proteins (Ilan and Ladd 2002). These substitutes do have limitations in their use. Allograft or xenograft processed bone carry the same risks as whole grafts of the same nature (disease transmission and immune responses). The materials must also be contained within the defect, which may require fixation of a cage at the graft site (Tang et al. 2009).

While there are several possibilities for the use of living or decellularised tissues to improve bone repair, it is desirable to find alternative solutions. Bone grafts are used as filler material and are not suitable for use in load bearing areas. These techniques are also unsuitable where there is the need for whole joint replacement. There are many examples of replacement of tissues with man-made alternatives, such as high weight polymer (UHMWPE) or titanium joints, surgical pins and whole artificial limbs. While these techniques do not mimic the native tissue, they are able to perform the structural functions required to grant the patient improved mobility. The mis-match between tissue and replacement material can cause further problems, such as the wear particles produced around titanium hip implants. As the replacement is much harder than the surrounding tissue, small debris particles are created during use of the joint. As well as aseptic loosening of the implant, the particles can lead to immune responses by the patient, leading to pain and further complications (St. Pierre et al. 2010; Ollivere et al. 2012;

Ingham and Fisher 2005).

The materials used in these kinds of replacements will not integrate with the surrounding tissue and such products have a lifespan of around 25 years. Due to the increasing life expectancy in the western world, it is possible that elderly patients may need further interventions as the replacements fail. There is also increasing need for suitable replacements in younger patients, or those who are remaining active later in their longer lives. In the case of very young patients, it is necessary that replacements not only last (to prevent the need for multiple revision surgeries), but are able to cope with the growth and development of the patient. This requires new approaches to tissue replacement and one possibility undergoing much current research is that of tissue engineering. The use of cells, growth factors and support materials may allow the creation of replacement tissues which can fully integrate with a patient, restoring function and reducing the burden on health care. It is likely that tissue engineering will be able to improve existing bone grafting materials and procedures, allowing better integration of the tissue and improving healing. An ambitious and long term goal would be the use of tissue engineering to aid in load bearing or whole joint replacement, and there are groups working towards this aim (Alhadlaq and Mao 2005; Alhadlaq et al. 2004; Mao et al. 2006). The complexity of such an engineered tissue makes this an unlikely prospect for some time.

1.4 Tissue Engineering

Tissue engineering is a constantly developing field of research, aiming to produce functional tissues or even whole organs *in vitro*. Such engineered tissues cover the whole range of bodily tissues, using a vast number of approaches and techniques.

The research may be undertaken for several reasons, including the production of replacement tissue for patients or for use in the pre-clinic testing of new treatments. Different techniques may be used to create suitable tissues, including bioreactor culture, mechanical stimulation or the use of scaffolds.

The production of tissues or organs *in vitro* is a challenging research area, with many different types, variables, outcomes and aims. The field is extremely multidisciplinary, using expertise from biology, chemistry, physics, engineering and medicine. Due to the shortage of donor organs for life saving surgeries, there is a need to produce replacements which are readily available and can be used to prolong the lives of patients. These replacements could even be tailored to individual patients, able to meet their needs and outperform current gold standards. There is also a need to reduce the use of animals in medical research. While animal testing is now strictly regulated and used as infrequently as possible, there are occasions where no suitable alternative exists before moving to human clinical trials. It is desirable to develop models based on human tissues which can be used to better assess the efficiency of new treatments. While routine cell culture with human cells may demonstrate simple inflammatory responses to new drugs, the complex interactions between cells in a whole tissue, organ or organ system are not predicted by this method. There is increasing interest in the development of more complex systems to use for testing of responses to treatments or compounds (Canton et al. 2010; Sun et al. 2006). If even a small 3D sample of a liver or kidney could be developed artificially, it would allow the effects of drugs to be tested on these organs before moving into humans, reducing the risk of drugs found safe in animal trials causing system failure in humans. Some implant solutions have had problems during *in vivo* use due to unexpected interactions with cells. For example, in coronary implants, complications may arise

from aggregation of cells within the implant, blocking the vessels and requiring further surgery. Research to address this includes attaching an endothelial layer to the inside of the implants prior to implantation to prevent thrombogenesis, requiring the use of tissue engineering (Feugier et al. 2005; Williamson et al. 2006).

Whole tissues or organs, produced *in vitro* and maintained in laboratory culture may serve another role. As the human body is a complex structure, there are many questions about its constituent parts that remain unanswered. The ability to study live organs under laboratory conditions may provide us with new insights into the functions and behaviour of tissues. As it is not acceptable to subject people or animals to many treatments which may provide information on normal and abnormal tissue and cell behaviour, the production of whole, functional organs in the laboratory would allow their study without fear of the effects on patients. While this is likely to be a costly endeavour, it may be an invaluable resource for furthering our understanding of disease and degeneration.

Many groups are working on engineered tissues, from simple 2D co-culture models to scaffold structures loaded with cells and subjected to chemical and mechanical stimulation. The following sections discuss some of the considerations necessary to produce a suitable tissue engineered construct. These include the cell types to be used, choice of support material, coatings, mechanical considerations and the mechanical stimulation of the construct. This is mainly focused on bone tissue engineering, with discussion of properties which may differ for other tissues. An overview of the tissue engineering process is provided in figure 1.6.

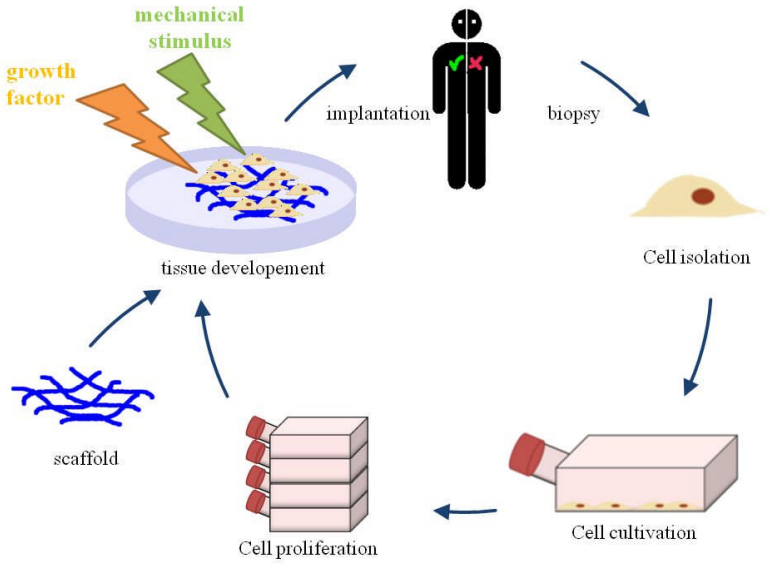

Figure 1.6: Overview of the Tissue Engineering process for tissue replacements. Image taken from (TE 2012), licensed under the Creative Commons Attribution 3.0 license, see (CC3 2012).

1.5 Cell Types for Tissue Engineering

The creation of tissues *in vitro* has a variety of requirements, not least the use of suitable cells. Species, cell type, ease of culture and culture requirements are all considerations in the choice of cells for experimentation and development of models
in vitro.

Many investigations into cellular behaviour and the creation of engineered tissues have been undertaken using animal cells. This is due mainly to the ease of availability of such tissue compared to human. While such experiments can provide insights into cellular behaviour, there is a need to move to human cells in order to answer questions about human genetics, conditions and diseases. In many cases the use of human cells is the preferable option as animal cells may not behave in the same way as human. Different cell sources (animal versus human,

as well as different cell harvest sites) have been shown to affect differentiation and response to osteogenic growth factors (Hoemann et al. 2009; Osyczka et al. 2009; Osyczka et al. 2004; Reilly et al. 2007). Despite these considerations, the use of primary human cells is not always possible as obtaining the cells can be expensive or difficult and primary cells cannot undergo many population doublings during culture before adopting abnormal behaviour. Problems with primary cells lead to a further decision for cell culture: primary cells or cell lines?

Primary cells are those which have been taken from a donor and placed into culture. Such cells are only able to undergo a small number of population doublings before losing their phenotype. This is presumably due to the loss of the correct cellular environment and aging effects as the cells divide. Primary cells may be taken from a fully differentiated tissue, such as osteoblasts from bone (Brounais et al. 2009; Goldstein et al. 2001; Tsigkou et al. 2009) or fibroblasts from skin (Hee et al. 2006; Canton et al. 2010; Sun et al. 2006), or be a form of stem cell. Stem cells are those which are able to undergo differentiation into a variety of different cell types. Embryonic stem cells are pluripotent: able to differentiate into any other bodily tissue, allowing the full range of tissue seen in an adult to develop. These cells can differentiate into other types of stem cells, such as haematopoietic or mesenchymal, both of which are of interest in the study of bone. Such multipotent stem cells are capable of differentiation into a limited number of other cell types and can be found in adult tissues (Salgado et al. 2004). Mesenchymal stem cells (MSCs) are able to differentiate into three different matrix producing cell types: chondrocytes (cartilage), osteoblasts (bone) and adipocytes (fatty tissue). Haematopoietic stem cells (HSCs) are able to differentiate into a variety of cells found in the bloodstream, such as red blood cells and lymphocytes. HSCs are the source of osteoclasts, which come from the fusion of cells in the

monocyte-macrophage lineage. Both types of stem cell are important components of the bone marrow niche.

The choice of cell type (differentiated or precursor) depends on the tissue being engineered. While it is possible to use many differentiated cell types (such as fibroblasts) with relative ease, it is difficult to maintain others (such as osteoblasts). There is increasing interest in the use of stem cells as a cell source for clinical therapies. For many adult stem cells, it is possible to extract small numbers of the cells directly from a patient. This means that the cells can be expanded *in vitro*, used to create a tissue engineered replacement and then implanted back into the patient without causing an immune response. MSCs are routinely extracted from animals and humans for use in cell culture. They are usually extracted from bone marrow aspirate, but the number of these cells is very low (approximately 1 in 100,000 (Heng et al. 2004; Heath 2000)). As MSCs are known to play important roles in the maintenance of normal bone tissue, as well as in recovery after musculoskeletal injury (Fong et al. 2011), it is desirable to use these cells for research *in vitro*. There is also some interest in the use of adipose tissue-derived stem cells (ASCs) for bone tissue engineering. ASCs have also been used to engineer bone and cartilage, but are easier to obtain and may be a more reliable source of cells in older patients compared to MSCs (Rada et al. 2009). Muscle derived stem cells have also attracted some interest for bone tissue engineering (Kimelman et al. 2007; Tuan et al. 2002). Human osteoblastic cells (hOB) obtained from explant cultures of trabecular bone fragments have shown multilineage differentiation capability (Nth et al. 2002), as have cells derived from human umbilical cord (Baksh et al. 2007; Lee et al. 2004). In addition to the use of progenitor cells, there is increasing research into the use of other cells types for osteogenesis, such as human dermal fibroblasts (HDFs). These cells can be obtained via a skin

biopsy and have been shown to respond to osteogenic stimuli by increasing alkaline phosphatase activity and matrix mineralisation (Delaine-Smith et al. 2012; Hee et al. 2006).

Another advantage of the use of MCSs for tissue engineering is the multipotency of the cells. As bone tissue is not formed from a single cell type, there may be a need to include different cell types within a tissue engineered structure (Meyer et al. 2004). *In vivo*, there are many different cell types interacting to form functional tissue and these are affected by age and other factors (Haynesworth et al. 1998). As an example, healing of defects in bone may occur via the formation and ossification of a cartilage template, requiring both chondrocytes and osteoblasts. Co-culture of multiple cells types allows the development of a more representative construct but can be difficult to achieve. For joint repair there is a need for osteochondral replacements to repair joint surfaces: both osteoblasts and chondrocytes can be obtained from MSCs for this purpose (Xin et al. 2007; Farrell et al. 2006). The ability of MSCs to produce both osteoblasts and chondrocytes for wound healing increased interest in bone tissue engineering using MSCs (Tuan et al. 2002). Many groups carry out research on the use of MSCs to produce both cell types and study their coculture (for examples see (Farrell et al. 2008; Farrell et al. 2006; Lennon et al. 1995; Meyer et al. 2004; Thompson et al. 2009; Haasper et al. 2008)). Other examples of co-culture include the addition of endothelial cells alongside osteoprogenitors (Grellier et al. (2009), reviewed in Hsiong and Mooney (2006)). The inclusion of HSCs to mimic the bone marrow environment may also be advantageous for complex cultures (Maggio et al. 2011). Coculture with and conditioned media from a variety of cell types has been shown to affect MSC differentiation (for a review see Heng et al. (2004)).

Despite the variety of available stem cell sources, there is much research into cell differentiation which avoids the need for a constant supply of primary cells. Some primary cells, such as cancerous cells, are able to undergo many divisions in *in vitro* culture without changing their behaviour. This observation has led to the production of a huge variety of different cell lines. Cell lines can be produced by the insertion of viral or bacterial genes into the cells of interest (Osyczka et al. 2002), or in some cases from selective pressure on embryonic cells (Karlsson et al. 2009). Cell lines are usually more robust than primary cells, can be expanded to greater passage numbers and are often used in preliminary work. It is important to remember that cell lines derived from cancers, such as the MG63 osteosarcoma cell line, may not show the same responses to stimuli or treatments as their non-cancerous counterparts. Primary cells from different sources may also show different expression pathways and functionality for tissue engineering, such as alkaline phosphatase production, matrix mineralisation or responses to stimuli (Hoemann et al. 2009; Diefenderfer et al. 2003; Diefenderfer et al. 2003). Suitable progenitor cell lines may help provide better reproducibility between laboratories, addressing the problem of donor variability in research (Karlsson et al. 2009; Osyczka et al. 2002).

During cell culture, cells are maintained under aseptic controlled conditions and bathed in culture media. For most cell types, cells are incubated at 37 °C in a humidified atmosphere containing 5% CO_2. For the culture media, there are a variety of different base formulations (such as Eagle's Media or Dulbecco's Modified Eagle's Media (DMEM)), which are supplemented to improve cell growth. Depending on the cell type and standard laboratory protocols, media may be supplemented with antibiotic and/or antifungal preparations. In addition, most cell culture medium is supplemented with serum, usually foetal calf or foetal

bovine serum (FCS and FBS respectively). This serum is part of the blood serum fraction from bovine sources and is heat inactivated prior to use in culture. The serum contains a variety of nutrients, growth factors and signalling molecules necessary for cellular growth and survival. As the serum is a natural product the composition will vary between batches and this may cause changes in the behaviour of cells due to differences in the signalling molecules present. The presence of soluble molecules or cellular material in the serum may also interfere with the detection of expression of similar factors by the cells. While the serum may be removed during specific periods of culture to investigate such changes, there are limited options for the culture of cells without serum.

Some chemical replacements exist, and there are a variety of options for the use of defined culture medium. For cell culture destined for clinical use in particular alternatives to serum need to be found. For cells cultured and destined for use in humans, the use of animal sera would introduce the risk of disease transmission, even when using autologous cells. Human platelet lysate is one possible alternative and autologous plasma has been shown to be effective for culture of MSCs (Sun et al. 2008; Lange et al. 2007; Shahdadfar et al. 2005; Mannello and Tonti 2007). Other approaches include the use of defined media containing appropriate growth factors and hormones (such as ITS+ Premix, EGF or insulin), or the use of a feeder layer of cells (Long et al. ; Mannello and Tonti 2007; Pytlk et al. 2009; Richards et al. 2008; Barnes 1980; Osyczka and Leboy 2005).

For bone tissue engineering, it is also important to ensure commitment of cells to an osteoblastic lineage, in order to allow proper bone matrix formation. This requires balancing of cell proliferation with differentiation, by the inclusion of stimulatory molecules or mechanical signals (Strehl et al. 2002). Cell density

has been shown to have effects on osteogenic differentiation of progenitor cells (Goldstein 2001). The use of mechanical conditioning to induce differentiation is discussed further in section 1.8. For chemically induced osteogenic differentiation, it is common to supplement media with ascorbic acid (vitamin c) and dexamethasone (a synthetic glucocorticoid) (Sittichokechaiwut et al. 2010; Porter et al. 2003; Rickard et al. 1994; Choi et al. 2008; Pytlk et al. 2009). These are important for proper organisation of collagen fibres and osteoblastic differentiation respectively. The use of bone morphogenic proteins (BMPs) is also under increasing investigation (Long et al. ; Rickard et al. 1994; Heng et al. 2004; Osyczka and Leboy 2005; Osyczka et al. 2009). A source of extracellular phosphate is also important for the mineralisation of the collagen matrix, often applied in the form of β-glycerophosphate (Farrell et al. 2007; Pittenger et al. 2002).

The choice of cell type for tissue engineering purposes ultimately depends on many factors. The intended use and stage of development of the research in producing the desired construct will play a role in this decision, as will the resources available within the laboratory. It is common to perform initial experiments with animal cells or human cell lines with high proliferative capacity. This reduces costs during initial development, before moving to more relevant cell types. The conditions under which cells are maintained also needs improvement to provide alternatives to the use of animal sera in routine cell culture. Cells may also need to be stored long term via cryopreservation and cells must be tested to ensure that they maintain their regenerative capacity once thawed (Liu et al. 2008).

1.6 Cells in their Natural Environment: ECM

For tissue engineering to provide suitable environments for the growth of tissues, it is necessary to understand the natural environment of a cell. During *in vitro* cell culture, there are noticeable differences in the behaviour of cells maintained in 2D versus 3D environments. Cells in the body are in a 3D environment, supported by extracellular matrix (ECM) and in communication with other cells embedded within this matrix. The organisation of fibres and mechanical properties of the ECM vary with tissue. In tendons, highly ordered collagen fibres are aligned in fibres and bundles, with cells present along the length of the fibres. This organisation allows the tendons to successfully resist tensile forces and provide anchorage and leverage between muscles and bone. In skin, a matrix of collagen and elastin provide a structure which is highly elastic and provides a barrier between the internal organs and the outside environment. Cortical bone has an ordered system of osteons, where concentric circles of mineralised matrix surround embedded osteocytes. Cancellous bone has a honeycomb structure, reducing the weight of the skeleton, whilst providing resistance to compressive forces and forming a container for the bone marrow. In all of these situations, cells are encased and supported within the 3-dimensional ECM, which contains a variety of molecules (such as collagen, fibronectin and glycosaminoglycans) and growth factors which provide cues to cells (Badylak 2004; Swartz and Fleury 2007).

Despite the 3D nature of the natural cellular environment, much routine *in vitro* work is carried out on flat, stiff culture plates, which provide an unrepresentative environment for the cells. While coating the surface of such plates with different molecules can provide chemical signalling cues similar to those in natural ECM, this still falls short of a natural cellular environment. The environment is

simplified and would not provide the variety of growth factors found *in vivo*. As an example, osteocytes *in vivo* are tightly encased within the bone matrix, residing in their lacunae. The space between membrane and bone is filled with the glycocalyx (connected to both surfaces), secreted proteoglycans and interstitial fluid. The fluid flows within the lacunae, providing nutrients to the encased cells and the flow is thought to be involved in mechanosensing by the osteocytes. By contrast, in 2D culture conditions only part of the cellular membrane is in contact with a surface, the internal structure of the cells is altered, in turn altering the ability of cells to respond to fluid flow stimulus (Thi et al. 2004). The cells are only partially attached to their surroundings, giving them a very different morphology to the same cells *in vivo* (Bacabac et al. 2008). It is likely that this will lead to the cells exhibiting different behaviour to native osteoblasts. The mechanical conditions to which they are exposed will differ greatly from the *in vivo* situation, altering the ability of the cells to respond to a given stimulus (Reilly and Engler 2010).

Previous studies have demonstrated that cells cultured in 3D can take cues from the physical environment they are in, such as the architecture (Tong et al. 2012) or substrate stiffness (Engler et al. 2006). These factors affect the differentiation and matrix production of progenitor cells (Farrell et al. 2007; Reilly and Engler 2010), cell conformation on the culture surface (Daud et al. 2012), signalling (Galli et al. 2012) and response to mechanical stimuli (Pedersen and Swartz 2005). The arrangement of stress fibres within cells and the attachments to the culture surface in 3D are very different to that in 2D, and this has been suggested as the mechanism by which cells respond to differences in substrate stiffness (Santis et al. 2011). Ideally, most cell culture work would be conducted in an environment as close as possible to the native tissue. While encouraging cells to produce their own

large 3D structures would be an ideal situation, this is not yet possible. Tissues have very complex structures, built up by a variety of cells working together in a 3D organisation during embryonic development. As the signalling mechanisms which regulate this behaviour are not well understood, much work on replicating the natural cellular environment instead involves the use of scaffolds to create the structure.

1.7 Scaffolds for Tissue Engineering: New Dimensions of Culture

Scaffolds are structures used to provide a template for cell growth in a 3D arrangement. A huge range of different types have been used for tissue engineering purposes and the type of tissue being produced has a major impact upon the requirements of the scaffold. For example, engineered skin and bone tissues will require different architectures and matrix elasticities to replicate the *in vivo* environment. Replacement bone tissue will need to perform load bearing functions on implantation, requiring a scaffold which can withstand these forces. Skin needs to perform a barrier function, as well as being elastic in nature to allow movement. Different materials and manufacturing processes may be used to produce a huge variety of scaffolds for different applications.

In the production of scaffolds for tissue engineering, there are a variety of factors which must be considered. These include porosity, stiffness, chemical structure, biocompatibility, biodegradability and ability to support cell attachment (Porter et al. 2009; Salgado et al. 2004; Wiesmann et al. 2004). The properties dictate whether cells are able to attach, proliferate, organise and produce matrix throughout the culture period. They must be carefully tailored to allow the cre-

ation of a functional tissue engineered construct. While the material used will be important in determining many of these properties, it is also important to consider the physical characteristics which are necessary for the desired application. The remainder of this section looks at different aspects of scaffold design, concentrating for the most part on bone tissue engineering.

1.7.1 A Question of Space

The main purpose of a scaffold for tissue engineering is to provide a 3D framework for the growth of cells. This 3D framework can be formed from a variety of materials with different architectures. When designing a scaffold able to support cell growth, there are several physical properties which are important to consider. Firstly, the overall shape and size of the scaffold has implications for the survival of cells seeded into it. *In vivo*, cells are no more than 200 μm from a medium supplying fresh nutrients and removing waste products. This limit is important as it is the distance over which diffusion is sufficient to maintain proper nutrient concentrations. When tissues are thicker than this, transport systems (such as a blood supply) are necessary to ensure cell survival (Hsiong and Mooney 2006).

For *in vitro* culture of cells, including tissue engineered constructs, it is important to ensure that the cells are able to exchange waste and nutrients with the surrounding culture media. This may be achieved by ensuring that the dimensions, porosity, pore size and interconnectivity within the scaffold are sufficient to allow the attachment of cells and movement of media throughout the construct (O'Brien et al. 2005; O'Brien et al. 2007; Melchels et al. 2010; Silva et al. 2006; Rose et al. 2004; Murphy et al. 2010). There is growing interest in the use of bioreactors to create movement of media during culture and these are discussed further in

section 1.8 (Wiesmann et al. 2004). While thin scaffolds (<400 μm) should allow the efficient transfer of materials into all the central regions of the scaffold, these would be of limited use during tissue engineering. Such scaffolds would not have sufficient structural properties for many tissues, such as bone or tendon, but may be useful in some circumstances. For example, such thin scaffolds may be appropriate for skin or circulatory system patches, where the tissue may not have load bearing functions but rather needs to provide a barrier. In cases where the scaffolds must be larger microstructure to allow mass transport or the use of fluid flow through scaffolds will be required in order to ensure cell survival.

Porosity of the scaffold is a measure of the volume of empty space within, sometimes referred to as the 'void space'. This gives an indication of the space available within the bulk volume of the scaffold for cell colonisation and media availability. The pore size is a measure of the sizes of individual pores and this measurement may be a range of values for inhomogeneous scaffolds. The pore interconnectivity is also important, as without sufficient interconnectivity there will be regions of scaffold where cells and media cannot penetrate. For a closed-cell foam scaffold, there is no interconnectivity between pores and cells would be unable to penetrate the scaffold. Open-cell scaffolds have a proportion of pores which are interconnected, allowing cells, nutrients and waste products to move within the structure. Sufficient pore interconnectivity will ensure cells are within reach of fresh media for nutrient supply and waste removal during the early stages of culture. As the cells proliferate within the scaffold, they will produce their own ECM. This will reduce the pore size and interconnectivity within the scaffold, reducing nutrient transfer as culture progresses at the same time that the demand for the process increases with cell proliferation. Although increasing the pore size and interconnectivity of the scaffold may address these problems, such changes

will affect the mechanical properties of the scaffold. A scaffold formed from a smaller volume of material with thinner struts will be highly porous but weaker than one with a lower porosity. This may make it unsuitable for applications which require the scaffold to be load bearing. Many groups have looked to the use of fluid flow to reduce problems of poor solute transfer, discussed in more detail in section 1.8. In bone tissue engineering, an open pore and highly porous scaffold will allow ingrowth and reorganisation of new bone tissue, as well as neovasuclatisation of the tissue construct after implantation to ensure its survival.

1.7.2 Scaffold Source: Natural or Synthetic?

The materials available for use as tissue engineering scaffolds are numerous. Many are synthetic materials with tuneable properties, allowing flexibility in the design and properties of the final scaffold. The use of natural materials is an approach which may be advantageous in terms of cell compatibility. Natural scaffolds introduce variability in material composition but include appropriate biological cues for cells. Scaffolds which are to be implanted in a patient must be biocompatible, that is it should not provoke any adverse response from the surrounding tissue. Bioinert materials will be in direct contact with tissues but provoke no response, whereas bioactive materials will promote a favourable biological response, including regeneration *in situ* (Bhat 2004; Bartolo and Bidanda 2008). This can be due to material properties or the inclusion of suitable signalling molecules. For bone tissue engineering scaffold, there are several properties which make a material bioactive. Osteoinductive materials encourage the recruitment of stem cells from the surrounding tissues and promote their osteogenic differentiation. Osteoconductive materials will instead guide and support the regeneration of the surrounding tissues into the implant (Salgado et al. 2004).

For natural scaffolds, there are two main approaches: the use of whole acellular tissues or of natural materials processed to form scaffolds. Either type should contain a range of tissue appropriate molecules derived from the ECM. In the case of whole acellular tissues, the ECM is left in the same configuration as in native tissue, with many of the component molecules that would be present normally (Badylak 2004). This is thought to aid the recreation of natural cell behaviour as cells which infiltrate the scaffold are in an environment close to their natural niche in terms of architecture and matrix components. If the scaffold is made from tissue appropriate for the cell type being cultured (such as dermal tissue for the growth of keratinocytes and fibroblasts), the ECM should stimulate the normal cellular behaviour desired (Canton et al. 2010). Recent work on tendons has suggested that replicating the tendon architecture in synthetic materials can be used to direct cell lineage (Tong et al. 2012). This research showed an effect separate from that of the tendon tissue, suggesting that the architecture alone can direct cell behaviour. A variety of tissue types have been successfully decellularised for use in TE, such as cardiac valves (Knight et al. 2008), bladder (Rosario et al. 2008; Bolland et al. 2007) and ligament (Ingram et al. 2007; Tischer et al. 2010). Work with demineralised bone matrix (DMB) has also been successful, allowing the differentiation of MSCs (Mauney et al. 2004; Mauney et al. 2004; Chakkalakal et al. 2001). Whole bovine trabecular bone has also been tested (David et al. 2008) and the matrix produced by osteogenic cells *in vitro* has been shown to influence the differentiation of MSCs (Dumas et al. 2010).

With the use of whole ECM scaffolds, there may be difficulties in encouraging cells to repopulate the tissue. Cells are removed from the scaffold by lysis before wash steps to remove the debris. This means that cells may be removed from areas of tissue which are very dense and which whole cells may not be able to

penetrate easily. The presence of cell attachment motifs on the scaffolds surface may help to encourage migration of cells into the inner regions of the scaffold, while vascular architecture may still be present within the material for the transfer of waste and nutrients.

There are many more examples of the successful use of whole ECM for TE, but other groups have focussed on the use of processed natural materials (Heng et al. 2004). Here, the material can be organised into a structure designed for the particular application whilst maintaining the presence of signalling factors found in the natural ECM. The porosity, pore size and overall scaffold shape can be tailored for the required application. The processing methods will depend on the type of material which is being used and the desired application. Scaffold materials of this type include gelatin hydrogels (Takagishi 2006), cellulose, agarose or alginate composites (Fang et al. 2009; Alcaide et al. 2009; Partap et al. 2007; Partap et al. 2006; Huang et al. 2012), collagen-glycosaminoglycan (collagen-GAG) (Farrell et al. 2008; Farrell et al. 2007; O'Brien et al. 2007) and silk films (Gupta et al. 2008).

For both types of natural scaffold it is likely that the base material can be degraded once implanted to allow remodelling of the tissue as necessary. For example, implanted bone may undergo normal remodelling such that the donor tissue is eventually replaced with the patient's own, which is integrated into the whole tissue and able to function normally under loading. This processes will occur using enzymatic pathways that occur normally within the body and should not produce any harmful byproducts. There is some evidence that treatments used on the tissue before implantation, such as crosslinking or sterilisation, may affect the remodelling response (Scheffler et al. 2008; Schmidt et al. 2012).

Although natural scaffolds may provide a complex stimulatory environment for cells, there are some limitations. The processes used in the removal of cells and sterilisation of such tissues can cause damage to the molecular components, reducing their efficiency as biological cues. As the tissue is a natural product, there may be problems with variability between samples. The size or composition of the matrix will vary with sample, which may in turn affect the behaviour of cells in contact with it. There are also concerns with the use of xenogenic tissue for implantation, as is the case for tissue grafts discussed previously. A suitable process for removal of the cells may overcome this problem by removing the cellular debris and molecules which can lead to rejection. These natural scaffolds may also be unable to perform appropriate mechanical functions within the body when first implanted. Pre-implant sterilisation methods may weaken the bone (Currey et al. 1997), leading to an unsuitable implant or longer recovery period than would be desirable. For other tissue types such as skin patches, the initial mechanical function may not be the most important factor in a treatment.

Many groups have instead focused on the use of synthetic materials to produce scaffolds. Such materials allow the production of a huge variety of scaffold types, with tuneable properties and low variability between batches. The scaffolds can be engineered to have different degradation rates (or no degradation), mechanical properties, exposed chemical groups, architectures and be produced in a range of different sizes. This allows production of scaffolds suitable for different tissues and culture conditions. Examples include ceramic materials (such as tricalcium phosphate or hydroxyapatite) (Hee et al. 2006; Yang et al. 2006; Cyster et al. 2005), bio-active glass (Reilly et al. 2007; Marion et al. 2005; Huang et al. 1997; Pamula et al. 2011), titanium (Fassina et al. 2009; Li et al. 2007), as well as many polymeric materials such as polyurethanes (PU) (Fassina et al. 2005; Fassina et al.

2006; Zanetta et al. 2009; Ramrattan et al. 2005; Khan et al. 2008), polycapralactone (PCL) (Daud et al. 2012; Li et al. 2005) and poly(lactide-co-glycolide) (PLGA) (Ngiam et al. 2009; reviews for bone and cartilage in Hutmacher 2000; Porter et al. 2009; Salgado et al. 2004).

For synthetic scaffolds there are a variety of approaches to fabrication which produce scaffolds with different architectures. They can be fabricated to have precise, ordered structures with defined characteristics or scaffolds with a range of pore sizes and a less uniform structure. Foam scaffolds can be produced which have random distributions of pore size and interconnectivity. The pore size can be tailored to give different ranges and the interconnectivity can be increased by altering the ratio of scaffold material to the filler used to create pores. Some examples of porous foam scaffold include polyurethanes (Zanetta et al. 2009; Guelcher et al. 2006), ceramic-polymer composites (Montjovent et al. 2007; Khan et al. 2008) and bioactive glasses (Fu et al. 2009). Other work has investigated the use of materials which are injected into a defect site containing cells and molecules of interest which form stable structure *in vivo* (Kim et al. 2009). 3D printing using suitable polymers, coupled with curing methods allows the production of precisely defined structures.

There are many groups producing scaffolds with specific characteristics to investigate the effects on specific cell types. They are being designed for specific applications, such as nerve guidance conduits (channels to direct neurite regrowth and aid nerve regeneration (Murray-Dunning et al. 2011)) and scaffolds with different motifs in different areas to attract cells and molecules to different areas of the scaffold (Viswanathan et al. 2012). Scaffolds can also be produced in sheets, such as through electrospinning. Electrospun scaffolds are usually thin,

although they can be rolled or folded to produce thicker scaffolds. Thin fibres are produced by a stream of polymer in solvent fired at a charged collector. They can be produced using a variety of materials, in random woven sheets, highly ordered aligned fibres or more complex arrangements (Bye et al. 2012; Blackwood et al. 2008; Puppi et al. 2010). Scaffold design through such methods provides a more tailored solution than a foam scaffold, but they may also be more labour intensive.

As mentioned previously, many synthetic scaffolds are produced from polymeric materials, where a polymer is a large molecule built from the combination of numerous smaller molecules (monomers). Many natural materials are polymers, such as cellulose (D-glucose monomers), starch (sugars), rubber and proteins (amino acids). There are an even greater number of synthetic polymers, which are often named according to their monomers. Examples include poly(ethylene), poly(propylene), poly(methyl methacrylate) (PMMA), poly(vinyl chloride) (PVC) and poly(styrene). Table 1.2 shows a list of some common polymer types, their medical applications and main features. Polystyrene is commonly used as a surface for tissue culture, which may pre treated prior to sale to improve cell attachment.

Commercial polymers are based on organic molecules (those with a carbon backbone) and are often classified in terms of size. This may be the molecular mass of the polymer or the number of repeated units (known as the degree of polymerisation, DP). Polymers can be divided into elastomers (able to withstand large deformations when a force is applied and return to their original dimensions afterwards) and plastics (rigid materials which undergo plastic deformation when loaded). The properties of plastic materials when they are exposed to a heat source can divide them further into two types - thermoset and thermoplastic polymers. Thermoplastic polymers soften on heating and can be reshaped during

Material	Uses	Notes
Poly(ethylene)	Acetabular cups, knee replacements, blood tubes	Chemical resistant, tough and flexible at low temperatures, cheap, easy to process
PTFE	Vascular grafts, arterial patches	Thermally stable, solvent and chemical resistant, no tissue reaction/inflammation, low thrombogenicity
PMMA	Bone cement, maxillofacial prostheses, lenses	Chemical resistant, biocompatibile, brittle, unreacted monomer can contaminate blood supply, exothermic reaction can cause tissue damage, can cause allergic reactions
Polyamides	Catheters, Dialysis devices, sutures, hypodermic syringes	Forms fibres readily, good mechanical properties, resistant to abrasion and breaking, thermal and chemical stability
Polyurethane	blood tubing, long term implants, adhesives, dental materials	biocomabtibility, low thrombogeniciy, good mechanical properties, hyrdolytically stable, non cytotoxic, no tissue reactions

Table 1.2: Example polymers for medical applications, compiled with information from Bhat (2004),Bartolo and Bidanda (2008), Lamba et al. (1998).

this time, where thermoset polymers deform permanently.

There are two general reactions which can be followed during polymerisation - step reactions or chain reactions. In a step reaction, a slow addition of monomers occurs throughout the reaction, with the highest molecular weight products formed only at the end of the process. The resultant solution consists of a mixture of all of the different possible sizes of polymer. In a chain reaction, there is a rapid buildup of high molecular mass polymer as monomers are added together, and the reaction solution contains only the finished molecules and single monomers. The presence of unreacted monomers in the final polymer may cause irritation on implantations, such as in PMMA bone cement (Bhat 2004).

While scaffolds may be used simply to provide the structural guidance of a 3D framework to cells in culture, they may also be able to perform mechanical functions. Different tissues have very different mechanical properties, tailored for their role in the body. Skin is thin and elastic, bone is designed to resist compressive force and provide structural support without being too heavy and tendon allows the transfer of forces between bone and muscle. Each different tissue type has a very different set of mechanical requirements, which require different scaffold solutions. If a scaffold is to be used for skin replacement, it mush be elastic to allow the development of skin which can move with the patient, as well as helping the migration of cells from the wound edge and creating an initial barrier over the wound against infection. Bone or tendon replacements would ideally be able to withstand the forces experienced during normal motion as soon as possible after implantation. A mismatch in the mechanical properties of tissue and scaffold can lead to stress shielding in bone implants. This causes a lack of appropriate mechanical cues to be transmitted to cells, which in turn leads to resorption of the surrounding bone (Bartolo and Bidanda 2008). Degradation of the scaffold too early will limit the efficiency of a scaffold's mechanical function, as discussed above. The scaffolds properties must be carefully tailored to provide a suitable environment for a given application. The mechanical properties of the scaffold are determined by the macroscopic architecture of the scaffold, as well as by the chemistry of the underlying polymer.

1.7.2.1 Polyurethanes for Tissue Engineering

One polymer of interest as a scaffold material for tissue engineering is polyurethane (PU). A huge range of different types of scaffold can be produced from PU due to the tunable nature of its chemistry and the effects this has on the macroscopic, microscopic, chemical and physical properties. Polyurethanes are thermoset plastics and are considered a block copolymer, meaning that they contain alternating hard and soft segments in their molecular chains. The urethane group (-O-CO-NH-) comes from the reaction of an isocyanate group with a hydroxy group, forming the basic reaction in PU chemistry. The hard polymer segments are formed from chains of highly reactive diisocyanate molecules linked with chain extenders (low molecular weight diols or diamines), with the soft segments consisting of a polyol (molecule with multiple OH groups). Oligomers (polymers consisting of only a few monomers) such as polyesters or polyethers may be used instead of monomers for the formation of polyurethanes. These molecules must terminate in OH groups, and are a common starting point in PU synthesis. Synthesis can be a 2 step process where the oligomer is first produced from a reaction of an excess of diisocyanate with an appropriate diol. The synthesis is then continued by the addition of diol or diamine chain extenders, producing the required multiblock copolymer.

Chain extenders are used to increase the hydrogen bond density and molecular weight in the final polymer and include 1,4 butanediol, ethylene diamine and ethylene glycol. If a small proportion of the monomers or oligomers are compounds with three functional OH groups (such as trimethylolpropane), crosslinks will form between the polymer chains during synthesis. Materials made only from linear oligomers are elastomers, lightly branched molecules are used to produce flexible foams and heavily branched molecules create rigid foams. The molar

ratios of the chain extender, polyol and isocyanate molecules also affect the final properties of the material. The hard segment in the polymer is responsible for the overall mechanical properties (tensile strength and hardness), where the soft segment is responsible for the elasticity and biodegradation properties. Polyester polyurethanes show the best mechanical properties, but the ester linkage in the backbone is susceptible to hydrolytic cleavage. Polyether polyurethanes are more useful when the environment is likely to require hydrophilic stability (Nicholson 2012; Bhat 2004; Bartolo and Bidanda 2008; Lamba et al. 1998; Campbell 2000).

There are many examples of polyurethane products commonly used in the medical industry, including bedding materials and disposable plasticware, although for most products there are cheaper polymers available. The main use of polyurethanes in the medical industry is for devices where biocompatibility of the product is important. Such devices include catheters, intra-aortic balloons and wound dressings in the form of hydrophilic foams. Polyurethane shows good haemocompatibility, including low thrombogenicity, so that implanted materials will not cause blood clotting and occlusion of blood vessels. For medical applications, there are some concerns over the use of some of the common isocyanate choices for PU synthesis as these molecules may be carcinogenic and can accumulate as the material degrades. While they show complete conversion during synthesis and leave no toxic residues, degradation of the polymer may release the molecules to harmful effect (Nicholson 2012). For example, polyurethanes synthesised with tolylene diisocyanate are thought to release toluene diisocyante when degradation occurs *in vivo* (Bartolo and Bidanda 2008). As such, there is some work using lysine or butyl diisocyanate molecules, which degrade to lysine and diamino butane (putrescene) respectively, both of which are non-toxic compounds.

1.7.3 Controlled Degradation

One of the concerns during tissue engineering for clinical applications is whether the materials placed within the body will remain inert or be degraded over time. For some replacements, such as hip and knee, the materials used are intended to be permanent replacements and should not degrade. There are known to be problems caused by wear of such implants, which can cause aseptic loosening. As the particles produced during wear remain within the joint, they can cause inflammation and degradation of healthy tissue (St. Pierre et al. 2010). The joint may need to be replaced, but the damage to surrounding tissue caused by loosening makes the revision surgery difficult (Ollivere et al. 2012). Revision surgery may require the use of bone grafting techniques as well as a new implant. For grafting which does not require the replacement of a complete joint, there is still a question of what materials will provide the best integration and functionality with the surrounding tissue. As people are remaining active later in their lives, which are also increasing in span, there is a growing need for materials with regenerative capacity and better functionality than the current gold standards.

Scaffolds for use in tissue engineering may be inert or undergo passive degradation or active remodelling by cells. For permanent materials, the scaffold will be populated by cells which produce healthy tissue, but the scaffold will be unchanged over time. Metal scaffolds (such as titanium foams (Li et al. 2007; Fassina et al. 2009)) should not undergo degradation, and will continue to perform structural roles over time. It may not be desirable to use a scaffold which is permanent, as this will become integrated within the tissue, but may suffer from wear issues similar to whole joint replacements, especially if the patient is young or very active. This would be problematic to replace if the surrounding tissue has partially integrated with the replacement. New tissue formed by the patient's own cells

can also never fully repair the defect, which may not be an ideal long term solution.

The use of scaffold materials which are remodelled or degrade could provide the initial structural support desired but be replaced in time with natural tissue. This would allow further remodelling and growth of the tissue, which is particularly important where the recipient is young. An engineered tissue will be functional as the patient grows and provide a better long term treatment option. This requires a construct which is able to change as the needs of the patient change and may be best achieved by a scaffold which is completely replaced by the patient's own healthy tissue. The use of natural materials (such as collagen) is ideal, as these can be broken down efficiently by the patient's body. The waste products from this breakdown can be metabolised through normal pathways used in the body during tissue turnover.

Polymers may undergo degradation via hydrolytic cleavage in the presence of water, via enzymatic degradation from bodily tissues, or by thermal degradation (Nicholson 2012; Campbell 2000). Biopolymers are susceptible to enzymatic degradation to allow their rearrangement during normal growth and development. Collagenase enzymes will break down collagen based materials and cellulose materials are hydrolysed by specific cellulases. Cellulases are found in vertebrates only where they have a symbiotic relationship with appropriate microorganisms (Bhat 2004). Any polymers for use *in vivo* would need to be thermally stable at 37°C in order to remain in the desired structure for any significant time after implantation. Some polymers (such as polyvinyl alcohol) are water soluble as their production includes hydrolysis, which may be reversible after implantation. Some polymer mixes may be susceptible to dissolution or erosion in moist environments depending on the pH, for example a mixture of methyl vinyl ether and maleic

anhydride (Bhat 2004). Polymers such as polyglycolic acid (PGA) and polylactic acid (PLA) undergo enzymatic degradation into waste products that are found normally within the body (in this example glycolic and acid respectively). If the scaffold is degraded in large volumes, there may still be problems with the waste products, even if they are naturally occurring compounds (Ngiam et al. 2009). Other materials, such as bioglass, have dissolution products (silicone, calcium and sodium) which have been demonstrated to be osteogenic (Tsigkou et al. 2009). If the degradation of such products is too high, cells growing in the dissolution media may have inhibited growth (Fu et al. 2009). Degradable scaffolds also allow the incorporation of growth factors into the scaffold, which are released over time into the developing tissue (Porter et al. 2009).

There are several degradation pathways of polyurethanes *in vivo*. Polyester polyurethanes are vulnerable to degradation by hydrolysis, in particular at the ester linkage. This leads to the release of isocyanate groups as well as hydroxy compounds ued in the fabrication process, for example diols. Cellular enzymes can bind to the polymer molecules and increase the rate of hydrolytic cleavage occurring within the material, increasing the overall degradation rate of a polyurethane product. As the rate of degradation also depends on the chemistry of the polyurethane, it is possible to tailor the rate of degradation by altering the monomers and isocyanate molecules used. Lower molecular weight polyurethanes are more susceptible to degradation than those with higher weights and any degradation *in vivo* should produce molecules with a low molecular mass which can be metabolised or excreted safely. Where the molecules are more hydrophilic, degradation is also seen to occur at a faster rate and deeper within the material. Some applications, for example bioresorbable sutures or bone constructs designed to integrate with the native tissue, require the use of biodegradable materials.

Polyurethanes can be tailored to the specific use such that the material degradation occurs at an appropriate rate. If sutures degrade too early, the wound may not heal sufficiently. In the case of a bone construct, the rate of degradation should be similar to the ingrowth of new bone, such that the mechanical integrity of the tissue is maintained. In contrast to the polyester polyurethanes, those made from polyether are not degraded by hydrolysis and are more stable in moist environments. They can be degraded by oxidation in the presence of metal ions.

For both natural and synthetic scaffolds it is important to make sure that any solutions used during the preparation of the scaffold are completely removed before use. As many synthetic solutions require harsh solvents, and natural the use of molecules to remove cells or break down the tissue, these could cause cytotoxicity problems if left within the scaffolds (Sachlos and Czernuszka 2003). This is especially important if the scaffold has low interconnectivity of pores, as solutions may become trapped and only released as the scaffold degrades or is subjected to mechanical forces.

1.7.4 Improving Culture Surfaces

There is an interest in tissue engineering research in the modification of culture surfaces to improve cell adhesion, migration, growth and development. This may be due to a property of the material used to create the culture surface, or a coating applied to the finished scaffolds after fabrication. The molecules or functional groups used will be dictated by the cell and tissue type to be used, as well as the desired function of the scaffold. For example, the scaffold may designed to direct cell shape, migration, or just improve the initial attachment of cells.

In order to produce a functional tissue, it is necessary that the attachment of cells to the scaffold is controllable. Is desirable that cells adhere sufficiently to the scaffold to remain in place when external forces are present. Hydrophilic surfaces will promote cell attachment over hydrophobic ones, for example. Bioreactors are commonly used to improve nutrient and waste transfer within constructs. While this can improve the cellular viability and mechanical characteristics of the constructs, it may also inhibit initial cell attachment to the scaffold. Shear stresses cause by the motion of fluid may lead to the detachment of cells which have only loosely adhered to the scaffold surface. As such, it is important to ensure that the scaffold material allows the secure attachment of cells in addition to other properties. For samples not cultured within bioreactors, but intended for use *in vivo*, it would be important for the cells to remain adherent once placed in the dynamic environment of the body. *In vivo*, cells attach to the ECM via integrins which bind to specific motifs, for examples the R-G-D peptide sequence in fibronectin (Ogura et al. 2004; Dolatshahi-Pirouz et al. 2011; Stevens and George 2005; Reilly and Engler 2010). Surface topography is also thought to be increasingly important in cell attachment and behaviour (Stevens and George 2005; Tong et al. 2012).

Simple surface modification techniques rely on adsorption of the molecule of interest onto the culture surface prior to the addition of cells. This usually involves leaving the culture surface under a solution of the molecule of interest (such as fibronectin or gelatin) for a period of time. The solution is then removed, the surface rinsed and culture continued as normal. In some cases, this is used as a default procedure during expansion (Karlsson et al. 2009), in others it is used to study effects on the behaviour of cells under experimental conditions. Examples of molecules adsorbed onto scaffolds include BMPs (Shen et al. 2009), serum and fibronectin (Yang et al. 2001), collagen mimetic peptides (Hennessy et al. 2009)

and carbonate apatite (Murphy et al. 2005). Direct coating of cells to improve differentiation has also been tested (Babister et al. 2009).

For polyurethanes, there are several options for modification of the polymer surface. During production of the material, bulk modification of the polymer can be used to introduce chemical groups of interest to the material. These groups may 'bloom' to the surface of the material and be used to allow the attachment of other molecules after production. Ionic groups and antioxidants such as vitamin E have been introduced to polyurethanes (and other polymers such as polyethylene (Bracco and Oral 2011)) in this manner. The molecules included in the bulk polymer may be able to influence cell behaviour without further modification, for example by making the surface more hydrophilic. The bulk modification of the polymer chemistry may have adverse effects on the mechanical properties of the final material and this must be considered during production.

Further surface modification can be achieved by reacting molecules of interest with those incorporated during bulk modification of the polymer. The inclusion of carboxyl groups in the bulk material will allow the attachment of different peptide sequences to the surface. These peptide sequences may encourage cell attachment or affect some other aspect of cell behaviour. As discussed previously, the R-G-D peptide sequence, found in fibronectin, is often used in experimental bone tissue engineering. Covalent attachment of molecules is also possible by first attaching diisocyanate bridges into the material. This can be achieved by reacting such molecules with urethane, hydroxy or amine groups within the polyurethane material. Further reaction can then be used to attach appropriate compounds, such as an albumin-heparin complex to improve haemocompatibility (Lamba et al. 1998). As mentioned previously, techniques such as plasma deposition have

been used successfully to deposit chemical groups or molecules on the surface of materials. For polyurethanes this includes polyethylene glycol, hydrophilic monomers and carbonyl or methyl groups (Lamba et al. 1998).

In order to characterise the bulk polyurethane and its surface, there are a variety of analysis techniques available. Infrared (IR) spectroscopy can be used to identify chemical groups within the material by splitting a beam of IR radiation and passing one beam through the sample. Comparing this to the reference beam allows the identification of molecules through their wave number. Differential scanning calorimetry (DSC) can be used to study the thermal properties of a material, including the melting point, degree of crystallinity and phase separation. Electron microscopy allows high magnification imaging of the material and mechanical testing (such as measurement of the stress and strain during loading or ultimate tensile strength) can be used to characterise the material properties (Sittichockechaiwut et al. 2009).

Surface characterisation methods include the use of imaging techniques such as atomic force microscopy (AFM), where the force of attraction between the surface and a nanometre scale needle is used to form a map of the surface. This can provide details on the distribution of charges of the molecular groups on the materials surface. The measurement of contact angle of the surface and a drop of water can be used to study the hydrophobicity of the surface. A drop of water on a material surface provides a junction of air with the liquid and solid materials. The technique looks at the tendency of the water to wet a surface - whether is will spread over the surface or bead up. The use of water may not be the best to test the biological relevance of a material surface as it does not contain any of the molecules found in biological fluids, such as proteins, salt or sugars. Attenuated fourier

transform IR spectroscopy (AT-FTIR) can be used to compare the surface of a material to the outer regions. As evanescent IR waves travel parallel to a surface, partial absorbtion and attenuated reflection will occur for two media with different refractive indices. XPS (x-ray photo-electron spectroscopy) can be used to find information on the specific atomic and molecular orbitals within the upper 30-100 $\mathring{A}$ of the material surface. The surface is irradiated with low, single energy x-rays which are able to excite electrons within the material. Some of these electrons will be ejected if they receive sufficient energy and this emission of electrons can be used to identify the particular bonds present. Another analysis method is SIMS (secondary ion mass spectrometry), where the surface is instead bombarded with an ion stream (such as argon, xenon or caesium). These ions strike the material's surface and cause the ejection of secondary ions which are then directed towards a quadrupole analyser. The intensity of these ejected ions and their mass/charge (m/z) ratio can be used to deduce the molecular structure of the species. The analysis can also detect the presence of hydrogen and high mass fragments, such as from proteins. This technique is only able to study they to 10 $\mathring{A}$ of the material, and as such characterises only the very surface of the material (Lamba et al. 1998).

The range of scaffolds which can be produced are tailored towards specific tissues or culture requirements. As tissue engineering develops and more is learned about the effects of the different scaffolds on cell behaviour, the relative importance of the different features may be elucidated. This may lead to more closely tailored scaffolds for the desired tissue.

1.8 Mechanical Conditioning of Tissue Engineered Constructs

The overall environment of cells can cause changes in behaviour, and it is necessary to carefully maintain the culture conditions as discussed previously within this chapter. *In vivo* there is another important factor which can affect cell behaviour: mechanical stimulation of the cells. The body is constantly moving, from the beating of a heart, movement of blood within blood vessels, or motion of limbs and joints through the combined action of muscles, tendons, ligaments and bones. Tissues must be able to cope with the normal mechanical environment in which they are found. In many tissue types, the cells respond to changes in the mechanical environment by changing their ECM or behaviour, such as in the increase in muscle mass found with an increase in suitable exercise. Distraction Osteogenesis is used to aid the creation of large volumes of new bone *in vivo*. It involves the application of controlled displacement to the bone, and modelling suggests this causes shear stresses and fluid flow within the bone (Isaksson et al. 2007). Mechanical conditioning of constructs *in vitro* is proposed to be a method to better prepare engineered tissues for use in an *in vivo* environment.

One method of stimulation of constructs is the use of bioreactors (Martin et al. 2004; Korossis et al. 2006). Many bioreactors have been designed to improve nutrient transfer, but their use may also provide appropriate mechanical conditioning to cells. Increasing the movement of culture medium can help to prevent cell death within the inner regions of scaffolds. For this reason, many fluid flow bioreactors were developed to improve construct homogeneity. There shear stresses passing over the surface of cells are increased which may lead to mechanical stimulation. In blood vessels, the cells must be able to withstand

the movement of pressurised blood along the vessel without detaching. *In vitro* conditioning of cells in constructs designed for this purpose may improve the performance of the vessel after implantation. In bone, which shows strong responses to changes in mechanical stimulation, it is unknown whether the response is caused my stimulation via fluid flow or matrix deformation.

Flow bioreactors may be used to stimulate cells to create better bone-like matrix. Many groups have looked at the use of bioreactors during culture of bone cells and the effects these have on osteogenic behaviour of the cells. Release of soluble signalling factors (Jaasma et al. 2008; Bakker et al. 2001; Bacabac et al. 2004; Genetos et al. 2007; Reilly et al. 2003; Jaasma and O'Brien 2008; Mullender et al. 2004), increased cell distribution and matrix production (Grayson et al. 2008; Fassina et al. 2005; Morris et al. 2010), ALP activity (Goldstein et al. 2001) and osteogenic gene expression (You et al. 2001; Owan et al. 1997) have been demonstrated with the use of fluid flow bioreactors. Computational analysis of fluid flow is also of interest to improve scaffold design for this type of stimulation (Cioffi et al. 2008; Jungreuthmayer et al. 2009).

There are a variety of other methods for mechanical stimulation of constructs in tissue engineering which have been tested *in vitro*. Simple methods include stirring of media (Ichinohe et al. 2008; Goldstein et al. 2001) and rotating (Botchwey et al. 2001) or rocking (Delaine-Smith et al. 2012) of the culture vessel. The application of mechanical compression causes deformation of the scaffold, which may be transmitted to the cells and cause bone remodelling. This process requires scaffolds which are able to maintain their shape despite the repeated application of such forces. A variety of different systems exist, with different parameters and results (Sittichockechaiwut et al. 2009; David et al. 2008; Sittichokechaiwut

et al. 2010; Wood et al. 2008, reviewed by Delaine-Smith and Reilly (2011)). Stretching of constructs may be applicable for tissues which naturally undergo tensile loading *in vivo*. Examples of this include skin and tendon, and research into the mechanical conditioning of such tissue to improve their properties *in vitro* is being carried out. Tension can be applied to such constructs by gripping the ends and stretching the material or stretching (Nguyen et al. 2009; Foolen et al. 2012; Butler et al. 2009; Nirmalanandhan et al. 2008; Thomas and El Haj 1996; Tang et al. 2006), or by bending of a surface (Peake et al. 2000; Owan et al. 1997). Other techniques include the use of magnetic particles to pull on cell membranes (Cartmell et al. 2005) or cytoplasm (Yuge et al. 2003) and the application of electromagnetic fields (Lohmann et al. 2003; Fassina et al. 2006; Fassina et al. 2009).

There is also growing interest in the use of vibration to alter the structure of bone tissue, both *in vivo* and *in vitro*. Low magnitude, high frequency (LMHF) vibration is applied to stimulate a response. For patients with diseases such as osteoporosis, it is not always possible for them to undertake high impact exercise to prevent bone degeneration. If their bones are already sufficiently weakened, this could increase the risk of breaks, leading to more complicated conditions. *In vivo* tests of LMHF vibration in animal and human subjects has shown increases in the bone mass, trabecular density and trabecular thickness from short periods of such stimulation (Gilsanz et al. 2006; Gusi et al. 2006; Judex et al. 2003; Rubinacci et al. 2008; Oxlund et al. 2003; Garman et al. 2007, reviewed in Rubin et al. (2001, Andrews (2010)). This form of stimulation usually involves the patient standing on a vibrating platform for a short period of time each day. However, the efficiency of this method is questionable, as some studies have not shown any significant effects (von Stengel et al. 2011; Torvinen et al. 2003).

The method of action of this type of stimulation is also poorly understood and it is not known which cells are affected by the stimulation to cause a response. Due to the possibilities of use in patients with compromised bone structures and the relative ease of applying the stimulation there is still much research into this kind of mechanical conditioning. This includes both animal (Lau et al. 2011; Rubinacci et al. 2008; Oxlund et al. 2003; Garman et al. 2007; Christiansen and Silva 2006) and *in vitro* work (Zhang et al. 2012; Suzuki et al. 2007; Pre et al. 2009). It is also theorised to have beneficial effects on other tissue types (such as muscle), and could be used to improve bone healing (Shi et al. 2010; Leung et al. 2009) or integration of tissue replacements (Zhao et al. 2009). Tables 1.3 and 1.4 provide examples of studies carried out, both *in vivo* and *in vitro*.

Reference	Species	Conditions	Measures	Outcomes
Rubin et al. (2002)	Ovine	0.3g, 30 Hz, 20 min/day, 5 days/week, 1 year	BMC, trabecular number, longitudinal stiffness and strength	↑(10.6%, 8.6%, 12.1%, 26.6%)
			trabecular spacing	↓ 11.3%
Judex et al. (2005)	Murine	Disuse versus vibration (45 Hz, 0.3g, 10 min/day, 5 days/week, 21 days)	BFR and mineralisation (trabecular and periosteal)	↑ BFR(32%, 93%), Min(18%, 69%)
			mRNA (Col I, osteonectin, osterix or MMP-2)	↓ in disuse.
Rubin et al. (2003)	Human	Force transmission through human spine to hip and spine, 15-35 Hz, 36 N	Reduced transmissibility above 20 Hz, resonance below 20 Hz.	
Gusi et al. (2006)	Human (PM women)	3 sessions per week, 8 months, vibration (12.6 Hz, 3 cm amplitude, 6 bouts of 1 min) or 1 hour walking and stretching	BMD (femoral neck), balance	↑ 4.3% and 29%
Rubin et al. (2004)	Human (PM women)	0.2g, 30 Hz, <20 mins/day, 7 days/week, 1 year	BMD	Small ↑ when compliance high
Oxlund et al. (2003)	Rat (OVX)	0.5g (17 Hz), 1.5g (30 Hz) or 3.0g (45 Hz) constant amplitude vibration, 30 min/day, 90 days	BFR	↑ (OVX and OVX + vib, highest for OVX + 45 Hz)
			Endocortical resorption	↑ (OVX), no change (OVX + vib)
			Maximum bending and compressive strengths	↓ (OVX), no change (OVX + vib)

Castillo et al. (2006)	Murine	Vibration (0-50 Hz), with or without carrier (sine wave), 30 s/day, 3 day/week, 4 weeks	Cortical BFR, geometry	No changes
Shi et al. (2010)	Rat (OVX)	35 Hz, 0.3g, 20 min/day, 5 days/week, 8 weeks	Fracture healing (callus formation, mineralisation, remodelling, energy to failure)	↓ OVX only
				↑ vibration (higher for OVX-vib than sham-vib)
Wenger et al. (2010)	Murine	18 month old, 0.5 and 1.5g, 32 Hz, 30 min/day, 12 weeks	Bone volume, strength	No changes
			High density bone, mineralisation, osteoclast numbers	↑ 0.5g (density), 1.5g (osteoclasts) or both (mineralisation)
			Pryridinoline crosslinks	↓ for vibrated
Rittweger et al. (2010)	Human	56 days bedrest or bedrest with vibration and resistive exercise (RVE, 11 times/week), 19-30 Hz, 5-10 mins (patient dependant)	Muscle size/function, bone volume	No change (RVE)
			BMC	↓ in controls
Sandhu et al. (2011)	Rat	0.3g, 30 Hz, 5 days/week, 5 weeks	Tendon cross section, stiffness	↑
			Strain to ultimate load	↓

Table 1.3: *In vivo* vibration research summary. BMC = bone mineral content, BFR = bone formation rate, PM = post menopausal.

Reference	Cells	Conditions	Measures	Outcomes
Tanaka et al. (2003)	MC3TC-E1	3 mins/day, 3 or 7 days, strain (3 Hz, 0-3000 μstrain, 0.33 s rest time), broad frequency vibration (0-50 Hz, ¡300μstrain or combination, collection on day 4 or 8)	Cell proliferation	$\downarrow$ (day 8, combined loading)
			mRNA (osteocalcin)	$\uparrow$ (2.6 fold, day 7)
			ALP activity, mRNA (col I, osteopontin, connexin 43, MMPs-1A, -3 and -13)	No change
Dumas et al. (2010)	MC3T3-E1, C3H10T1/2 (MSC)	MC3T3 cells stimulated (15-40 μstrain, 400 Hz, 20 min/day for 1, 3 or 7 days)	NO secretion, mRNA (fibronectin, osteopontin, bone sialoprotein, col I)	$\uparrow$
			Cell number, viability	No change
		C3H10T1/2 cells cultured on decellularised MC3T3 matrix (7 days with/without stimualtion)	Attachment, focal adhesions, osteogenic mRNA	$\uparrow$
			Adipogenic mRNA	$\downarrow$
Tjandrawinata et al. (1997)	MC3T3-E1	Serum deprivation, 2 mins vibration at 7.838g followed by 6 mins at 4.098g	mRNA (c-fos, c-myg)	initial $\uparrow$
			mRNA (osteocalcin, TGF-β, HisH4, cPLA$_2$, COX-2 or β-actin), PGE$_2$	No changes
(Bacabac et al. 2006)	MC3T3-E1	5, 30, 60 and 100 Hz, 5 mins, varying amplitude	Cell shape, alignment or detachment	No change

			NO release	↑ with ↑ maximum acceleration
			PGE_2 release	↑ with ↓ maximum acceleration
Suzuki et al. (2007)	Goldfish scale	0.5, 1, 2, 4 or 6g vibration, 5 or 20 min/day, 6 or 24 hr incubation	Osteoblast activity (ALP)	↑ with ↑ g
			Osteoclast activity (TRAP)	↓ at 24 hr with vibration (highest suppression 2g
Lau et al. (2010)	MLO-Y4	0.3g, 30, 60 or 90 Hz, 1 hour	mRNA (Cox-2)	↑ (90 Hz highest)
			mRNA (RANKL), soluble RANKL, PGE_2	↓ for all
			Osteoclast formation	Inhibited by vibrated conditioned media
Pre et al. (2009)	SAOS-2	11 mm displacement, 30 Hz, each day, 4 days, varying duration	mRNA (ALP, Col-I, osteonectin, fibronectin, Col-III)	↑, highest for 45 or 60 minutes
			Cell proliferation	↓

Table 1.4: *In vitro* vibration research summary

1.9 Summary

Tissue engineering is a fast growing field of research, aimed at improving our understanding of cells and tissues and providing solutions to clinical problems. There are many different aspects which must be considered, such as the cell type, scaffold material and architecture, culture conditions and mechanical conditioning. The ability to produce viable tissues, patient specific if necessary, would have a profound effect on many standard medical treatments. It would also allow more robust testing of drugs and compounds prior to human testing, reducing the necessity of animal experimentation. The ability to investigate cellular behaviour in more relevant culture conditions than currently available has the potential to provide social and economic benefits in many areas.

The following research investigated the use of a recently released, commercially available mesenchymal progenitor cell line for bone tissue engineering. The attachment of the cells in 2D and a 3D polyurethane scaffold was studied, followed by the effects of low magnitude, high frequency (LMHF) vibration on the cells in both 2D and 3D culture. An early differentiation marker is investigated, as well as the production of mineralised matrix by the cells. The main aim of the research was to study the effects of low magnitude, high frequency vibrations on the osteogenic differentiation of the chosen cell line. This would help elucidate whether this type of stimulation could be used during the production of tissue engineered bone constructs from progenitor cells. The research also provides more information on the possible cell types involved during *in vivo* responses to such loading.

1.10 Chapter Outline

- Chapter 2 details the materials and methods used throughout the work.
- Chapter 3 describes work on the attachment of cells to a 3D polyurethane foam scaffold and the imaging of the attached cells and mineralised matrix.
- Chapter 4 begins investigation into the effects of LMHF vibration on the hES-MP cell line. This chapter looks at the behaviour of the cells in 2D.
- Chapter 5 continues to work on LMHV vibration and hES-MP cells, moving to a 3D environment using several different scaffold types.
- Chapter 6 provides a final discussion of the research as a whole, including future research topics suggested by the results.

Chapter 2

Materials and Methods

2.1 Cell Culture

Three cell lines were used during experimental work. The expansion of cells was carried out in T75 tissue culture flasks (Nunc) incubated at 37 °C in a humidified 5% CO_2 atmosphere. Normal experimental culture was carried out in the required culture vessels under the same incubator conditions as expansion. Chemicals were obtained from Sigma Aldrich, Dorset, UK (abbreviated to Sigma) unless otherwise specified.

The MG63 human osteosarcoma cell line was used to help develop culture techniques and mechanical compression regimens. These cells show high proliferation and osteogenic behaviour, with minimal culture requirements. For these cells, basal media consisted of Dulbecco's modified Eagles medium (DMEM) (Biowhittaker), 10% FCS, 1% penicillin/streptomycin (p/s), 1% l-glutamine and 0.25% fungizone (f).

The hMPC 32F cell line, developed by Osyczka et al. and kindly donated for use was tested for cell attachment in the PU foams. The cell line is a mesenchymal progenitor cell line which displays all the properties of normal MSC cells isolated from bone marrow. These cells may be used over a much longer period of time than primary cells as they can proliferate for over 20 passages without changing their differentiation potential (Osyczka et al. 2002) . The cells were maintained in basal culture media of Alpha minimum essential medium (α-MEM) (Lonza), 10% FCS, 1% p/s and 1% l-glutamine.

The hES-MP 002.5 human mesenchymal progenitor cell line (Cellartis, Lot hESMP002.5EL) was used throughout the project. Expansion of these cells was the same as detailed above, except that T75 flasks were coated with 0.1% (w/v) autoclaved gelatin solution for 30 minutes prior to seeding of cells, as recommended by the vendor. This promotes rapid and continued attachment of the cells to the substrate. Basal culture media used was α-MEM (Lonza), 10% FCS, 1% p/s and 1% l-glutamine.

In experimental cultures, several additives were included in culture medium to promote osteogenic differentiation and improve matrix production and mineralisation. Ascorbic acid-2-phosphate (Sigma) was added to a 50 μg.ml^{-1} final concentration, as well as β-glycerophosphate (5 mM final concentration) (Fisher Scientific). Dexamethasone (Sigma) was added to some culture media to induce osteogenic differentiation in hES-MP cells at a working concentration of 10 nM, specified in the experimental details. Some conditioned media experiments also included indomethacin (Sigma) at a working concentration of 10^{-6}M. Table 2.1 details the additives and the abbreviations used for them. Examples of media formulations and their abbreviations are given in table 2.2.

Additive	Abbreviation	Concentration
Ascorbic acid	a	50 μg.ml^{-1}
β-glycerophosphate	b	5 mM
Dexamethasone	d	10 nM
Gelatin	g	0.1% (coating)
Indomethacin	i	10^{-6}M

Table 2.1: Media additives during cell culture, including working concentrations.

Abbreviation	Details
ab	Basic supplementation, ascorbic acid and β-GP
abd	As above with dexamethasone
abdg	As above with gelatin coated well plates
abg	Basic supplementation with gelatin coated plates
abi	Basic supplementation with indomethacin
abdi	As above with dexamethasone
C:abd.T:ab	Cells cultured initially in abd media, receiving conditioned media containing ab at each transfer point during culture.

Table 2.2: List of abbreviations for media formulations

2.2 Scaffold Preparation

For much of the 3D work, a readily available foam scaffold previously studied within the lab was used. The foam was an interconnected open pore polyether polyurethane (PU) foam, grade XE1700V (Caligen Foam Ltd, donated by Professor A.J. Ryan, University of Sheffield). The foam is made of a polyether polyurethane, synthesised using an ether polyol (MW 3500) and toluene di-isocyanate. Water and methylene chloride were used as blowing agents, siloxane silicone as a stabiliser and an amine catalyst (BDMAEE). The foams were characterised previously in the lab by a PhD student using SEM images to estimate pore size and strut width. Mechanical properties were tested by compressive loading to 50% strain using the Bose ELF3200 mechanical testing machine (strain rate 0.2 mm.s^{-1}) and the Young's modulus calculated. The average pore size is approximately 400 μm, with a range of 150-1000 μm. Average strut width was 65 μm (ranging from 43-96 μm) and the Young's modulus was 2.07$\pm$0.02 in dry conditions (2.87$\pm$0.02 in wet conditions).

This foam was chosen as it had been used previously within the lab, supporting both osteogenic cell lines and primary mesenchymal stem cells through calcified matrix production. Compressive mechanical loading had been able to increase the matrix production and differentiation markers as reported by (Sittichockechaiwut et al. 2009),(2010). Also this scaffold does not undergo degradation this was thought to be advantageous during these studies, as the mechanical properties of the scaffold would not change and affect force transmission during the experiments.

Ten mm diameter cylindrical scaffolds were cut from the foam block, either 4 mm or 10 mm high depending on the requirements of the experiment. These were sterilised by soaking in 70% ethanol overnight or by autoclaving in PBS. Scaffolds were pre-rinsed with basal culture media immediately before seeding. Prepared polyurethane scaffolds were placed in 12 well tissue culture plates within 1 cm internal diameter stainless steel rings. Figure 2.1 shows examples of a foam cylinder and scaffolds within metal rings after seeding with cell suspension. Samples were squeezed gently to remove excess media prior to placement in the rings. Scaffolds were seeded to a density of $5x10^4$ cells per mm of scaffold height, distributed evenly over the scaffold using a micropipette. This was done using a low volume of media (50 μl) to prevent leakage of the suspension from the porous scaffold. Samples were incubated for 2 hours to allow initial cell attachment, at which point sufficient basal culture media was added to cover both the ring and scaffold. After 24 hours, the metal rings were removed and samples were placed in fresh well plates in either ab or abd supplemented media. Figure 2.2 shows the seeding process in more detail.

Other scaffold types (see below) had the same 2 hour incubation before adding media to cover the scaffolds. The other scaffold types were not of a suitable size to use with the stainless steel rings and were instead seeded in a small volume

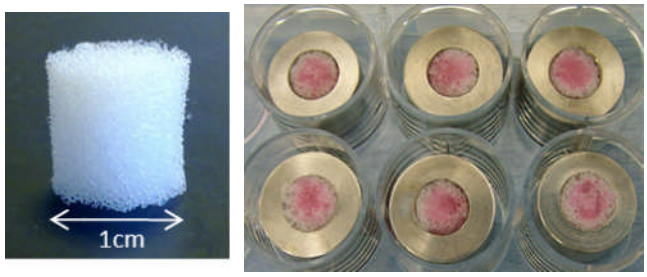

Figure 2.1: Cylindrical polyurethane foam scaffolds

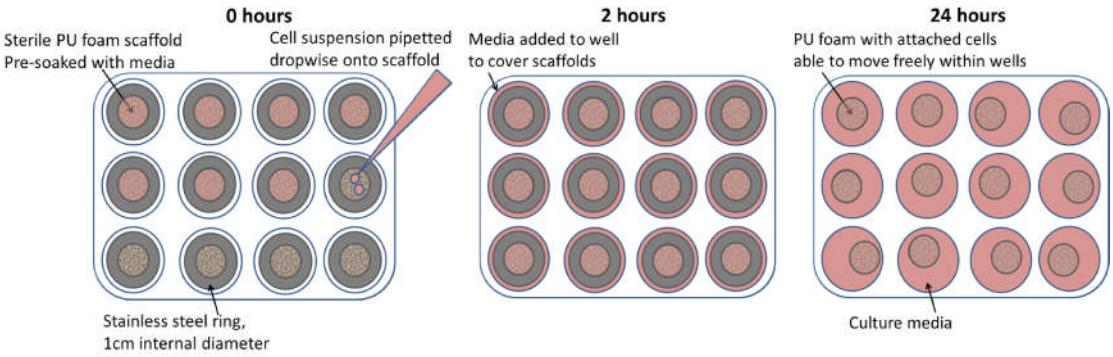

Figure 2.2: Cell seeding method for PU foam scaffolds

of media to ensure the cell suspension did not leak from the scaffold. They were transferred to fresh plates in the required media after 24 hours. More detailed descriptions of these scaffolds are presented in section 5.5 and cell numbers used during the final experiments are detailed in table 5.2, along with further details of the experimental setup.

Further preparation was required for each of the other scaffold types used. Borosilicate glass scaffolds (Orla) were prepared by sterilisation in 0.1% peracetic acid for 2 hours on a plate rocker. The samples were then washed thoroughly in PBS (3 washes for 30 mins each on the rocker) before transferring to a 12 well plate for seeding.

Alvetex scaffolds (Reinnervate) were prepared as described in the product information. They were presoaked in 70% industrial methylated spirit (IMS)

overnight, before washing 3 times with PBS. While the scaffolds are supplied in sterile conditions, soaking in IMS is required to pre-wet the scaffolds. The hES-MP cell line used requires gelatin treatment for normal culture and pre-treatment of the scaffolds to aid attachment was also recommended by the scaffold manufacturer. Therefore these scaffolds were coated with a 0.1% autoclaved gelatin solution for 30 minutes prior to cells seeding, as for the T75 flasks. The gelatin solution was removed and scaffolds washed once with PBS prior to cell seeding. Cells were seeded in 1 ml of the required media type per scaffold to ensure even coverage.

3D Insert scaffolds (3D Biotek) were provided sterile and pre-treated with a sterile 0.1% gelatin solution as for the Alevetex scaffolds. They were seeded with the cell suspension in as low volume as possible (approximately 20 μl) to ensure cells remained within the scaffolds.

Collagen-glycosaminoglycan (CGAG) scaffolds, kindly donated by F. O'Brien, were cut from a sterile sheet into 10 mm diameter cylinders aseptically. Cells were seeded directly onto the scaffolds without pre-wetting, as the scaffolds contract when placed in media. Adding the cells in media to dry scaffolds helped ensure the cell suspension remained within the scaffold rather than leaking on to the culture plate. Cells were seeded in as low a volume as possible (approximately 40 μl) to aid with the retention of cells in the scaffold.

2.3 Mechanical Loading

Mechanical loading of scaffolds was carried out using a Bose ElectroForce 3200 (ELF3200) mechanical testing device. For compressive loading, samples were loaded under sterile conditions within a biodynamic chamber. The biodynamic

chamber was sterilised by autoclave and opened within a laminar flow hood. Samples were placed between the loading platens for mechanical compression, in approximately 200 ml of loading media (as normal MG63 media with only 2% FCS, (Allen et al. 2000)). Paired, non loaded control samples were placed in a T25 flask with 40 ml of loading media. These samples were kept next to the Bose during loading to control for differences in temperature, humidity and CO_2. The biodynamic chamber was secured on the testing machine, and used to apply 5% cyclic compressive strain. All samples were loaded for 7,200 cycles with variations in loading day and frequency of compressions. Samples were cultured in well plates in appropriate ab or abd media between loading cycles.

The ELF3200 was also used to investigate the effects of low magnitude, high frequency vibrations on hES-MP cells. A perspex plate was attached to the motor at the top of the machine. A second piece of perspex and grips were used to clamp the well plate onto the machine. Sinusoidal vibrations were applied to the plate at various frequencies and for different time periods. This information is provided later in the individual experiment descriptions.

2.4 Metabolic Activity Assay

Samples were tested for metabolic activity using either an MTT (Sigma) or MTS (Cell Titer 96 AQueous One Solution Cell Proliferation Assay, Promega) assay. MTT (A3-(4,5-dimethylthiazol-2-yl)-2,5-diphenyltetrazolium bromide) is applied as a yellow solution, which is converted to an insoluble purple formazan salt within the mitochondria of viable cells. An MTS assay (3-(4,5-dimethylthiazol-2-yl)-5-(3-carboxymethoxyphenyl)-2-(4- sulfophenyl)-2H-tetrazolium) was used in scaffolds which are to be analysed further, due to the soluble nature of the

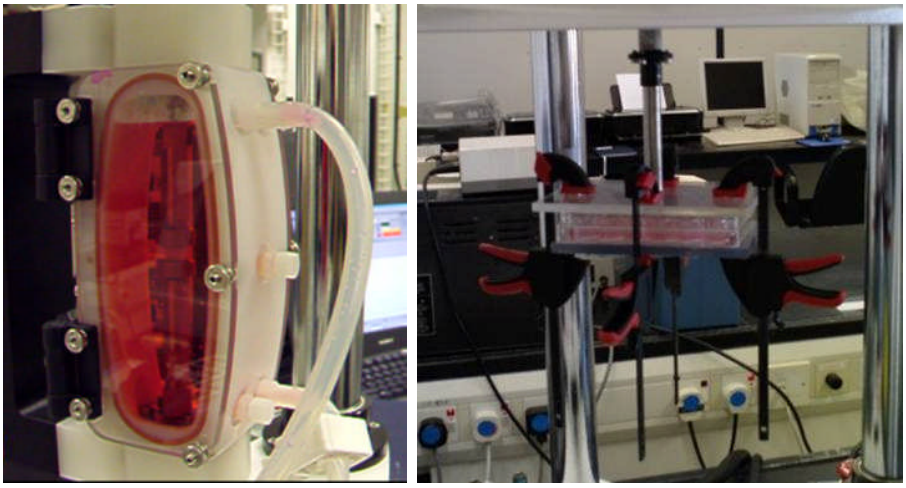

Figure 2.3: Images of Bose ELF3200 set up for mechanical stimulation. Left shows the biodynamic chamber used for application of cyclic compressions. Right shows the setup for the vibration of whole culture plates.

pink formazan product. The purple colouration produced by MTT allows viable cells to be visualised easily within scaffolds and was used to study cell distribution. Both assays are usually performed to asses the cell viability within cultures.

MTT assays were performed using a 0.5 $mg.ml^{-1}$ solution of MTT in sterile PBS. After rinsing 3 times with PBS, scaffolds were immersed in 4 ml of MTT solution and incubated at 37°C for 40 mins. Samples were then rinsed thoroughly in PBS before being cut into sections to observe cell distribution.

For MTS assays, samples were washed gently with PBS to remove culture media. Stock solution was diluted 1:10 in sterile PBS and 220 μl (500 μl for 3D) of the resulting solution was added to each sample before incubation at 37 °C for 2 hours. For 3D samples, scaffolds were assayed in fresh well plates and placed in metal rings to contain the MTS solution within the scaffold. After 2 hours incubation, 200 μl samples of solution were placed in a 96 well plate and the optical density measured at 490 nm using a spectrophotometer (Biotek).

2.5 Extracellular Matrix Production

Formalin fixed samples were analysed for collagen and calcium content to investigate extracellular matrix production. After analysis of cell viability, samples were rinsed 3 times with PBS and fixed in 10% formalin for 20 minutes. Samples were rinsed a further 3 times with PBS before staining. For the PU scaffolds, samples were cut into 2 mm high circular sections after the final PBS wash. Alizarin red was used to stain calcium present within the samples, which binds with calcium to give a bright red staining (Gregory et al. 2004). Alizarin red dye (Sigma) was dissolved in distilled water (1 $mg.ml^{-1}$), and the pH adjusted to 5.5 using ammonium hydroxide. Samples were placed under 2 ml of the solution and left at room temperature for 40 minutes on a plate rocker. Excess dye was removed by thorough washing with distilled water until clear. Samples were photographed before destaining with 5% perchloric acid (Sittichockechaiwut et al. 2009; Sittichokechaiwut et al. 2010). 1 ml per scaffold of destain solution was applied for 30 minutes under mild shaking. Destain solution was used in small volumes for 2D samples in 12 well plates (220 μl), due to the relatively low presence of calcium. 200 μl samples of the resulting solution were measured for absorbance at 410 nm.

For collagen analysis samples were stained with sirius red, an anionic dye which binds strongly to and aligns with collagen fibres (Tullberg-Reinert and Jundt 1999). Samples were washed thoroughly with distilled water prior to staining. Direct red 80 (Fluka) was dissolved in saturated picric acid (Fluka) at a concentration of 1 $mg.ml^{-1}$. Samples were covered with 1 ml per well (12 well plate, 4 ml per well for scaffolds) or 2 ml (6 well plate) of stain solution for 2 hours on a plate rocker. Unbound dye was removed by washing in distilled water until no more stain was eluted. Samples were destained using 450 μl per well (12 well plate, 1 ml for

scaffolds) of destain solution for 30 minutes on a plate rocker. Destain solution consists of a 1:1 solution of methanol and 0.2 M sodium hydroxide. Duplicate 200 μl samples of the resulting solution were measured for absorbance at 490 nm.

2.6 Fluorescence Microscopy

Fluorescence microscopy was used to study cell viability, cell attachment and mineral deposition within scaffolds. Samples were imaged using either a Zeiss LSM510 Meta confocal microscope or Axon Instruments ImageXpress Automated Cellular Imaging and Analysis System.

Cell viability was investigated by live-dead staining with the nuclear stains Syto-9 and propidium iodide (PI). Syto-9 (5 mM in DMSO, Invitrogen) is a fluorescent dye which enters cells and fluoresces when excited at 488 nm. PI (1 mg.ml $^{-1}$, Invitrogen) is only able to enter cells with compromised cell membranes and fluoresces when excited at 543 nm. Combining images taken at these wavelengths for the same field of view shows which cells were dead (those in which PI has entered the cell) and which where alive (those stained only with Syto-9). Syto-9 (1.5 μl.ml^{-1}) and PI (3 μl.ml^{-1}) were added to basal culture media. Samples were incubated in 1.5 ml staining media for 15 mins, before gentle rinsing with PBS prior to imaging. Although rinsing must ensure the removal of unbound dye, vigourous washing may remove dead cells from the samples and was avoided. False coloured images were produced where green denotes live cells and red dead cells.

Cell attachment in 2D and in scaffolds was investigated using phalloidin TRITC and DAPI. Phalloidin TRITC (Sigma P1951, 0.5 mg.ml $^{-1}$) is a fluorescently la-

belled molecule which binds to f-actin within cells. This allows imaging of the cell cytoskeleton when the sample is excited at 543 nm. DAPI ([4'-6-Diamidino-2-phenylindole], Sigma) is a fluorescent stain which binds to DNA and is used to image cell nuclei, helping to locate cells within the field of view. Samples were first fixed in 10% formalin for 20 minutes at room temperature. After washing 3 times with PBS, a 1% solution of Triton-X100 was added to samples for 5 minutes to permeabalise cell membranes. Samples were then washed 3 times with PBS and placed in 1.5 ml staining solution, consisting of a 1:5,000 dilution of Phalloidin TRITC and 1:10,000 dilution of DAPI in PBS. After incubating for 30 minutes, samples were washed thoroughly in PBS to remove excess stain solution. Samples were cut into sections to reveal the centre of the scaffold, allowing imaging of all regions of the scaffold. For imaging using the confocal microscope, samples were held under PBS on the bottom of 6 well plates using metal wire holders, using the mercury lamp to find regions of interest and avoid the possibility of laser reflections. Images were taken using a water dipping lens. For imaging with the Axon ImageXpress, samples were placed in 24 well plates in a small volume of PBS such that they remained on the bottom of the culture plate during imaging.

In order to follow the production of mineralised matrix by hES-MP cells, calcein was added to culture medium. Calcein is a chelating agent which can bind to metal ions, in this case the ions of interest were Ca^{2+} ions. The calcein is then incorporated into the hydroxyapatite matrix produced by osteoblasts during mineralisation. As the molecule binds to the matrix during mineralisation occurring when the molecule is present in the media, it may be used to show mineral deposited during a certain time frame. Fluorescence microscopy may then be used to visualise the sites of mineral deposition throughout culture. Excitation occurs at 543 nm, and the emission occurs at 509 nm. Calcein (Sigma 21030)

was dissolved in dH_2O to produce stock concentrations of 20 mM. Stock solutions were filter sterilised to make them suitable for cell culture. A variety of working conditions were tested and are described later in the experiment detail.

As well as using calcein to identify the deposited calcium ions within the matrix produced, a collagen I antibody (COL1) was used after fixation to allow imaging of the organic matrix component. The antibody (Sigma C2456.2ML) is a monoclonal anti-Collagen I antibody, produced in mice. Samples for staining with the antibody were fixed in 2.5% glutaraldehyde in PBS for 10 minutes before washing throughly with PBS. Samples were then blocked in 5% powdered milk in PBS for one hour before further washing. Primary antibody was added at a dilution of 1:1000 in 1% milk, in enough volume to ensure complete coverage of the sample. Samples were kept in the solution at 4°C overnight. The following day, samples were washed several times with PBS before the addition of a biotinylated anti-mouse secondary antibody (1:1000 in 1% milk in PBS). Samples were maintained in the solution for one hour at room temperature before thorough washing. Streptavidin conjugated texas red was then added to samples for 30 minutes (1:100 in 1% milk). Four PBS washes of 5 minutes each were carried out and the first wash contained DAPI at a dilution of 1:1000. Samples were stored in PBS in foil covered well plates at 4°C prior to imaging, which was carried out no more than 24 hours after staining.

2.7 Alkaline Phosphatase Activity

Alkaline phosphatase (ALP) activity was used as a marker of osteoblastic differentiation (Hoemann et al. 2009; Hessle et al. 2002). The assay was performed after digestion of the cells to free the membrane components. The assay required cell assay buffer (CAB) (1.5 M Tris (pH adjusted to 9.0 with concentrated HCL),

1 mM $ZnCl_2$, 1 mM $MgCl_2$ in 500 ml dH_2O), cell digestion buffer (CDB) (1:10 dilution of CAB:dH_2O, including 1% Triton X-100) and ALP solution (Alkaline Phosphatase Yellow (pNPP) Liquid Substrate System for ELISA, Sigma). At the end of culture, usually after an MTS assay, samples were rinsed thoroughly with PBS and 200 μl CDB added per well (12 well plate). In 3D experiments, scaffolds were cut into small pieces and placed into 500 μl eppendorf tubes. 300 μl CDB was added per scaffold and mixed thoroughly to digest cells. All samples were freeze thawed 3 times in order to improve the release of cellular material. This method was tested and did not cause significant changes in the ALP activity measured (data not shown), but is necessary for later steps to quantify total DNA.

The resulting solution was removed from the scaffolds or plates and transferred to new eppendorfs, to be stored at 4°C overnight if necessary. Samples were then incubated for 30 mins at 37°C before mixing 20 μl of sample with 180 μl ALP solution (or 10 μl and 190 μl for longer timepoint samples) in a 96 well plate. Optical density was measured at 410 nm using an absorbance spectrophotometer, programmed to take a reading once every minute for 30 minutes. ALP activity was expressed as nmol p-nitrophenol present at each time point according to equation 2.1. This allowed calculation of the rate of activity of ALP within each sample by plotting a graph of ALP activity with time and calculating the gradient of the linear region. This was expressed as the nmol p-nitrophenol converted per minute (nmol p-nitrophenol min^{-1}). Note that VSample is 10 or 20 μl, as it is the final volume of sample present in the solution used for the measurement of absorbance. VTotal is the volume of CDB used initially to collect the sample. A_{410} is the absorbance of the sample measured at 410 nm (equation 2.2). The value of κ was calculated from a standard curve produced by another PhD student within the laboratory group. The standard curve was produced by

measuring absorbance of different concentrations of p-nitrophenol in PBS in the same absorbance spectrophotometer used in experiments.

$$\frac{A_{410} \times \kappa}{V_{Sample}} \times V_{Total} \tag{2.1}$$

$$1A_{410} = 22.5nMofproduct(\kappa) \tag{2.2}$$

2.8 Determination of Cell Number

In order to determine cell number within samples, a Quant-It PicoGreen (PG) DNA assay (Invitrogen P7589) was performed on the cell lysate obtained for ALP assays. A calibration curve was produced using both calf thymus DNA (Invitrogen 15633-19) at known concentrations and the lambda standard included in the kit. This allowed the calculation of the total amount of DNA present within cell lysate samples. Samples were taken from the lysate produced for the ALP assay after the freeze thaw process. 100 μl of sample was mixed with 200 μl of freshly diluted 1x sample buffer containing 5 μl PicoGreen per 2 ml sample buffer. Samples were vortexed briefly before transferring duplicate 100 μl samples to a 96 well plate. Fluorescence was measured immediately using a fluorescence spectrometer (485 nm excitation with 528 nm emission). The concentration of DNA in the sample can then be calculated using equation 2.3, allowing the total DNA present in the cell lysate to be calculated.

$$Concentration(ng.ml^{-1}) = 0.1367 \times Fluorescence \tag{2.3}$$

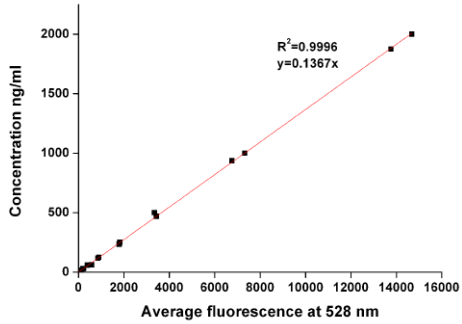

Figure 2.4: PicoGreen standard curve for DNA quantification. Uses data from the assay kit standard and calf thymus DNA.

2.9 Statistical Analysis

Graphs are shown as mean ± standard deviation. Two-way ANOVA analyses were performed using Graphpad Prism 5.04 (GraphPad Software, Inc.) with post hoc testing (Bonferroni). * is used in graphs to denote significant values ($p < 0.05$). Significance of the differences in ALP activity between samples cultured in ab or abd supplemented media were tested during one experiment (figure 4.7), but were not included every time to reduce complexity of the statistical analysis. ImageJ software was used for nucleus counting (ImageJ Nucleus Counter plugin) and removal of background in scaffold images taken on the Axon ImageExpress.

Chapter 3

Cell Attachment in 3D

3.1 Introduction

As discussed in the introduction, there is growing interest in the routine use of 3D culture of cells. The use of a synthetic scaffold to provide spatial organisation of cells and allow the application of mechanical load is one method for creating a 3D environment. This chapter studies the attachment of several cells lines to a synthetic foam scaffold through metabolic assays and confocal microscopy.

3.2 Scaffold Pre-treatment and Cellular Behaviour

Initial cell culture involved the development of suitable culture methods for 3D work in open cell polyurethane (PU) foam scaffolds. These scaffolds were to be used for 3D experiments investigating mechanical stimulation of the hES-MP cell line towards osteogenesis. The foam was chosen due to its mechanical properties making it suitable for the repeated application of mechanical load, as well as its porosity (150-1000 μm, average approximately 400 μm), which is in the range

thought suitable for cell growth and migration. In an open pore foam scaffold, it is useful to understand how the cells are attached to the surface. Cells may spread along the surface of the material, stretch across the pores, or clump together, forming loose attachments to the scaffold (Reilly and Engler 2010). The degree to which the cells form close attachments with the scaffold may be important in understanding how the cells respond to scaffold deformation and fluid movement. In order to investigate cell attachment in the scaffolds, several pre-treatment methods and cell types were used. Different imaging methods were used to study the cells within the scaffolds.

Foam sections 10 mm high and 10 mm in diameter were sterilised in 70% ethanol overnight, or by autoclaving in phosphate buffered saline (PBS). Scaffolds were pretreated by soaking for 3 hours in either PBS, normal culture media, foetal calf serum (FCS) or fibronectin. Fibronectin is known to promote cell attachment via the R-G-D peptide sequence and can be used to ensure cell adhesion to tissue culture plates. Most cell culture media is supplemented with FCS or FBS (foetal bovine serum), as these contain growth factors and nutrients necessary for cell survival. Some of these compounds can adsorb to the scaffold during pretreatment, having a positive influence on cell growth and survival (Sawyer et al. 2005).

Cells were seeded into scaffolds held inside a stainless steel ring using a low volume of media (100 μm), as described in section 2.2. Samples were then cultured for 24, 48 or 72 hours in basal culture media, with some samples kept for 7 days. At the appropriate time point, samples were analysed by MTT or fixed for staining and microscopy. MTT was used to visualise the overall distribution of cells within the scaffolds and fluorescence microscopy to look at cell viability, shape and spreading. Specifically, live-dead staining with Syto-9 and PI was

used to look at the distribution of live and dead cells within the scaffolds. Later experiments involved f-actin and nuclei staining (using phalloidin TRITC and DAPI respectively) to look at the cell shape and spreading. Other experiments studied the collagen and mineral matrix components using fluorescent molecules.

Samples were cut after staining to allow imaging of the central regions of the scaffolds. The MG63 and hMPC 32F cell lines were used for initial testing and later the hES-MP cell line was used to see if progenitor cells responded differently to the treatments. Initial experiments with hES-MP cells studied 2D attachment of the cells with and without gelatin, while 3D work involved autoclaving the scaffolds in the gelatin solution.

3.2.1 Scaffold Pre-treatment and Metabolic Activity

An MTT assay was used to ensure that the method of seeding cells into the PU scaffolds was efficient and that the coatings tested could be used to improve initial cell attachment (figure 3.1). As the MTT product is insoluble, it provides information on the location of metabolically active cells.

MTT staining in the scaffolds over a period of 72 hours showed cells distributed within the scaffold throughout the culture period. The purple colouration indicates the number of metabolically active cells increased for all conditions over the culture period and cells appeared to be present throughout the inner regions of the scaffolds. The scaffolds pre-treated with media appear to contain higher cell numbers than the PBS treated scaffolds. Treatment with FCS prior to seeding appears to cause further increases in the metabolic activity within the scaffolds over the culture period. This suggests that the treatment of scaffolds with FCS prior to cell seeding may be a useful technique to improve the initial cell retention within the scaffold

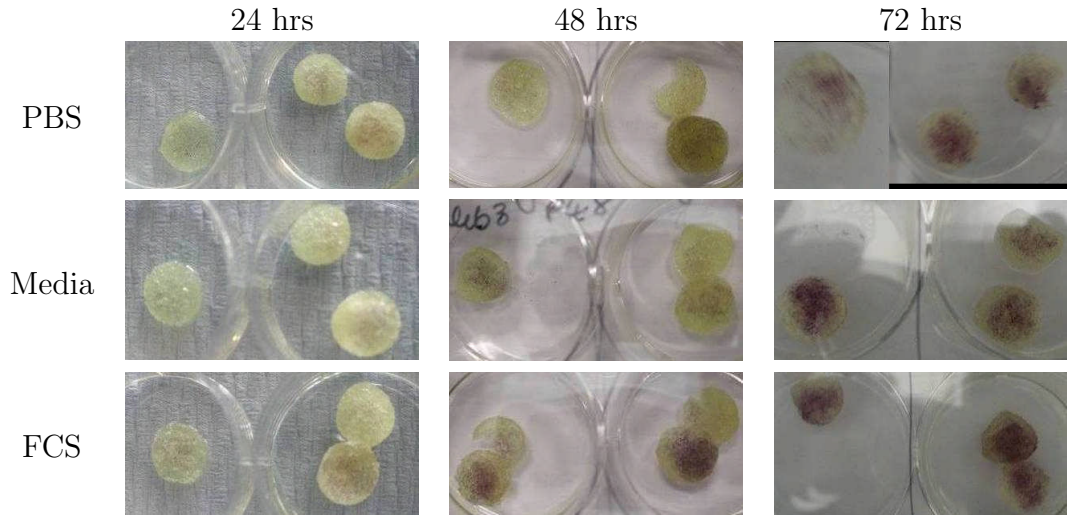

Figure 3.1: MTT staining in pre-treated 1 cm diameter, 1 cm high scaffolds cultured for 24, 48 or 72 hours. Purple colouration indicates metabolically active MG63 cells. Representative images shown.

for *in vitro* work.

3.2.2 Imaging of Live Cells on Pre-treated Scaffolds

After initial experiments with MTT, confocal microscopy was used to further investigate the viability of the cells within the scaffold. A live-dead assay was used to establish whether cells were evenly spread or clumped together and whether there were areas of dead cells present. Scaffolds were pre-treated with either PBS, culture media or FCS and cultured in basal culture media for 24, 48 or 72 hours as before. Scaffolds were sectioned and imaged after staining with Syto-9 and PI as described in the Materials and Methods chapter and the results are presented in figures 3.2 and 3.3.

The live-dead assay demonstrated that there were live cells present within scaffolds in each pre-treatment group. At 24 and 48 hours, it was noted to be much more difficult to locate cells within media and PBS treated scaffolds than

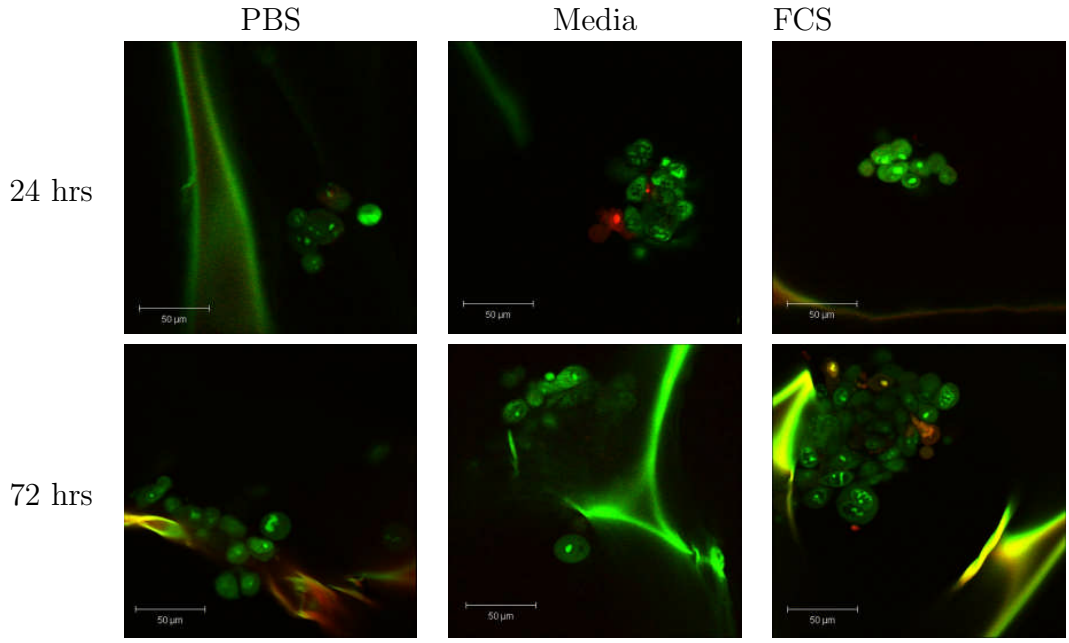

Figure 3.2: Scaffold pre-treatment with MG63 cells, live-dead staining. Confocal images showing live (green) and dead (red) stain of MG63 cells in PU scaffolds. Cells were found in small clumps around the scaffold rather than spread over the surface. Representative images shown, n=6. Scale bar shows 50 μm.

FCS treated. As the MTT showed fainter purple colouration within these scaffolds than the FCS treated, this suggests that the cells were failing to adhere to the scaffolds initially without the pre-treatment. There were also noted to be few cells stained with PI, suggesting that there were few dead cells present in the samples. Using Z-stacked images it could be seen that clumps of cells were forming within the scaffolds, which was especially noticeable for the FCS treatment (figure 3.3). While there were higher numbers of cells present within these samples, the number apparently increasing with time, cells appeared to be only loosely adhered to the scaffold, instead attaching preferentially to one another. It was also noted that the scaffold was visible during the imaging, especially for the samples excited at 488 nm. In some cases, this made it difficult to obtain clear images of the cells, as the background from the scaffolds was so high.

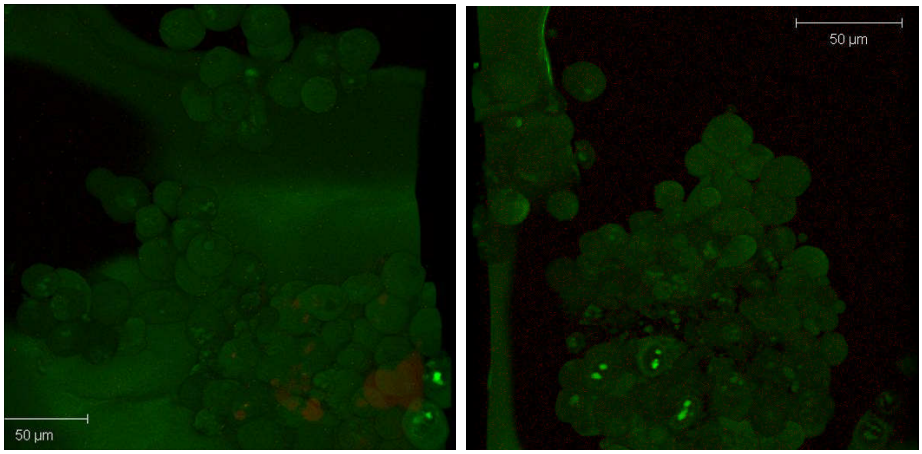

Figure 3.3: Z-stacked confocal images showing live-dead stain of MG63 cells after 48 hours culture. Images demonstrate the close association of cells to one another in clumps rather than spreading over the scaffold. Live cells appear green, dead cells would appear red if present. Representative images shown, scale bar 50 μm.

3.2.3 Scaffold Autofluorescence

The autofluorescence of the PU scaffold was further investigated due to its potential to interfere with fluorophores used to label cells. Cell-free scaffolds were imaged using lambda scan settings on the confocal microscope. The method allows the excitation of a sample and the emission to be measured at set wavelength intervals. In this case excitation occurred at 488, 543 and 633 nm and emission was measured at approximately 10 nm intervals above the excitation wavelength. Scaffold pre-treatments were used to rule out the possibility that it was a component of the culture media which contributed to this autofluorescence. The treatments were water, PBS, serum free media, media with 10% FCS and FCS alone, with results shown in figure 3.4.

These experiments showed that the scaffold had high levels of autofluorescence under excitation at 488 nm, with an emission peak around 590 nm. The position and intensity of this peak did not seem to be affected by the pre-treatments tested. This suggested that the use of labels which were excited at 543 nm would be more

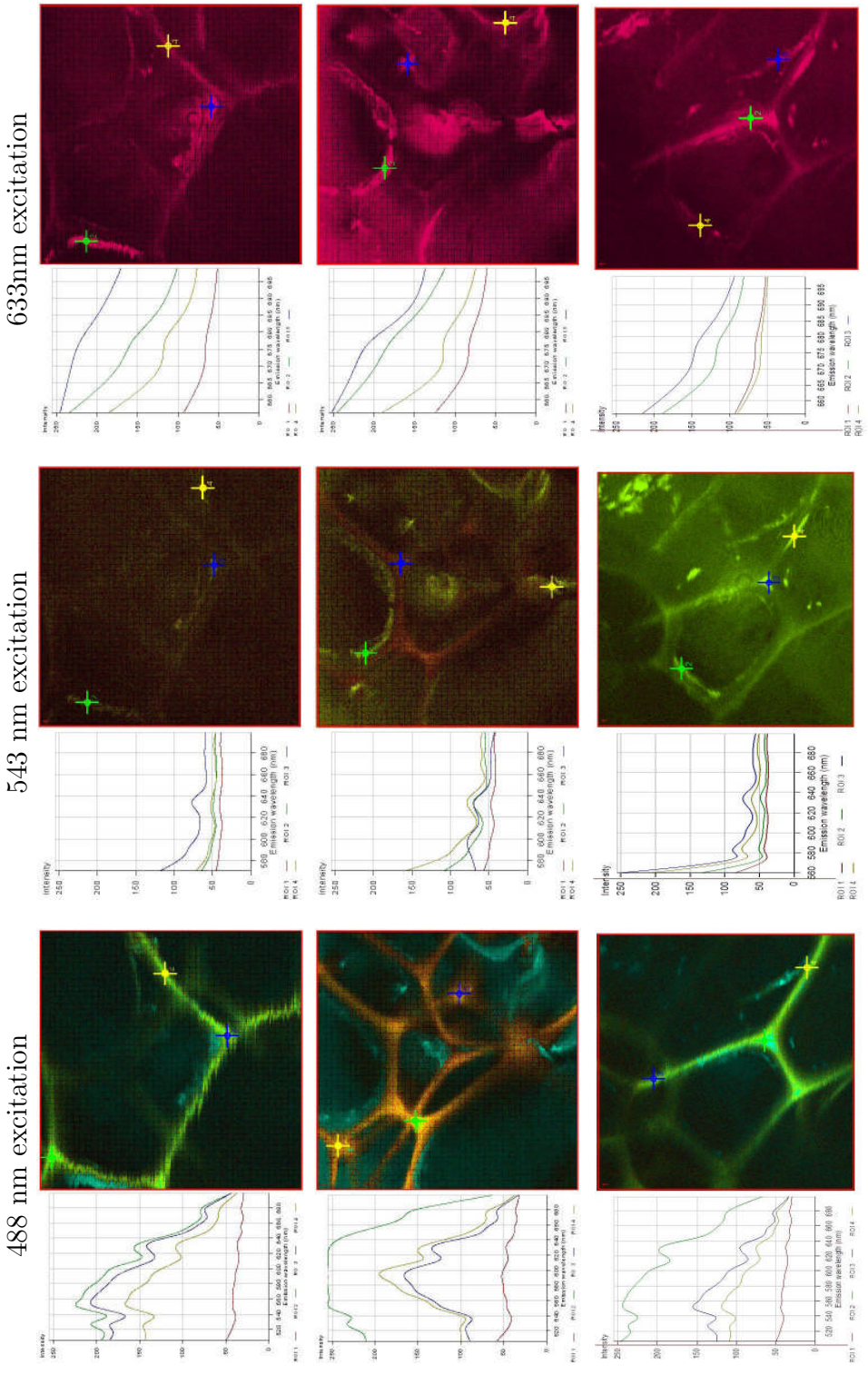

Figure 3.4: Fluorescence spectra for marked areas of polyurethane scaffold at different excitation and absorbance wavelengths following different pre-treatments.

suitable for experiments, allowing the cells to be imaged without interference from the scaffold. It would also allow imaging of the scaffold separately, showing the positioning of the cells in relation to the scaffold. As such, experiments to look at cell shape were conducted with a phalloidin TRITC (rhodamine-based) rather than FITC (fluorescein-based) conjugation.

3.2.4 Cell Shape Within Pre-treated Scaffolds During Early Culture

To further investigate the attachment of MG63 cells to the PU foams, the three day pre-treatment experiment was repeated with the addition of a fibronectin treatment. At each timepoint (24, 48 and 72 hours), samples were fixed in 10% formalin. These samples were then stained with DAPI and Phalloidin TRITC as described in the Materials and Methods chapter. Results of this staining are presented in figure 3.5.

Again, samples pre-treated with FCS showed better cell attachment than other conditions (figure 3.5). While this may not be important with cell lines that have high proliferative capacity (such as cancerous cell lines including MG63), this improved initial cell number is important in the use of primary cells. As primary cells show lower proliferation rates and must be kept at low passage numbers to maintain phenotype, it is important that as many of the cells as possible adhere quickly and securely to scaffolds. Fibronectin treatment did not appear to be as effective as FCS. Visualisation of the cytoskeleton confirmed that the cells formed clumps in preference to spreading over the scaffold surface.

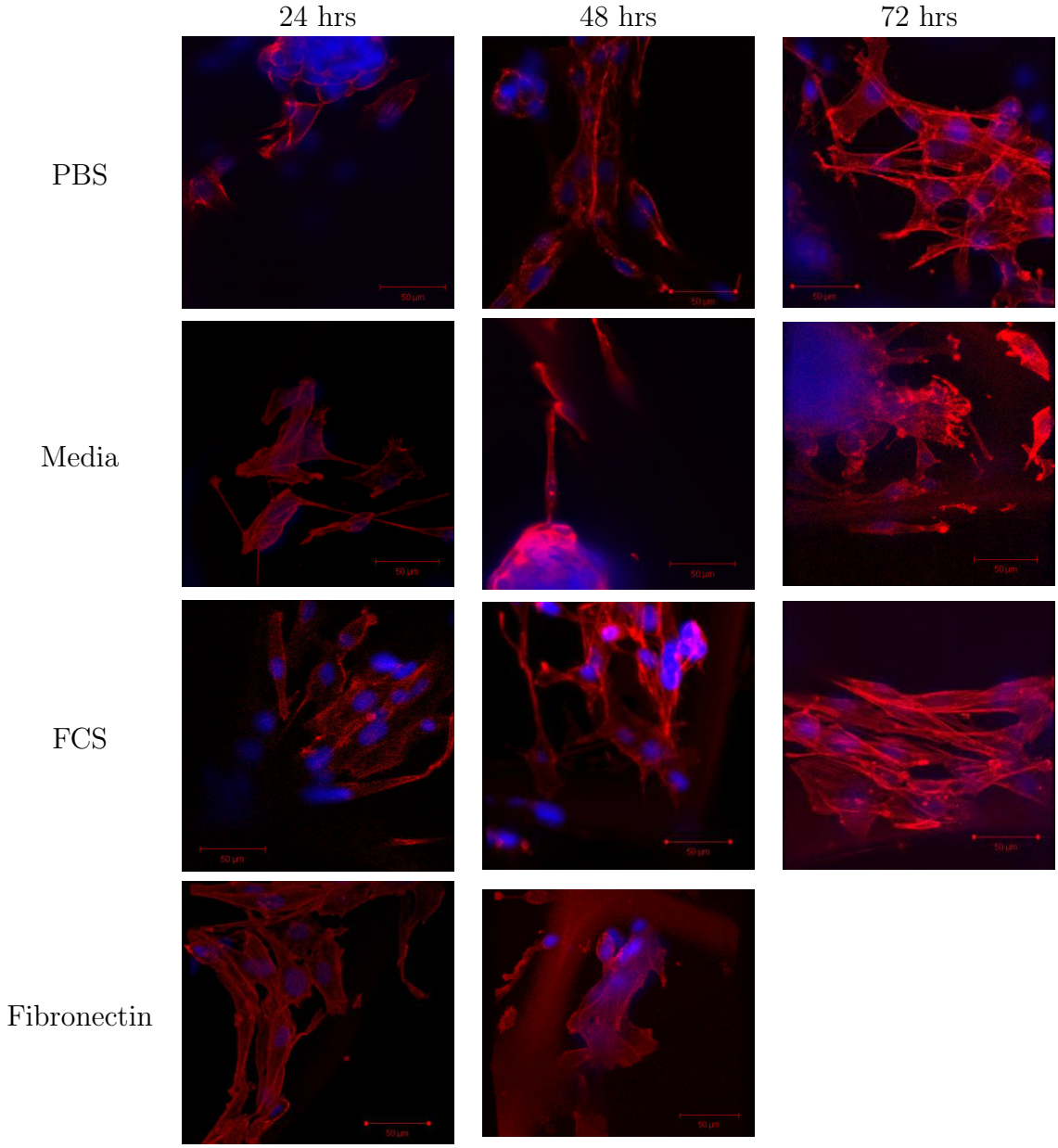

Figure 3.5: Confocal images showing f-actin staining of MG63 cells on pre-treated scaffolds. The actin cytoskeleton of cells is shown in red (Phalloidin TRITC) and the cell nuclei in blue (DAPI). Representative images, scale bar shows 50 μm.

Although MG63 cells are simple to maintain in culture and useful for *in vitro* work, constructs for use *in vivo* would require different cell types. Osteoblasts are difficult to extract from a patient and expand for re-implantation, and it is expected that mesenchymal progenitor cells may prove a useful alternative. These cells have been extracted from various sources (such as bone marrow and adipose tissue) and have the ability to undergo osteoblastic differentiation. As there is an interest in using these cells for clinically useful constructs, *in vitro* work using similar cells may provide more robust models for investigation into manipulation of cellular behaviour. Primary MSCs are expensive to obtain and show large variability between patients and some groups are focusing on the development of progenitor cell lines. The attachment of the hMPC 32F cell line (Osyczka et al. 2002) to the scaffold was tested with media and fibronectin pre-treatment alongside testing for the MG63 cells. FBS was not tested as the fibronectin was expected to perform better for the primary cells and these were available in lower numbers. Example images from this experiment are shown in figure 3.6.

While the hMPC 32F cells did remain within the scaffold, they did not show even attachment and were not spread across the scaffold surface. Further experiments in 2D with these cells were showing high variability in their proliferation rate and response to differentiation media (data not shown). This was thought to be due to the high passage number of the cell stock and an alternative cell line was sourced. The hES-MP 002.5 cell line (Cellartis) has been shown to display behaviour similar to mesenchymal precursor cells in culture up to passage 20. It also shows differentiation capabilities along the osteogenic, adipogenic and chondrogenic pathways (Karlsson et al. 2009). This cell line was tested for growth and osteogenic differentiation before being chosen for further experiments.

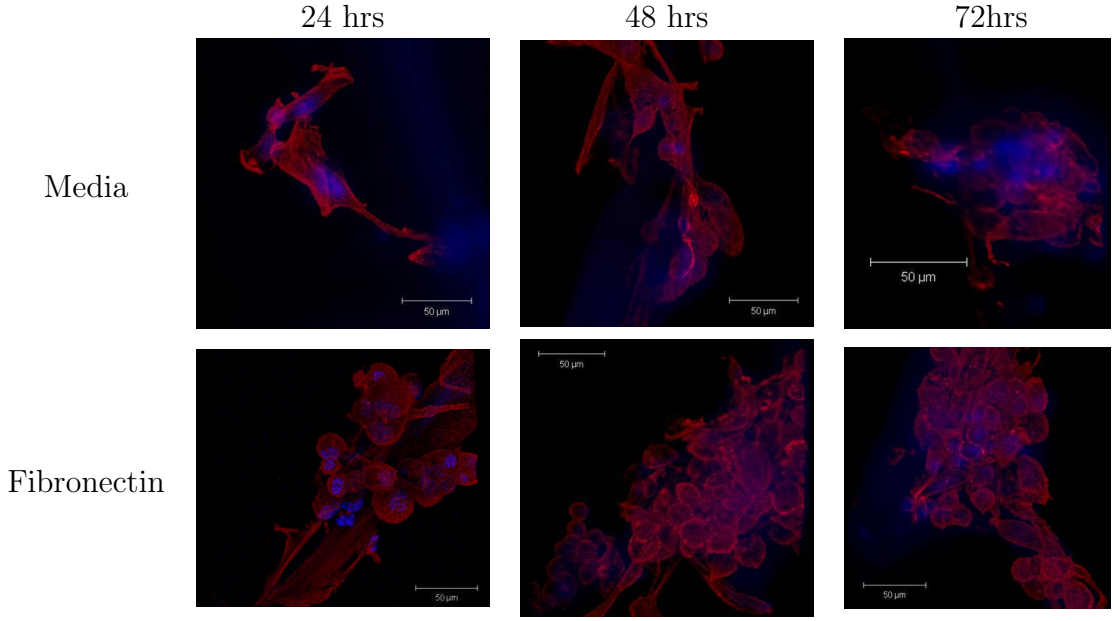

Figure 3.6: hMPC 32F cells on pre-treated PU scaffolds. Cells were not well spread over the scaffold surface. The actin cytoskeleton of cells is shown in red (Phalloidin TRITC), and the cell nuclei in blue (DAPI). Representative images, scale bar shows 50 μm.

3.2.5 Gelatin Coating Improves Cell Attachment and Spreading

Initial work in 2D with the hES-MP cell line was used to check the cell proliferation with and without gelatin, along with the capability for osteogenic differentiation. When the cell line was initially sourced, there was limited published data on its capabilities and culture. In order to establish their suitability for further work, the cells were tested in simple 2D experiments to ensure they could be differentiated towards osteogenesis under our laboratory conditions. The hES-MP cell line is cited as requiring the coating of tissue culture plates with gelatin to aid cell attachment. For this, a 0.1% solution of gelatin in dH_2O was prepared and sterilised by autoclaving. Well plates and T75 flasks were coated in the solution for 30 minutes prior to seeding cells on the surface. Cells were cultured in 12 well plates with 5,000 cells per well and maintained in ab or abd supplemented

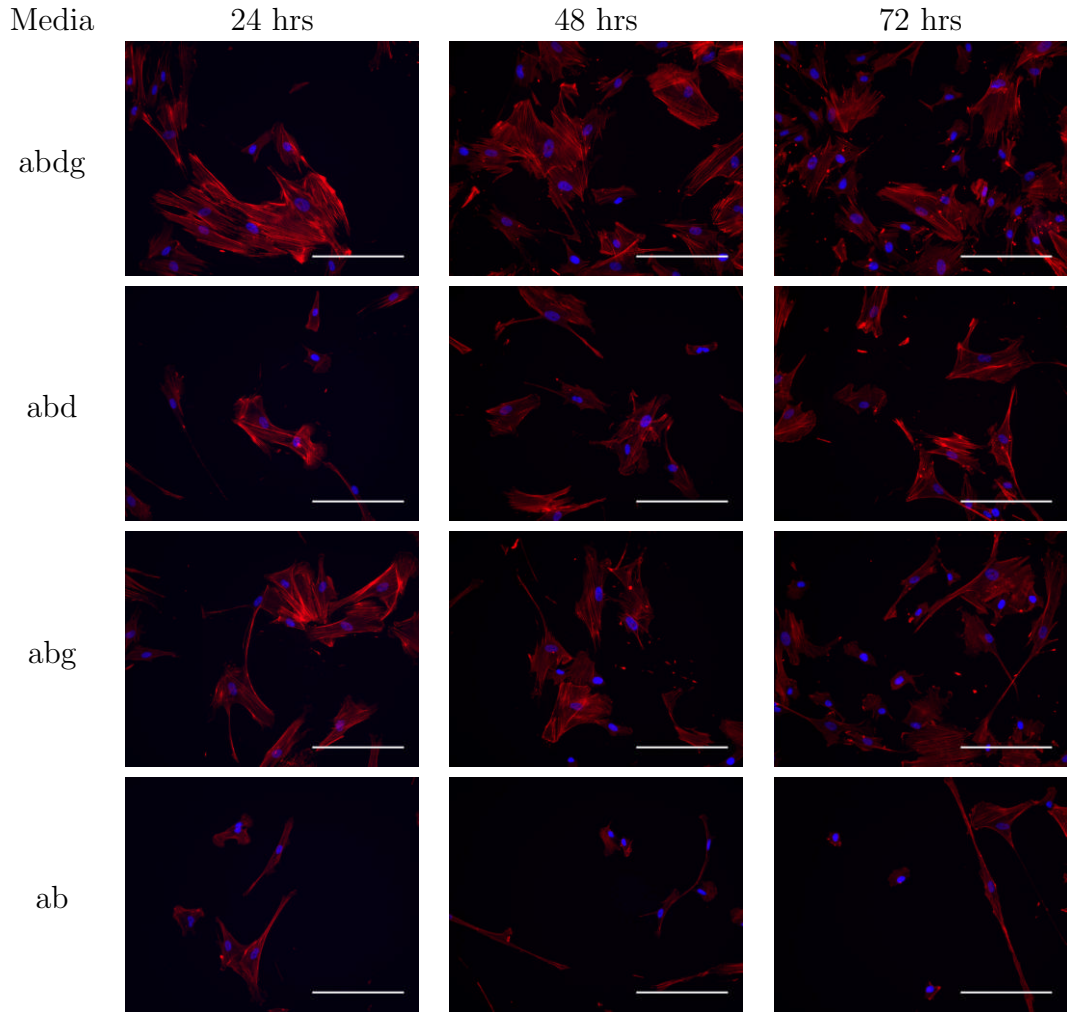

Figure 3.7: hES-MP 2D attachment over 72 hours. Images show the actin cytoskeleton in red (Phalloidin TRITC) and nuclei in blue (DAPI). The effects of gelatin coating and media type on the cells was investigated. Images are taken from the central portion of the well, representative of repeat experiments. Scale bar shows 200 μm.

media. After 24, 48 or 72 hours, cells were fixed in 10% formalin, before staining with DAPI and phalloidin TRITC as described previously. Images were obtained using the Axon ImageXpress (figure 3.7) and cell numbers estimated using ImageJ (figure 3.8).

To investigate the behaviour of hES-MP cells in gelatin coated PU foams, the previous 72 hr experiment was repeated in 3D using the foam scaffolds. As the

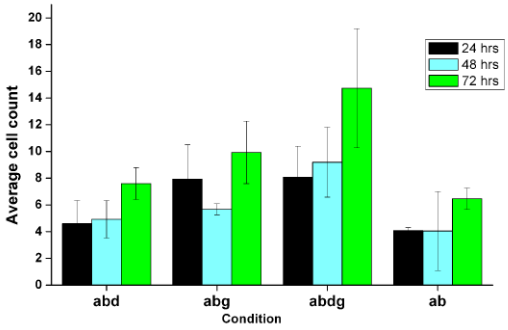

Figure 3.8: hES-MP 2D cell counts over 72 hours. Counts are averages from multiple points in multiple wells, in an area of 0.3mm^2.

gelatin solution has to be autoclaved prior to use, sections of PU foam were cut into required sized cylinders (10 mm diameter, 4 mm high) and placed in 0.1% gelatin solution. These were then autoclaved to sterilise the foams and allow the gelatin to coat the scaffolds. Scaffolds were then seeded with 2x10^5 cells and cultured for 24, 48 or 72 hours. Samples were transferred to ab or abd supplemented media after 24 hours. Samples were fixed in 10% formalin, stained with phalloidin TRITC and DAPI and imaged using the Axon ImageXpress. Images were obtained by moving to a random area of the scaffold and focusing through the sample until adherent cells could be clearly seen and examples are shown in figure 3.9. No images are shown for 24 hours as all scaffolds were maintained in basal media during this time so no comparison could be made.

In order to estimate the cell numbers in 3D, images were obtained from the same samples, using a different image acquisition technique. Random areas of scaffold were chosen as before, but images were captured in 50 μm increments through the scaffold. This gave large numbers of images quickly to obtain a more accurate estimate of cell number. Nuclei counts were performed for each image and the area which the cells occupied was estimated for each image. Cell counts are shown in figure 3.10.

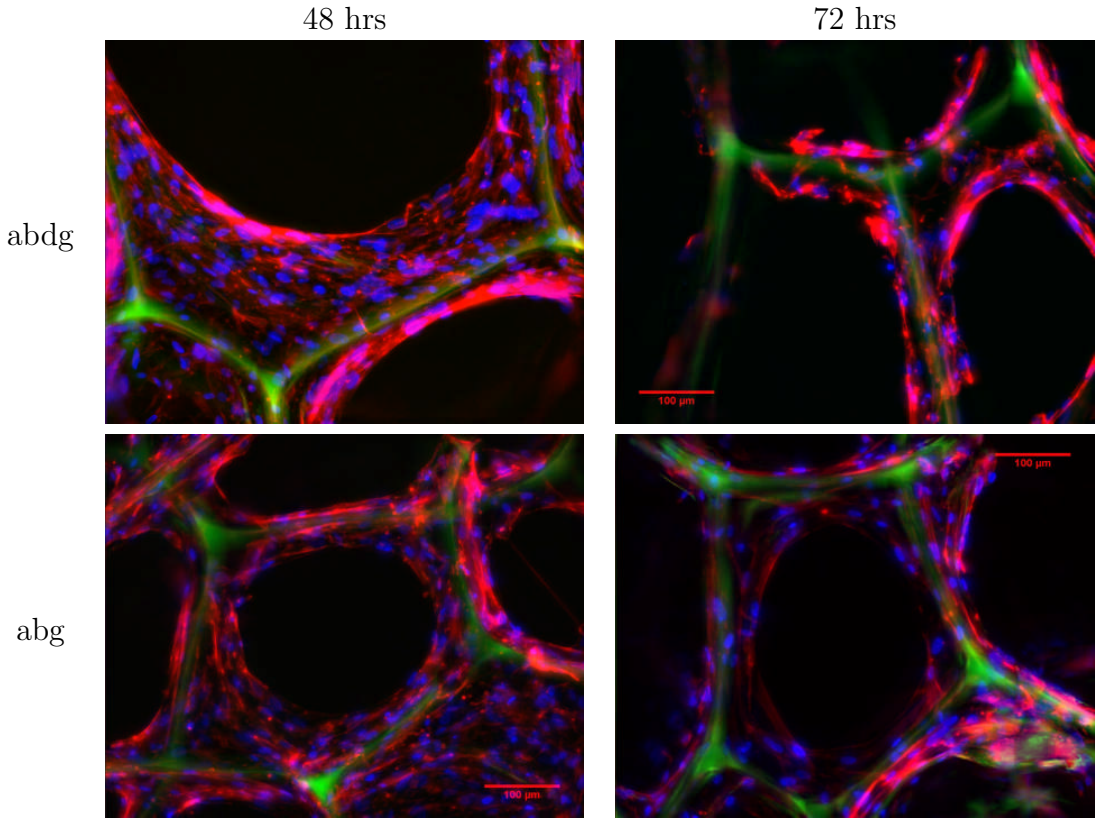

Figure 3.9: hES-MP 3D attachment over 72 hours. Images show the actin cytoskeleton in red (phalloidin TRITC) and nuclei in blue (DAPI). Cells can be seen spread over the surface of the scaffold (green) around scaffold pores. Images are representative projected z-stacks of repeat experiments, scale bar shows 100 μm.

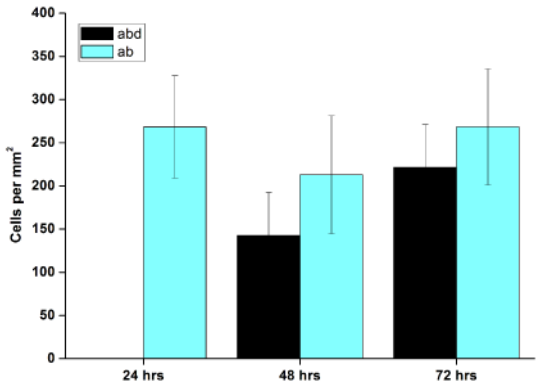

Figure 3.10: hES-MP 3D cell counts over 72 hours. Counts are averages from multiple points in multiple wells, given as cells per mm^2.

There were no significant differences in the number of cells found in either media formulation at 48 or 72 hours and the number of cells increased over this period. The high initial cell number may be to do with loss of loosely adhered cells from the scaffold during the initial culture period.

3.3 Monitoring of Matrix Mineralisation Using Calcein

During long term experiments to develop cell culture methods, it is necessary to monitor cellular behaviour during culture. Where the production of a properly formed matrix is the desired end product, it is advantageous to use methods which allow the monitoring of matrix development in samples over time. For bone matrix, mineralisation is an indication of a maturing ECM. While sirius red and alizarin red can be used to study the matrix produced at the end of experiments, the state of matrix mineralisation would be an interesting factor to monitor throughout culture.

Calcein is a calcium chelator, which has been shown to be incorporated into bone matrix if it is present during mineralisation of the collagen matrix (Judex et al. 2005; Castillo et al. 2006; Oxlund et al. 2003; Li et al. 2007). In order to test the use of calcein *in vitro* with osteogenically differentiated hES-MPs, calcein was added to the culture medium. Cells were cultured in abd media up to 3 weeks to allow the onset of mineralisation. On day 15, filter sterilised calcein in dH_2O was added to the media at working concentrations of 0.2, 0.1, 0.05 or 0.01 mM. These were estimated to be a suitable dose based on the use of calcein for labelling bone *in vivo*. Cells were cultured up to day 21 before fixation in 10% formalin and imaged using the Axon ImageExpress.

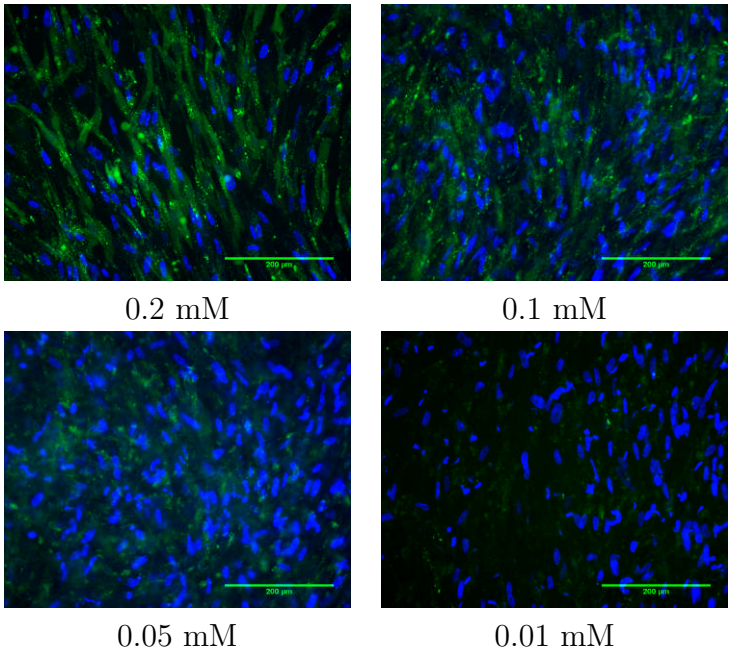

Figure 3.11: Calcein staining of hES-MP mineralised matrix in 2D. Calcein fluorescence was seen most clearly in the higher concentration conditions. Staining occurred in small nodules, consistent with the onset of mineralisation. Green shows calcein bound into the matrix, blue cell nuclei (DAPI). Representative of repeat experiments.

The calcein was visible around the cells in 2D and the form of the staining suggested mineralised nodules, consistent with early mineralisation. As the higher concentration gave good images and did not appear to affect cell behaviour, this was tested in 3D samples.

3.3.1 Calcein Staining of Mineralised Matrix in 3D

After testing the dose of calcein for matrix incorporation and imaging in 2D, further tests were carried out in 3D. 4 mm high PU foam scaffolds were sterilised in 0.1% gelatin and seeded with $2x10^5$ cells as described previously. Calcein was added to the media (0.2 mM working concentration) on day 15 and at every subsequent media change. On day 21 samples were incubated for 40 minutes in MTT solution to show the overall distribution of cells throughout the scaffold. After washing 3 times with PBS, samples were fixed in 2.5% glutaraldehyde. In

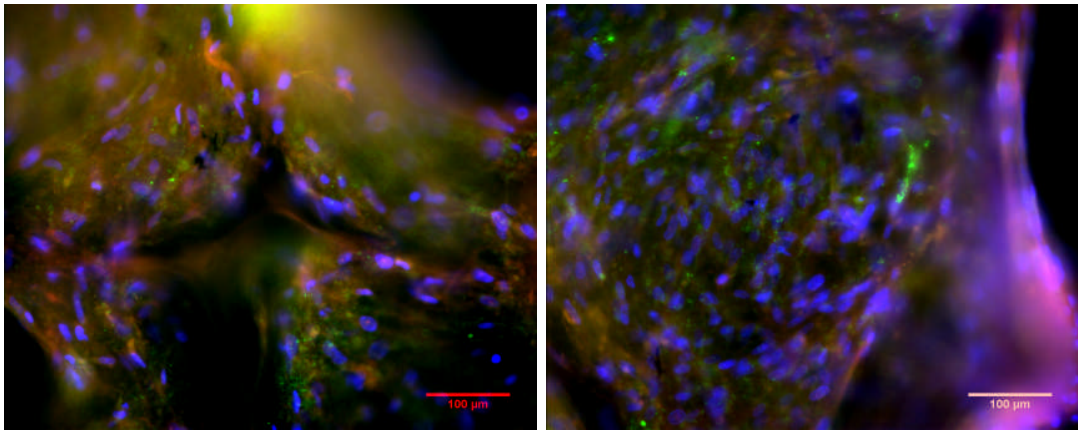

Figure 3.12: Calcein staining of hES-MP mineralised matrix in PU scaffolds. Cell nuclei are shown in blue(DAPI), deposited mineral in green (calcein) and collagen matrix in red (Texas red conjugated anti-collagen I antibody). Representative images, scale bar shows 100 μm.

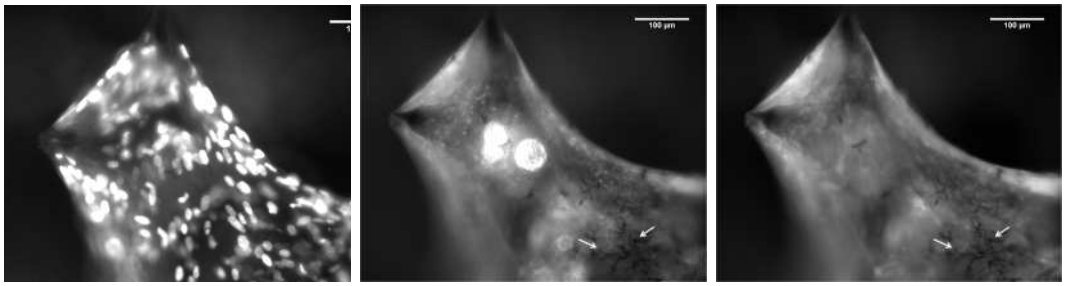

Figure 3.13: Fluorescence microscopy images showing MTT shadows. Images show cell nuclei (DAPI, left), calcein staining (centre) and collagen I (right). Representative images, scale bar shows 100 μm.

order to visualise the organic part of the deposited matrix, a collagen I antibody was used. Although this technique would be unsuitable for use throughout culture, it should provide more information about the matrix at the end point of an experiment. The full staining method is given in the Materials and Methods chapter and results are shown in figure 3.12.

It was noted during the imaging of scaffolds that there were dark, feather-shaped patches in some of the images. These were most noticeable on the images using excitation wavelengths of 480 nm, as seen in figure 3.13. The patches were suspected to be caused by the MTT still localised within the mitochondria of the

cells. As the calcein was still visible and comparable to that seen in the previous 2D experiment, the MTT was included in later experiments to provide data on overall cell distribution. While solubilisation of the MTT from within the cells could remove the patches, it had the potential to damage the structures of interest, causing much greater disturbance in the fluorescence images.

3.4 Discussion

Pre-treatment of scaffolds for cell culture is used to improve the attachment of cells to a surface which may not be ideal for cell adhesion, but which have mechanical properties suitable for the desired tissue. Increasing the number of cells which adhere to the scaffold initially is an important consideration in tissue engineering. The use of primary cells for patient therapies requires strong attachment to the scaffold, as these cells are in limited supply. Losing cells due to poor adherence would increase the proliferation needed to fill the scaffolds, which is a limiting factor when using primary cells to provide timely treatments.

During the live-dead staining of MG63 cells in the PU scaffold, it was noted that the cells seemed to form clumps, in close association with each other but not the scaffold (similar to the attachment noted by (Sittichockechaiwut et al. 2009)). This suggests that the scaffold surface is not ideal for cell adherence. Treatment with FCS appeared to improve the attachment: a higher number of cells is seen in the first few days of culture compared to non-treated controls. There were also very few dead cells found within the scaffolds over the first 3 days of culture. As these cells would likely be loosely adhered, it is possible that there were more present during culture, but that these have been removed during preparation for the staining.

Fibronectin did not appear to improve the cell spreading within the scaffolds for the MG63 of hMPC 32F cells. The R-G-D peptide sequence in fibronectin is known to enhance cell attachment and spreading of MSCs (Ogura et al. 2004; Dolatshahi-Pirouz et al. 2011), as well as promoting osteogenic differentiation of precursor cells (Wang et al. 2013; Moursi et al. 1996; Moursi et al. 1997). In mature osteoblasts, fibronectin is thought to be important in cell survival, as agonists lead to apoptosis (Globus et al. 1998). As cells produce bone like matrix, they will deposit fibronectin within where it may act as a signalling molecule for osteoblasts, osteocytes or precursor cells recruited during remodelling. As the MG63 cells are already differentiated, it is possible that the use of fibronectin coating would not drastically improve their attachment, but may have affected their longer term survival. It is surprising that the hMPC 32F cells did not show improvements in attachment on the scaffolds, but there were other problems noted with the behaviour of these cells in 2D differentiation experiments. They showed variable proliferation and mineralisation rates, a problem noted by several members of the group. As the hES-MP cell line was available at this time, the use of the hMPC cells was not continued. It is also possible that the fibronectin did not adhere to the scaffold in such a way that the R-G-D sequence was presented to cells consistently, which would have reduced its efficiency in improving cell attachment.

While increasing the cell number within the scaffold is one aim of the pre-treatments, it is also desirable that the cells are well spread within the structure. This will allow the efficient transmission of any mechanical conditioning applied via the scaffolds to all of the cells. If the cells are only partly attached, mechanical deformation of the scaffold is unlikely to provide a suitable stimulus. Only the cells with secure attachment to the scaffold would be subject to the full substrate

deformation, with the majority of cells experiencing no direct forces. While fluid flow may provide stimulus to these loosely adhered cells, it would likely lead to the detachment of such cells from the scaffold. This idea is presented in figure 3.14.

Cytoskeletal staining revealed that the cells still clumped together, rather than spreading over the scaffold surface for the FBS treatment. The use of gelatin coating with the hES-MP cells demonstrated much better coverage of the scaffold and a more even spreading of the cells. As gelatin is a mixture of denatured collagens, it is likely that this provides a more natural attachment substrate to the cells compared to FBS. It is also possible that the nature of the two cells types (osteoblastic lineage compared to undifferentiated or early differentiation states) causes a difference in the cell attachment.

For *in vitro* work, FCS may be an appropriate treatment of scaffolds prior to cell seeding, as it is easily available, low cost and is already routinely used in cell culture. It would be unsuitable for work which requires non-xenogenic components, such as constructs destined for clinical use. The natural variation between batches of FCS may also make the method unsuitable for a routine coating. Batch variation in serum would introduce variability into the cell attachment, much as it may do during cell culture. Another consideration is that, while the treatment with FCS offers some improvement in cell number, it is still evident that the cells are not spread evenly over the scaffold. As many treatments to improve this further may be more expensive and time consuming, initial work to look at mesenchymal progenitors was carried out with simple techniques.

Gelatin coating of well plates for the culture of the hES-MP cell line showed an improvement in the cell number compared to non treated plates over 72 hours. The

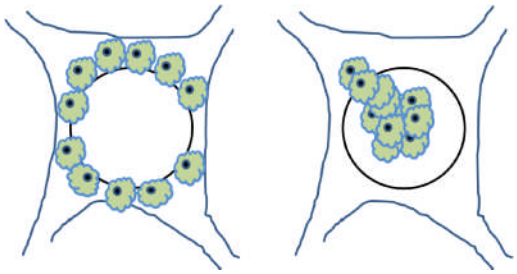

Cell attachment: spreading (left) vs clumping (right)

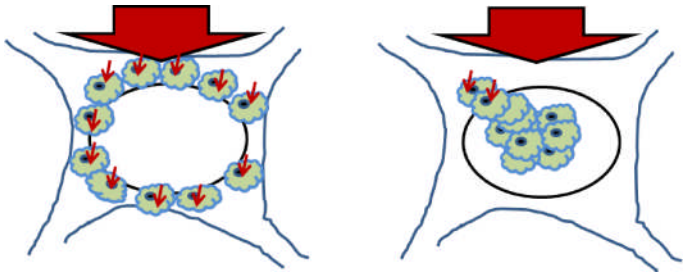

Scaffold under compression

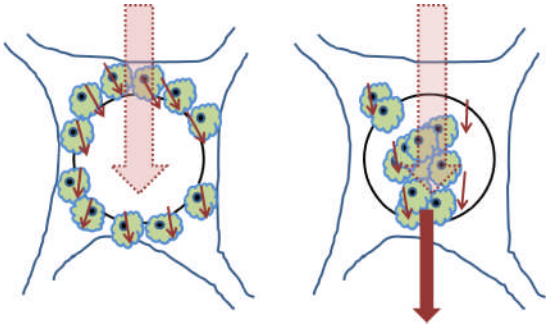

Fluid flow through scaffold

Figure 3.14: Stimulation of clumped cells within a porous scaffold. Diagram shows possible attachment of cells to scaffold. Large arrows from top of images show application of force. Smaller arrows denote cells which are likely to experience mechanical loading. During compression, most spread cells will be subject to some form of direct strain (the magnitude will depend on the orientation of the strut to which they are attached). For clumped cells, most cells will not be directly stimulated. For flow, spread cells will all receive some stimulation whereas clumped cells may detach from the scaffold, although outer cells of the clump will all be stimulated.

cells also appeared to be more spread on the plate surface, suggesting osteogenic rather than adiopogenic differentiation (Reilly and Engler 2010). For the gelatin coated PU scaffolds, the phalloidin staining showed that the cells had spread over the scaffold surface, forming layers around the pores. As this method of coating culture surfaces is cheap and simple, it is a useful method for improving the attachment of these cells over the initial culture period. While porcine gelatin would not be suitable for an animal free model, there are alternatives available which should show the same improvement. For example, there are several products available consisting of human collagen. It may be sourced from placenta, harvested from the ECM of cultured fibroblasts, or produced in bacteria (Sigma Aldritch catalogue). These products consist of different types of collagen, for example that produced by fibroblasts is described as containing mainly type I collagen with some type III. As gelatin is a mix of collagens produced by boiling animal skin, the use of human collagen as a coating is likely to produce similar results.

For the monitoring of mineralisation during culture, calcein was added to culture medium to test its use with osteogenic cells during culture. The technique was based on previous *in vivo* studies using a variety of calcium chelators to study the deposition of mineral in bone over time (O'Brien et al. 2002). While the technique was successful, showing mineralisation in differentiated cells with time, it did not provide information about the cells or the organic component of the matrix. Combining this with collagen I and nuclear staining at the end of culture allows visualisation of both the organic and inorganic matrix components. Relative locations of collagen deposition and mineralisation can then been seen with fluorescence microscopy. These stains for organic matrix components cannot be used during culture, as the techniques used are unsuitable for use with live cells. DAPI binds to DNA and inhibits normal cellular function and division

and phalloidin is produced from a potent toxin, binding to and preventing rearrangement of the cytoskeleton which is necessary for normal cellular function. Additionally, to allow phalloidin to enter the cells the cell membranes must first be permeabalised, which would cause cell death. As a result, this technique was employed only at the end of culture.

The repeated imaging of samples over a culture period may allow the monitoring of the onset and progression of mineral deposition, but it has several drawbacks. The primary problem was the extra manipulation required for samples to be imaged with the equipment available at the time. Increased amounts of manipulation increase the risk of infection, as well as disturbances to the cells via deformation of the scaffold. Samples could not be imaged on the confocal as the set up did not allow the samples to be maintained in sterile environment due to the use of a water dipping lens. While the Axon ImageExpress allowed the samples to be kept sterile while imaging it was also not ideal. Scaffolds had to be transferred to new plates for imaging and could move within the well, causing difficulties in obtaining images. The scaffolds were also kept out of the incubator for periods of time, disrupting the normal culture conditions (later work in Chapter 4 discusses this in more detail). The technique could still prove useful for studying bone matrix deposition throughout culture by osteogenic cells *in vitro* if suitable microscopy facilities and culture vessels are available.

It is also possible to apply agents with different fluorescence characteristics to the cells at different timepoints (such as calcein and xylenol orange) (Lee et al. 2000; O'Brien et al. 2002). This could be used to study the deposition occurring during specific periods in culture. This would allow more indepth studies of the effects of mechanical stimulation at different timepoints on osteogenesis as alter-

nating layers of different fluorescent molecules are built up within the mineralised matrix. It is possible that the incorporation of these molecules into the matrix will have an effect on the matrix structure. The molecules may alter the deposition pattern of the mineral in the bone matrix, causing structural problems. There is a long history of the use of these molecules *in vivo* however, with no noted structural problems, suggesting that the matrix is not disrupted in a detrimental fashion.

3.5 Chapter Summary

This chapter investigated the attachment of a variety of cell types to an open cell polyurethane foam scaffold. Several staining techniques were used to study different properties of the constructs. The work in this chapter has:

- Demonstrated the attachment and proliferation of hES-MP cells within an open cell polyurethane scaffold.
- Shown that pre-coating of scaffolds with a 0.1% gelatin solution promotes attachment and cell spreading.
- Used fluorescence microscopy to study the cells within the scaffolds.
- Optimised the use of calcein in the culture media to allow visualisation of mineral deposition by the cells.

Chapter 4 studies the mechanical stimulation of the hES-MP cells with the aim of causing their osteogenic differentiation. A number of stimulation regimens are used, considering early differentiation markers and the deposition and mineralisation of their extracellular matrix.

Chapter 4

Low Magnitude, High Frequency Vibration and the Differentiation of the hES-MP Cell Line

4.1 Introduction

While the application of mechanical compression to individual scaffolds can be used to improve the matrix produced by the cells, it has several limitations. With the Bose system, there is a limited diameter of scaffold which can fit between the platens to ensure the whole scaffold is compressed. While this could be improved by the addition of an extra fitting within the biodynamic chamber, the number of samples which can be maintained is still limited. The shape of the scaffold is also important in this setup, as in order to allow the application of a uniform force across the scaffold, the two opposite faces of the scaffold must be parallel. While this is acceptable in the case of standard laboratory experiments, it is not ideal for constructs which would be used to fill clinical defects. These defects are not likely to be uniform in shape and will vary for individual patients. Producing larger constructs which are later cut down to the required dimensions would be one solution, although this option may be wasteful, especially if the supply of cells is limited. The extra processing may also damage the construct or provide opportunities for the sterility of the construct to be compromised. It is therefore

desirable to try and develop stimulation techniques which are suitable for scaffolds of varying shape and size.

While there are many different, well explored techniques available for mechanical stimulation (see section 1.8 for further discussion), one that can be used with the Bose ELF3200 is that of vibration. The use of low magnitude, high frequency (LMHF) vibration and its effects on bone properties have been investigated *in vivo* in both human and animal models and examples are given in table 1.3. Research suggests that the technique may be used to improve the structure of bone in osteoporotic patients (Beck et al. 2006; Rubin et al. 2006). Applications of short periods of LMHF vibration for long term treatment *in vivo* have shown beneficial effects on trabecular thickness, as well as trabecular number and bone mineral density (Beck et al. 2006; Rubin et al. 2006; Andrews 2010). Clinical trials using LMHF vibration have been conducted in humans and animals (Rubin et al. 2002; Gusi et al. 2006; Rubin et al. 2001; Flieger et al. 1998), and research groups are investigating LMHF vibration as a method of *in vitro* stimulation to promote osteogenesis (Zhang et al. 2012; Suzuki et al. 2007; Lau et al. 2010). The response to LMHF vibration is poorly understood, and there is some debate over the efficacy of the stimulus and the mechanisms behind its effects (Andrews 2010). There are several possible cellular targets for this type of stimulation, including recruitment of or inducing differentiation in precursor cells, direct stimulation of osteoblasts or osteocytes, or the inhibition of osteoclast formation and activity. Studying the behaviour of cells subjected to this stimulation *in vitro* may provide clues as to the *in vivo* effects. It could also prove a useful tool for the stimulation of 3D constructs.

The first chapter looked at the attachment of a variety of cell types to a PU foam scaffold, shown previously to support the growth, differentiation and

matrix production of primary MSCs. This resulted in the choice of the hES-MP mesenchymal progenitor cell line for further experiments. This chapter concentrates on the investigation of mechanical stimulation of these cells in 2D via the application of LMHF vibrations.

4.2 Variability and Limitations with Mechanical Compression

Initial experiments using mechanical compression were performed using a protocol established previously within the group. The method used PU foams which were seeded with cells before exposing them to direct mechanical compression. Work on both human MSCs and a mouse osteoblastic cell line (MLO-A5) has shown that the technique could be used to improve matrix deposition and mineralisation by the cells (Sittichokechaiwut et al. 2010; Sittichockechaiwut et al. 2009). 5% cyclic mechanical strain at a frequency of 1 Hz was applied to each cell seeded foam for 2 hours on days 5, 10 and 15 of a 20 day culture period. The technique was limited in that it only allowed stimulation of a single scaffold at a time and required in a large volume of media. The dimensions of the scaffold used were also limited by the internal diameter of the platens inside the biodynamic chamber. Preliminary experiments during this poroject used MG63 cells and investigated whether the same number of compression cycles could be applied at a higher frequency to produce a similar increase in bone matrix. While this would still be limited to one sample per run, the run time would be significantly shorter, allowing more samples to be stimulated in one day. This should allow the production of larger numbers of samples for analysis by a wider range of methods.

Timepoint	Step	Details
Day 0	Seeding	Scaffolds seeded with $5x10^5$ cells
Day 1	Media	Transfer of scaffolds to new well plates with required culture media
Days 7,10,14,17	Stimulation	Compressive mechanical loading of scaffolds
Day 21	Endpoint	MTS assay before fixation of cells and staining of ECM (sirius red, alizarin red)

Table 4.1: Timepoints in 10 Hz vs paused compressive mechanical loading regimen. Media changed every 2-3 days as required.

Several regimens were tested to look at the collagen and calcium production within the scaffolds, as well as cell viability. In order to allow collagen and calcium staining, the metabolic activity was measured using MTS, where the formazan product is soluble. As this does not require solubilisation of the product, there is no disruption to the tissue matrix when quantifying the metabolic activity. The regimens tested were compression at 3 vs 30 Hz and 10 Hz vs 10 Hz with rest periods inserted. Details of the loading regimen are given in table 4.1. Rest periods during fluid flow have been shown to cause increased responses to the stimulus *in vitro* (Batra et al. 2005) and may also have an effect during compressive loading. For these rest periods, the total loading time was the same as for the 10 Hz samples (12 minutes) but after a single compression (0.1 s) the loading was paused for 9.9 s. For both the 3 vs 30 Hz and 10 Hz vs 10 Hz paused experiments there were no differences in metabolic activity or collagen production compared to the static controls for any compression regimen (3 vs 30 Hz - preliminary data not shown, 10 Hz vs 10 Hz paused data shown in figure 4.1). Alizarin red staining was also used to investigate calcium levels but the stain eluted was below the detection limit of the spectrometer.

The variety of compressive loading regimens tested did not produce any significant differences between loaded and non-loaded samples. Due to the low

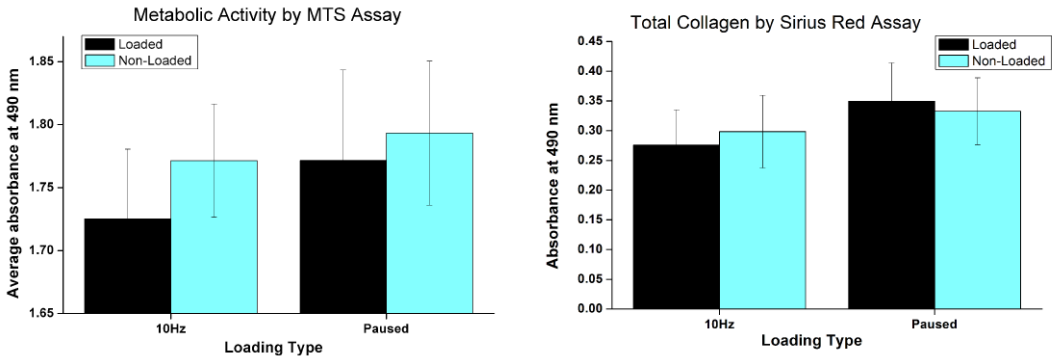

Figure 4.1: Mechanical compression experiments, 10 Hz vs paused data. Results showed high variability and no significant effect of mechanical compression on cell viability or matrix mineralisation. Mean ± standard deviation, n=12 over 3 experiments.

sample number produced via this method of stimulation and the high risk of infection of samples, I decided to use a completely different method of stimulation - that of low magnitude, high frequency (LMHF) vibration. Results and discussion for this investigation comprise the remainder of this chapter and data is later summarised in tables 4.6 to 4.11.

4.3 10 Minutes Low Magnitude, High Frequency Vibration

Initial experiments with LMHF vibration stimulation used short term (10 minute) bouts of loading on day 6 of culture of cells in 2D. 12 well plates were pre-coated with 0.1% autoclaved gelatin solution for 30 mins prior to cell seeding. hES-MP 002.5 cells were used and cultured in ab or abd supplemented media (see tables 2.1 and 2.2 for media additives and formulations). The loading was applied using a Bose Electroforce 3200, with a vertical displacement of ±0.05 mm. The cycle number was adjusted to give 10 minutes of stimulation at each of the frequencies used (15, 30, 45 and 60 Hz). Samples were assayed 24 or 48 hours after stimulation to investigate the osteogenic differentiation of the cells; table

Timepoint	Step	Details
Day 0	Seeding	hES-MP cells seeded in 12 well plates
Day 6	Vibration	Plates vibrated at specific frequencies for 45 minutes each day
Day 6	Media	Final media change (ab or abd media)
Day 7	Endpoint 1	MTS* assay on samples before collection of cell lysate for ALP activity and DNA quantification
Day 8	Endpoint 2	MTS* assay on samples before collection of cell lysate for ALP activity and DNA quantification

Table 4.2: hES-MP vibration regimen over 8 days, detailing two different collection times. Media changed every 2-3 days as required. Where both endpoints were used, half of samples were collected on day 7 and the rest on day 8. Later experiments used only endpoint 2. *MTS assay where used in experiment.

4.2 gives details of the vibration regimen timepoints. ALP assays, along with estimation of DNA quantity using PicoGreen were used as the assessment methods.

Analysis of the displacement measurements taken by the BOSE showed that these initial experiments did not maintain constant amplitude variations across the frequencies. The maximum amplitude was seen to decrease with increasing frequency. Further analysis showed that this was due to machine compensation to create a constant acceleration across the conditions. This was calculated to be $0.03g$ (where g is the acceleration due to gravity). It is possible to switch amplitude control on, causing the Bose to keep the same maximum amplitude for the different frequencies. Example vibration traces for 60 Hz are shown in figure 4.2. Later experiments compared the effects of constant acceleration with constant amplitude. The results of the experiments using 10 minutes LMHF vibration at $0.03g$ are presented in figure 4.3.

The application of LMHF vibration for a short period (10 minutes) had few noticeable effects on the ALP activity or DNA content of samples. The one significant effect was a small reduction in ALP activity by total DNA for cells

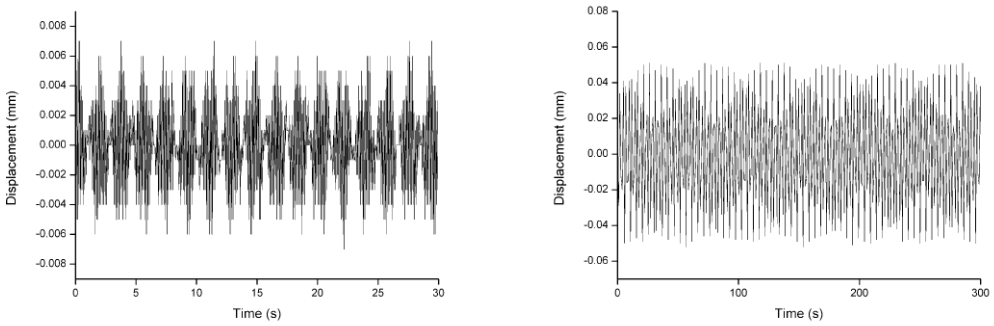

Figure 4.2: Example vibration traces for 60 Hz LMHF vibration. Left shows trace from constant acceleration vibration (amplitude is reduced and the acceleration is the same as other conditions), right from constant amplitude vibration. Graphs show peak-to-peak displacement, but sampling frequency was too slow give accurate representation of individual sine wave sections.

cultured in abd media (30 Hz, collection 48 hours after vibration, figure 4.3). Further investigation looked at whether a longer bout of vibration was necessary to elicit a response. The experiment was repeated using 45 minutes of vibration for the different conditions.

4.4 45 Minutes of LMHF Vibration Increases ALP Activity

Experiments were conducted to assess the effects of LMHF vibration on the hES-MP cells with a 45 minute stimulation period. These experiments used the timepoints described in table 4.2, using the same vibration frequencies and constant acceleration for the longer time period. Results for the longer stimulation period are presented in figure 4.4.

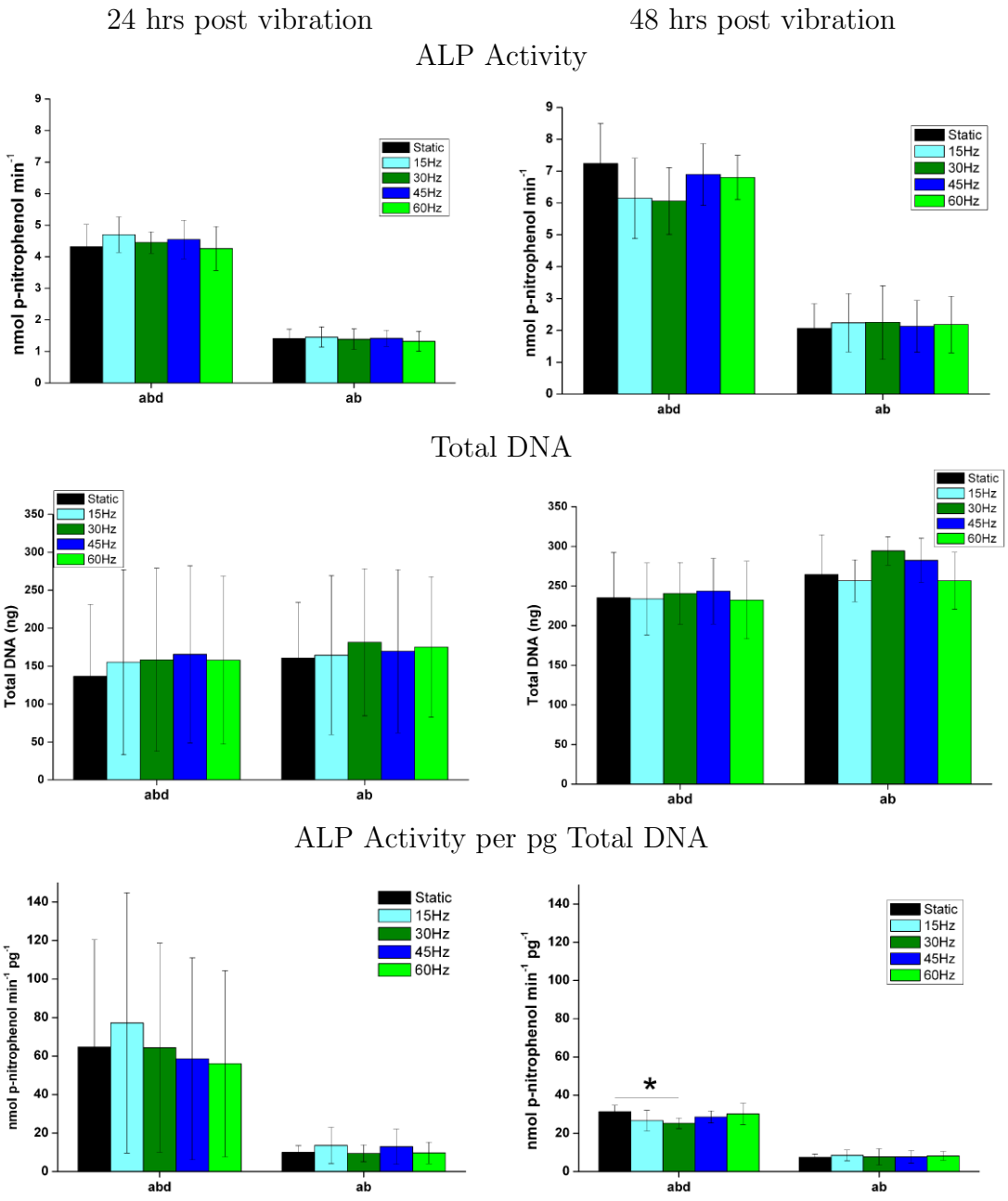

Figure 4.3: 10 minutes LMHF vibration of hES-MP cells in 2D. Times given are those between vibration and collection of cell lysate. A single significant effect occurred for ALP:DNA in abd media ($p < 0.05$). Mean ± standard deviation, n=12 over 3 experiments.

After application of 45 minutes of vibration to the hES-MP cells, a trend of decreasing total DNA and increasing ALP:DNA was seen. This was significant under some conditions and clearest for samples grown in abd media. For all samples grown in this media there was significantly higher ALP activity of vibrated samples compared with static controls. There were also significant changes in the total DNA content for some conditions. The higher ALP activity alongside a reduced amounts of DNA suggests that the stimulus has pushed the cells towards osteogenic differentiation and slowed their proliferation. It is also possible that the stimulus caused some of the cells to lift off the plate shortly after vibration. In order to test these hypotheses, further experiments were conducted where cells were fixed and stained shortly after vibration to look at cell detachment. Longer term experiments investigating matrix composition and LMHF vibration were then conducted.

4.5 LMHF Vibration and Cell Morphology

As a reduction in DNA content (and therefore cell number) was noted for vibrated cells in the previous section, fluorescence microscopy was used to investigate this effect further. The lower cell numbers may be due to changes in the behaviour of the cells (reduced proliferation), or to the peeling off of cells caused by the applied forces. Cells were seeded into 12 well plates as before and cultured in ab or abd supplemented media. In order to reduce the number of samples, only static culture and 60 Hz vibration were compared. Samples were subjected to vibration on day 6 and fixed in 10% formalin 0 or 2 hours after vibration had ceased. Samples fixed after 2 hours were maintained under normal culture conditions in an incubator at 37°C until that time. Samples were then stained with phalloidin TRITC and DAPI as described in the Materials and Methods section. The Axon fluorescence

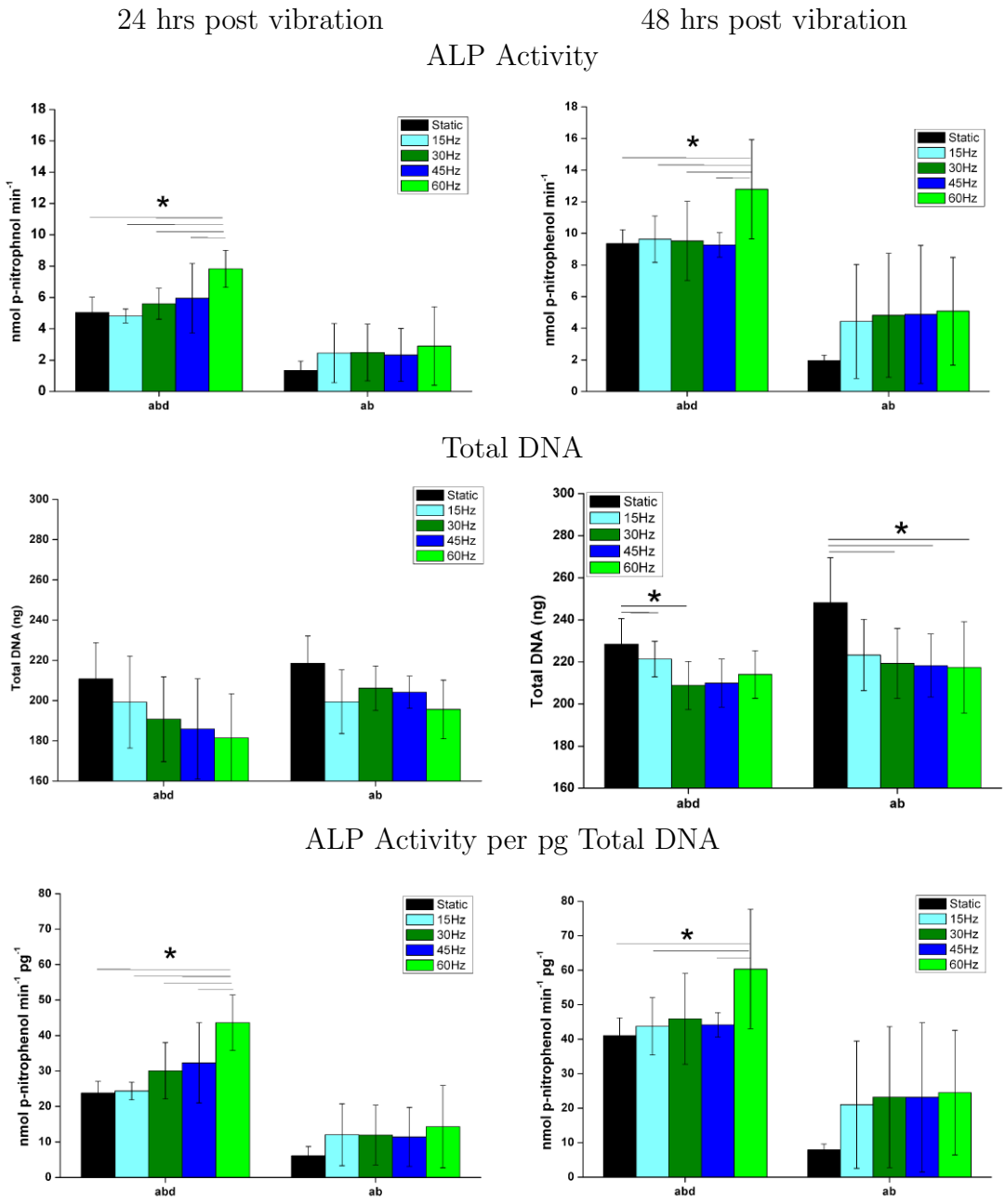

Figure 4.4: 45 minutes LMHF vibration of hES-MP cells in 2D. Times given are those between vibration and collection of cell lysate. At 48 hours, most vibrated samples showed a significant reduction ($p < 0.05$) in DNA compared with static controls. For both timepoints, 60 Hz gave significantly higher values for ALP activity (abd media, all other frequencies) and ALP:DNA (abd media, all frequencies except 30 Hz at 48hrs) . Mean ± standard deviation, n=12 over 3 experiments.

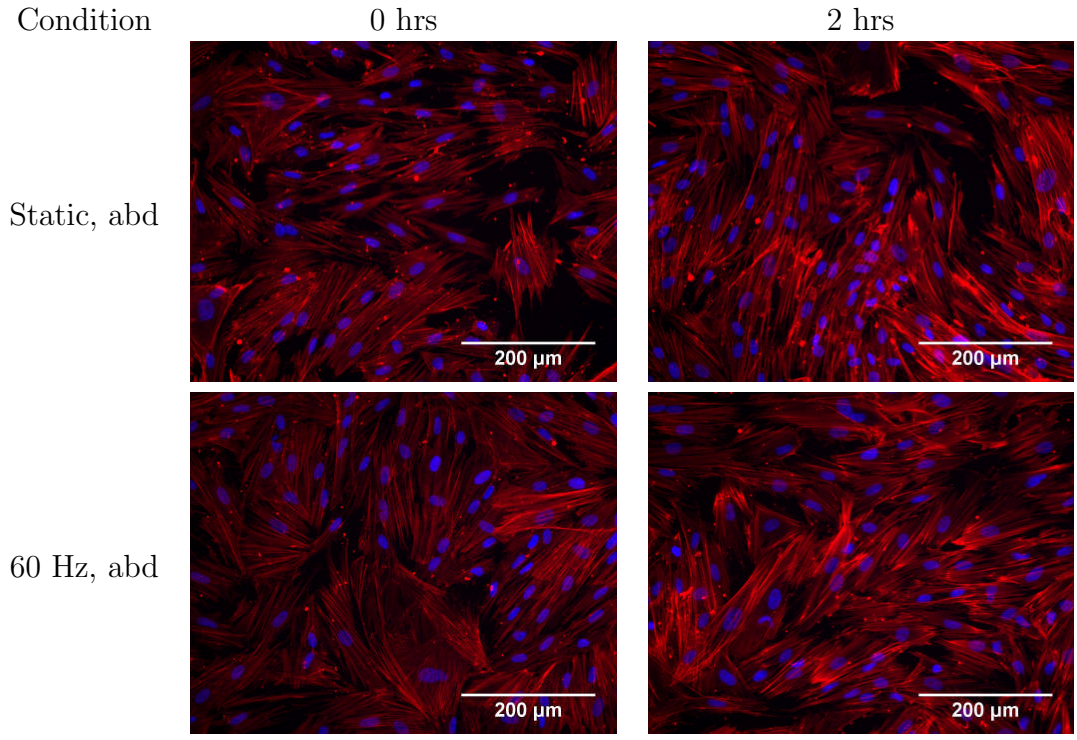

Figure 4.5: hES-MP f-actin staining, post vibration. Cells on gelatin coated well plates, pre and post vibration or static treatment. Images show cellular f-actin (red) and nuclei (blue) for samples in abd media. Vibrated and static samples show the same general morphology and cell number. Representative images, scale bars show 200 μm.

microscope was used to obtain multiple images from each well (at the centre and 4 points around the well) and representative images are shown in figure 4.5. Images shown are for cells in abd media only as in ab media there were higher cell numbers but neither media formulation showed differences between static or vibrated samples at either timepoint.

The cell number was quantified from the microscopy images using the ImageJ Nucleus Counter plugin and results for each time point are shown in figure 4.6. There were no significant changes in the number of cells on the plates between the cells which were vibrated and those kept in static conditions on the bench. The fluorescence microscopy showed no discernible effects on cell shape, suggesting that the vibration did not cause cells to detach from the culture plate.

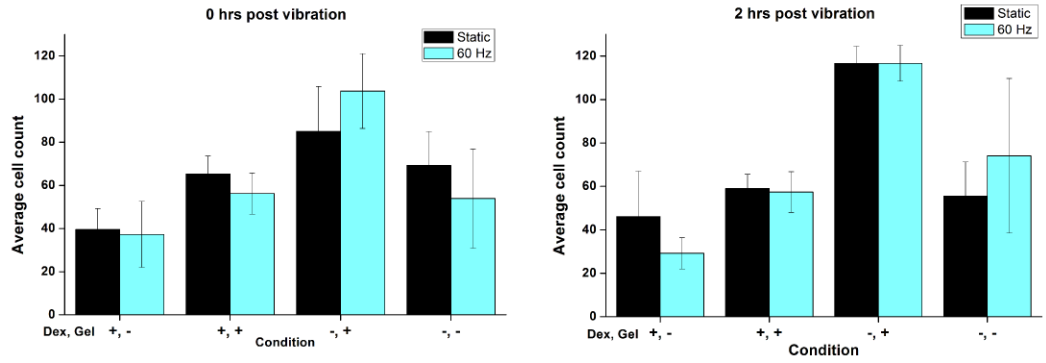

Figure 4.6: Cell counts from DAPI staining, hES-MP cells, post vibration. Data shows average cell number in $0.3mm^2$, mean ± standard deviation, n=6 over 2 experiments.

4.6 Serum-Free and Constant Acceleration versus Constant Amplitude Vibration

The addition of FCS to culture medium allows the culture of a wide variety of cells for *in vitro* experiments, but there are some limitations to its use. FCS is a natural product, and there is variability in composition between batches. While overall cell growth may not be affected, a change in the serum composition may affect signals which the cells are subjected to. As molecules present in FCS may be part of signalling pathways, it is possible that the inclusion of serum during some experiments may reduce or inhibit the responses being investigated. The effect of using serum free media during vibration stimulus was investigated. Normal culture media (ab or abd supplemented) was replaced with serum free media (no FCS, no supplements) immediately prior to vibration. This was replaced with fresh supplemented culture media (ab or abd) post vibration. Samples were otherwise treated as for 45 minutes vibration stimulation detailed earlier.

To test the effects of keeping cells in non-standard culture conditions during vibration, an extra control condition was included where plates were kept in the incubator throughout culture. The static plates were placed on the bench for the same time as samples undergoing vibration and compared to the incubator condition. This was to confirm that a period of at least 45 minutes out of the incubator did not affect the cell behaviour. Experimental results are presented in two figures - the two control conditions (incubator and static) in figure 4.7 and then vibrated compared to the static controls in figures 4.8 and 4.9.

These results show that removing the cells from the incubator for 45 minutes (static condition) has no significant effect on the cells compared to those maintained in the incubator throughout culture. For further experiments, static plates (on the bench for the vibration period) were kept as the control condition. For the main experiment, the presence of serum during vibration was investigated for a variety of vibration conditions, in ab or abd supplemented media. Constant amplitude versus constant acceleration vibrations were considered, at 60 and 120 Hz. 60 Hz gave a response in the previous experiments, and higher vibration frequencies tested in the literature had been shown to cause increased mRNA expression of matrix components (Dumas et al. 2010). The results of these experiments are shown in figure 4.8.

Surprisingly, these experiments did not show the same effect as in the previous 45 minute stimulation experiments (figure 4.4 compared to 4.8) and there are few differences between conditions. For the serum free vibration in ab supplemented media, there are significantly higher amounts of DNA for the 0.03 g, 60 Hz samples compared to all other vibrated samples. This is the opposite effect to that seen previously where responses were seen in abd media.

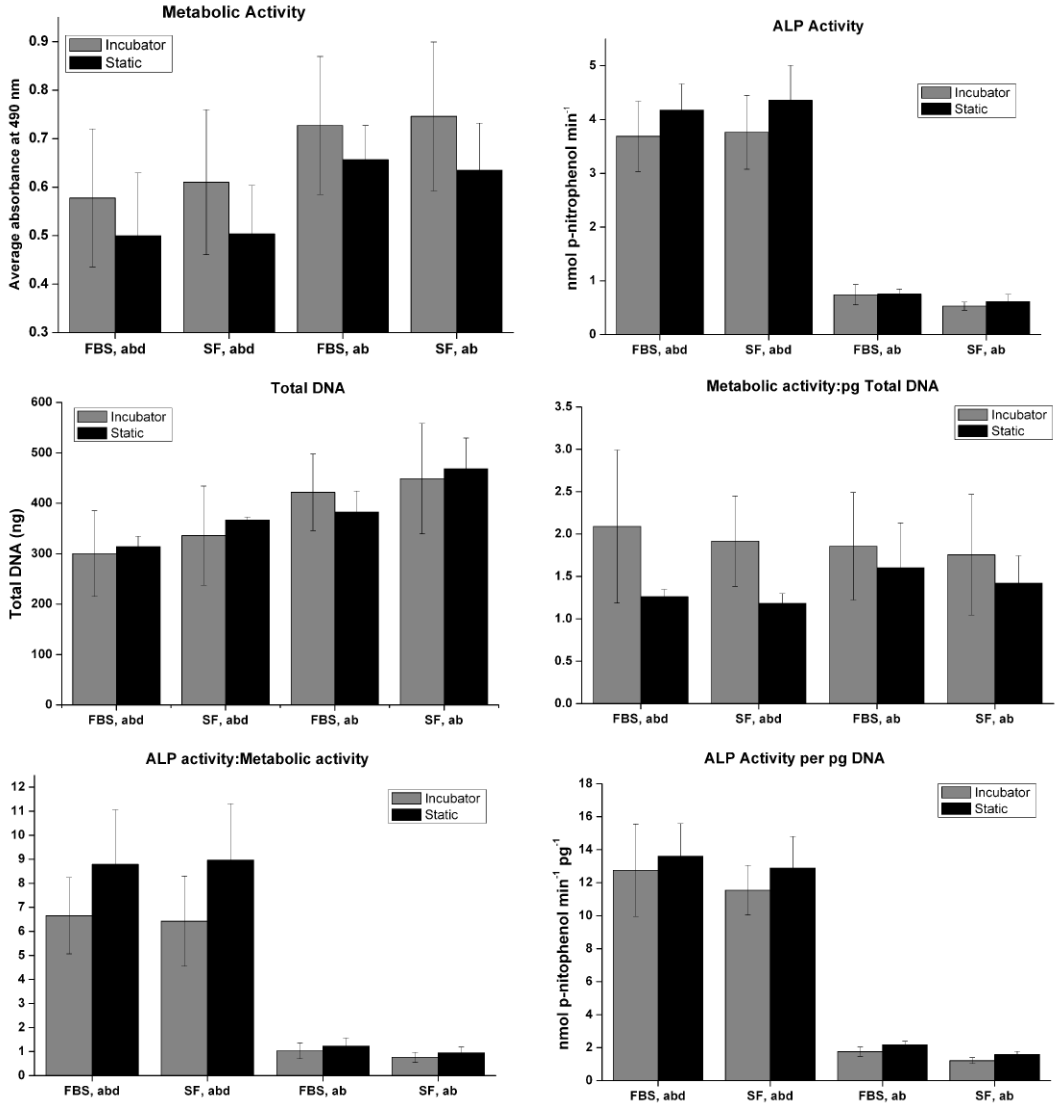

Figure 4.7: Controls for LMHF vibration of hES-MP cells under different serum conditions. Removing cells from incubation at 37°C for 45 minutes had no significant effects on metabolic or ALP activity or DNA content. There was an overall significant effect of dexamethasone treatment on the ALP activity of the cells as was expected ($p < 0.05$). Future work did not test the significance of this for each experiment to reduce analysis complexity. No other significant effects were observed, static samples show a trend for lower MTS and higher ALP (abd media). Mean $\pm$ standard deviation, n=6 over 2 experiments.

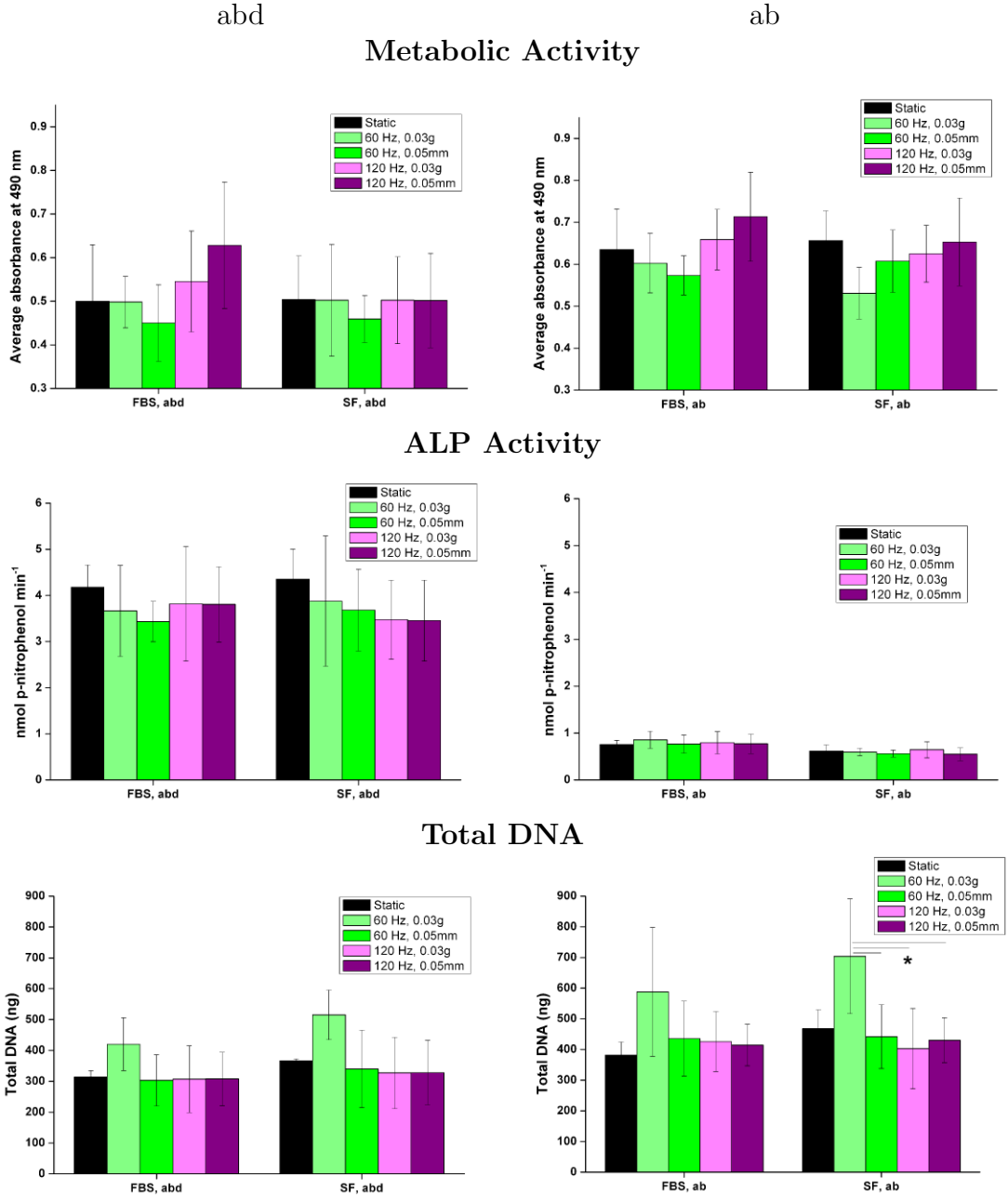

Figure 4.8: LMHF vibration of hES-MP cells under different serum conditions. Significant differences ($p < 0.05$) were found in total DNA content between $0.03g$, 60 Hz vibration and all other vibration frequencies for serum free media. A trend was seen for increasing metabolic activity with 120 Hz vibration (FBS containing media). Mean ± standard deviation, n=6 over 2 experiments.

The ALP:DNA, ALP:MTS and MTS:DNA ratios were calculated for the samples (figure 4.9). There were no significant differences in these ratios for any of the conditions. As the presence of serum did not seem to affect the response to vibration, further work vibrated cells in normal culture media.

4.7 Long Term Culture of hES-MP Cells with Repeated Vibration

While one bout of LMHF vibration for 45 minutes had an effect on the ALP activity of hES-MP cells, this did not provide information on the effects of vibration on the matrix production of the cells. Long term culture of hES-MP cells with repeated LMHF vibration was carried out to investigate possible changes in the matrix production and mineralisation. The cells were seeded in 12 well plates in either ab or abd supplemented media as for the initial 8 day experiments. On 10 occasions during culture (once per day on days 6-10 and 13-17), the cells were subjected to 45 minutes of constant acceleration vibration. Table 4.3 provides details of the long term time points. Many *in vivo* studies have applied stimulation on 5 days each week and this was thought to be a good starting point for *in vitro* work. 90 Hz vibrations were included to further study the effects of vibration at higher frequencies in the long term. Metabolic activity was measured on day 21 via MTS assay, before fixation in 10% formalin. Alizarin red and sirius red staining were used after fixation to investigate the matrix production and mineralisation and results are presented in figure 4.10.

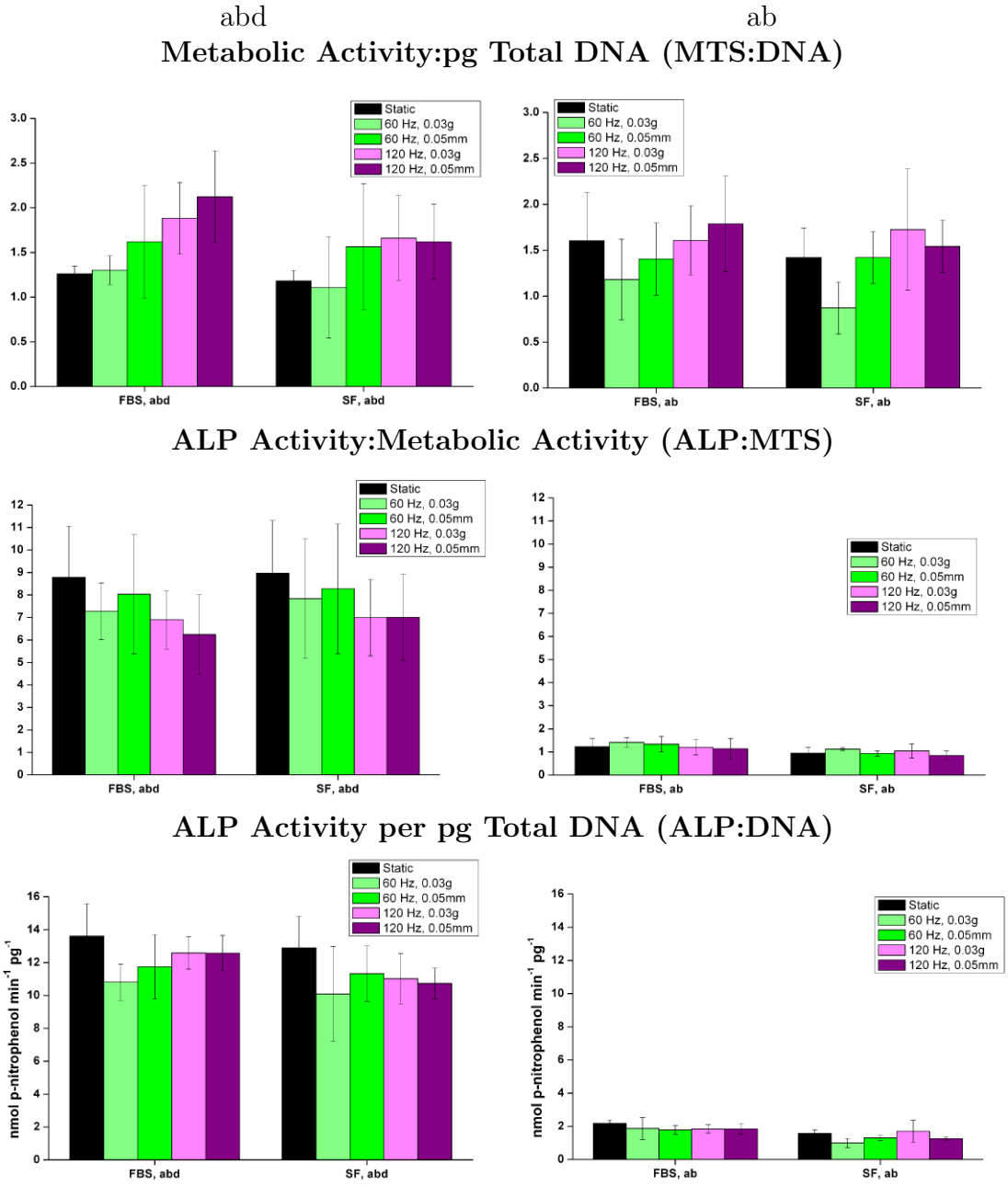

Figure 4.9: LMHF vibration of hES-MP cells under different serum conditions (ratios). Although trends were seen in the MTS:DNA ratio in abd media including FBS, no significant differences were found by 2-way ANOVA. Mean ± standard deviation, n=6 over 2 experiments.

Timepoint	Step	Details
Day 0	Seeding	hES-MP cells seeded in 12 well plates
Days 6-10 and 13-17	Vibration	Plates vibrated at specific frequencies for 45 minutes each day
Day 21	Endpoint	MTS assay before fixation of cells and staining of ECM

Table 4.3: Timepoints in long term LMHF vibration regimen. Media changed every 2-3 days as required.

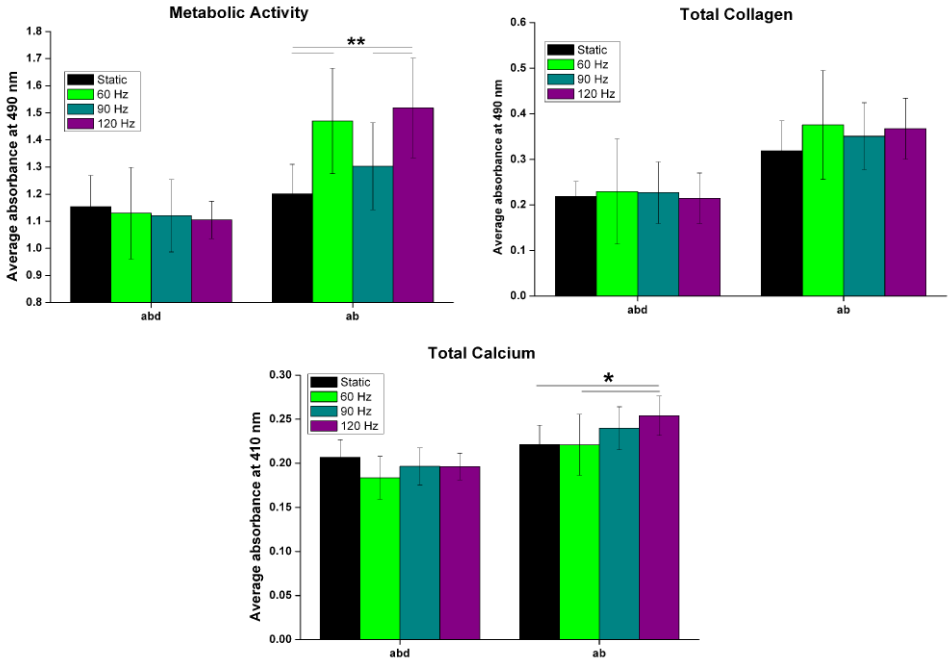

Figure 4.10: Long term vibration and matrix production in hES-MP cells, 0.05 mm. Significantly higher values ($p < 0.05$) were seen for metabolic activity and total calcium with 120 Hz vibration (ab media). Mean $\pm$ standard deviation, n=12 over 2 experiments.

For samples cultured in ab supplemented media, metabolic activity was significantly higher for several conditions (60 and 120 Hz compared with static, 120 Hz compared with 90 Hz). There were no significant differences in collagen production, but significantly higher total calcium in some cases (120 Hz compared with static and 60 Hz). Ratios of collagen and calcium per metabolic activity (Col:MTS and Ca:MTS respectively) and calcium to collagen (Ca:Col) were calculated to further investigate this response (figure 4.11).

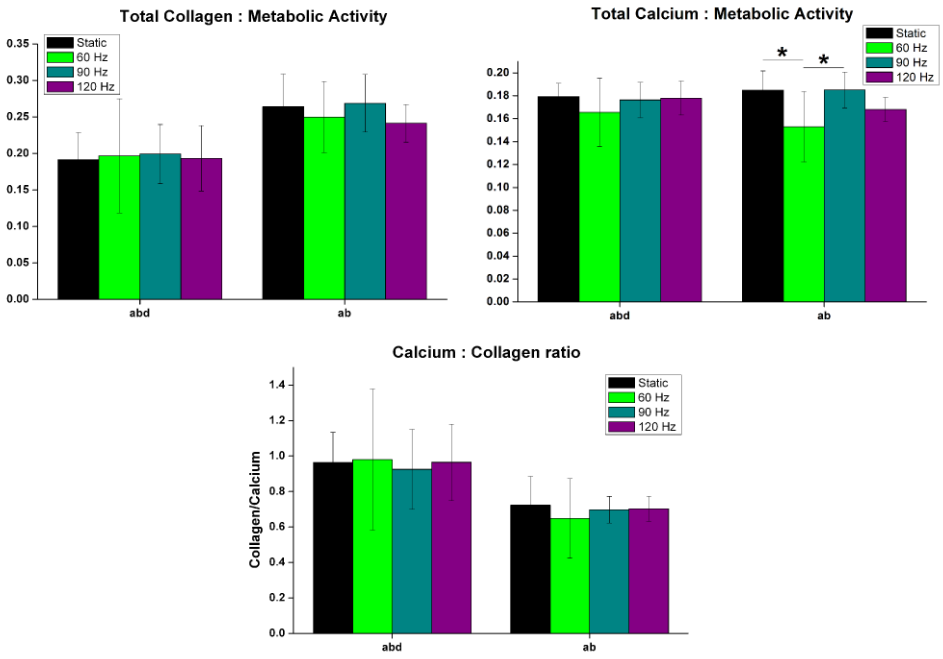

Figure 4.11: Long term vibration and matrix production in hES-MP cells, 0.05 mm, ratios. Ca:MTS significantly lower ($p < 0.05$) in 60 Hz samples (ab media) than static and 90 Hz samples. Mean ± standard deviation, n=12 over 2 experiments.

The calculated ratios show little trend with frequency. Ca:MTS values were significantly higher values for static and 90 Hz compared with 60 Hz in samples cultured in ab supplemented media. There is a similar small but non significant difference for the samples grown in abd media. The experiment was repeated using the constant acceleration vibration in order to compare the two different conditions with results presented in figure 4.12. 30 Hz vibration was included to cover a larger range of frequencies, as the previous experiment showed changes in matrix that had not been suggested in short term experiments.

For the constant acceleration vibration in abd media, metabolic activity was seen to increase slightly with increasing frequency, but this was not significant. In ab media there was significantly higher metabolic activity in cells vibrated at 120 Hz compared with static, 60 or 90 Hz samples. Alizarin red staining showed a

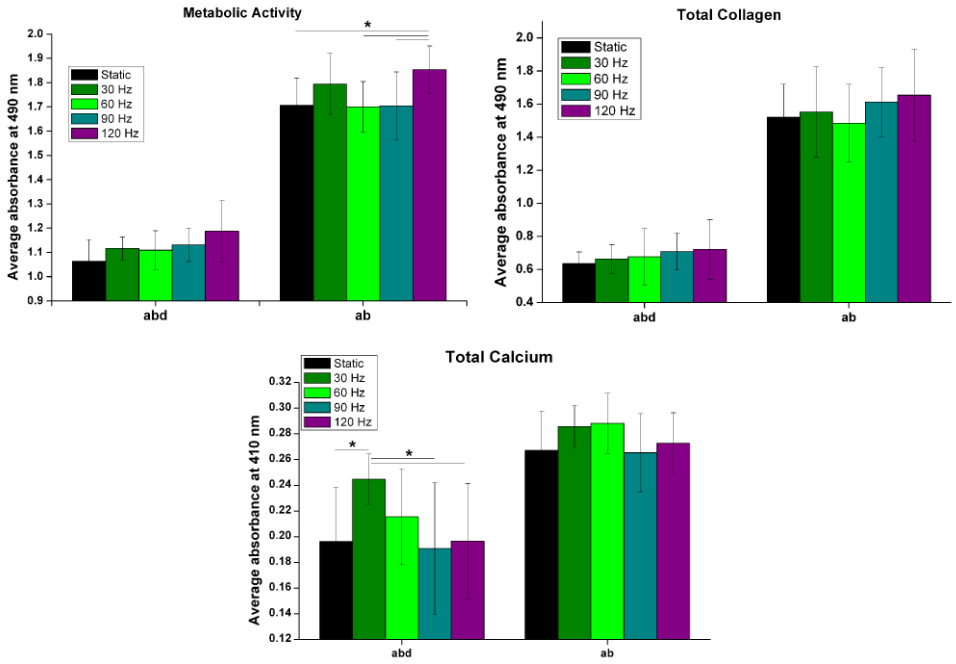

Figure 4.12: Long term vibration and matrix production in hES-MP cells, 0.03g. 120 Hz vibration caused significantly higher ($p < 0.05$) metabolic activity than other conditions (ab media) and 30 Hz showed significantly higher calcium (abd media). Mean ± standard deviation, n=12 over 2 experiments.

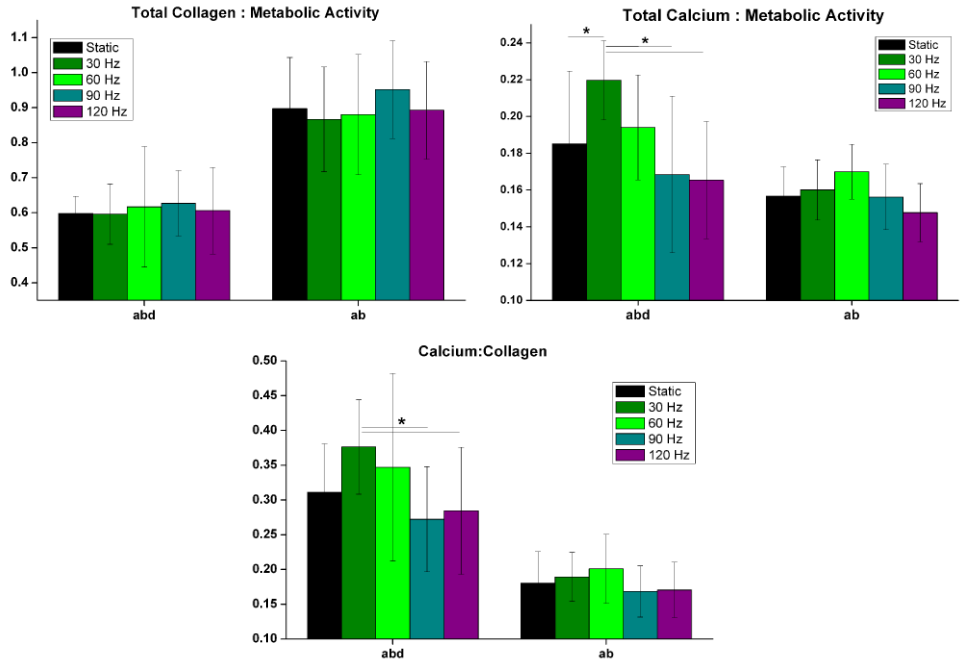

Figure 4.13: Long term vibration and matrix production in hES-MP cells, 0.03g, ratios. Ca:MTS and Ca:Col were significantly higher ($p < 0.05$) for 30 Hz samples compared with other frequencies (abd media). Mean ± standard deviation, n=12 over 2 experiments.

significant increase in calcium deposition (30 Hz compared with all except 60 Hz, abd media) and a similar trend was seen for the ab media samples, but this was not significant.

The ratios of Col:MTS, CA:MTS and Ca:Col were calculated (figure 4.13) and showed significantly higher Ca:MTS, as had been seen for the raw calcium. There is also a significant change in the composition of the matrix (as shown by the Ca:Col ratio) for samples vibrated at 30 Hz (compared with 90 and 120 Hz, abd media). This suggests that the cells are being stimulated to produce a more mature mineralised matrix.

4.8 Media Transfer from Vibrated Cells to Non-Stimulated Cells

As previous work had demonstrated a response in hES-MP cells to stimulation by LMHF vibration, the effects of media from these vibrated cells on statically cultured cells was investigated. As the mechanism of the response was unknown, this would help elucidate whether the cells released any soluble factors in response to the stimulation. Such soluble factors may be of use to stimulate constructs which are difficult to directly vibrate, but could be treated with conditioned media (CM)

4.8.1 Media Transfer and Early Differentiation

Vibrated cells were cultured in gelatin coated 12 well plates as for previous experiments. For the recipient cells, gelatin coated 24 well plates were used to allow comparison of ab and abd media from vibrated cells on static cells cultured in

Timepoint	Step	Details
Day 0	Seeding	Seeding of cells which will be vibrated
Day 2	Seeding	Seeding of cells which will receive conditioned media (CM)
Day 6	Vibration	Cells seeded on day 0 subjected to 45 minutes of LMHF vibration
Day 8	Transfer	Cells seeded on day 2 receive CM from vibrated cells
	Endpoint	MTS assay on vibrated cells before lysate collection for ALP activity and DNA quantification
Day 10	Endpoint	MTS assay on cells which received conditioned media before lysate collection for ALP activity and DNA quantification

Table 4.4: Timepoints in short term media transfer experiments. Media changed every 2-3 days as required before day 6.

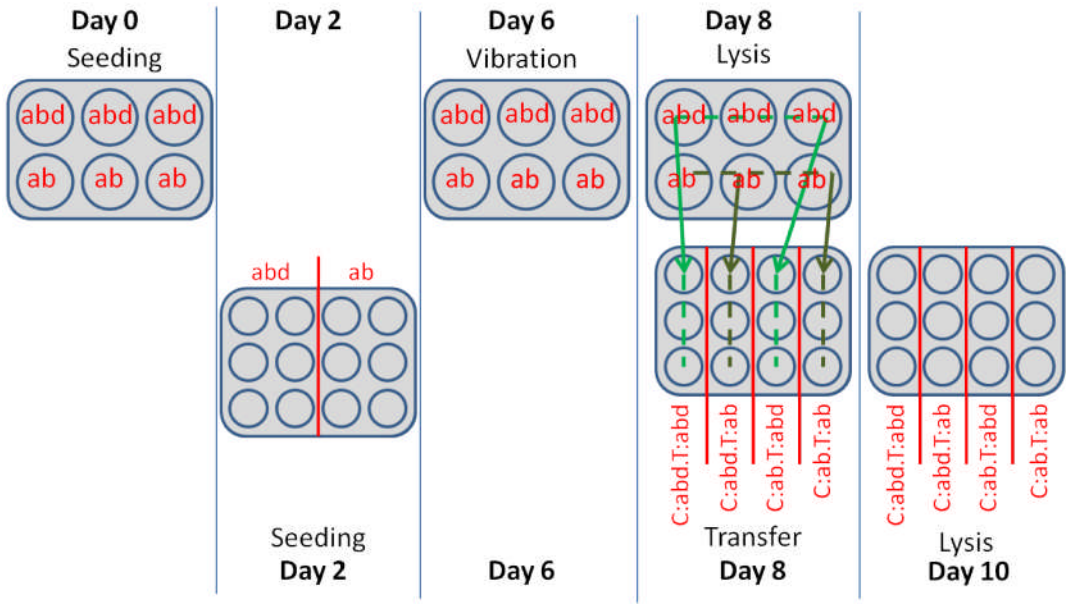

Figure 4.14: Media transfer in short term culture. Lysis refers to the MTS assay and subsequent lysate collection for measurement of ALP activity and DNA quantification.

both media types prior to transfer. 2,400 cells were seeded into each well, keeping the cell number per mm^2 constant. Cells were seeded such that day 0 for the cells receiving conditioned media (T:) coincided with day 2 for the vibrated cells. Media was transferred from the vibrated cells before lysate collection on day 8 , detailed in table 4.4 and figure 4.14. This meant that the cells being stimulated by conditioned media received this stimulation on day 6 of culture, equivalent to the application of LMHF vibration. Samples were assayed for metabolic activity, ALP activity and total DNA. Media transfer experiments where conducted using 0.05 mm amplitude vibration as the application of constant amplitude vibration was more consistent. The results of experiments for the vibrated cells are shown in figures 4.15 and 4.16.

Several differences seen between vibrated and static cultures across the different conditions (figure 4.15). There was a small reduction in metabolic activity for samples vibrated at 30 or 60 Hz compared to static (all media), which was not present in samples vibrated at 120 Hz (all media). This was significant only for 120 Hz compared with 60 Hz in abd media. For total DNA, significantly lower values compared to static controls were seen at all vibration frequencies in ab media. The same trend was observed in the abd media where it was not significant.

For the calculated ratios, there were no obvious trends. Significantly higher values were found only for ALP:DNA (60 Hz) and MTS:DNA (120 Hz) in abd media compared with static controls. This is very different to the situation observed previously. 120 Hz now appears to be more effective in creating a response than 60 Hz, although this is not of the same magnitude.

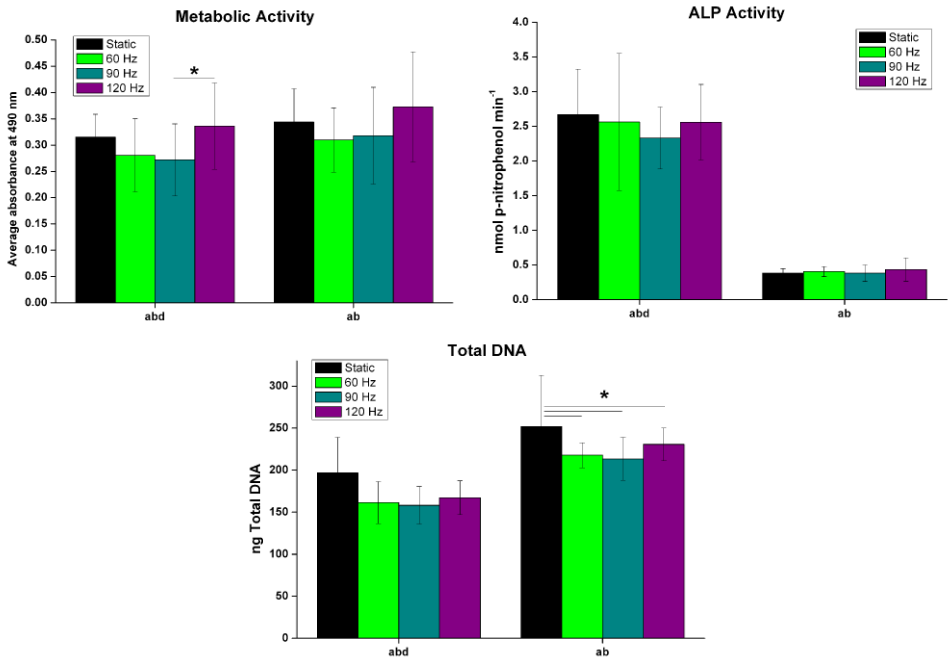

Figure 4.15: 45 minutes LMHF vibration (day 6 of 8 day culture) of hES-MP cells for transfer experiments. Significant differences ($p < 0.05$) were found for metabolic activity and total DNA content. Mean ± standard deviation, n=24 over 4 experiments.

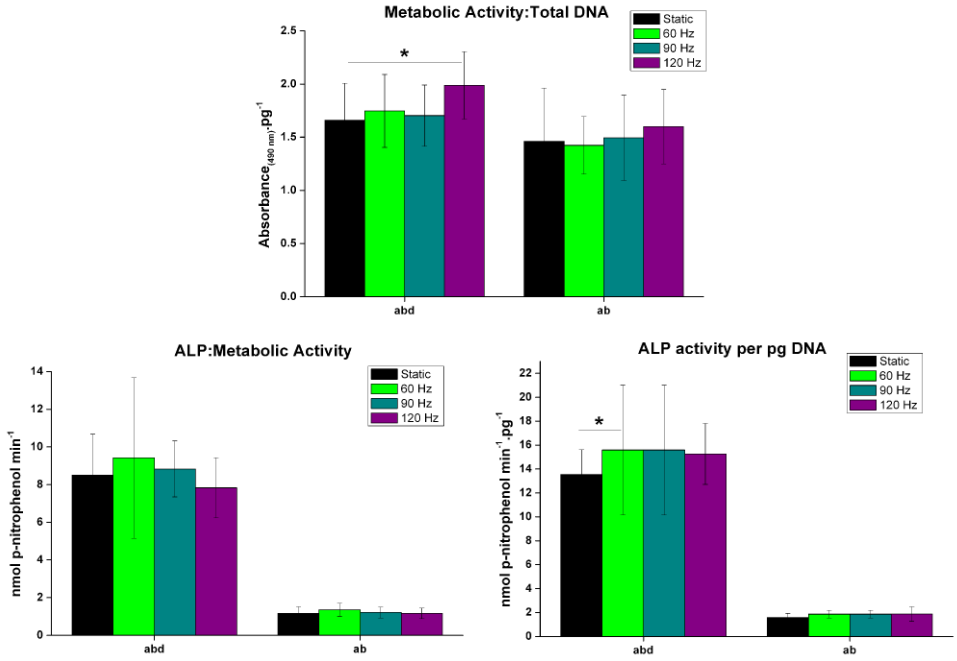

Figure 4.16: 45 minutes LMHF vibration of hES-MP cells for transfer experiments, ratios. Values significantly higher than static controls ($p < 0.05$) were found in abd media samples for ALP:DNA (60 Hz) and MTS:DNA (120 Hz). Mean ± standard deviation, n=24 over 4 experiments.

The results for cells receiving conditioned media are shown in figures 4.17 and 4.18. Control cells were given fresh media instead of CM at the same experimental time points. This allowed a comparison between cells cultured normally with fresh media at each media change and those receiving CM from other cells, some of which had been previously stimulated with LMHF vibrations. Media formulations describe the supplements in the initial culture media (C:) and the media transferred from other cells (T:).

For the CM samples, most of the differences observed occurred between fresh media controls (ie where the transfer media has not been conditioned by other cells) and C:abd.T:abd samples. ALP activity was significantly higher in 120 Hz(CM) samples (C:abd.T:abd media) compared with static controls. 60, 90 and 120 Hz(CM) were only significantly higher for the C:abd.T:abd media when compared with fresh controls. Metabolic activity increased for all media types with increasing frequency, although this was not significant for any condition.

Ratios in the transfer experiment (figure 4.18) also showed almost all significant differences at 120 Hz(CM) compared with fresh samples. ALP:MTS was higher for 60 Hz(CM) than static(CM) and decreased at higher frequencies (all media conditions). The effect was less pronounced in the C:ab.T:abd and C:.T:ab conditions and was not significant. The ALP:DNA was significantly higher for 90 Hz(CM) (C:abd.T:abd and C:abd.T:ab) and 120 Hz(CM) (C:abd.T:abd) compared with fresh controls. There were also significantly higher values of MTS:DNA for 120 Hz(CM) samples compared with fresh (all media except C:abd.T:ab). There appeared to be a general trend in MTS:DNA (lower for 60 Hz(CM) compared to static(CM), increasing afterwards with increasing frequency), but this was not significant. These results suggest that 120 Hz may be the most appropriate condition for producing conditioned media with 0.05 mm vibration.

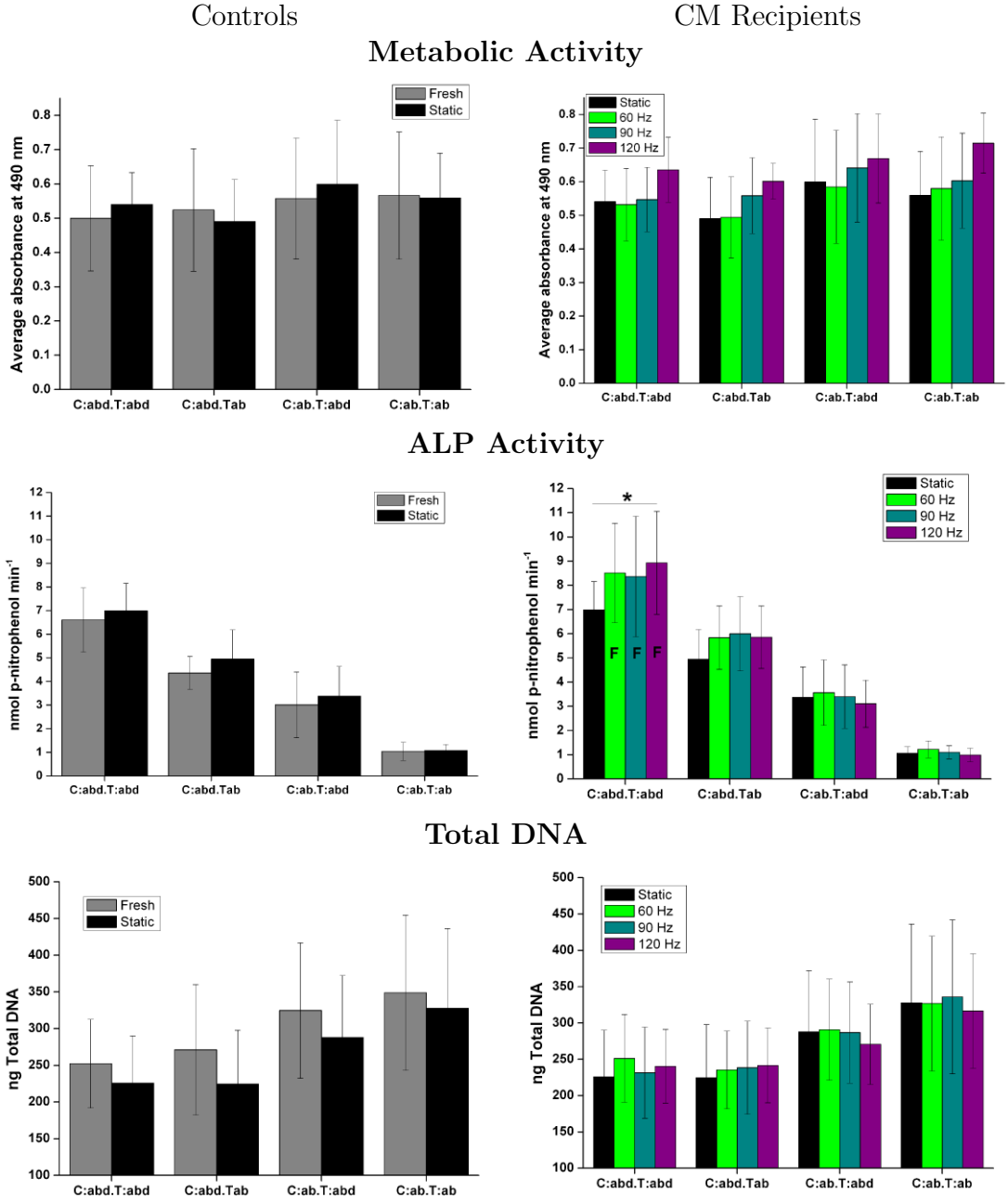

Figure 4.17: Short term media transfer in hES-MP cells. In Control graphs, T: media was either fresh media (Fresh condition) or transferred from cells kept on the bench during vibration (Static condition). 120 Hz vibration was significantly higher than static controls (C:abd.T:abd $p < 0.05$). F denotes a significantly higher value compared to fresh controls. Mean ± standard deviation, n=12 over 4 experiments.

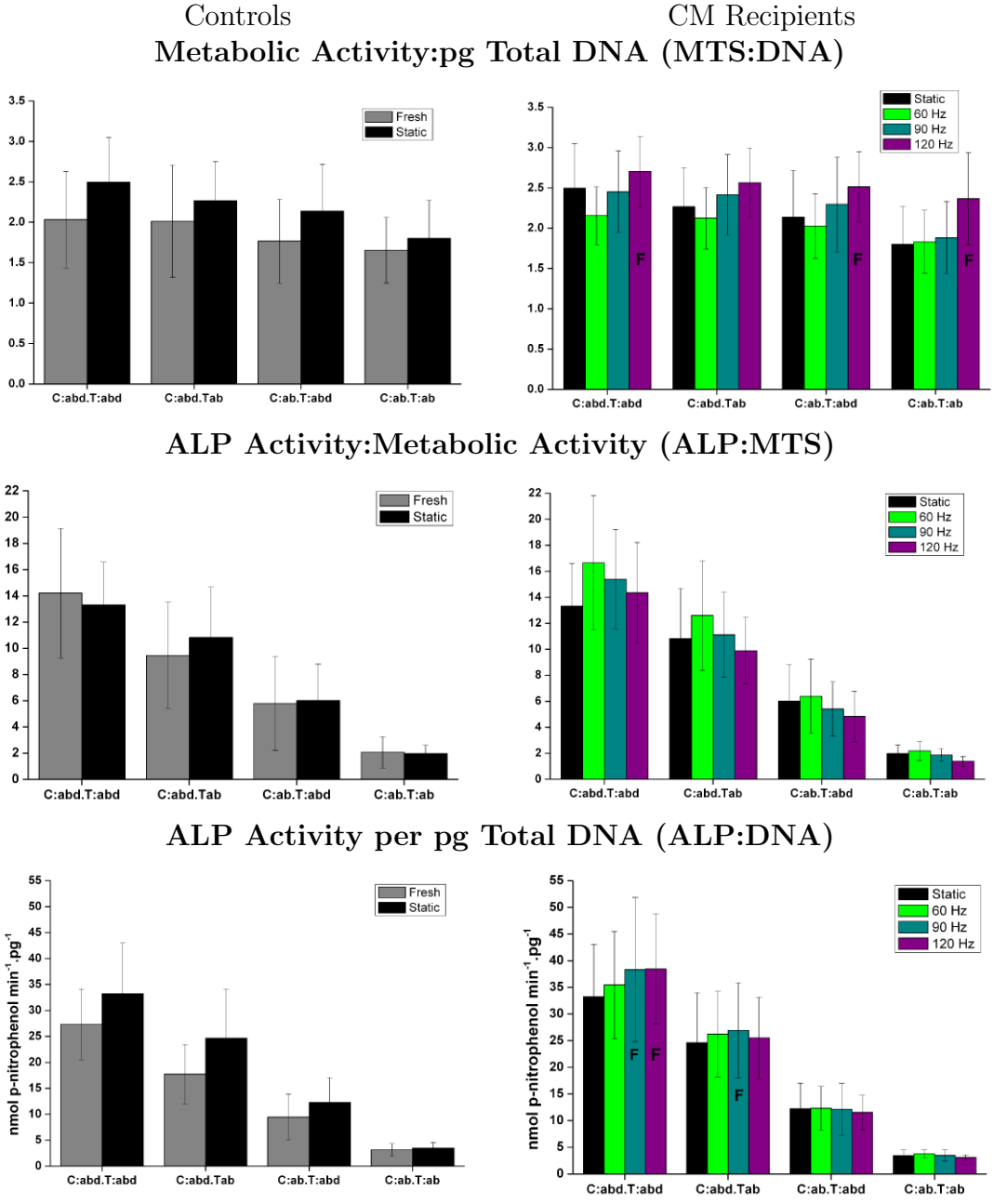

Figure 4.18: Short term media transfer in hES-MP cells, ratios. In Control graphs, T: media was either fresh media (Fresh condition) or transferred from cells kept on the bench during vibration (Static condition). F denotes a significantly higher value ($p < 0.05$) compared to fresh controls. Mean ± standard deviation, n=12 over 4 experiments.

There are also apparent differences between the media formulations at a given frequency. For the vibrated samples (figure 4.15 and 4.16), there are significant differences between abd and ab supplemented cultured samples for all frequencies (ALP, DNA, ALP:MTS and ALP:DNA), demonstrating the normal response to differentiation media. There were no significant differences between groups for metabolic activity. For the CM samples, MTS activity was similar for all media formulations. Total DNA showed slightly higher amounts of DNA for the samples with ab supplemented culture media (C:ab). ALP activity showed a steady decrease for all frequencies moving from C:abd.T:abd to C:ab.T:ab media. This suggests that the combination of supplements in both culture (C:) and transfer (T:) media has an effect on the ALP activity, but only the culture medium affects the metabolic activity and cell number.

4.8.2 Media Transfer and Matrix Production

The long term effects of conditioned media were also investigated, using the long term vibration regimen at 0.05 mm. The timepoints for the media changes and transfers are shown in table 4.5). Media was transferred on days 6, 8, 10 and 13, 15 and 17 to coincide with media changes on the vibrated cells. Control cells were given fresh media instead of conditioned media (CM) from static or vibrated cells. The same cell numbers were seeded for the experiments as in the short term experiments (5,000 per well in 12 well plates for vibrated cells and 2,400 per well in 24 well plates for CM recipients). The vibrated samples which provided the conditioned media were those from the 0.05 mm long term experiment detailed in figures 4.10 and 4.11.

The control samples (fresh media) were notably different to the static controls for this experiment (figure 4.19). These higher values are significant for metabolic

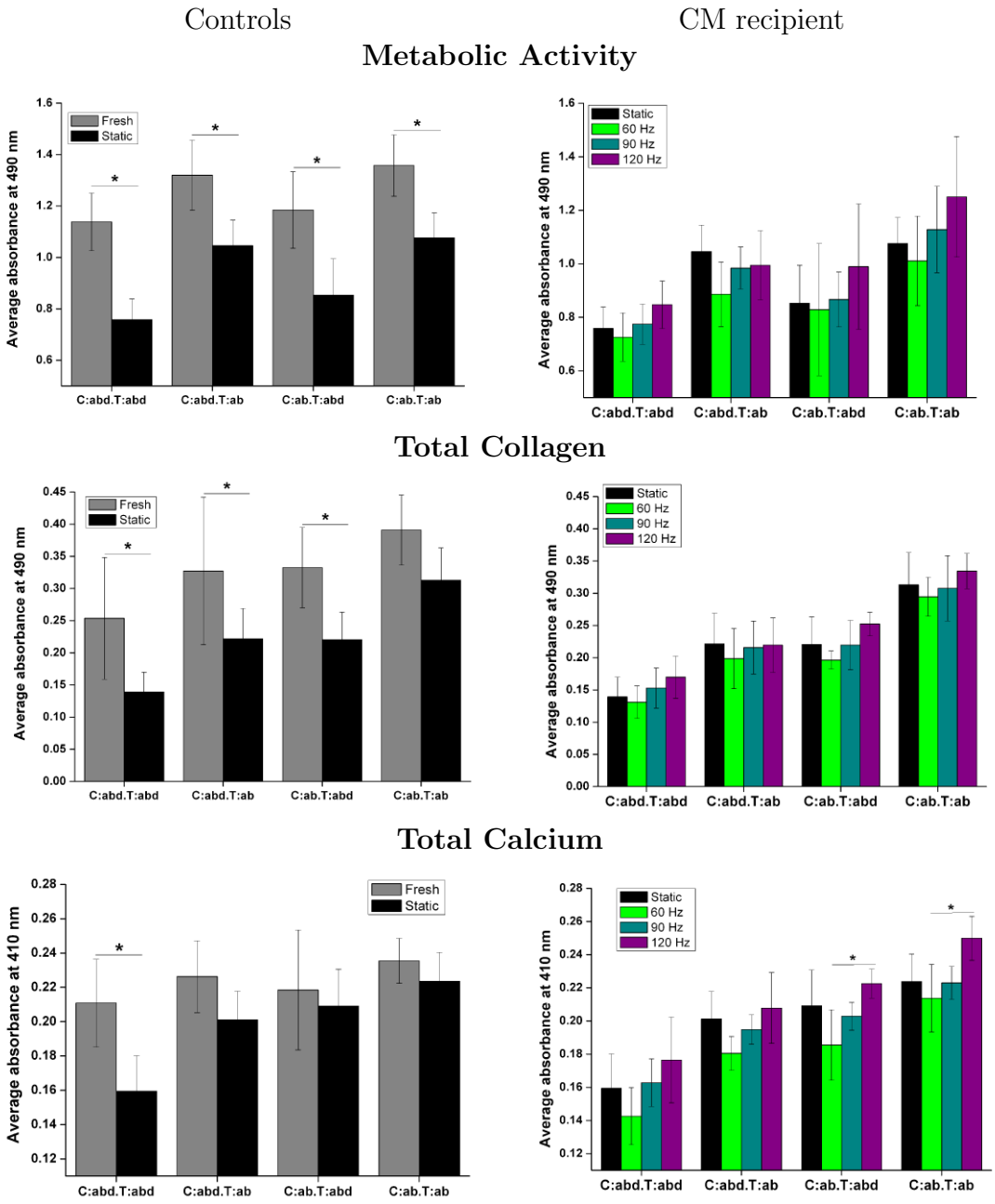

Figure 4.19: Long term media transfer and matrix production in hES-MP cells. In Control graphs, T: media was either fresh media (Fresh condition) or transferred from cells kept on the bench during vibration (Static condition). Fresh controls showed significantly higher values compared with static controls (MTS, collagen (all except C:ab.T:ab) and calcium (C:abd.T:abd), $p < 0.05$). Higher calcium was noted for 120 Hz(CM) samples, significant compared to static for C:ab media. Mean ± standard deviation, n=6 over 2 experiments.

Timepoint	Step	Details
Day 0	Seeding	Seeding of all cells (i.e. those to be vibrated or receive conditioned media). 12 well plates for vibrated cells and 24 well plates for conditioned cells
Day 6-10 and 13-17	Vibration	Cells in 12 well plates subjected to 45 minutes of LMHF vibration
Days 6,8,10,13,15,17	Transfer	Conditioned media from vibrated cells transferred to cells in 24 well plates
	Media change	Fresh media given to vibrated cells
Day 21	Endpoint	MTS assay on all cells before fixation for staining of the ECM

Table 4.5: Timepoints in long term media transfer experiments. Media changed every 2-3 days as required before day 6.

activity (all media), collagen (all but C:ab.T:ab) and calcium (C:abd.T:abd only). There was a general trend of higher MTS, collagen and calcium readings across all frequencies moving from C:abd.T:abd to C:ab.T:ab media. For individual media types, metabolic activity is significantly higher in fresh compared with CM samples, except for 90 Hz(CM) (C:ab.T:ab) and 120 Hz(CM) (C:ab). For collagen production, the differences are not significant for 60 and 90 Hz(CM) (C:ab.T:ab) or 120 Hz(CM) (only C:abd.T:ab is significantly lower than fresh). The results are more apparent for the calcium deposition: significant decreases compared to fresh media are seen only for 60 Hz(CM) (C:abd) and 90 Hz(CM) (C:abd.T:abd).

When considering only the samples where transfer media came from static or vibrated cells, there are no significant changes for metabolic activity or collagen production compared to static transfer medium. Total calcium for samples cultured in ab supplemented medium initially was significantly higher for 120 Hz compared to 60 Hz.

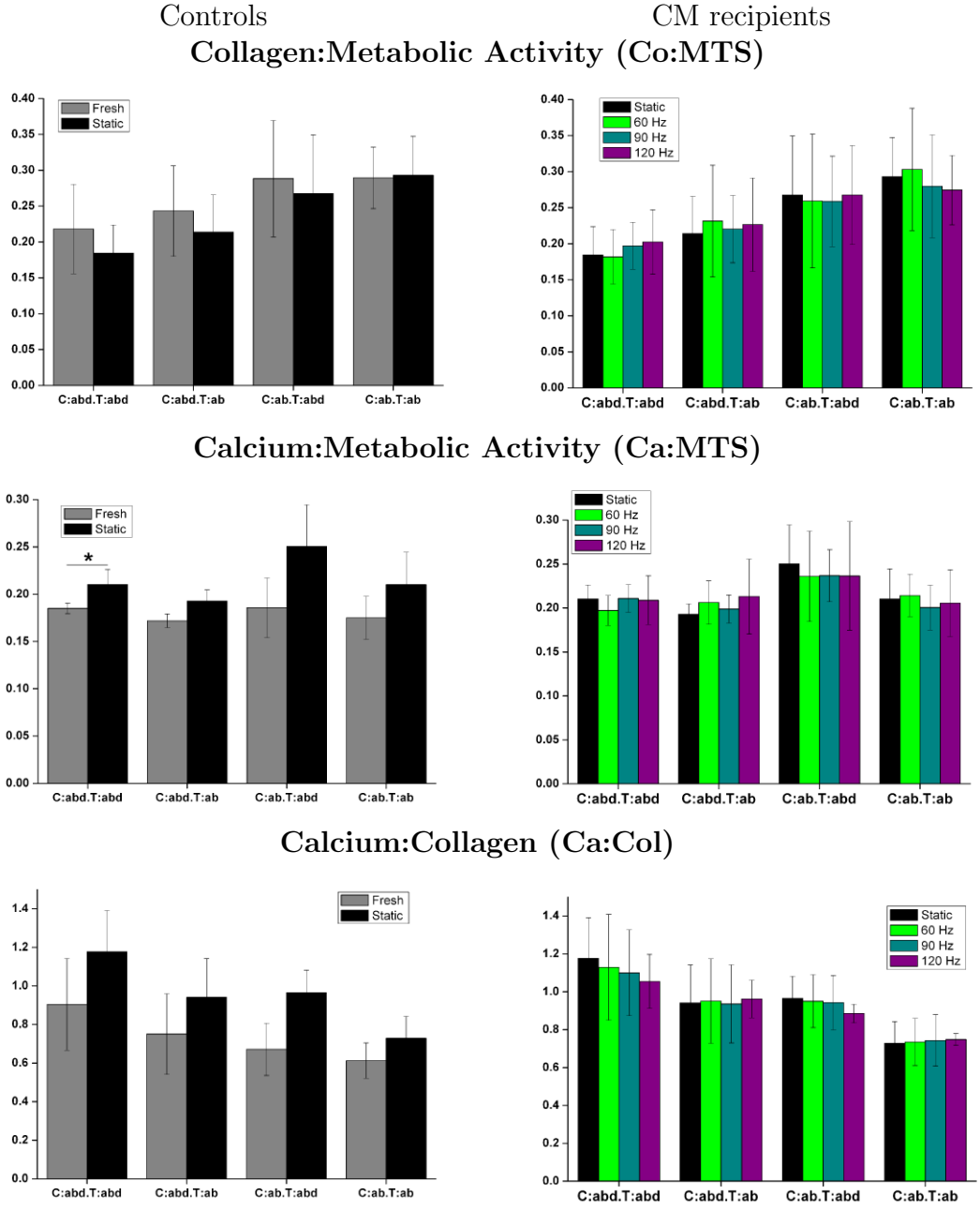

Figure 4.20: Long term media transfer and matrix production in hES-MP cells. In Control graphs, T: media was either fresh media (Fresh condition) or transferred from cells kept on the bench during vibration (Static condition). Shows ratios of collagen and calcium to metabolic activity, only fresh compared with static (Ca:MTS, C:abd.T:abd) was significant ($p < 0.05$). Mean ± standard deviation, n=6 over 2 experiments.

No trends were evident for Col:MTS, Ca:MTS or Ca:Col. The only significant difference was an increase in Ca:MTS for static transfer media compared with fresh. The variability in values was much higher than that seen for the raw data, suggesting that the changes in matrix composition were not consistent between samples.

4.9 Prostaglandin Signalling and LMHF Vibration

One possibility for the effects of conditioned media on recipient cells is that the vibrated cells release prostaglandins as signalling molecules (Morris et al. 2010). In order to test this, the short term transfer experiments were repeated with the addition of indomethacin to half of the donor cells. Indomethacin has been used to disrupt prostaglandin signalling in bone marrow stromal cells undergoing mechanical stimulation (Thomas and El Haj 1996). The donor cells were kept static next to the ELF3200 or vibrated at 60 or 120 Hz, using the 0.03 g regimen. This also allowed the investigation of the short term transfer effects of 0.03 g vibration. Cells in the recipient group were seeded in 24 well plates at 2,400 cells per well. Indomethacin was added to the media of vibrated cells one hour before vibration was applied. After vibration, stimulated cells were returned to the incubator for 2 hours before media transfer as in previous experiments to allow the accumulation of soluble factors.

Results for the vibrated samples treated with indomethacin are shown in figures 4.21 and 4.22. Samples vibrated at 120 Hz showed higher metabolic activity compared with static controls for all conditions. These differences were significant

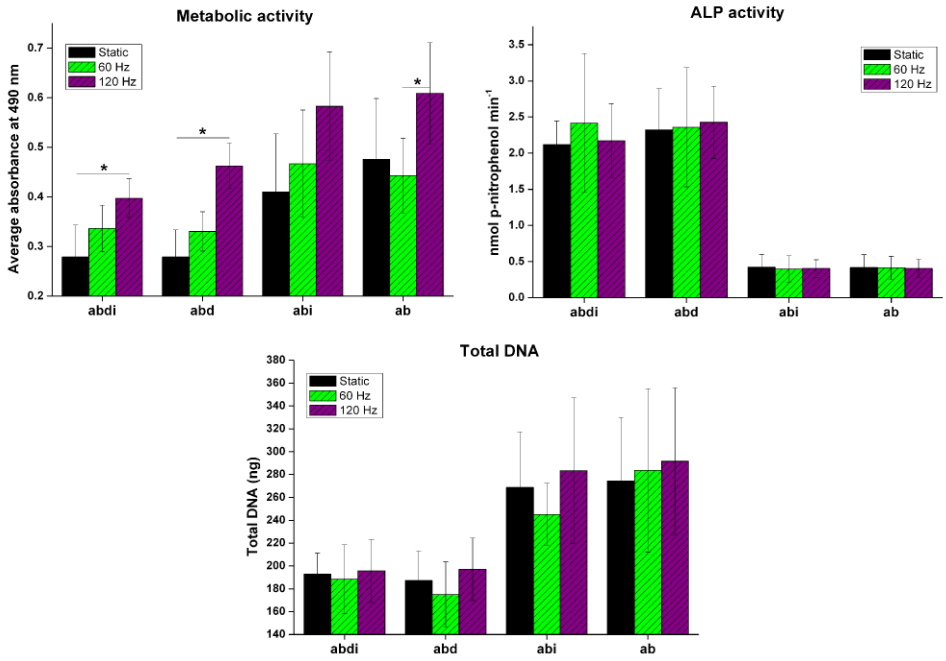

Figure 4.21: Effects of indomethacin on vibrated cells. Indomethacin did not show any effects on samples. Mean ± SD, n=6 over 2 experiments

in all cases except abdi supplemented media. There were no significant differences in ALP activity or total DNA between conditions. Increases in metabolic activity at 120 Hz are more pronounced than those seen previously in figure 4.15, and there are no significant changes in total DNA.

Ratios were calculated as for other experiments and are presented in figure 4.22). ALP:MTS was significantly reduced in samples vibrated at 120 Hz compared with static controls in differentiation media with no indomethacin. A similar trend was seen for the abdi media condition, but this was not significant. There was also no effects of indomethacin on ALP:DNA. The ratio of MTS:DNA was significantly higher at 120 Hz compared with static for all media conditions. During culture, the media from these treated cells was used as conditioned media for other cells. The same seeding densities were used as in previous transfer experiments and the timepoints were the same as the previous short term transfer

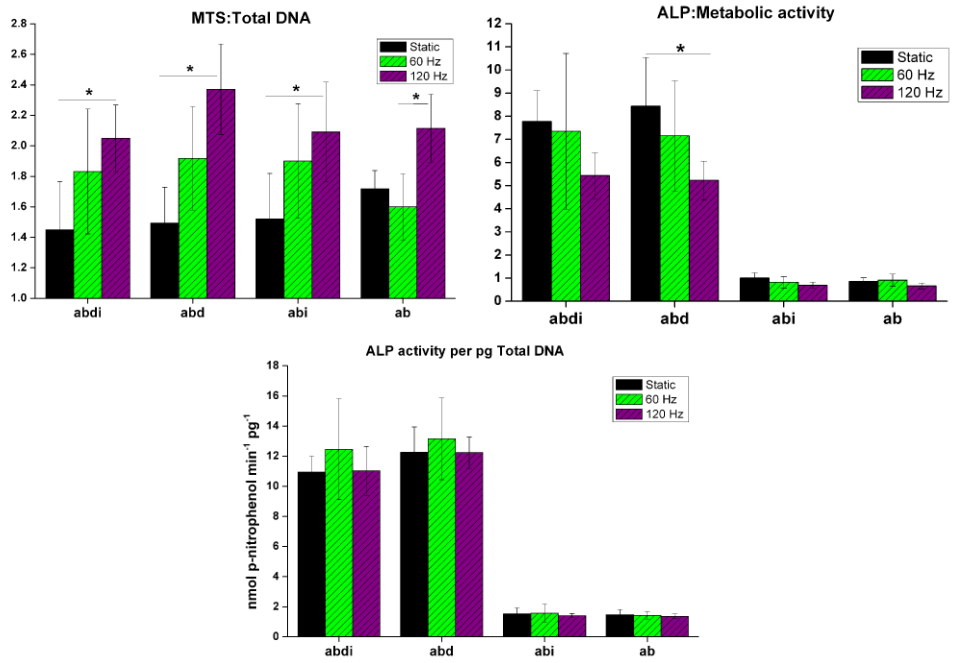

Figure 4.22: Effects of indomethacin on vibrated cells, ratios. Mean ± SD, n=6 over 2 experiments

(table 4.4 and figure 4.14).

The results for the CM samples treated with indomethacin are shown in figure 4.23. The only significant effect found was a reduction in the total DNA for 120 Hz compared with static (C:ab.T:ab media). However, variability for ALP activity and DNA was high and may mask other effects. The response to differentiation culture media is maintained through the experiment, demonstrating that the cells are still able to differentiate. Ratios (figure 4.24) also showed high variability, particularly for samples with abd media through the initial culture period and there were no significant differences. The cells still show a response to dexamethasone in the initial culture media, but not in the transfer media.

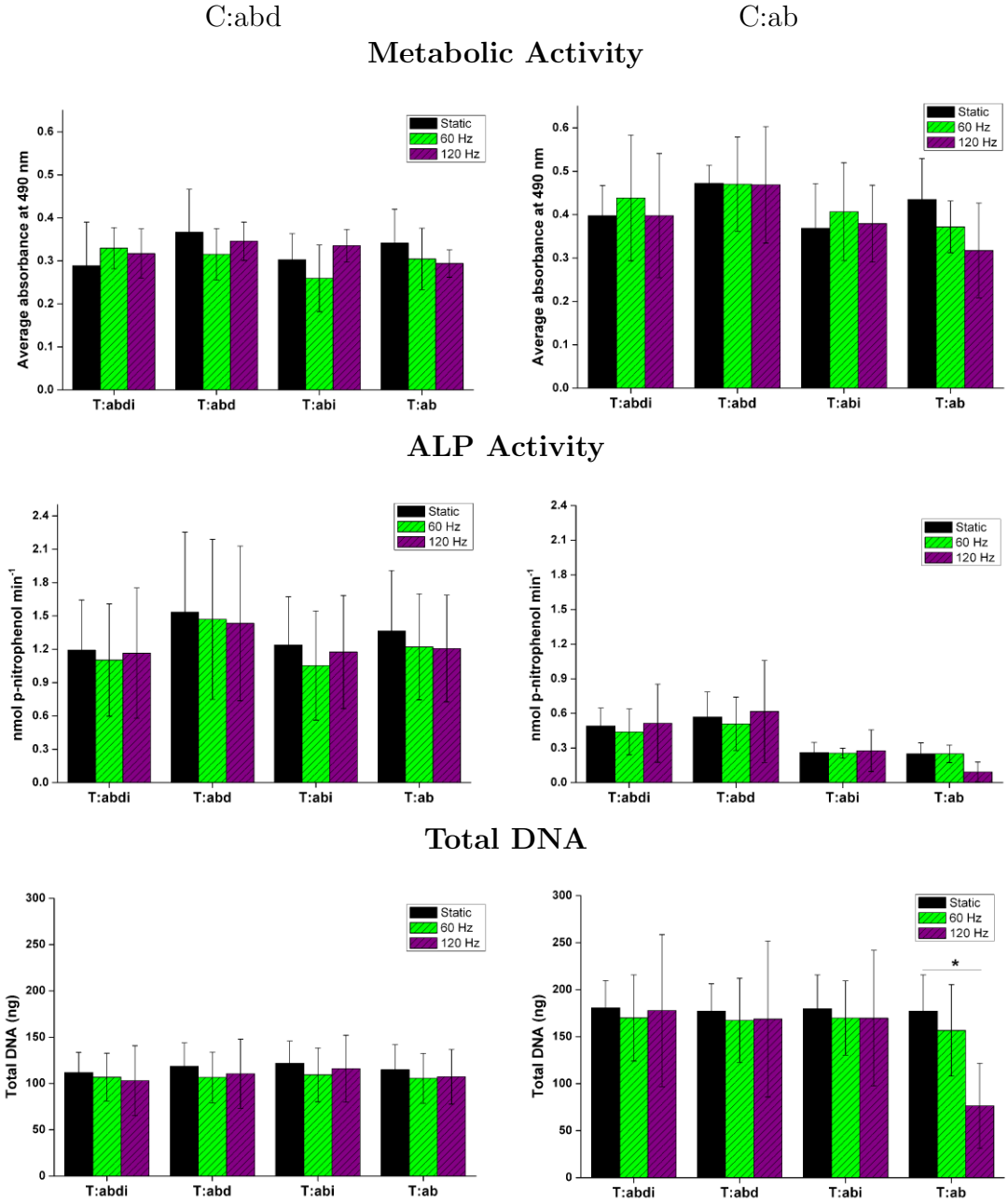

Figure 4.23: Effects of indomethacin in conditioned media on recipient cells. Headings refer to initial culture media, legends to transfer media. Mean ± SD, n=6 over 2 experiments

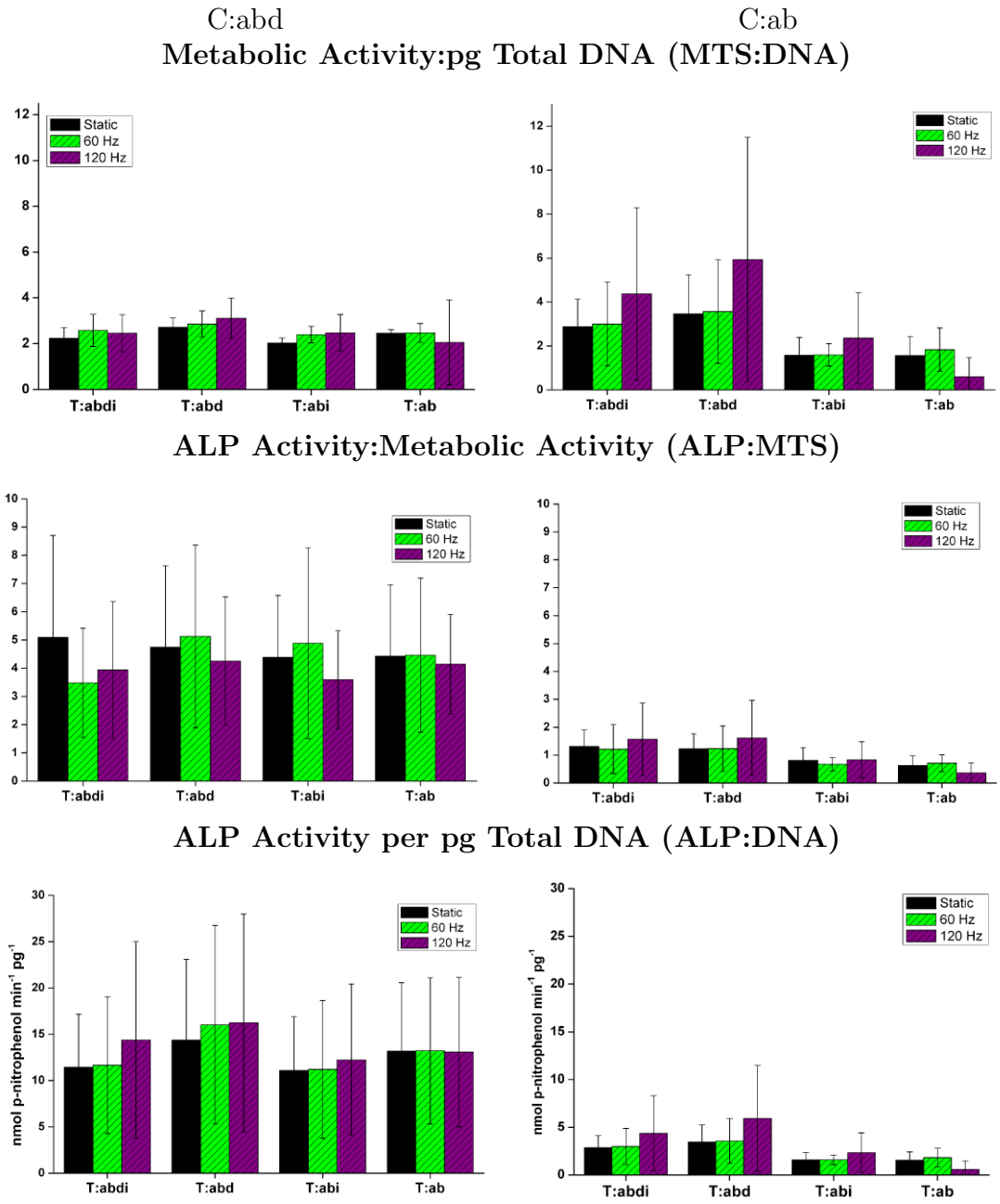

Figure 4.24: Effects of indomethacin in conditioned media on recipient cells, ratios. Headings refer to culture media, legends to transfer media. Mean ± SD, n=6 over 2 experiments

4.10 Discussion

This section of work studied the effects of low magnitude, high frequency (LMHF) vibration on the differentiation and matrix mineralisation of a mesenchymal progenitor cell line during 2D culture. The use of mechanical stimulation to affect the behaviour of cells is likely to be important in the production of tissues which are representative of those found in the body. For such stimulation methods, it is important that the cells can be stimulated in different configurations as required with minimal manipulation.

For the osteogenic differentiation of mesenchymal progenitor cells, LMHF vibrations are of interest as *in vivo* studies in several species have shown beneficial effects of this kind of loading on bone structure. The method is simple and requires little manipulation of cells over that normally required by tissue culture. The mechanisms causing these responses are however unknown and some studies have shown no improvements in bone structure. In previous *in vitro* studies, a variety of stimulation protocols have been tested, producing a range of responses (Lau et al. 2010; Bacabac et al. 2006; Pre et al. 2010; Pre et al. 2009; Shikata et al. 2008; Suzuki et al. 2007). Responses have been shown for a variety of vibration frequencies and osteogenic cell lines, and are discussed in more detail later in this chapter. Some examples are also provided in tables 1.3 and 1.4 in the introduction chapter. The work presented in this chapter looked for changes in the osteogenic differentiation of a mesenchymal progenitor cell line (hES-MP 002.5) following stimulation with LMHF vibrations. Tables 4.6 through 4.11 provide an overview of the results obtained.

Figure	Experiment	Response	Media	Comparing
4.15, 4.16	ST vib	MTS	abd	120 Hz higher than 90 Hz
		MTS:DNA	abd	120 Hz higher than static
4.17	ST CM	MTS:DNA	C:abd.T:abd, C:ab.T:abd, C:ab.T:ab	120 Hz(CM) higher than fresh
4.21, 4.22	Ind vib	MTS	abdi, abd	120 Hz higher than static
			ab	120 Hz higher than 60 Hz
		MTS:DNA	abdi, abd, abi	120 Hz higher than static
			ab	120 Hz higher than 60 Hz

Table 4.6: Comparison of short term LMHF vibration effects: MTS. Media indicates media types affected. ST = short term, Ind = indomethacin.

Figure	Experiment	Response	Media	Comparing
4.3	10 min	ALP:DNA	Dif	30 Hz lower than static
4.4	45 min	ALP	abd	24 and 48 hours, 60 Hz higher than static and 15, 30, and 45 Hz
		ALP:DNA	abd	24 hours 60 Hz higher than static and 15, 30, and 45 Hz
				48 hours 60 HZ higher than static, 15 and 45 Hz
4.9	ST vib	ALP:DNA	abd	60 Hz higher than static
4.17	ST transfer	ALP	C:abd.T:abd	120 Hz(CM) higher than static, 60, 90 and 120(CM) Hz higher than fresh
		ALP:DNA	C:abd.T:abd, C:abd.T:ab	90 Hz(CM) higher than fresh
			C:abd.T:abd	120 Hz(CM) higher than fresh
4.22	Ind vib	ALP:MTS	abd	120 Hz lower than static

Table 4.7: Comparison of short term LMHF vibration effects: ALP. Media indicates media types affected. ST = short term, Ind = indomethacin.

Figure	Experiment	Response	Media	Comparing
4.4	45 min	DNA	abd	48 hours, 15 and 30 Hz lower than static
			ab	48 hours, 30, 45 and 60 Hz lower than static
4.8	SF	DNA	SF	$0.03g$, 60 Hz higher than all other vibrated samples
4.15	ST vib	DNA	ab	Static higher than all vibrated samples
4.23	Ind transfer	DNA	C:ab.T:ab	120 Hz(CM) lower than static

Table 4.8: Comparison of short term LMHF vibration effects: DNA. Media indicates media types affected. ST = short term, Ind = indomethacin.

Figure	Experiment	Response	Media	Comparing
4.10, 4.11	0.05 mm	MTS	ab	60 and 120 Hz higher than static
				120 Hz higher than 90 Hz
		Ca:MTS	ab	60 Hz lower than static and 90 Hz
4.12, 4.13	$0.03g$	MTS	ab	120 Hz higher than static, 60 and 90 Hz
		Ca:MTS	abd	30 Hz higher than static, 90 and 120 Hz
4.19, 4.20	0.05 mm CM	MTS	All	Static(CM) significantly lower than fresh(CM)
			C:ab.T:ab	90 Hz(CM) not significantly lower than fresh(CM)
			C:ab.T:abd, C:ab.T:ab	120 Hz(CM) not significantly lower than fresh(CM)
		Ca:MTS	C:abd.T:ab	Static(CM) significantly higher than fresh(CM)

Table 4.9: Comparison of long term LMHF vibration effects:MTS. Media indicates media types affected.

Figure	Experiment	Response	Media	Comparing
4.19	0.05 mm CM	Col	C:abd.T:abd, C:abd.T:ab, C:ab.T:abd	Static(CM) significantly lower than fresh(CM)
			C:ab.T:ab	60, 90 and 120 Hz(CM) not significantly lower than fresh(CM)
			C:abd.T:abd, C:ab.T:abd	120 Hz(CM) not significantly lower than fresh(CM)

Table 4.10: Comparison of long term LMHF vibration effects: Collagen. Media indicates media types affected.

Figure	Experiment	Response	Media	Comparing
4.10, 4.11	0.05 mm	Calcium	ab	120 Hz higher than static and 60 Hz
		Ca:MTS	ab	60 Hz lower than static and 90 Hz
4.12, 4.13	$0.03g$	Calcium	abd	30 Hz higher than static, 90 and 120 Hz
		Ca:MTS	abd	30 Hz higher than static, 90 and 120 Hz
		Ca:Col	abd	30 Hz higher than 90 and 120 Hz
4.19, 4.20	0.05 mm CM	Ca	C:abd.T:abd	Static(CM) significantly lower than fresh(CM)
			C:ab.T:abd, C:ab.T:ab	120 Hz(CM) significantly higher than 60 Hz(CM)
			C:abd.T:abd	60 and 90 Hz(CM) significantly lower than fresh(CM)
			C:abd.T:ab	60 Hz(CM) significantly lower than fresh(CM)
		Ca:MTS	C:.abd.T:ab	Static(CM) significantly higher than fresh(CM)

Table 4.11: Comparison of long term LMHF vibration effects: Calcium. Media indicates media types affected.

The initial experiments using 10 minutes of vibration produced only one significant difference between conditions, in the form of a reduction in ALP activity per pg DNA (figure 4.3). The inclusion of the two different collection time points showed the increase in ALP activity and DNA content continuing for some time after the vibration had been applied. This suggests that the cells are still proliferating at roughly the same rate across conditions. As the literature suggested that longer stimulation periods may be required to induce a response, the experiment was repeated with 45 minutes LMHF vibrations on day 6. This change in conditions produced significantly higher ALP activity at both timepoints where the cells had been stimulated at 60 Hz. There was also a significantly lower amount of DNA present within samples for those vibrated at higher frequencies after 48 hours. Interestingly, while the change in ALP activity was seen only for the cells cultured in abd media, the decrease in total DNA was also seen in cells cultured in ab supplemented media. The amount of DNA present increased between the two timepoints (24 and 48 hours after vibration), but was significantly lower than static controls after 48 hours. When taken together with the increase in ALP activity, this suggests an additive effect of vibration and chemical stimulation with dexamethasone, where cells are pushed further towards an osteogenic phenotype.

The change in DNA content could be due to loss of loosely adhered cells after vibration and this was investigated separately. Fluorescence microscopy of the cells with and without vibration showed no differences in the cell shape or cell number (figures 4.5 and 4.6. The cells did not appear to be changing shape or lifting from the surface. As the cell counts showed no significant differences between static and vibrated samples, the reduction in DNA content in vibrated samples is likely due to changes in cellular behaviour resulting in reduced proliferation. In the case of the 60 Hz vibration, the increased ALP activity suggest osteogenic

differentiation of the cell line. Although the 2 hour timepoint was relatively soon after vibration, a 24 hour timepoint may not have provided clear data due to changes in proliferation expected over the time period.

In other experiments, the effect of keeping the cells on the bench during vibration compared with keeping them in the incubator throughout culture was investigated. The change from 37°C to room temperature, along with an altered humidity and CO_2 pressure may be expected to have an effect on cell behaviour. Although the change in conditions produced a slight inhibition of metabolic activity this was not significant. There were also no significant differences in total DNA or ALP activity of the cells. Future experiments continued to use the static control which was kept on the bench alongside the stimulated cells.

Serum free media was tested and had no effect on the ability of cells to respond to vibration. Two different modes of vibration (constant amplitude and constant acceleration) were also tested to look for different effects on the cells. Interestingly, the change in ALP activity seen previously in cells vibrated at 60 Hz and constant acceleration was no longer evident. It is possible that this is due to a change in the batch of FCS used for general culture within the lab. The cells were tested for normal growth behaviour before using the new serum for experiments, but it is possible that a change in the growth factors and signalling molecules present within the new batch had effects on the differentiation of the cells. Although the cells were vibrated in serum free media, they were subsequently returned to normal media for culture. This may have acted to quench any signalling response the cells were initiating. Alternatives to the use of serum with the hES-MP cells were tested by an undergraduate student under my supervision, but the cells were found to respond poorly to the culture conditions. Passage number was unlikely

to have had an effect as this was kept between 7 and 14 for experiments, and the cells have been shown to exhibit consistent behaviour up to passage 20 (Karlsson et al. 2009). The cells exhibited the expected response to the inclusion of dex in the media, showing increased ALP activity and a reduction in cell number. The use of differentiation media (abd) does not appear to have any significant effects on the metabolic activity of the cells.

Long term vibration experiments were conducted using both constant amplitude and constant acceleration vibration. Both conditions were used after the results from the serum free experiments gave unexpected results. Samples were vibrated for five days with two days rest for two weeks of the culture period. Several *in vivo* LMHF vibration protocols have applied the stimulation on 5 or fewer days of each week (Flieger et al. 1998; Gusi et al. 2006; Rubinacci et al. 2008). Although such *in vivo* stimulation was applied for months, the three week protocol was used during these experiments to look for early changes in the behaviour of the mesenchymal progenitor cell line. For the long term vibration at 0.05 mm, cells showed higher metabolic activity for samples cultured in abd media. For this condition, the significant increases are for 60 Hz compared to static and 120 Hz compared to both static and 90 Hz. There is no change in the collagen matrix but a change in mineral content is present for cells in ab supplemented media (120 Hz vs static and 60 Hz). This suggests that the presence of dexamethasone may be masking a response to the mechanical stimulus for some vibration regimens. The ratios of calcium to collagen show no significant changes, while there is a significant decrease in calcium:metabolic activity for 60 Hz samples compared to static or 90 Hz. This shows that the vibration at 60 Hz and 0.05 mm constant amplitude has different effects on the metabolic and ALP activity of cells than 60 Hz vibration at $0.03g$. This seems to indicate that

maintaining constant amplitude is more important than constant acceleration with changing frequency.

For the long term $0.03g$ vibration with ab supplemented media, there was significantly higher metabolic activity for samples vibrated at 120 Hz compared to all conditions except 60 Hz. While there were no significant differences in collagen production for any of the samples, calcium levels were significantly higher for the 30 Hz samples compared to all but 60 Hz samples in abd medium. This effect is different from that seen with the 0.05 mm vibration and is interesting as it suggests that the vibration at 120 Hz has some effect on metabolic activity (either an increase in cell number or change in the metabolic behaviour), but that 60 Hz affects the mineralisation. This is a further difference to the 0.05 mm results as the effect of LMHF vibration is seen only with samples treated with dexamethasone. The differences in loading regimen may be affecting cells in different ways, with the two regimens suited to cells in differentiation states (0.05 mm for progenitors, $0.03g$ for chemically differentiated).

While none of the vibration conditions affect the amount of collagen produced, the increase in mineral present with the 60 Hz suggests the presence of a more bone like matrix. The ratio of calcium to collagen shows significant increases for 60 Hz with respect to 90 and 120 Hz for the abd media samples. This again suggests a shift in the composition of the matrix. As the cells may produce a collagen based ECM via other differentiation pathways, this data suggests vibration may be useful for osteogenesis. Further work looking at the type of collagen present in various conditions may show changes in the composition, rather than amount of the collagen matrix. Taken together, the data gathered suggests that sensitivity of cells to LMHF vibration may only occur for exact sets of stimulation condi-

tions (Judex et al. 2007; Uzer et al. 2012; Shikata et al. 2008; Bacabac et al. 2006).

Cells undergoing mechanical or chemical stimulation may undergo changes in the expression of a variety of molecules due to cell differentiation or responses to stimuli. Although this response may be confined to the stimulated cells, it is also possible that it may involve the release of soluble factors into the surrounding environment. To investigate soluble factors, conditioned media taken from vibrated cells was placed onto non-stimulated cells. The osteogenic differentiation of these cells was investigated for long and short term experiments. The 0.05 mm vibration was chosen as the vibration regimen as it was the most reliable method of stimulation with the equipment.

In the short term, the main effects seen were between samples maintained in fresh media throughout the culture period and those receiving media from vibrated cells (C:abd.T:abd media, CM recipients, see figure 4.17). This caused an increase in the ALP activity, which was also significant for 120 Hz compared to static (cells kept on the bench for 45 minutes without vibration). Ratios showed that the ALP:DNA was significantly higher in samples treated with media from the higher frequencies (90 and 120 HZ) compared to fresh. Interestingly, the ratio of MTS:DNA was significantly higher in samples receiving media from cells vibrated at 120 Hz compared to fresh for most media formulations. These results suggest that the vibration may cause cells to release soluble factors which change the ALP production and metabolic activity of other cells. The cells vibrated at 120 Hz showed a reduction in the DNA content, as well as an increase in metabolic activity:DNA seen in the cells receiving their media during transfer.

For the long term transfer experiments, there was a significant decrease in the metabolic activity measured by MTS assay of vibrated samples compared to static controls, with exceptions for 3 conditions (C:ab.T:abd for static vs 120 Hz and C:ab.T:ab for static vs 90 or 120 Hz). This uniform decrease in viability in samples with conditioned media compared to fresh media suggests a lack of available nutrients or a build up of harmful waste products in the conditioned media. The media did not change significantly in colour from fresh media, suggesting that there had not been a large change in pH (results not shown). Such a change in pH would have been indicative of build up of waste products within the media. The reduced metabolic activity is accompanied by a similar reduction in the production of the collagen by the cells, which may be indicative of the osteogenic differentiation of the cells. Calcium production was significantly lower in several conditions compared with static controls. For the samples with ab supplemented initial culture media the only significant difference is higher levels of calcium production at 120 Hz compared with 60 Hz. This occurred despite the apparent detrimental effects of the conditioned media on metabolic activity and may further suggest increased osteogenic differentiation. The ratios calculated for this data set give a single significant difference (calcium:metabolic activity, C:abd.T:abd, control vs 90 Hz).

A preliminary experiment was conducted to see if the vibration stimulus caused NFκB activation in the cells. Fluid flow stimulation in MLO-A5 cells has been shown to cause translocation of the NFκB subunit p65 to the cell nuclei (Morris et al. 2010). The results are presented in figure 4.25 and showed that vibration at the frequencies tested did not elicit a similar response. Due to a limited supply of the required antibodies, only static, 30 Hz and 60 Hz conditions were tested.

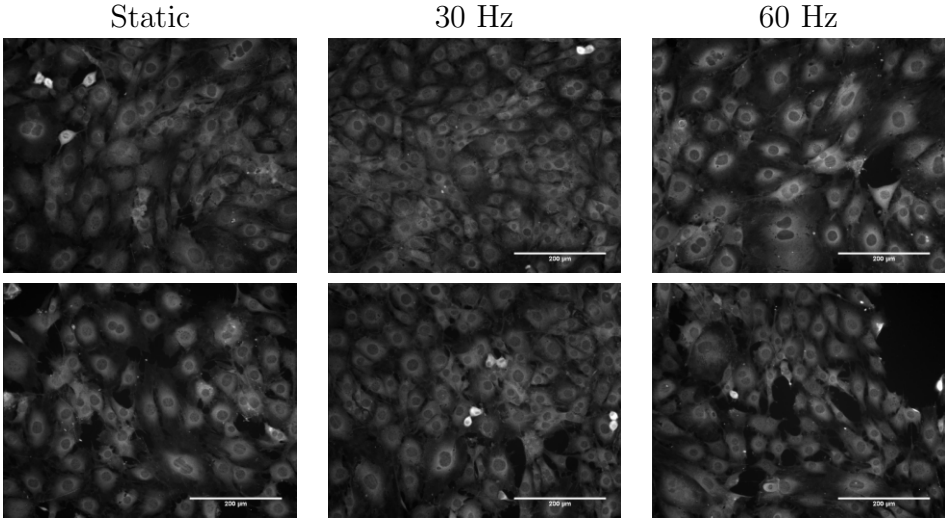

Figure 4.25: NFκB staining in vibrated hES-MP cells.

In order to further investigate the responses of the cells to the vibration stimulus, cells were treated with indomethacin 30 minutes before vibration and for 2 hours after vibration. This was used to block cell signalling by prostaglandins, which may play a role in the transmission of the vibration stimulus (Thomas and El Haj 1996). Prostaglandin E_2 has been shown to be involved in the response of osteocytes to fluid flow (Morris et al. 2010), and there may be a similar response to other forms of stimulation in bone cells. Blocking this response may reduce the efficiency of vibration as an osteogenic stimulus for stimulated cells or those receiving conditioned media. There were significant increases in the metabolic activity of cells vibrated at 120 Hz compared to static (abd and abdi media) or 60 HZ vibration in ab supplemented media only. There were no effects on the ALP activity or total DNA within the samples. There was a significant decrease in ALP activity per metabolic activity for the 120 Hz vs static samples in abd media. There were significant increases in the metabolic activity per ng DNA for the 120 Hz samples compared with static (abdi, abd and abi conditions) or 60 Hz (ab). This shows that the MTS assay in this case has not been an accurate reflection of the cell number within the samples. A change in the metabolic activity of the

cells has not been accompanied by an increase in the total DNA content, which suggests that the increased activity is not due to cell proliferation.

The indomethacin experiment was also used to test the effects of indomethacin in the transfer media on the behaviour of the cells. There were no significant differences in any of the measures of cellular behaviour used. While this may suggest that it is not the appropriate pathway for the communication of cells during application of vibration stimuli, it is important to note that for these experiments, there was no increase in ALP activity in the vibrated cells either. There was also high variability in the results and it is possible that prostaglandin signalling may still be involved in the response to transfer media.

The ALP response seen in the initial vibration experiments does not appear to have been translated into corresponding increases in matrix deposition, or alterations in the matrix composition. It has been noted previously in the literature that levels of ALP activity may not be proportional to mineralisation (Hoemann et al. 2009). Although there were some responses with the long term vibration resulting in changes in the matrix composition, consistent long term effects on matrix deposition were not found. Responses were seen at different frequencies to those predicted by short term experiments and large differences between samples cultured in ab or abd supplemented media were not seen in the long term experiments. This may be due to over confluence in the cells in all conditions, meaning that cells which were proliferating more slowly (due to differentiation) will reach comparable numbers to faster proliferating cells by the end of culture. It would be interesting to look at the total DNA content present within cells after 3 weeks of culture, which would indicate whether there were differences in the cell number between conditions or if comparable numbers were

reached. This was not investigated during these experiments as lysing of the cells after culture would have caused damage to the ECM before staining.

As the results from the indomethacin experiment showed a change in the ratio of metabolic activity to total DNA, it is possible that there are differences in the cell number not seen by the MTS assay. As the amount of DNA is constant per cell, a change in the MTS assay with respect to this shows a change in the cellular behaviour. This could be due to changes in gene or protein expression, rearrangement of cellular structure or a response to stress or apoptosis. The data also highlights limitations in the use of metabolic activity assays as an indicator of relative cell number when there is the possibility of changes in behaviour. This is especially likely when cells are being stimulated to study a particular effect. While the metabolic activity may drop drastically if a treatment is detrimental to the cell viability, it is possible that more subtle changes in cell number and relative metabolism in cells treated differently may be missed. It has also been suggested that there may be problems with the use of many common cell proliferation assays when moving to high density 3D cultures (Ng et al. 2005).

In vivo work has shown much variability in the success of LMHF vibration in improving bone mineral density (BMD) and structure. Many studies have demonstrated positive effects of LMHF vibration on bone in postmenopausal women (balance improvement and reduction in fall frequency (Gusi et al. 2006; von Stengel et al. 2011), increase BMD in some areas (Beck et al. 2006; Rubin et al. 2004; Rubin et al. 2001, reviewed in Rubin et al. (2006, Andrews (2010)), but studies by other groups have shown different results. For example, studies in healthy patients have not shown any effects on bone mass, structure or strength at any bone site (Torvinen et al. 2003). Research has also shown that vibration does

not enhance exercise in osteoporotic patients other than a reduction in falls (von Stengel et al. 2011), although they did not examine the effects of vibration alone. Bone turnover markers were also unchanged and the only altered physical test was an increase in jump height. Stimulation at $0.3\,g$ was shown to be osteogenic for children with disabling conditions (90 HZ) (Ward et al. 2004) and young women with a low BMD (30 Hz) (Gilsanz et al. 2006), as well as reducing IVD swelling during extended bed rest (30 Hz, also $0.5\,g$) (Holguin et al. 2009). Most studies also only require short periods of loading to have effects (10-20 minutes), which is advantageous in increasing compliance. It has been suggested that there may be a benefit of the application of LMHF vibration to improve implant integration (Zhao et al. 2009), but most human trials suggest benefits only for diseased, damaged or sub-standard tissue.

There has been a much greater body of research in animal models. 30 Hz, $0.3\,g$ vibration can improve BMD and trabecular structure in healthy sheep (Rubin et al. 2002; Rubin et al. 2002), as well as increasing trabecular stiffness and providing more uniform distribution of strain within trabecular bone models (Judex et al. 2003). Research in rats and mice has provided data on healthy and ovariectomised (OVX) animals, including beneficial effects on bone for a variety of stimulation conditions in healthy (Christiansen and Silva 2006), growing (Xie et al. 2008; Xie et al. 2006) and OVX animals (Flieger et al. 1998; Judex et al. 2007; Oxlund et al. 2003; Rubinacci et al. 2008; Sehmisch et al. 2009). The use of LMHF to reduce the effects of disuse or bedrest in mice and rats has also proved successful (Judex et al. 2005; Garman et al. 2007; Rubin et al. 2001). Benefits in fracture healing in OVX and healthy rats have been described (Shi et al. 2010; Leung et al. 2009), as well as some effects on muscle tissue (Oxlund et al. 2003; Murfee et al. 2005). Lack of effect in cortical bone has been noted (Sehmisch et al. 2009; Rubin

et al. 2002), as well as no change for healthy animals (Castillo et al. 2006). The beneficial effects include trabecular number, thickness and spacing, bone strength, prevention of bone loss, increased bone formation and inhibition of osteoclast formation or activity. The conditions used vary greatly, although $0.3\,g$ is often used, as are frequencies of 45, 60 and 90 Hz.

In vitro studies are fewer in number, but also show large ranges of vibration regimens, as well as cell types and responses. Broad frequency vibrations have been shown to upregulate osteocalcin and MMP-9 mRNA levels in MC3T3 cells, but have no effect on ALP activity or other matrix components (Tanaka et al. 2003). Upregulation of ALP and collagen I expression have been seen in another cell line, using 60 Hz vibration for 45 minutes (Pre et al. 2009). Higher levels of osteoblast activity, as well as suppression of osteoclast activity has been demonstrated in fish (Suzuki et al. 2007) and regulation of osteoclast size and activity by vibrated osteocytes (Lau et al. 2010). There is also interest in the effects of LMHF vibration on mesenchymal progenitor cells. This includes demonstrating both an increase (hBMSCs, (Pre et al. 2010)) and decrease (rat MSCs, (Lau et al. 2011)) in the mineral deposition by MSCs in osteogenic culture media. Collagen deposition and fibre organisation has also been shown to be improved in vibrated adipose derived stem cells (Pre et al. 2011). Decellularised matrix produced by vibrated osteoblasts shows improved attachment of MSCs, as well as promoting their osteogenic (rather than adipogenic) differentiation (Dumas et al. 2010). Again, *in vitro* studies are usually carried out at $0.3\,g$, and much research has focused on the use of 30 Hz vibration.

The $0.03g$ vibration used in the 2D studies detailed in this chapter was a much lower acceleration than that used in *in vivo* studies. Research has shown that

applied vibrations are not transmitted fully through the musculoskeletal system (Rubin et al. 2003; Kiiski et al. 2008), demonstrating significant reductions in energy through the lower half of the body. Computer modelling has also suggested that the shear stresses occurring in bone marrow during vibration may be similar to those found stimulatory *in vitro*, but may cause much higher stresses on the endosteal bone surface (Coughlin and Niebur 2012). As such, it is possible that the low acceleration loading is sufficient for a simple 2D model which does not suffer from damping effects of muscle and bone tissue. There are a variety of other factors which may affect the response of bone cells to LMHF vibration *in vitro*. It is possible that small changes in the media volume, viscosity or temperature may have much greater effects on the forces applied to the cells during stimulation. For example, ambient temperature changes over the year may be enough to affect the responses seen in cells kept outside the incubator for short periods. A difference of 10% media volume may be enough to significantly alter the behaviour of the fluid during LMHF vibration and therefore affect the cellular response. For experiments using small volumes of media ($<$1 ml), a 10% error may be caused by an accumulation of insufficient removal of media during media changes and minor pipette inaccuracies. Modelling of the fluid behaviour in a variety of different conditions may help provide an insight into the sensitivity of cells to a vibration stimulus.

4.11 Chapter Summary

This chapter has studied the mechanical stimulation of the hES-MP cells with the aim of inducing osteogenic differentiation. A number of stimulation regimens were used, considering early differentiation markers and the deposition and mineralisation of their extracellular matrix. The main results have shown:

- 10 minutes LMHF vibration at $0.03g$ produced a small response.
- 45 minutes gave a significant increase in ALP activity for 60 Hz vibration at $0.03g$. This did not occur consistently in later experiments.
- Constant acceleration ($0.03\,g$) and constant amplitude (0.05 mm) during vibration produced different responses (60 Hz or 120 Hz respectively) indicating sensitivity to exact loading conditions.
- In the long term, the vibration caused changes in the matrix composition under some conditions (90 or 120 Hz, most effects with 0.05 mm vibration).
- High frequency vibrations appeared to increase the metabolic activity of cells.
- The response may not be caused by prostaglandin signalling or NFκB p65 subunit activation.

Further work investigating the response of the cells to different conditions may help to elucidate the mechanisms involved. The final chapter studies the effects of the LMHF vibrations in 3D to see if any responses are found in such an environment. Vibration in 3D is carried out using a selection of mechanically different scaffolds.

Chapter 5

3D Vibration

5.1 Introduction

As discussed in Chapter 3, there are many reasons for the use of a 3D culture environment for tissue engineering. This chapter looks at the effects of vibration in mechanically different scaffolds on the osteogenic behaviour of hES-MP cells.

Initial 3D experiments were conducted by applying direct mechanical compression to single scaffolds, but this method proved inefficient in terms of time. Each sample required 2 hours of loading, plus transfer time, on each day where mechanical stimulation was applied. This made it difficult to produce large sample numbers per experiment. Shorter periods of loading were attempted (see figure 4.1), but with the equipment available this required increased manipulation of the scaffolds, increasing the risk of infections and damage to samples. The low magnitude, high frequency vibration used in 2D experiments (see chapter 4) would allow the stimulation of many scaffolds at once. An increase in the number of scaffolds would allow larger datasets for research and a more commercially viable process for clinical use. The method should also allow the stimulation of con-

structs of different sizes, making it more flexible for different applications. There would be reduced manipulation of the constructs as the vibration could be performed within the culture plate, reducing the risk of construct damage or infection.

As the hES-MP cells had been shown to proliferate well within the gelatin coated PU scaffolds, the combination was used to test the response of mesenchymal progenitors in 3D culture to LMHF vibration. Later experiments included the use of mechanically different scaffolds to see if these produced different cellular responses to LMHF vibration. A scaffold formed from glass pellets was used as a stiff scaffold in an attempt to improve force transmission to the cells. Collagen-glycosaminoglycan (CGAG) scaffolds, which contracted around cells during culture, were used to study cells in a dense matrix environment. Alvetex scaffolds represented a non-woven sheet scaffold, and 3D Insert scaffolds were used as a stiff scaffold with defined architecture. Both Alvetex and 3D Insert are commercially available polystyrene scaffolds, the same material used for standard tissue culture flasks and plates. Further details on the scaffolds are provided later in this chapter and previously in Materials and Methods.

5.2 Cell Distribution and Mechanical Compression

Initial 3D experiments studied the effect of mechanical compressive loading on the distribution of cells within the PU foam scaffolds. Diffusion of nutrients and waste into and out of a scaffold is only possible over a small distance. As mentioned previously, this is approximately 200 μm, after which a flow of nutrients is required to ensure cell survival. In the body, this flow comes from the movement of blood through vessels and capillaries. *In vitro*, pump systems

are often used to ensure a supply of fresh media throughout scaffolds. Such systems have been shown to improve cell viability and construct homogeneity (Goldstein et al. 2001), as well affecting the matrix deposition of osteogenic cells (Morris et al. 2010). During mechanical compression of a scaffold, it is likely that some movement of the surrounding media into and out of the scaffold will occur, increasing nutrient transfer (Sittichockechaiwut et al. 2009). For this project a preliminary study was undertaken by modifying a loading regimen developed previously in the lab to see if frequency of compression cycles affected cell viability.

MG63 cells were seeded into the open cell polyurethane (PU) foam scaffold studied in Chapter 3. Scaffolds were prepared and seeded as described in the Materials and Methods chapter, using 1 cm high cylinders and $5x10^5$ cells. The scaffolds were maintained in ab supplemented media after an initial incubation of 2 hours in a low volume of media. Some samples were collected on day 5 to provide a picture of cell distribution in early culture. On days 5, 10 and 15, samples were subjected to compressive mechanical loading (table 5.1). Regimens were based on previous work using sinusoidal mechanical compression of 5% strain at a frequency of 1 Hz for 2 hours. A Bose ELF3200 was used to apply compression to samples held between metal platens inside the Bose biodynamic chamber. Further samples were subjected to the same number of compression cycles (7,200), but at a frequency of 10 Hz (reducing the loading time to 12 minutes). Control samples were treated as described in Materials and Methods. After loading, samples were transferred to new culture plates and maintained in ab media.

On day 5 or 20 of culture, samples were analysed by MTT assay. Scaffolds were cut into sections to allow imaging of the central regions of the scaffold, and were photographed to check distribution throughout (figure 5.1).

Timepoint	Step	Details
Day 0	Seeding	Scaffolds seeded with $5x10^5$ cells
Day 1	Media	Transfer of scaffolds to new well plates with required culture media
Days 5,10,15	Stimulation	Compressive mechanical loading of scaffolds
Day 20	Endpoint	MTS assay before fixation of cells and staining of ECM (sirius red, alizarin red)

Table 5.1: Timepoints in original compressive mechanical loading regimen.

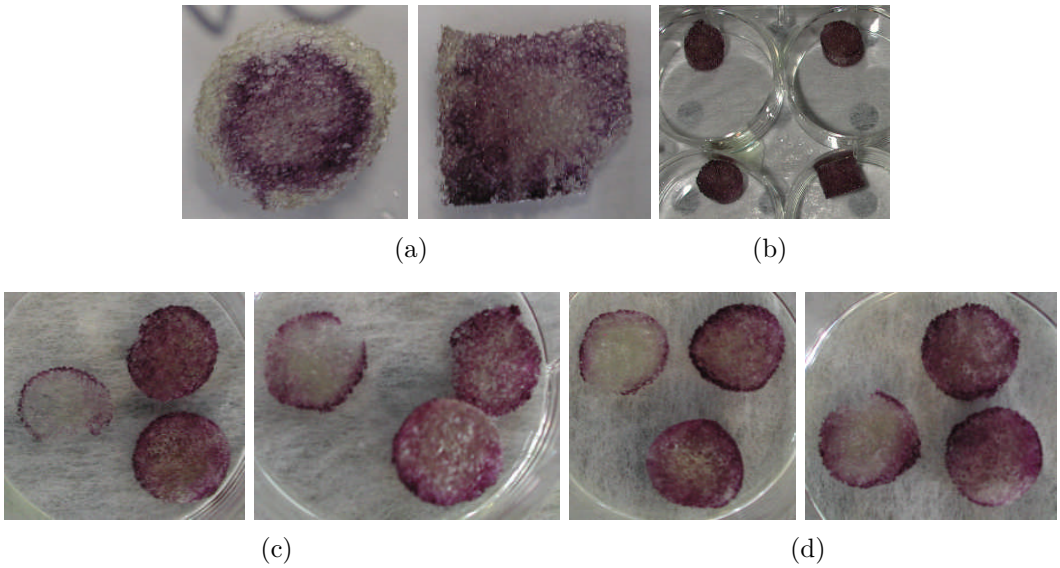

Figure 5.1: MTT images in 1 cm diameter PU scaffolds from 20 day 1 and 10 Hz loading experiment. (a) MTT sections from samples collected on day 5. (b) View of MTT treated 1 Hz samples before cutting on day 20. (c)&(d) Examples of cell distribution in central scaffold regions on day 20. (c) shows 1 Hz and (d) 10 Hz non-loaded (left image) and loaded (right image) samples. Images are representative of repeat experiments, showing slight differences observed between loaded and non-loaded cell distribution.

Samples collected on day 5 showed an even distribution of cells in the centre of the scaffolds, to within a few millimetres of the edge. This showed that the seeding method was effective in introducing cells to the scaffold. After incubating in MTT solution on day 20, samples showed dark purple staining across the whole outside of the scaffolds, indicating high cell numbers due to proliferation. After scaffolds were cut into sections it became apparent that cells were present only in the peripheral regions. This suggests that there may have been cell death in the central regions or migration of cells to the scaffold's outer regions during culture. There were slight differences between samples which had undergone mechanical compression and those which had not. Cells appeared to have remained viable closer to the central regions of the scaffolds where cyclic loading had occurred. The purple colouration appeared more intense in stimulated scaffolds and the band of cells around the scaffold periphery appeared slightly wider than unstimulated counterparts.

Although mechanical compression provided some improvement in the cell distribution within scaffolds, further experiments with mechanical stimulation used LMHF vibrations to stimulate the cells within a variety of scaffolds. This method allows larger numbers of samples to be processed at a time. Shorter scaffolds were used in an attempt to limit the problems with cell distribution noted above.

5.3 LMHF Vibrations and hES-MP Cells in Polyurethane Foams

hES-MP cells were cultured in 4 mm high, 10 mm diameter PU scaffolds to test the effects of LMHF vibration in 3D. Scaffolds were first sterilised by autoclaving

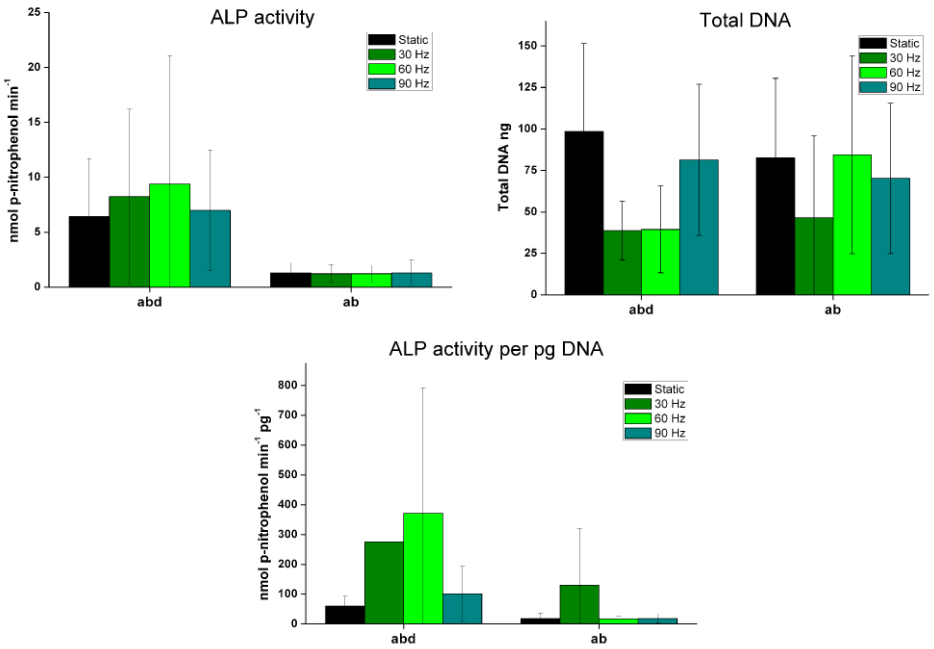

Figure 5.2: 3D LMHF vibration in PU foams, vibrated in 1 ml culture media. Samples vibrated at 30 or 60 Hz showed slightly higher in ALP activity and lower amounts of total DNA (abd and ab media), but results were highly variable and not significant. Mean ± standard deviation, n=9 over 2 experiments.

in 0.1% gelatin to improve the attachment of the hES-MP cells. 2x10 ^{5} cells were seeded in each scaffold in a low volume of media. The media was topped up after 2 hours and scaffolds were maintained in ab or abd supplemented media for 6 days. On day 6 of culture, scaffolds were vibrated at 30, 60 or 60 Hz at constant acceleration, or kept as static controls in 1 ml media. They were returned to the incubator and maintained until day 8, as for 2D experiments (see table 4.2, using only day 8 collection points). Cell lysate was collected for measurement of ALP activity and DNA quantification. These methods are the same as used for the 2D experiments, except that 300 μl of cell digestion buffer was added to scaffolds in 500 μl eppendorfs to ensure coverage of the scaffold.

The results were variable across the different conditions, with no significant differences between frequencies. It was of note that some of the scaffolds could

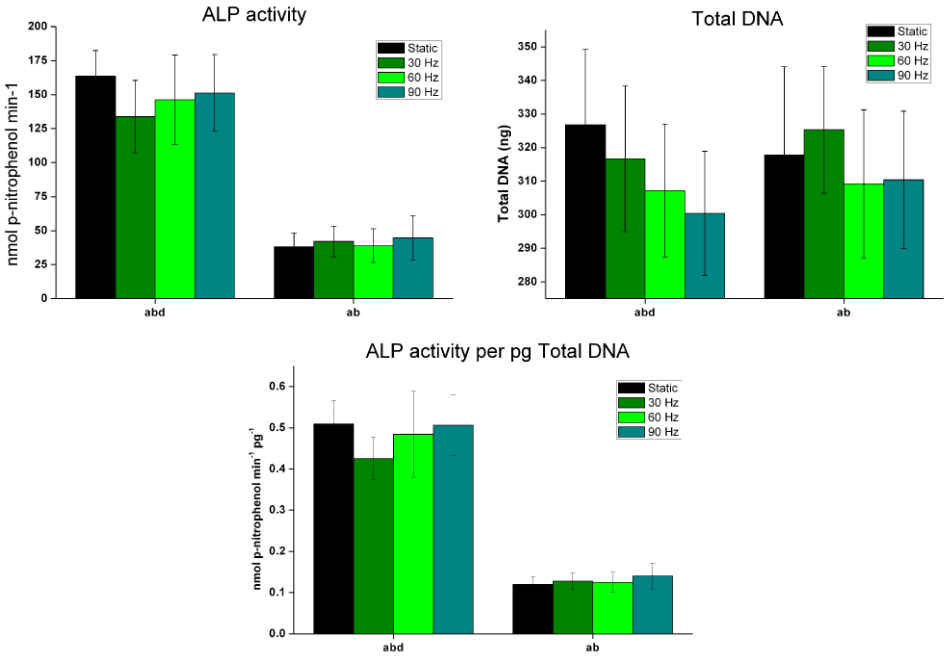

Figure 5.3: 3D LMHF vibration in PU foams, low volume vibration. Data shows lower variability than previous experiment and similar trends in ALP activity and DNA content (abd media). Mean ± standard deviation, n=6 over 2 experiments.

move easily within the media in the plate, suggesting inconsistent contact and transmission of forces. Further experiments were conducted using 500 μl of media during vibration in an attempt to improve contact between the scaffold and the base of the culture plate. The volume was sufficient to just cover the scaffolds whilst preventing them from floating within the media.

Using a lower volume of media reduced the variability between repeat samples. Percentage error in results for the 1 ml vibration was between 45 and 144%, reduced to 5-27% in experiments with a lower volume of media during vibration. However, while there is still a reduction in cell number with increasing frequency this is inconsistent and the higher ALP activity seen in 2D is not present. There is no difference in ALP activity at 60 Hz and a slight reduction in the ALP activity of samples at 30 Hz, although this is not significant.

5.4 Glass Scaffolds Suggest Scaffold Shape is Important as well as Stiffness

In order to investigate whether the loss of an ALP response in 3D compared with 2D experiments was caused by poor force transmission to the cells, a small batch of glass scaffolds was sourced. These scaffolds consist of fused borosilicate glass pellets in cylindrical sections. This type of glass is typically used for microscope slides. As this produces a very stiff scaffold, it was thought that they would allow improved transmission of forces through the scaffold to the cells. Although there are scaffolds available made from bioactive glass, such scaffolds would undergo changes in mechanical properties throughout culture, adding an extra variable to the experiments.

Scaffolds were sterilised as described in the Materials and Methods section and seeded with $2x10^5$ cells in approximately 50 μl of media. After one hour, abd media was added to cover the samples; no samples were cultured in ab supplemented media due to the low sample number available. Samples were subjected to vibration at 60 Hz or kept as static controls in 500 μl of media. As scaffolds would not fit in eppendorf tubes for the collection of cell lysate, they were instead placed in 24 well plates and 300 μl of CDB pipetted through the scaffolds repeatedly.

In the first experiment (set 1), there is a small (though not significant) increase in ALP activity for scaffolds vibrated at 60 Hz compared to static controls. However, this was not repeatable and the higher activity is not seen in experiment 2, which also shows a small non-significant increase in ALP activity but no other effects. There is a large difference in the amount of DNA measured within scaffolds by experiment (an approximately 6-fold increase in experiment 2). This could

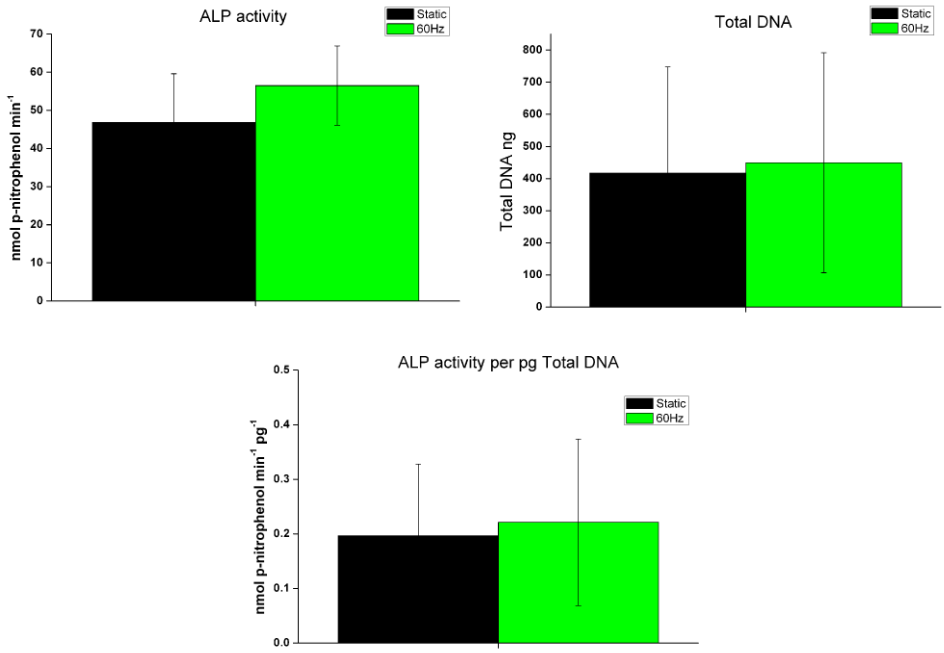

Figure 5.4: 3D LMHF vibration in glass scaffolds. No differences were observed between static or 60 Hz vibrated samples. Mean ± standard deviation, n=6 over 2 experiments.

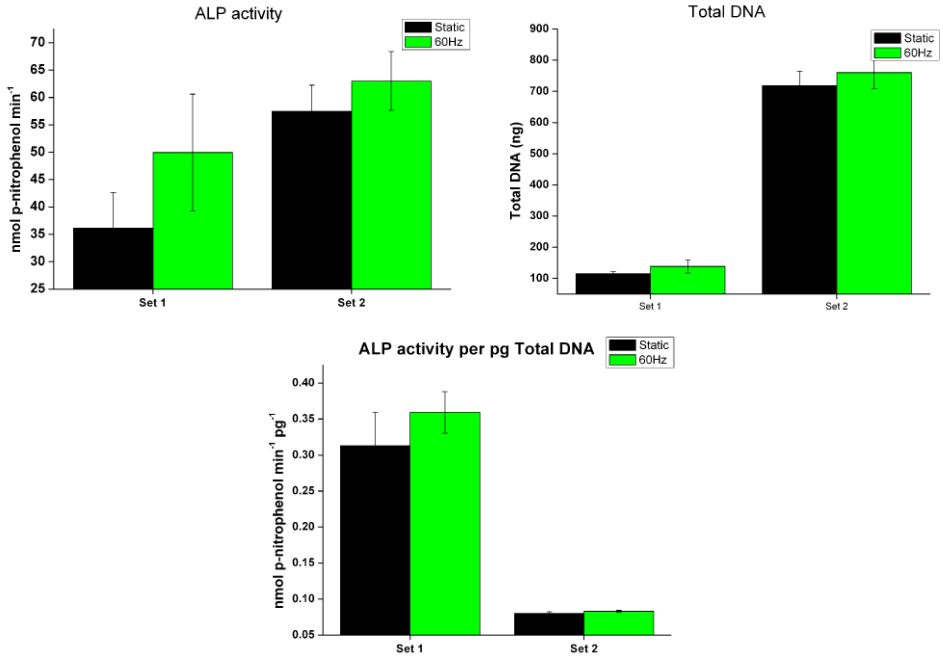

Figure 5.5: 3D LMHF vibration in glass scaffolds by experiment. Individual experiments showed a trend of higher ALP activity in vibrated samples (more pronounced in set 1). Mean ± standard deviation. n=3 for each condition

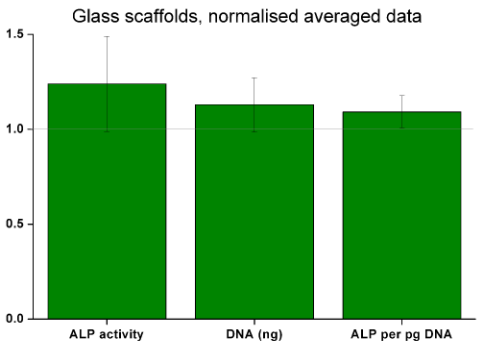

Figure 5.6: 3D LMHF vibration in glass scaffolds (normalised data). Slight increases could be seen for all measures after normalising to static controls. Mean ± standard deviation, n=6 over 2 experiments.

be due to difficulties in extracting the cell lysate within the rigid scaffolds. Normalisation of the data suggested slightly higher values of the outcomes measured, but variability was still high (figure 5.6). Due to the lack of further scaffolds, the experiment could not be repeated.

Although the high variability makes it difficult to interpret this data, the response seemed to be less variable than for the PU foams. Considering the whole data set, the error varied between 18-80%, which is less than that seen in the 1 ml PU experiment, but more variable than the 0.5 ml. For the normalised data, the error was reduced to 7-20%, which is slightly lower than the PU at 0.5 ml. This suggests that rigid scaffolds may be beneficial when using LMHF vibration to stimulate cells. The small effects on ALP activity and reduction in overall variability may indicate that the glass scaffold is slightly better than PU at transmitting vibration forces. Any effect is still difficult to detect and the variability may be due to the inhomogeneity of the scaffold.

5.5 LMHF Vibration, Mechanically Different Scaffolds and Matrix Production

To further investigate the effects of scaffold type on the behaviour of hES-MP cells subjected to LMHF vibration, three scaffolds with differing mechanical properties were investigated. 3D Insert scaffolds (3D Biotek) made from polystyrene were used as a defined, rigid scaffold type with the same chemical properties as normal tissue culture plastic. These scaffolds are designed to fit in a 96 well plate and are approximately 200 μm thick. They have a porosity of 200 μm and a uniform structure with 150 μm diameter fibres. Alvetex scaffolds (Reinnervate) are thin sheets, providing a limited depth 3D environment for cells. They are also made from polystyrene and are sized to fit a 12 well plate. These scaffolds are described as providing an improvement in culture over normal 2D, without creating problems in nutrient and waste transfer. Alvetex scaffolds are 200 μm thick and have a porosity of greater than 90%. For both of these scaffold types, it is recommended to pre-coat the scaffolds to aid cell attachment. As a 0.1% gelatin solution has been used in the previous work, this method was employed for the new scaffolds.

A final scaffold type, a collagen-glygosaminoglycan foam, was kindly donated by Fergal O'Brien. These scaffolds are soft and gel-like and are known to contract around cells during cell culture, providing very high levels of contact between the cells and the scaffold. This could provide a more biologically relevant environment for the cells, providing close contact with an ECM mimicking that found *in vivo*. As low volumes of media would be used during vibration, these scaffolds should remain on the base of the well plate for force transmission. Although the scaffolds are non-rigid, they may be able to provide better transmission of forces to the cells than PU as the material is more closely associated with the cells. In a preliminary

experiment, these scaffolds were tested with mechanical compression, but due to the contraction of the scaffolds they were too small to remain within the platens during loading. Finally, the previously studied gelatin coated PU scaffolds were used as a control.

For these experiments, it was decided to employ calcein staining of the deposited mineral over long term culture of the cells. At the end of the experiments, cells could be examined by fluorescence microscopy for matrix production and mineralisation and the overall distribution of the cells. Further staining of the collagen and calcium was also carried out for relative quantification by sirius red and alizarin red staining.

Cells were seeded on day 0 of culture and scaffolds were prepared as in the Materials and Methods chapter. PU foams were seeded in metal rings in 12 well plates, and Alvetex in 12 well plates using the provided plastic rings. For 3D Insert and CGAG scaffolds, seeding was carried out in 24 well plates in as small a volume of media as possible to prevent leakage from the scaffolds. Table 5.2 shows the cell number for each scaffold type, which varied due to large size differences in scaffolds. Cell number was adjusted to keep similar numbers of cells per unit total volume across the different scaffolds, based on the initial scaffold volume. After 24 hours, samples were transferred to ab or abd supplemented media in 12 well plates ready for vibration.

Samples were subjected to 60 or 120 Hz vibrations ($0.03g$) on days 6-10 and 13-16 of culture (see table 5.3 for regimen details). Vibration was carried out by removing sufficient media such that the scaffolds were still bathed but in full contact with the bottom of the plate. This media was kept in separate 12 well

Scaffold Type	Approx. Volume (mm^3)	Cell Number	Seeding Volume (μl)
PU foam	300	$2x10^5$	40
Alvetex	76	$5x10^4$	1000
3DInsert	32	$5x10^3$	15
CGAG	300*	$2x10^5$	40

Table 5.2: Cell culture information for final scaffolds used. * due to contraction, the value given is much higher than the final volume of the scaffolds after culture. Cell number was calculated based on the initial volume.

Timepoint	Step	Details
Day 0	Seeding	Scaffolds seeded with the cell numbers detailed in table 5.2
Day 1	Media	Transfer of scaffolds to new well plates with required culture media
Days 6-10 and 13-16	Vibration	Plates vibrated at specific frequencies for 45 minutes each day. Scaffolds were vibrated in a small volume of media, allowing them to remain in contact with the culture plate
Day 14+	Calcein	Calcein (0.2 mM) included in all media from this point
Day 20	Endpoint	MTS assay, sample fixation and staining of ECM (collagen antibody, sirius red, alizarin red)

Table 5.3: Timepoints in long term LMHF vibration regimen. Media changed every 2-3 days as required.

plates in a cell culture incubator and replaced once vibration had finished. Calcein was added to the media (working concentration 0.2 mM) from day 14 and to all subsequent media changes. This was to allow the incorporation of the fluorescent molecule into any mineralised matrix produced from day 14 onwards. On day 20, samples were washed once with PBS before covering with MTT solution for 40 minutes. After rinsing gently with PBS, samples were photographed to show cell distribution. The samples were then fixed in 2.5% glutaraldehyde for 10 minutes. After washing with PBS, samples were kept in PBS at 4 °C overnight before immunostaining for collagen I (as described in Materials and Methods).

Figure 5.7: Cell distribution in mechanically different scaffolds, MTT assay. Images shown are of samples in a 12 well plate, internal diameter of each well is 22 mm. Purple colouration shows the location of actively respiring cells. Representative images are shown for each condition and scaffold type which demonstrate the arrangement of cells in each case.

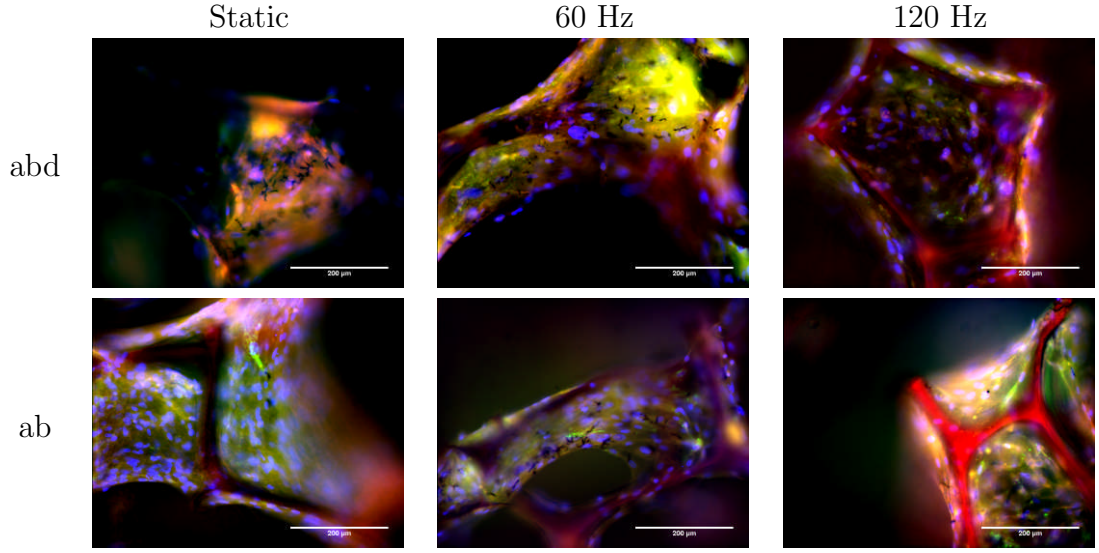

Figure 5.8: Calcein fluorescence and collagen I staining, PU, Axon. Images show calcein (green), collagen I (red) and DAPI (blue). Cells were spread over all scaffold surfaces and mineralisation was evident in many small nodules over the ECM in all conditions. Representative images, scale bar shows 200 μm.

The MTT results (figure 5.7) suggest that there is more metabolic activity for cells seeded in all scaffolds in ab supplemented media. This is consistent with 2D MTS results. 3DInsert and Alvetex scaffolds showed visibly darker colouration in those scaffolds subjected to 120 Hz vibrations compared to other conditions.

After immunostaining for collagen I and the addition of DAPI to label cells, the samples were imaged using the AXON ImageXpress system (figures 5.8 to 5.11). 5 Image sets, consisting of DAPI, calcein and collagen images, were taken from each sample.

The images show the dark patches seen previously during imaging (figures 3.12 and 3.13), but demonstrate the presence of mineralised matrix within all of the scaffolds. However, in some cases (particularly the PU and CGAG scaffolds), there were high levels of background interference in the images. This is due to the presence of large quantities of fluorescent material outside the focal plane. In order

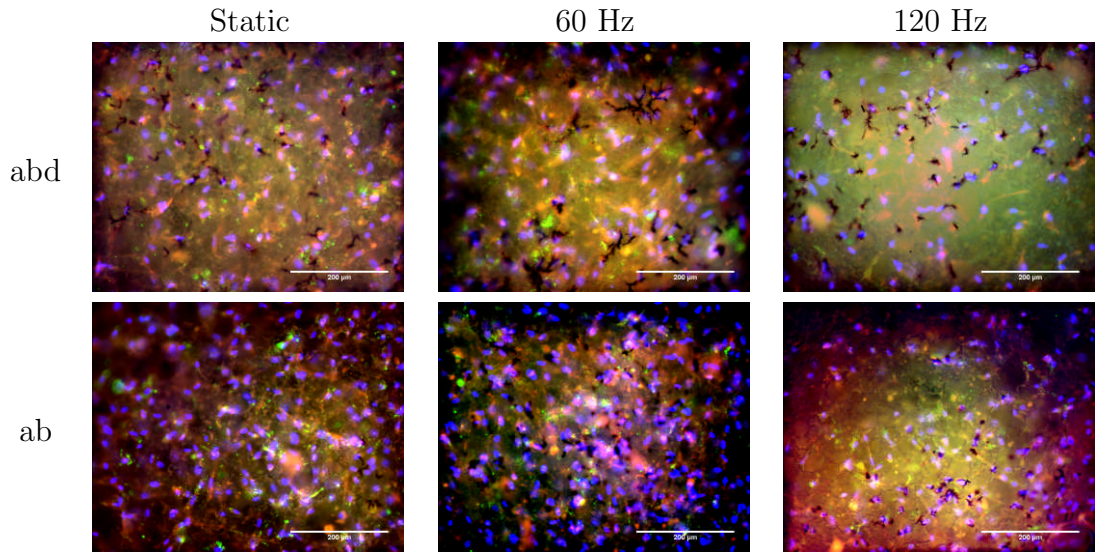

Figure 5.9: Calcein fluorescence and collagen I staining, Alvetex, Axon. Cells were spread over the scaffold surface in some areas and showed some larger calcium deposits. Images show calcein (green), collagen I (red) and DAPI (blue). Representative images, scale bar shows 200 μm.

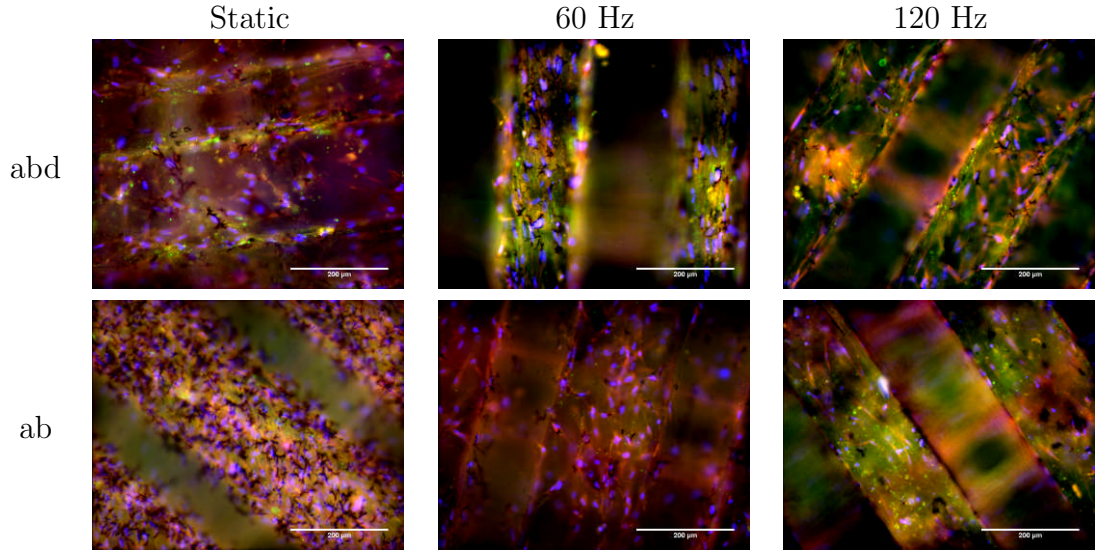

Figure 5.10: Calcein fluorescence and collagen I staining, 3D Insert, Axon. Cells were well spread over the scaffold surface, with cell density appearing higher in ab media. Mineralisation was evident in all conditions, especially for samples vibrated at 60 Hz (abd) media or 120 Hz (ab media). Images show calcein (green), collagen I (red) and DAPI (blue). Representative images, scale bar shows 200 μm.

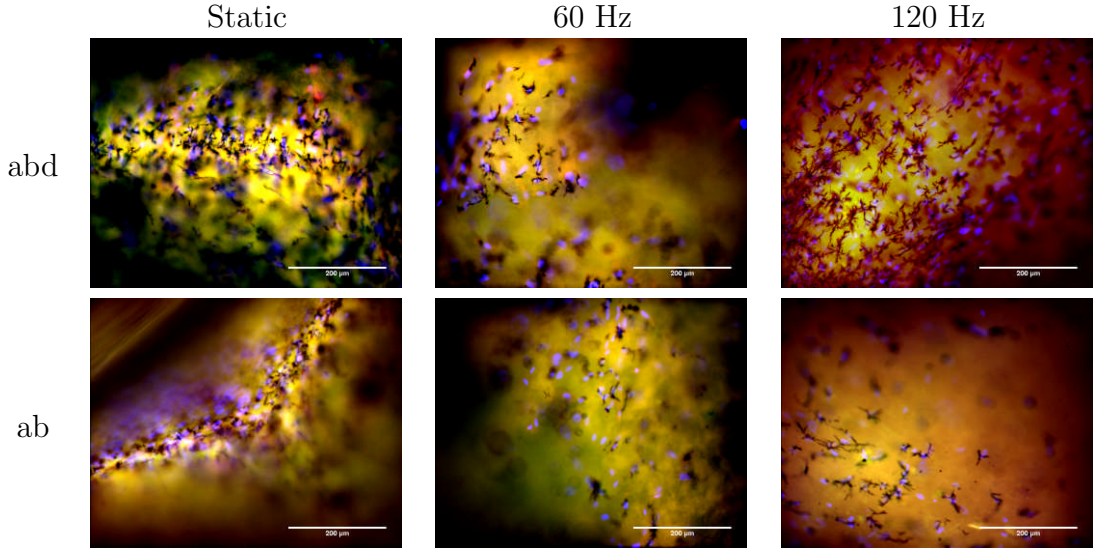

Figure 5.11: Calcein fluorescence and collagen I staining, CGAG, Axon. Samples were difficult to image due to high interference from out of focus scaffold regions. Mineralisation was evident in all conditions but collagen staining was non-specific between cell ECM and scaffold. Images show calcein (green), collagen I (red) and DAPI (blue). Representative images, scale bar shows 200 μm.

to combat this interference, further images were obtained using a Zeiss LSM520 confocal microscope. After obtaining images from several scaffold types with the confocal microscope, it was observed that there were much larger amounts of calcein present than expected (figure 5.12). These bright patches had a feather like appearance and appeared to correlate with the dark patches seen in the collagen I images taken on the Axon.

These patches were theorised to be the MTT, which had not previously interfered with the imaging of calcein. As the axon uses a mercury lamp to excite the specimen, whereas the confocal uses a laser, it was suspected that the difference in images came from the intensity of light exciting the specimen. Mercury lamps show a very low intensity of emission around 480 nm compared to 543 nm. As the laser provides high intensity light at the required wavelength, it appears to be exciting the formazan product present in cells after the MTT assay, causing it

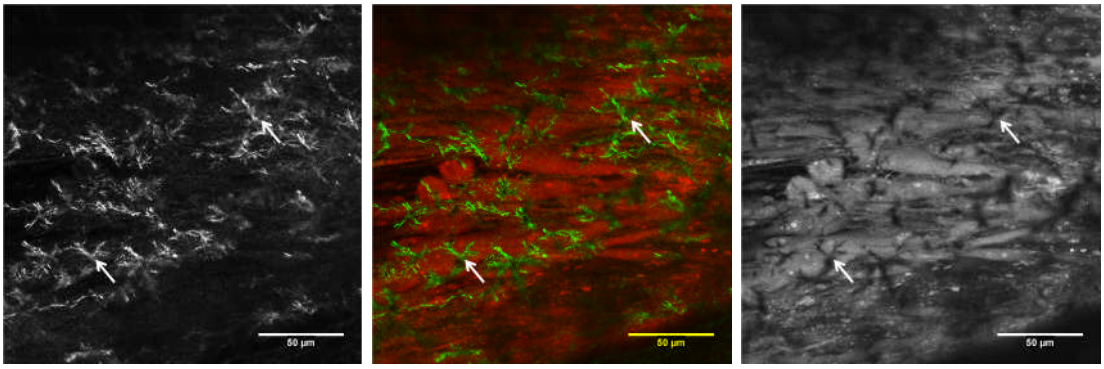

Figure 5.12: Confocal images in 3D Insert scaffolds showing feather patches. Calcein (left), collagen (right) and combined (centre) images of cells and matrix. Arrows indicate feather patches in the collagen staining and corresponding fluorescence on the calcein imaging. Scale bar shows 50 μm.

to fluoresce. As this fluorescence was stronger than the calcein (possibly due to greater levels of formazan compared to calcein), it prevented successful imaging of the mineralised matrix. Control samples (MTT only, calcein only and calcein with MTT) were used to study this phenomenon and attempt to negate the MTT signal. Initially, images were taken from the MTT or calcein only samples to demonstrate the differences in structure seen. These were taken using the initial filter set with a 488 nm excitation and a band-pass emission filter of 480-520 nm (figure 5.13).

Lambda stacked images were then obtained to investigate whether the peaks in emission of the two compounds can be separated. Image stacks were obtained using the filter set described above before changing the collected emissions filter to wavelengths between 512 and 522 nm (figure 5.14).

It was found that narrowing the wavelength range of the light which was collected from the samples, as well as reducing the gain on the detector was sufficient to remove the bright fluorescence and show the calcein. Samples were then reimaged using the confocal microscope and new settings to study the matrix

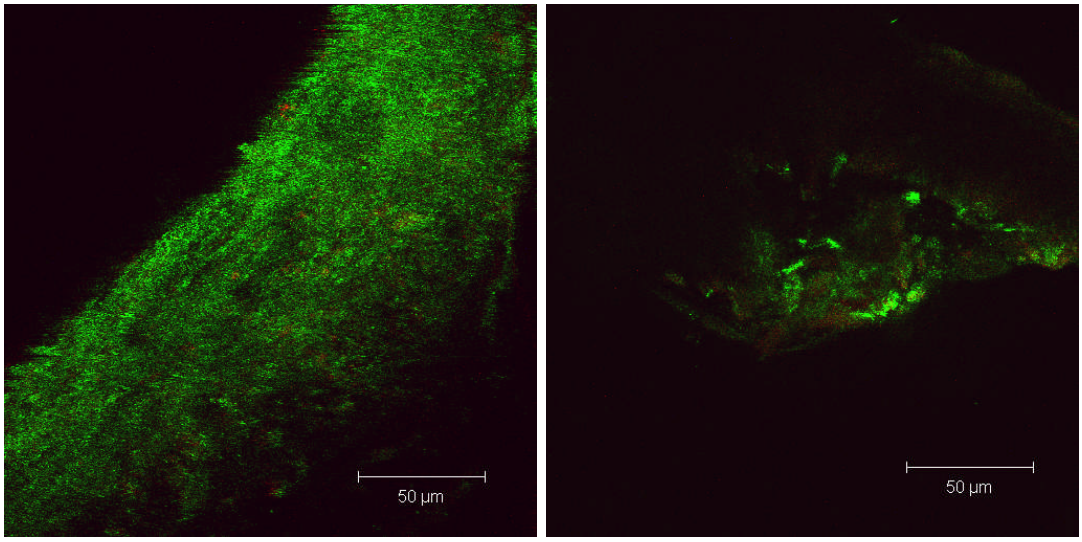

Figure 5.13: Calcein and MTT scaffold controls. Left image shows signal from samples stained with calcein only, right sample with MTT only. Scale bar shows 50 μm.

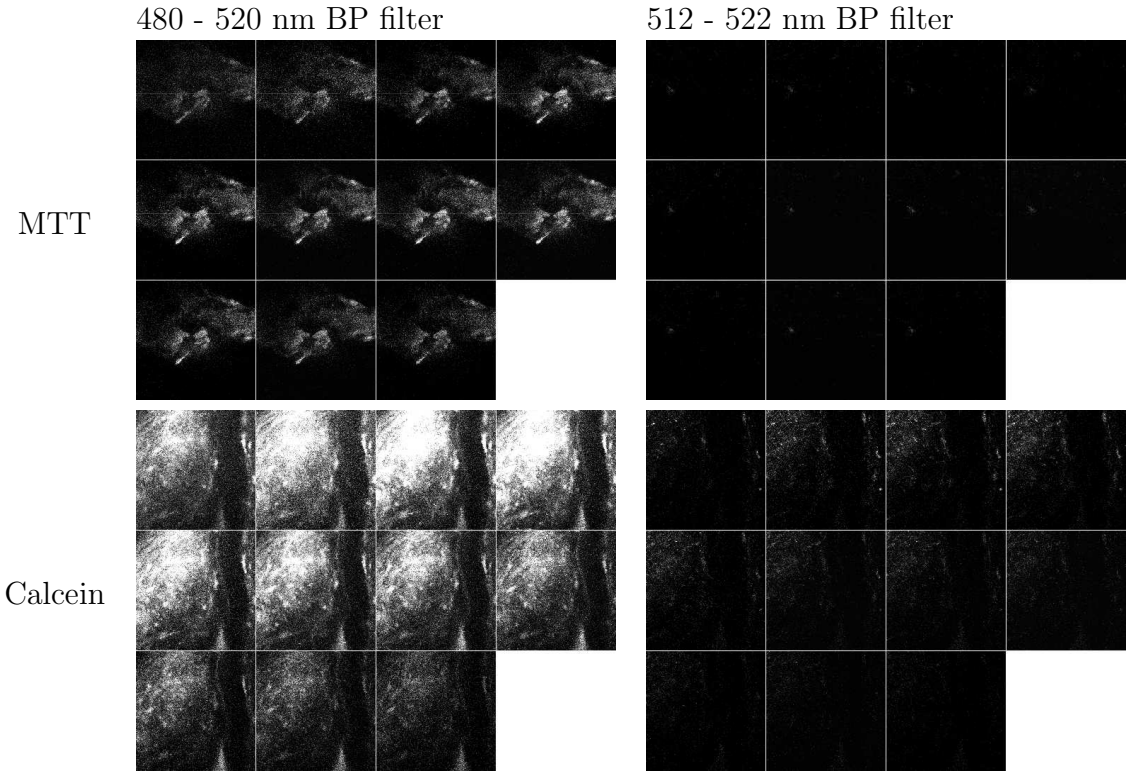

Figure 5.14: Lambda stacked images showing formazan and calcein fluorescence. For each condition, images from left to right show emissions at approximately 10 nm intervals, starting at 506 nm. Images demonstrate the loss of the MTT signal using the 512-522 nm BP filter, which could still be used to image calcein.

3D Vibration

	0 Hz	60 Hz	120 Hz
Dif	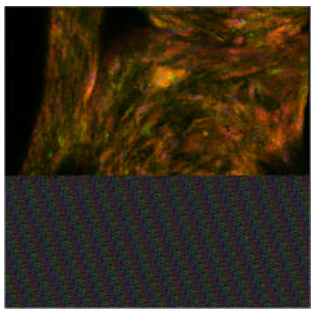		

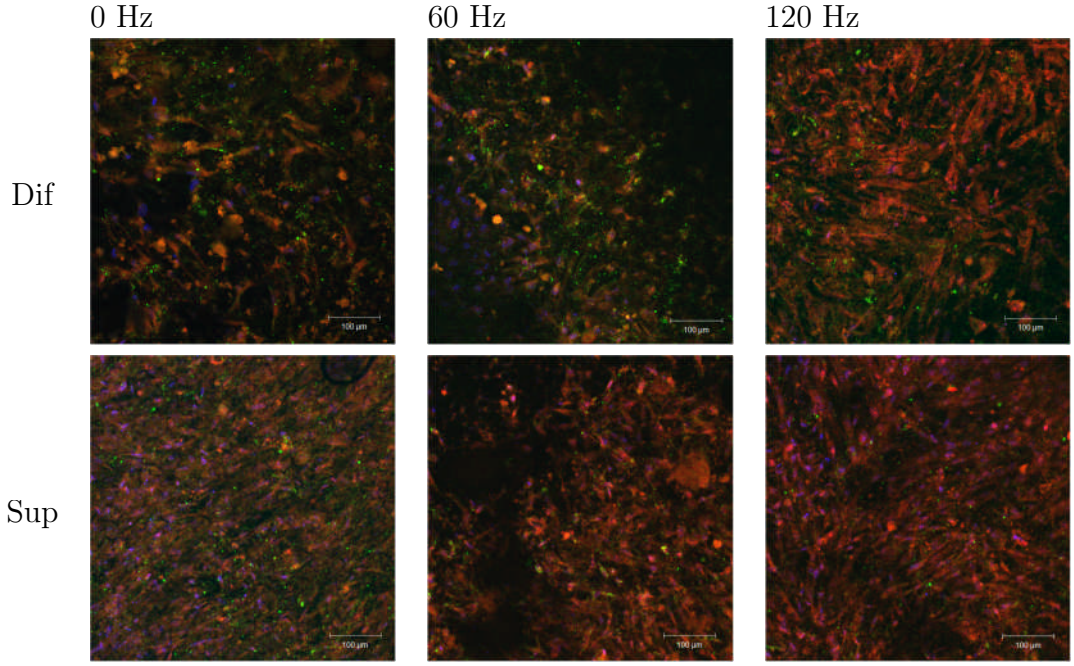

Figure 5.16: Calcein fluorescence and collagen I staining, Alvetex, confocal. Reduction in background fluorescence shows cells more clearly, demonstrating higher cell spreading in ab media and more calcein in abd media. Images representative and show calcein (green), collagen I (red) and DAPI (blue), scale bar shows 100 μm.

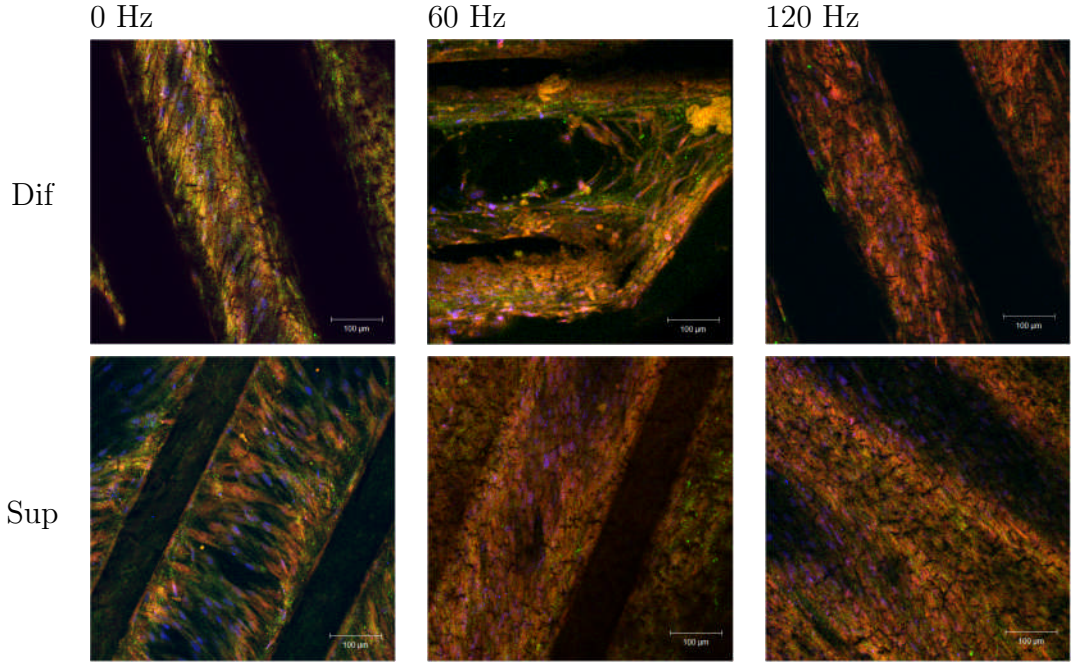

Figure 5.17: Calcein fluorescence and collagen I staining, 3D Insert, confocal. Confocal imaging showed the spread of mineralised matrix (particularly for abd media) more clearly than previously. Images are representative and show calcein (green), collagen I (red) and DAPI (blue), scale bar shows 100 μm.

in the scaffold and producing a mineralised matrix. The cells have also started stretching across the pores, as can be seen in the 60 and 120 Hz images (figure 5.15. This suggests that the cells are creating a mineralised ECM which may begin to have effects on the porosity of the scaffold over a few weeks of culture. Cells were sometimes difficult to locate within Alvetex scaffolds, but there was still evidence of mineralised matrix.

After the fluorescence imaging, samples were then stained using sirius red, followed by alizarin red in an attempt to quantify the matrix production and results are presented in figures 5.18 to 5.20. These assays showed no differences between groups which were statistically significant, however there was some indication that collagen deposition was higher at higher frequencies (figure 5.18). Some samples showed higher calcium levels for 60 Hz, but this was also not significant. Changes in the ratio of matrix components were not consistent, as seen in figure 5.20. PU and Alvetex scaffolds contained the highest levels of collagen after culture, almost double that of the other scaffold types. Alvetex also seemed to promote mineralisation of the matrix in samples vibrated at 120 Hz (ab media, figure 5.19). Several scaffolds demonstrated higher values the ratio of calcium:collagen for vibration at 60 Hz compared to static, suggest increasing mineralisation of the deposited matrix (PU, 3D Insert, CGAG, 120 Hz for Alvetex). In abd media, PU, Alvetex and CGAG showed a reduction in the ratio with increasing frequency, suggesting that the dexamethasone may be masking a mineralisation response to vibration. 3D Insert scaffolds showed a higher ratio at 60 Hz for both media types, although this was not significant.

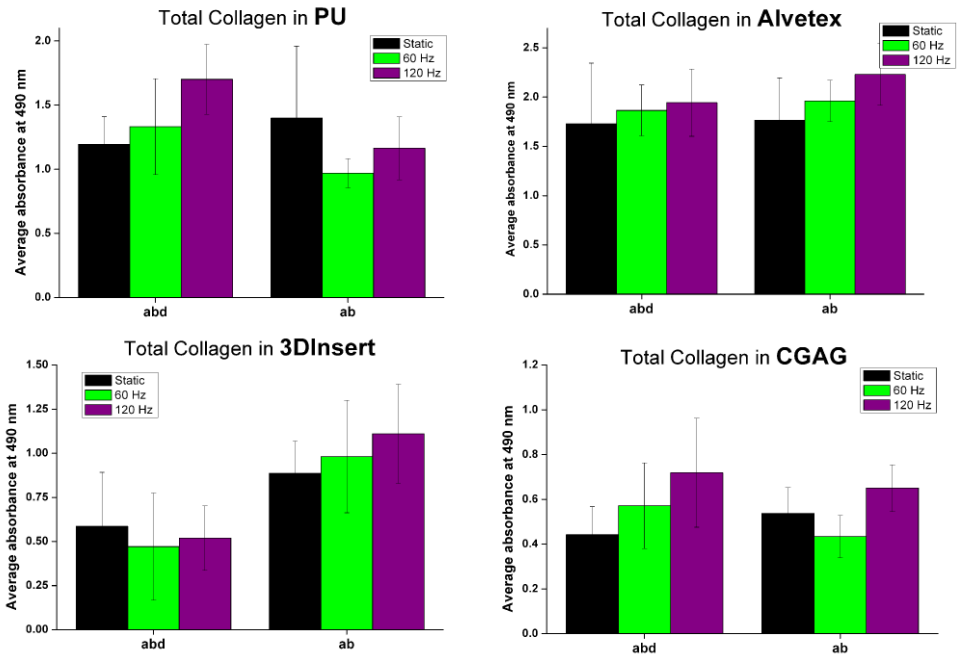

Figure 5.18: Collagen production of hES-MP cells in mechanically different scaffolds. A trend for higher levels of collagen with increasing frequency was seen for some conditions (PU [abd], Alvetex [ab, abd], 3D Insert [ab], GAG [abd]) but was not significant. PU and Alvetex showed highest collagen levels. Mean ± SD, n=4 over 2 experiments

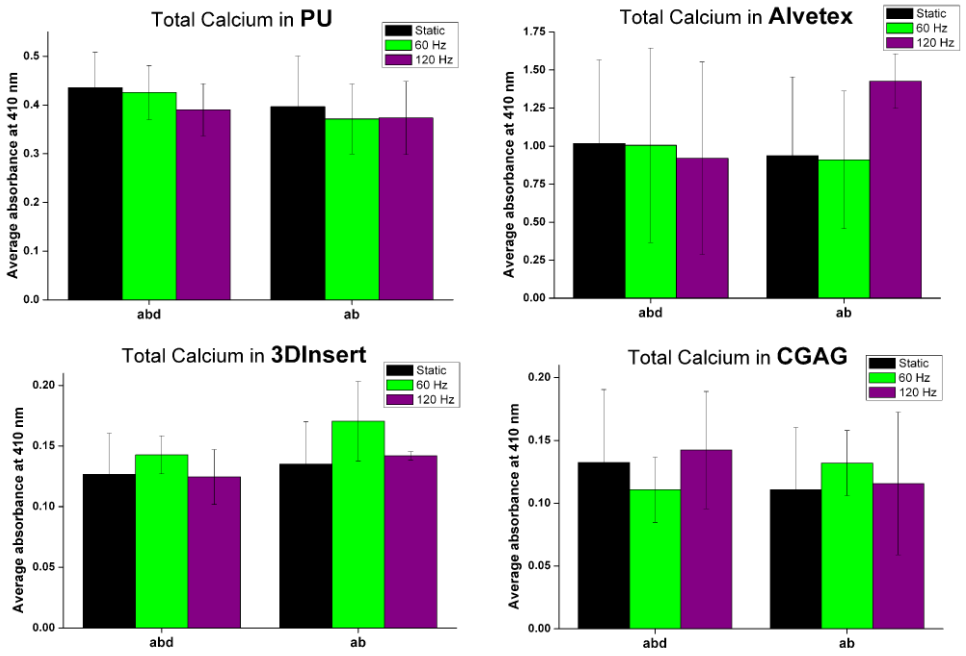

Figure 5.19: Calcium production of hES-MP cells in mechanically different scaffold. Alvetex scaffold contained larger amounts of calcium than any other scaffold type. 3D Insert scaffold showed a trend for higher levels of calcium at 60 Hz in both media types (not significant). Mean ± SD, n=4 over 2 experiments

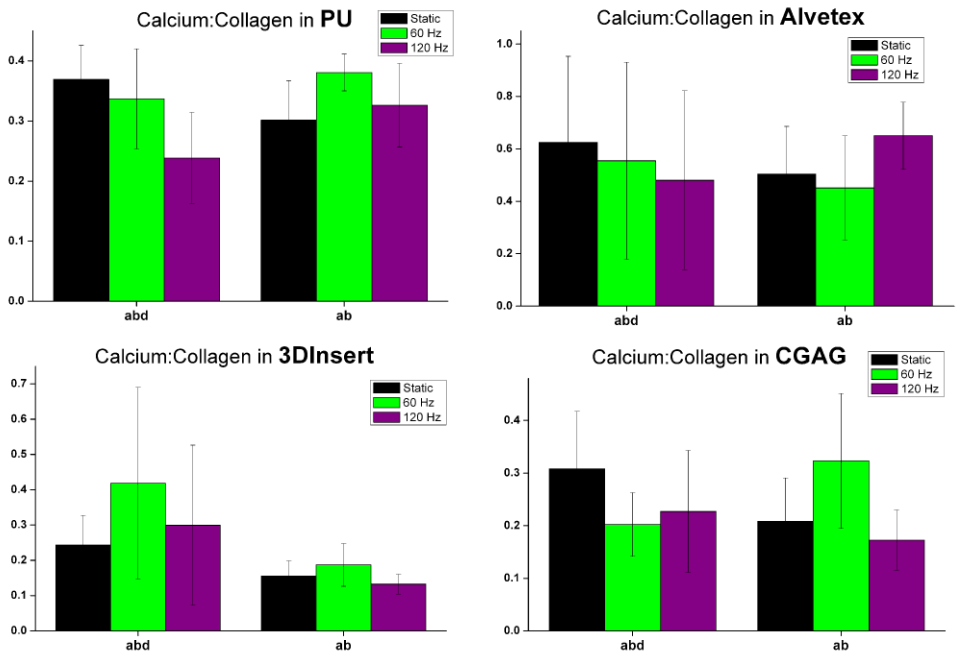

Figure 5.20: Ratio of collagen and calcium production of hES-MP cells. An increase in mineralisation of the matrix under 60 Hz vibration compared to static is seen in some conditions (PU [ab], 3D Insert [ab, abd], CGAG [ab]) or a decrease with increasing frequency in abd media (PU , Alvetex) but no differences are significant. Mean ± SD, n=4 over 2 experiments

5.6 Discussion

This chapter investigated the effects of mechanical stimulation via LMHF vibrations on the behaviour of hES-MP cells in a variety of mechanically different scaffolds. The cell attachment work in 3D in chapter 3 showed that the hES-MP cells could be encouraged to attach to and spread over the surface of PU foam scaffolds by gelatin coating. These scaffolds were ideal for loading via direct compression of the scaffold as their elastic nature allowed the loading to be applied without permanent deformation of the scaffold. Their suitability for use with LMHF vibrations was investigated and it was found that a different scaffold type may be required for this type of stimulation.

Initial experiments investigated the application of mechanical compressive loading to cell seeded scaffolds, following on from previous work within the research group. Several loading regimens were tested, but did not produce any significant changes in matrix production or mineralisation and gave highly variable results (preliminary data not shown). To check the cell seeding efficiency and the effects of compressions on cell distribution, experiments were performed using 1 or 10 Hz compressions (as detailed in Materials and Methods), and analysed by MTT assay (figure 5.1). The results showed that cells were initially found within the central regions of the scaffold, but by day 20 of culture were present only in the peripheral regions. This may be due to poor nutrient availability and waste removal within the centre of the scaffolds, causing cells to migrate outwards. This would put them within 200 μm of the fresh media and diffusion would be sufficient to maintain conditions conducive to cell growth and survival.

As well as migration of cells, it is possible that the cells merely proliferate outwards (as the scaffold is initially less densely populated in the outer regions initially) and those in the centre die as culture progresses. The increase in cell number within the scaffold, as well as the onset of matrix deposition by the cells, may reduce the efficiency of the transport of media through the scaffolds by blocking of the pores. Another effect of increasing cell numbers is an increase in the nutrient requirements and waste production. These factors mean there is unlikely to be a hospitable environment in the central regions of the constructs. Therefore it seems likely that cell death is at least partly responsible for the lack of metabolically active cells within the central regions. Further investigation, either with live-dead staining and imaging of specific scaffold regions, or through the use of hypoxia markers, could increase understanding of what is occurring. The use of other metabolism assays, such as Alamar blue, may allow the visualisation of viable cell distribution throughout scaffolds during culture without detrimental effects on cells. Closer monitoring of the pH of the solutions, as well as testing media for waste products or the depletion of glucose may provide further insights into the changes in culture environment with time.

There did appear to be a slight increase in the thickness of the band of viable cells around the periphery of the scaffold at the higher compression frequency. This may be due to increased flow of fluid in and out of the scaffold pores, increasing the distance over which nutrient and waste transfer occurred. As the scaffold is highly elastic, fluid will be forced out in small volumes when it is compressed. When the force is removed, the scaffold will return to its original shape and media will flow back into the scaffold. This change in the volume of the scaffold should create limited fluid flow in the outer regions of the scaffold. Fluid movement in and out of the scaffold may help maintain concentrations of waste and nutrients

favourable to the cells. This fluid flow may also be responsible in some degree for the cellular responses to loading seen in previous work (Sittichockechaiwut et al. 2009). It is unknown whether the cells respond to the direct deformation of the scaffold or the movement of fluid within the pores causing a shear stress response; much as the mechanisms of mechanotransduction *in vivo* are still not well understood (Jacobs et al. 2010).

The early 3D experiments with LMHF vibrations and the PU foams were carried during some of the earlier 2D vibration experiments. Moving directly to 3D culture would have allowed more thorough investigation into the use of LMHF vibrations in the production of tissue engineered constructs. 4 mm high scaffolds were used, as the cell distribution experiments showed that the 10 mm high scaffolds could not support cells in the central scaffold regions over 20 days of culture. The vibration experiments did not show any significant changes in ALP activity or total DNA content, although the cells did still respond to dexamethasone. This may be indicative of poor transmission of the vibrations through the scaffold to the cells. The volume of media used during vibration was reduced to see if this was due to a lack of contact between the scaffolds and the surface of the culture plate during stimulation. While this second set of data was less variable, no significant effect of vibration was noted. This suggested another possibility that, due to the elastic nature of the scaffold, forces are not being transmitted efficiently to the adhered cells. The elastic nature of the scaffold may serve to damp the vibrations such that they do not stimulate the cells. The vibration may be enough to remove any cells loosely adhered to the scaffold in clumps (reducing the cell number), without being transmitted through the scaffolds sufficiently to have any effect on adhered cells (figure 3.14).

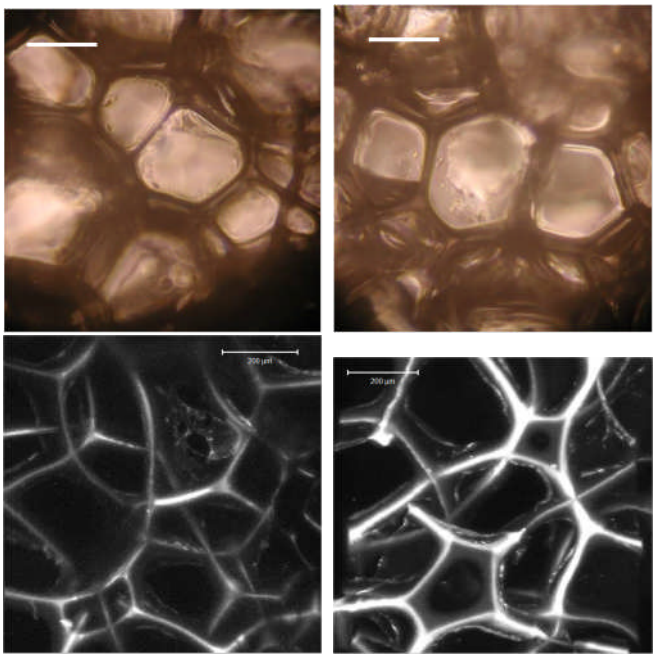

Figure 5.21: Microscopy of PU scaffolds. Upper images show scaffolds under light microscopy, lower images using confocal microscopy and scaffold autofluorescence (z-stacked). Scale bars show 200 μm.

It is also of interest that there were large variations in the results for the control (static) samples. This could be indicative of problems with scaffold inhomogeneity, providing different surface areas and spatial configurations within different samples. Example light microscope and confocal images of the PU scaffolds are shown in figure 5.21. This inhomogeneity will affect the area available for growth, nutrient transfer and force transmission between samples. The use of scaffolds with strictly defined or more consistent structures may help reduce this variability.

For the glass scaffolds, there was high variability in results, and still no significant differences in cell number or ALP activity. For the DNA results, this variability seems to be due to a large difference in the amount of DNA detected between the two experimental repeats. While there is a reduction in the ALP activity alongside the reduction in DNA, it does not appear to be of the same magnitude, and indicates a problem when processing the samples. Insufficient

scaffolds were available to repeat the experiment, but there did appear to be less variation than for the PU scaffolds even when the two experiments had such different results. As the scaffolds are created from fused glass pellets, the scaffolds are also not a homogeneous structure. The pellets are randomly arranged within the scaffold structure, creating differences in the total surface area of the scaffolds. Pore size, porosity and interconnectivity will also be affected by this random arrangement of pellets. The number of pellets in contact with the plate will also vary between scaffolds, providing a different surface area in contact with the plate for each scaffold. This will have effects on force transmission to different regions of the scaffolds. While the faces of the scaffold may not be perfectly parallel, it is possible that they are more so than the PU foams sectioned by hand, further reducing the variability in overall dimensions. However, the rigid nature of the scaffolds may have better force transmission properties than the PU due to its stiff structure and reduced damping.

Another possibility for the differences between 2D and 3D behaviour is that, due to the altered physical environment, the cells underwent osteogenic differentiation at a different rate. As the activity of ALP has been shown to vary over time (Hoemann et al. 2009), it is possible that the stimulation and collection time points at which differences in ALP were detected in 2D (24 and 48 hours after stimulation on day 6 of culture) were not suitable to detect ALP differences in 3D. As there is a much larger surface area for the cells to spread upon within the 3D scaffold, it is likely that they will take a longer time to reach confluence, even with a higher initial cell number. This may affect the differentiation pattern of the cells, or change the time point at which they are able to respond to mechanical stimuli.

Cellular communication is likely important in the response to loading, either through the release of soluble signalling molecules into the media or directly via cell-cell contacts. Osteocytic cells are known to communicate via gap junctions (Yellowley et al. 2000), and mechanotransduction signals seem to be transmitted in this manner (Lohmann et al. 2003; Genetos et al. 2007; Donahue 2000). In 2D the cells reach confluence quickly and are therefore in close contact with other cells at an early stage in culture. In the 3D situation, it is likely that the cells will need more time in order to become confluent, meaning that the cell-cell contacts are not available as early in the culture process. This may reduce the efficiency of a cellular response to loading, as cells may not be able to communicate effectively via direct pathways. Cells may need to be vibrated at a later timepoint for loading to be effective in 3D compared with 2D. The optimal collection timepoint may also need adjusting to allow for the altered culture environment.

The use of calcein labelling to monitor mineralisation by osteogenic cells could prove a useful technique for bone tissue engineering. Phenol red free culture media would allow the imaging of cells directly from the incubator, without the necessity to switch the cells to PBS during imaging. Short periods of time (45 minutes) out of the incubator have been shown to have no significant effects on the metabolic activity or ALP production of the hES-MP cells (figure 4.7), which is ample time for imaging of cells. The use of multiple labelling agents, such as xylenol orange, would allow labelling with different fluorescence markers at different stages in culture. Initial tests were carried out xylenol orange, but the fluorescence emissions were not as visible as calcein using the Axon and this method was not used further (preliminary data not shown). It may be more feasible where access to a microscope using laser excitation is possible throughout experiments. Laser excitation will provide a higher power and may allow the imaging of incorporated

xylenol. This type of sequential labelling has been successful *in vivo* (Oxlund et al. 2003; Castillo et al. 2006; Li et al. 2007) and may prove useful for *in vitro* development. For this work, imaging was only carried out on fixed scaffolds. As the calcein was present within the culture media, scaffolds would have needed to be washed before imaging in PBS, which may have had effects on the behaviour of the cells. Imaging only at the end of culture in fixed scaffolds prevented these problems in this study.

For the experiments comparing the mechanically different scaffolds, the MTT assay produced darker staining in scaffolds vibrated at 120 Hz, suggesting an increase in the metabolic activity. This is consistent with the response seen in the 2D experiments using long term vibration or indomethacin vibration.

Imaging of the matrix deposition within CGAG scaffolds was difficult due to the contraction of the foams. Repeat experiments could inhibit the contraction by gluteraldehyde fixation (Keogh et al. 2010; Haugh et al. 2011). Mineralisation in the other scaffolds was good, with samples showing good coverage of cells and matrix. For the PU foams in particular, the cells could be seen to be spreading across the pores and producing matrix. 3D Insert scaffolds had cells covering the scaffold struts in layers, and there was some evidence of spreading across gaps around the edges of the scaffolds.

Scaffolds were further investigated using standard bone matrix staining procedures within the lab (sirius and alzarin red). From the results, it is surprising that the lowest values for collagen come from the collagen-based scaffolds. Although these scaffolds should have shown very high collagen content, by the end of the experiment they had vastly reduced in volume. This creates a very small surface

area, and very dense internal configuration of cells and matrix, as seen from the Axon and MTT images. Due to the short times over which the destain solution was applied compared to staining times, it is presumed that the samples did not have time to properly diffuse from the dense scaffolds. In the case of the sirius red stain, it was not possible to increase the time in the destain solution as the methanol involved in the destain begins to evaporate. This would alter the optical properties of the solution and solubility of the stain, providing an inaccurate reading. As the scaffolds had also proved difficult to image, the destain time was kept the same as the other scaffolds rather than being increased.

There were no significant differences in the matrix production within any of the scaffold groups. Higher amounts of collagen were detected in the Alvetex and PU scaffolds compared to other scaffold types and a trend for higher levels of collagen with increasing frequency was seen for some conditions (PU [abd], Alvetex [ab, abd], 3D Insert [ab], GAG [abd]). The PU scaffolds had the largest bulk volume by the end of culture, providing the largest area for cell growth and matrix production. For the Alvetex, this increase is interesting as the area available for cell growth is lower than that in the PU foams. Some calcium levels were also higher in vibrated samples, particularly noticeable for Alvetex (ab media, 120 Hz compared to control).

The ratios calculated (calcium:collagen) suggest that the vibration is having an effect on mineralisation of any matrix produced. For most scaffold types, there was a trend for a decrease in the ratio with increasing frequency in media containing dexamethasone. For all scaffold types, there was an increase in the ratio in ab media with vibration compared to control (120 Hz for Alvetex, 60 Hz for other scaffold types). These results suggest that the dexamethasone may be causing a

change in response to vibration in the hES-MP cells. A similar effect was seen for MTS activity and calcium production in long term 2D experiment (figure 4.10). Surprisingly, this effect was seen with 0.05 mm vibration in 2D but 0.03g in 3D, suggesting that the move to a scaffold is altering which vibration regimen is most effective. For 3D Insert scaffolds in abd media the increase in ratio is seen in both media types (much lower in the ab media), suggesting that the nature of the scaffold also has an effect. As this scaffold is made from the same material as normal tissue culture plastic, it is perhaps not surprising to find a response at a frequency which promoted a response previously in 2D. This response was seen in the ALP activity and not the matrix production, however. As the scaffolds were very different in architecture, it is likely that the porosity, pore shape and surface area available for growth affected the matrix deposition and mineralisation in the hES-MP cells. As all of these properties are known to affect the growth of cells within scaffolds, it is difficult to determine which properties may have had the greatest effects during the experiments. A more rigourous study of fabricated scaffolds with evolving properties may provide more information on these effects.

The use of scaffolds with defined structures may also improve the repeatability of experiments in 3D. If the scaffold structure for each sample is identical, this greatly reduces the possibilities for variations in the cellular environment. Cells will always have the same surface area for expansion, the same diffusion characteristics for waste and nutrients and more predictable forces acting on them. While this may change over time as the cells proliferate, it should be more consistent during the early stages of culture. Keeping the same surface area in contact with the plate, with the same structure for force transmission should reduce any variation in the transmission of mechanical stimulation, making 3D Insert or similar scaffolds ideal for experiments. Standardising the scaffold may be particularly important

when developing methods for the culture of primary cells. Due to the genetic differences in patients, there will be differences in the responses of their cells to treatment. Robust protocols for the production of new tissue should reduce variability wherever possible to reduce the impact of patient variability.

5.7 Chapter Summary

This chapter investigated the effects of the LMHF vibrations in 3D, in a selection of mechanically different scaffolds. The work showed that:

- The polyurethane foam scaffolds were not idea for this kind of stimulation.
- Glass scaffolds showed some improvement, but were still not suitable.
- High frequency LMHF vibrations appeared to increase metabolic activity in hES-MP cells.
- hES-MP cells were suitable for culture in the selection of different scaffolds.
- Long term vibrations did not produce any significant changes in matrix composition.

Chapter 6

Conclusions and Future Work

Work in this project has studied the early attachment and spreading of several cell lines in an open cell polyurethane foam, before moving to the use of low magnitude, high frequency (LMHF) vibration for the mechanical stimulation of mesenchymal progenitor cells in 2D. A range of frequencies were tested, looking at an early differentiation marker and the longer term matrix production in the hES-MP cell line. Finally, several mechanically different scaffolds were used to study the response of the cells to LMHF in 3D.

While there are many scaffold options available, polyurethane has been suggested for use as a scaffold material in tissue engineering (Zanetta et al. 2009; Williamson et al. 2006; Ramrattan et al. 2005; Guelcher et al. 2006; Fassina et al. 2005). For tailored applications, the structure of the polyurethane may be tailored to give different properties and degradation rates (Jozwiak et al. 2008; Guelcher 2008). The scaffold used in this study had been used previously within the lab to apply mechanical compressive loading, supporting both osteoblast-like cells and MSCs (Sittichokechaiwut et al. 2010; Sittichockechaiwut et al. 2009). While the foam is not biodegradable, this is an advantage during the *in vitro* study of

mechanical loading on cells. Degradation of the scaffold would lead to changes in the mechanical properties, complicating the understanding of the forces being applied to the cells.

Cells were shown to attach and proliferate well within the scaffold after pretreatment with gelatin solution (figure 3.9). Several other coatings were tried, including FCS, and while this appeared to improve the number of cells within the scaffold during early stages of culture (figure 3.1), cells formed clumps loosely adherent to the scaffold rather than being well spread over its surface (figure 3.5). These clumps, while not large enough to cause problems with nutrient diffusion to the centre, may prevent the application of mechanical forces in a consistent way to the cells. Mechanical deformation of the scaffold would not be applied to all the cells within a clump, as few are in direct contact with the scaffold. Movement of fluid may also cause the detachment of cells from the scaffold due to a small anchor point (see figure 3.14 in chapter 3). The use of gelatin solution encouraged cells to spread over the whole surface of the scaffold with the hES-MP cells. As the use of MSCs may be more appropriate for *in vivo* work, these cells were used through the rest of the project. Although it was not envisaged that the work would require a move to *in vivo*, the method of stimulation used in later experiments would be ideal for culture of autologous MSCs *in vitro* if it could direct them along an osteoblastic lineage for bone repair. Further investigation into the attachment of the cells would provide more data on the attachments to the scaffold initially, and how these alter as the cell number increases. It would also be interesting to study the formation of gap-junctions between the cells. As discussed in the previous chapter, these junctions are important for signalling and understanding any differences in their formation between 2D and 3D culture may provide more insight into differences found in 2D and 3D responses to stimuli.

Calcein labelling of mineral deposition was used to allow investigation of the deposited matrix using fluorescent microscopy (figures 3.12, 5.8-5.17). Coupled with collagen I labelling, this showed the matrix formation in cells around scaffold pores. As several such calcium chelators may be used to sequentially label bone (O'Brien et al. 2002; Lee et al. 2000), these could be applied to follow matrix production with time. Use of microscopy facilities with controlled temperature, humidity and CO_2 would allow the imaging of cells throughout culture. Any changes in initialisation or rate of mineralisation due to treatments could be investigated. It is possible that decalcification of the matrix after culture may allow quantification of the calcium present, by detecting the fluorescence of the calcein present in the resulting solution.

Low magnitude, high frequency (LMHF) vibration was shown to have variable effects on hES-MP cells. In initial short term experiments, $0.03\,g$ stimulation at 60 Hz for 45 minutes showed higher ALP activity than all other conditions. Accompanied by a reduction in total DNA for vibrated samples, this suggested that the stimulation was pushing the cells to an osteogenic phenotype. In further experiments, different responses to LMHF vibration were seen. Serum free vibration found only a significant increase in the total DNA under the same stimulation conditions. For other short term experiments, as well as the transfer of media to cells, responses were seen for 120 Hz vibration instead of 60 Hz. The 120 Hz showed increased levels of metabolic and ALP activity, as well as ALP:DNA. This suggests that there are soluble factors which can alter the differentiation of non-vibrated cells. Changes in ALP expression with LMHF vibration have varied in the literature, with some studies finding no change with borad frequency vibration (Tanaka et al. 2003) and others upregulation (Pre et al. 2009). This upregulation was seen in mRNA levels after vibration at 60 Hz for 45 minutes. Other frequencies

were not as effective, suggesting that the response is very dependant on the use of specific stimulation conditions. The results of the work presented here suggest a similar dependance as changing from constant acceleration to constant amplitude vibrations changes the cellular response.

When indomethacin was applied to the vibrated cells, there were increases in the metabolic activity of the 120 Hz stimulated cells compared to static or 60 Hz. Indomethacin in the transfer media resulted in a loss of the responses seen in the previous transfer experiment, which could indicate prostaglandin signalling which was inhibited. There were also no responses in samples which did not receive indomethacin in the transfer media, suggesting that the cell responses to loading did not occur or were hidden by high variability. As such, the indomethacin experiments are inconclusive. The variety of experiments which have been conducted using LMHF vibrations in the literature suggest that the response is highly dependent on the exact state of cells (summarised in tables 1.3 and 1.4). For the *in vivo* situation, there will be variability between patients (such as muscle mass, age and disease state) which will affect the overall response to loading. This suggests that subtle differences in the cellular behaviour (such as lower than normal proliferation rates or slight differences in the general laboratory conditions) may be enough to affect the cellular response to loading.

Interestingly, the 120 Hz vibration also demonstrated a change in the ratio of MTS:DNA, which was not affected by the indomethacin. Metabolic activity assays are often used to give an estimate of cell number, but this research demonstrates that this may not be a valid measure for samples undergoing mechanical stimulation. As the metabolic activity per ng of DNA varied with the different conditions tested, this suggested that changes in the metabolic activity did not correlate with changes in cell number. Metabolic activity may vary connection

with processes other than cell proliferation, such as protein production. It has been suggested that methods to assess cell viability in 2D conditions may not be applicable in 3D (Ng et al. 2005) and this research also suggests that comparing static and dynamic culture may require different assay techniques.

In long term experiments (figures 4.10 to 4.13), $0.03g$ vibration at 30 Hz did show an improvement in the matrix production. For the 0.05 mm experiment, 120 Hz produced a significant increase in calcium deposition. Differences in matrix mineralisation may signify matrices different mechanical properties (when produced in sufficient volume) or which have different effects on other cells in contact with them (such as undifferentiated progenitor cells or osteoclasts). If the ratio of mineralisation is being affected it is likely that other matrix components (such as signalling factors eg fibronectin, osteopontin or osteonectin) are undergoing changes in expression due to the LMHF vibration. This would be similar to the situation seen in the literature (for examples see table 1.4 and the discussion section in chapter 4). There are also examples described in the literature of both positive and negative effects of LMHF vibration on calcium deposition (Pre et al. 2010; Lau et al. 2011), though these experiments used primary MSCs. However, the two studies used human and rat cells respectively and differences may be due to the species alone. In transfer experiments (figures 4.19 and 4.20), the stimulation at 120 Hz was able to prevent the negative effects of transfer media on metabolic activity and calcium deposition. It would be interesting to quantify the cell number during long term transfer. This may indicate whether the transfer media is causing an increase in cell number, or causing differentiation and increased matrix deposition.

The move to 3D demonstrated the importance of the scaffold properties during mechanical stimulation. The polyurethane foam scaffolds used previously within the group were found not to be suitable. They showed high variability in results, although this was partly due to a lack of contact with the culture plate. The use of a more rigid scaffold (glass) reduced the error, although there was a large discrepancy between experiments and a small sample number. It is likely that the elastic nature of the PU foams caused damping of the vibrations, reducing the forces transmitted to the cells. This may be similar to the damping of vibrations *in vivo* by the muscles (Rubin et al. 2003; Kiiski et al. 2008).

Final experiments were conducted using scaffolds with different mechanical properties to further investigate this effect. Cells were shown to attach and proliferate within all of the scaffolds, as well as producing mineralised matrix. Imaging within the collagen-GAG foams was difficult due to contraction of the foams during culture. Cells within the 3D Insert and PU foams were shown to spread over the scaffold surface and cells could be seen to be creating matrix over the pores in the scaffold, most noticeable for the PU foams. The use of sirius red and alizarin red to stain the samples after fluorescence microscopy were inconclusive. For the CGAG scaffolds especially, the elution of stain from the scaffolds was difficult. For future work, it would be interesting to quantify cells within the scaffolds, as well as using an MTS assay in conjunction with the MTT. This would provide information on the cell number, spread within the scaffolds and how metabolically active the cells were. The use of calcein and other calcium chelators to study the mineral deposition over time may also provide information on the onset and progression of mineralisation for the hES-MP cells. Fixation of the scaffolds to the culture plate during vibration (for example using a fibrin glue) may also allow better transmission of the forces. Although reducing the volume of media within the plate prior to loading did stop large movements of the scaffolds, this may not

provide consistent force transmission. Scaffolds could be held in place with fibrin glue, and used to perform further investigations. Larger, crosslinked versions of the CGAG scaffolds would also be of interest, as the tight matrix connection with the cells may be similar to that *in vivo* with natural ECM.

The results presented here showed some evidence that the use of LMHF vibrations has an effect on the matrix composition of hES-MP cells, altering the ratio of collagen to calcium. Investigation of the matrix components and structure could characterise these effects. The orientation of collagen may be altered, as well as the ratios of different collagens and other matrix proteins. The use of second harmonic generation (SHG) or scanning electron microscopy (SEM) would provide more detail on the matrix structure. Western blotting or immunohistochemistry could be used to label molecules of interest and better characterise the matrix. The matrix orientation may also shed light on how the cells are orientated within the scaffolds, and on the number of gap junctions that the cells have formed with one another. If cells form gap junctions later in certain conditions, this may be enough to disrupt the response to loading. It may also account for differences in response between 2D and 3D, as it may take longer for cells to produce a network in 3D, but which will be much larger once complete. The use of biodegradable scaffolds over longer time periods could also answer questions about the changes in matrix and transmission of LMHF vibrations with time. If the scaffold degraded at a rate that allowed the cells to create their own matrix, the use of LMHF in natural tissues may be better understood. It may also be possible to use acellular natural scaffolds which have been reseeded with progenitor cells.

The use of LMHF vibrations to stimulate mesenchymal progenitor cells *in vitro* has shown some success. The method is simple to apply and is suitable for a variety of different culture conditions and scaffold types. A range of different frequencies were used, investigating both short term and longer term application. The difference in responses when constant amplitude vibrations were used compared to constant acceleration suggests that the conditions must be strictly defined to promote the required response from cells. Improvements in ALP activity and matrix production were seen for some of the conditions tested, but increased ALP activity did not predict increases in matrix production. Changes in the ratios of metabolic activity to total DNA were seen in some experiments, suggesting such assays may not be accurate predictors of cell number. Higher metabolic activity in short term experiments was observed for the same conditions in longer culture. This suggests that LMHF vibration has a continuing effect on the metabolic activity of cells which does not appear to be only matrix production or mineralisation. Cells vibrated over a longer time period showed differences in collagen and calcium production depending on the vibration conditions. A change in the ratio of these components seen in some conditions suggested that the stimulation was having effects on the composition and maturation of extracellular matrix produced, as well as the overall volume.

Bibliography

Alcaide, M., M.-C. Serrano, R. Pagani, S. Snchez-Salcedo, M. Vallet-Reg, and M.-T. Portols (2009). Biocompatibility markers for the study of interactions between osteoblasts and composite biomaterials. *Biomaterials 30*(1), 45 – 51.

Alhadlaq, A., J. H. Elisseeff, L. Hong, C. G. Williams, A. I. Caplan, B. Sharma, R. A. Kopher, S. Tomkoria, D. P. Lennon, A. Lopez, and J. J. Mao (2004). Adult stem cell driven genesis of human-shaped articular condyle. *Annals of Biomedical Engineering 32*, 911–923. 10.1023/B:ABME.0000032454.53116.ee.

Alhadlaq, A. and J. J. Mao (2005). Tissue-engineered osteochondral constructs in the shape of an articular condyle. *The Journal of Bone & Joint Surgery 87*(5), 936–944.

Allen, F., C. Hung, S. Pollack, and C. Brighton (2000). Serum modulates the intracellular calcium response of primary cultured bone cells to shear flow. *Journal of Biomechanics 33*(12), 1585 – 1591.

Andrews, N. A. (2010). Vibration therapy: Does it have a future in the bone field? *IBMS BoneKEy 7(3)*, 97–102.

Athanasiou, K., C.-F. Zhu, D. Lanctot, C. Agrawal, and X. Wang (2000). Fundamentals of biomechanics in tissue engineering of bone. *Tissue Engineerng 6(4)*, 361–381.

Babister, J. C., L. A. Hails, R. O. Oreffo, S. A. Davis, and S. Mann (2009). The effect of pre-coating human bone marrow stromal cells with hydroxyapatite/amino acid nanoconjugates on osteogenesis. *Biomaterials 30*(18), 3174 – 3182.

Bacabac, R. G., D. Mizuno, C. F. Schmidt, F. C. MacKintosh, J. J. V. Loon, J. Klein-Nulend, and T. H. Smit (2008). Round versus flat: Bone cell

morphology, elasticity, and mechanosensing. *Journal of Biomechanics 41*(7), 1590 – 1598.

Bacabac, R. G., T. H. Smit, M. G. Mullender, S. J. Dijcks, J. J. V. Loon, and J. Klein-Nulend (2004). Nitric oxide production by bone cells is fluid shear stress rate dependent. *Biochemical and Biophysical Research Communications 315*(4), 823 – 829.

Bacabac, R. G., T. H. Smit, J. J. W. A. Van Loon, B. Z. Doulabi, M. Helder, and J. Klein-Nulend (2006). Bone cell responses to high-frequency vibration stress: does the nucleus oscillate within the cytoplasm? *The FASEB Journal 20*(7), 858–864.

Badylak, S. F. (2004). Xenogeneic extracellular matrix as a scaffold for tissue reconstruction. *Transplant Immunology 12*(34), 367 – 377. Organogenesis and Tissue Engineering in Transplantation Medicine.

Baker, E. L. and M. H. Zaman (2010). The biomechanical integrin. *Journal of Biomechanics 43*(1), 38 – 44. Special Issue on Cell Mechanobiology.

Bakker, A. D., K. Soejima, J. Klein-Nulend, and E. H. Burger (2001). The production of nitric oxide and prostaglandin e2 by primary bone cells is shear stress dependent. *Journal of Biomechanics 34*(5), 671 – 677.

Baksh, D., R. Yao, and R. S. Tuan (2007). Comparison of proliferative and multilineage differentiation potential of human mesenchymal stem cells derived from umbilical cord and bone marrow. *Stem Cells 25*(6), 1384–1392.

Barnes, D. (1980). Serum-free cell culture : a unifying approach. *Cell 22*, 649–655.

Bartolo, P. and B. Bidanda (Eds.) (2008). *Bio-materials and prototyping applications in medicine*. New York, N.Y : Springer.

Batra, N., R. Kar, and J. X. Jiang (2012). Gap junctions and hemichannels in signal transmission, function and development of bone. *Biochimica et Biophysica Acta (BBA) - Biomembranes 1818*(8), 1909 – 1918. The Communicating junctions, composition, structure and characteristics Part 1.

Batra, N. N., Y. J. Li, C. E. Yellowley, L. You, A. M. Malone, C. H. Kim, and C. R. Jacobs (2005). Effects of short-term recovery periods on fluid-induced signaling in osteoblastic cells. *Journal of Biomechanics 38*(9), 1909 – 1917.

Bauer, T. (2007). Bone graft substitutes. *Skeletal Radiology 36*, 1105–1107. 10.1007/s00256-007-0377-4.

BDB (2012, Sept). http://en.wikipedia.org/wiki/file:Transverse_Section_Of_Bone.png.

Beck, B. R., K. Kent, L. Holloway, and R. Marcus (2006). Novel, high-frequency, low-strain mechanical loading for premenopausal women with low bone mass: early findings. *Journal of Bone and Mineral Metabolism 24*, 505–507. 10.1007/s00774-006-0717-9.

Bhat, S. V. (2004). *Biomaterials* (2ed. ed.). Harrow : Alpha Science International.

Blackwood, K. A., R. McKean, I. Canton, C. O. Freeman, K. L. Franklin, D. Cole, I. Brook, P. Farthing, S. Rimmer, J. W. Haycock, A. J. Ryan, and S. MacNeil (2008). Development of biodegradable electrospun scaffolds for dermal replacement. *Biomaterials 29*(21), 3091 – 3104.

Bolland, F., S. Korossis, S.-P. Wilshaw, E. Ingham, J. Fisher, J. N. Kearney, and J. Southgate (2007). Development and characterisation of a full-thickness acellular porcine bladder matrix for tissue engineering. *Biomaterials 28*(6), 1061 – 1070.

Bonewald, L. F. (2006). Mechanosensation and transduction in osteocytes. *Bonekey Osteovision 3(10)*, 7–15.

Botchwey, E. A., S. R. Pollack, E. M. Levine, and C. T. Laurencin (2001). Bone tissue engineering in a rotating bioreactor using a microcarrier matrix system. *Journal of Biomedical Materials Research 55*(2), 242–253.

Bracco, P. and E. Oral (2011). Vitamin e-stabilized uhmwpe for total joint implants: A review. *Clinical Orthopaedics and Related Research 469*(8), 2286–2293.

Brounais, B., E. David, C. Chipoy, V. Trichet, V. Ferr, C. Charrier, L. Duplomb, M. Berreur, F. Rdini, D. Heymann, and F. Blanchard (2009). Long term oncostatin m treatment induces an osteocyte-like differentiation on osteosarcoma and calvaria cells. *Bone 44*(5), 830 – 839.

Burger, E. H. and J. Klein-nulend (1999). Mechanotransduction in bonerole of the lacuno-canalicular network. *The FASEB Journal 13*(9001), 101–112.

Butler, D. L., S. A. Hunter, K. Chokalingam, M. J. Cordray, J. Shearn, N. Juncosa-Melvin, S. Nirmalanandhan, and A. Jain (2009). Using func-

tional tissue engineering and bioreactors to mechanically stimulate tissue-engineered constructs. *Tissue Engineering: Part A 15(4)*, 741–9.

Bye, F. J., L. Wang, A. J. Bullock, K. A. Blackwood, A. J. Ryan3, and S. MacNeil (2012). Postproduction processing of electrospun fibres for tissue engineering. *Journal of Visualized Experiments 66*, e4172.

Campbell, I. M. (2000). *Introduction to synthetic polymers* (2ed. ed.). Oxford University Press.

Canton, I., D. Cole, E. Kemp, P. Watson, J. Chunthapong, A. Ryan, S. MacNeil, and J. Haycock (2010). Development of a 3d human in vitro skin co-culture model for detecting irritants in real-time. *Biotechnology and Bioengineering 106*(5), 794–803.

Cartmell, S. H., A. Keramane, G. R. Kirkham, S. B. Verschueren, J. L. Magnay, A. J. E. Haj, and J. Dobson (2005). Use of magnetic particles to apply mechanical forces for bone tissue engineering purposes. *Journal of Physics: Conference Series 17*(1), 77.

Castillo, A. B., I. Alam, S. M. Tanaka, J. Levenda, J. Li, S. J. Warden, and C. H. Turner (2006). Low-amplitude, broad-frequency vibration effects on cortical bone formation in mice. *Bone 39*(5), 1087 – 1096.

CC1 (2012). Creative commons public domain mark.

CC3 (2012). Creative commons attribution-sharealike 3.0 license.

Cellpath. Osteoclast image.

Chakkalakal, D. A., B. S. Strates, K. L. Garvin, J. R. Novak, E. D. Fritz, T. J. Mollner, and M. H. McGuire (2001). Demineralized bone matrix as a biological scaffold for bone repair. *Tissue Engineering 7(2)*, 161–177.

Choi, K.-M., Y.-K. Seo, H.-H. Yoon, K.-Y. Song, S.-Y. Kwon, H.-S. Lee, and J.-K. Park (2008). Effect of ascorbic acid on bone marrow-derived mesenchymal stem cell proliferation and differentiation. *Journal of Bioscience and Bioengineering 105*(6), 586 – 594.

Christiansen, B. and M. Silva (2006). The effect of varying magnitudes of whole-body vibration on several skeletal sites in mice. *Annals of Biomedical Engineering 34*, 1149–1156. 10.1007/s10439-006-9133-5.

Cioffi, M., J. Kffer, S. Strbel, G. Dubini, I. Martin, and D. Wendt (2008). Computational evaluation of oxygen and shear stress distributions in 3d

perfusion culture systems: Macro-scale and micro-structured models. *Journal of Biomechanics 41*(14), 2918 – 2925.

Coughlin, T. R. and G. L. Niebur (2012). Fluid shear stress in trabecular bone marrow due to low-magnitude high-frequency vibration. *Journal of Biomechanics 45*(13), 2222 – 2229.

Crapo, P. M., T. W. Gilbert, and S. F. Badylak (2011). An overview of tissue and whole organ decellularization processes. *Biomaterials 32*(12), 3233 – 3243.

Currey, J. D., J. Foreman, I. Laketi, J. Mitchell, D. E. Pegg, and G. C. Reilly (1997). Effects of ionizing radiation on the mechanical properties of human bone. *Journal of Orthopaedic Research 15*(1), 111–117.

Cyster, L., D. Grant, S. Howdle, F. Rose, D. Irvine, D. Freeman, C. Scotchford, and K. Shakesheff (2005). The influence of dispersant concentration on the pore morphology of hydroxyapatite ceramics for bone tissue engineering. *Biomaterials 26*(7), 697 – 702.

Daud, M. F., K. C. Pawar, F. Claeyssens, A. J. Ryan, and J. W. Haycock (2012). An aligned 3d neuronal-glial co-culture model for peripheral nerve studies. *Biomaterials 33*(25), 5901 – 5913.

David, V., A. Guignandon, A. Martin, L. Malaval, M.-H. Lafage-Proust, A. Rattner, V. Mann, B. Noble, D. Jones, and L. Vico (2008, Jan). Ex vivo bone formation in bovine trabecular bone cultured in a dynamic 3d bioreactor is enhanced by compressive mechanical strain. *Tissue Engineering Part A 14*(1), 117–26.

Delaine-Smith, R. and G. Reilly (2011). The effects of mechanical loading on mesenchymal stem cell differentiation and matrix production. *Vitamins and Hormones 87*, 417–80.

Delaine-Smith, R. M., S. MacNeil, and G. C. Reilly (2012). Matrix production and collagen structure are enhanced in two types of osteogenic progenitor cells by a simple fluid shear stress stimulus. *European Cells and Materials 24*, 162–174.

Diefenderfer, D. L., A. M. Osyczka, J. P. Garino, and P. S. Leboy (2003). Regulation of bmp-induced transcription in cultured human bone marrow stromal cells. *The Journal of Bone & Joint Surgery 85*, 19–28.

Diefenderfer, D. L., A. M. Osyczka, G. C. Reilly, and P. S. Leboy (2003). Bmp responsiveness in human mesenchymal stem cells. *Connective Tissue Research 44*(1), 305–311.

Doblar, M., J. Garia, and M. Gmez (2004). Modelling bone tissue fracture and healing: a review. *Engineering Fracture Mechanics 71*(1314), 1809 – 1840.

Dolatshahi-Pirouz, A., T. Jensen, K. Kolind, C. Bnger, M. Kassem, M. Foss, and F. Besenbacher (2011). Cell shape and spreading of stromal (mesenchymal) stem cells cultured on fibronectin coated gold and hydroxyapatite surfaces. *Colloids and Surfaces B: Biointerfaces 84*, 18–25.

Donahue, H. (2000). Gap junctions and biophysical regulation of bone cell differentiation. *Bone 26*(5), 417 – 422.

Dumas, V., B. Ducharne, A. Perrier, C. Fournier, A. Guignandon, M. Thomas, S. Peyroche, D. Guyomar, L. Vico, and A. Rattner (2010). Extracellular matrix produced by osteoblasts cultured under low-magnitude, high-frequency stimulation is favourable to osteogenic differentiation of mesenchymal stem cells. *Calcified Tissue International 87*, 351–364. 10.1007/s00223-010-9394-8.

Engler, A. J., S. Sen, H. L. Sweeney, and D. E. Discher (2006). Matrix elasticity directs stem cell lineage specification. *Cell 126*(4), 677 – 689.

Fang, B., Y.-Z. Wan, T.-T. Tang, C. Gao, and K.-R. Dai (2009). Proliferation and osteoblastic differentiation of human bone marrow stromal cells on hydroxyapatite/bacterial cellulose nanocomposite scaffolds. *Tissue Engineering: Part A 15(5)*, 1091–1098.

Farrell, E., E. M. Byrne, J. Fischer, F. J. O'Brien, B. C. O'Connell, P. J. Prendergast, and V. A. Campbell (2007, January). A comparison of the osteogenic potential of adult rat mesenchymal stem cells cultured in 2-d and on 3-d collagen glycosaminoglycan scaffolds. *Technol. Health Care 15*(1), 19–31.

Farrell, E., O. v. d. Jagt, J. Koevoet, N. Kops, C. v. Manen, C. Hellingman, H. Jahr, F. O'Brien, J. Verhaar, H. Weinans, and G. v. Osch (2008, December). Chondrogenic priming of human bone marrow stromal cells: A better route to bone repair? *Tissue Engineering. Part A*.

Farrell, E., F. J. O'Brien, P. Doyle, J. Fischer, I. Yannas, B. A. Harley, B. O'Connell, P. J. Prendergast, and V. A. Campbell (2006). A Collagen-glycosaminoglycan Scaffold Supports Adult Rat Mesenchymal Stem Cell

Differentiation Along Osteogenic and Chondrogenic Routes. *Tissue Engineering 12*(3), 459–468.

Fassina, L., E. Saino, M. Sbarra, L. Visai, M. Cusella De Angelis, G. Mazzini, F. Benazzo, and G. Magenes (2009). Ultrasonic and electromagnetic enhancement of a culture of human saos-2 osteoblasts seeded onto a titanium plasma-spray surface. *Tissue Engineerning Part C Methods 15(2)*, 233–42.

Fassina, L., L. Visai, L. Asti, F. Benazzo, P. Speziale, M. Tanzi, and G. Magenes (2005). Calcified matrix production by saos-2 cells inside a polyurethane porous scaffold, using a perfusion bioreactor. *Tissue Engineering 11(5/6)*, 685–700.

Fassina, L., L. Visai, F. Benazzo, L. Benedetti, A. Calligaro, M. G. C. D. Sngelis, A. Farina, V. Maliardi, and G. Magenes (2006). Effects of electromagnetic stimulation on calcified matrix production by saos-2 cells over a polyurethane porous scaffold. *Tissue Engineering 12(7)*, 1985–1999.

Feugier, P., R. Black, J. Hunt, and T. How (2005). Attachment, morphology and adherence of human endothelial cells to vascular prosthesis materials under the action of shear stress. *Biomaterials 26*(13), 1457 – 1466.

Flieger, J., T. Karachalios, L. Khaldi, P. Raptou, and G. Lyritis (1998). Mechanical stimulation in the form of vibration prevents postmenopausal bone loss in ovariectomized rats. *Calcified Tissue International 63*, 510–514. 10.1007/s002239900566.

Fong, E. L., C. K. Chan, and S. B. Goodman (2011). Stem cell homing in musculoskeletal injury. *Biomaterials 32*(2), 395 – 409.

Foolen, J., V. S. Deshpande, F. M. Kanters, and F. P. Baaijens (2012). The influence of matrix integrity on stress-fiber remodeling in 3d. *Biomaterials 33*(30), 7508 – 7518.

Fu, H., Q. Fu, N. Zhou, W. Huang, M. N. Rahaman, D. Wang, and X. Liu (2009). In vitro evaluation of borate-based bioactive glass scaffolds prepared by a polymer foam replication method. *Materials Science and Engineering: C 29*(7), 2275 – 2281.

Galili, U. (1993). Interaction of the natural anti-gal antibody with a-galactosyl epitopes: a major obstacle for xenotransplantation in humans. *Immunology Today 14(10)*, 480–482.

Galli, C., M. Piemontese, S. Lumetti, E. Manfredi, G. Macaluso, and G. Passeri (2012). The importance of wnt pathways for bone metabolism and their regulation by implant topography. *European Cells and Materials 24*, 46–59.

Garman, R., G. Gaudette, L.-R. Donahue, C. Rubin, and S. Judex (2007). Low-level accelerations applied in the absence of weight bearing can enhance trabecular bone formation. *Journal of Orthopaedic Research 25* (6), 732–740.

Genetos, D. C., C. J. Kephart, Y. Zhang, C. E. Yellowley, and H. J. Donahue (2007). Oscillating fluid flow activation of gap junction hemichannels induces atp release from mlo-y4 osteocytes. *Journal of Cellular Physiology 212*(1), 207–214.

Gilbert, T. W., T. L. Sellaro, and S. F. Badylak (2006). Decellularization of tissues and organs. *Biomaterials 27*(19), 3675 – 3683.

Gilsanz, V., T. A. Wren, M. Sanchez, F. Dorey, S. Judex, and C. Rubin (2006). Low-level, high-frequency mechanical signals enhance musculoskeletal development of young women with low bmd. *Journal of Bone and Mineral Research 21*(9), 1464–1474.

Globus, R. K., S. B. Doty, J. C. Lull, E. Holmuhamedov, and M. J. H. C. H. Damsky (1998). Fibronectin is a survival factor for differentiated osteoblasts. *Journal of Cell Science 111*, 1385–1393.

Goldstein, A. S. (2001). Effect of seeding osteoprogenitor cells as dense clusters on cell growth and differentiation. *Tissue Engineering 7(6)*, 817–827.

Goldstein, A. S., T. M. Juarez, C. D. Helmke, M. C. Gustin, and A. G. Mikos (2001). Effect of convection on osteoblastic cell growth and function in biodegradable polymer foam scaffolds. *Biomaterials 22*(11), 1279 – 1288.

Grayson, W. L., S. Bhumiratana, C. Cannizzaro, P.-h. G. Chao, D. P. Lennon, A. I. Caplan, and G. Vunjak-novakovic (2008). Effects of initial seeding density and fluid perfusion rate on formation of tissue-engineered bone.

Gregory, C. A., W. G. Gunn, A. Peister, and D. J. Prockop (2004). An alizarin red-based assay of mineralization by adherent cells in culture: comparison with cetylpyridinium chloride extraction. *Analytical Biochemistry 329* (1), 77 – 84.

Grellier, M., P. L. Granja, J.-C. Fricain, S. J. Bidarra, M. Renard, R. Bareille, C. Bourget, J. Amde, and M. A. Barbosa (2009). The effect of the co-

immobilization of human osteoprogenitors and endothelial cells within alginate microspheres on mineralization in a bone defect. *Biomaterials 30*(19), 3271 – 3278.

Guelcher, S. (2008). Biodegradable polyurethanes: Synthesis and applications in regenerative medicine. *Tissue Engineering Part B: Reviews 14(1)*, 3–17.

Guelcher, S., V. Patel, K. Gallagher, S. Connolly, J. Didier, J. Doctor, and J. Hollinger (2006). Synthesis and in vitro biocompatibility of injectable polyurethane foam scaffolds. *Tissue Engineering 12(5)*, 1247–1259.

Gupta, S., M. Hunter, P. Cebe, J. M. Levitt, D. L. Kaplan, and I. Georgakoudi (2008). Non-invasive optical characterization of biomaterial mineralization. *Biomaterials 29*(15), 2359 – 2369.

Gurkan, U. and O. Akkus (2008). The mechanical environment of bone marrow: A review. *Annals of Biomedical Engineering 36*, 1978–1991. 10.1007/s10439-008-9577-x.

Gusi, N., A. Raimundo, and A. Leal (2006). Low-frequency vibratory exercise reduces the risk of bone fracture more than walking: a randomized controlled trial. *BMC Musculoskeletal Disorders 7*, 1–8. 10.1186/1471-2474-7-92.

Haasper, C., J. Zeichen, R. Meister, C. Krettek, and M. Jagodzinski (2008). Tissue engineering of osteochondral constructs in vitro using bioreactors. *Injury 39*(1, Supplement), 66 – 76. Cartilage Repair.

Han, Y., S. C. Cowin, M. B. Schlaffler, and S. Weinbaum (2004). Mechanotransduction and strain amplification in osteocyte cell processes. *Proceeding of the National Academy of Sciences 101(47)*, 16689–16694.

Haugh, M. G., C. M. Murphy, R. C. McKiernan, C. Altenbuchner, and F. J. O'Brien (2011). Crosslinking and mechanical properties significantly influence cell attachment, proliferation, and migration within collagen glycosaminoglycan scaffolds. *Tissue Engineering Part A 17(9-10)*, 1201–1208.

Haynesworth, S. E., D. Reuben, and A. I. Caplan (1998). Cell-based tissue engineering therapies: the influence of whole body physiology. *Advanced Drug Delivery Reviews 33*(12), 3 – 14. Tissue Engineering.

Heath, C. A. (2000). Cells for tissue engineering. *Trends in Biotechnology 18*(1), 17 – 19.

Hee, C. K., M. A. Jonikas, and S. B. Nicoll (2006). Influence of three-dimensional scaffold on the expression of osteogenic differentiation markers by human dermal fibroblasts. *Biomaterials 27*(6), 875 – 884.

Heest, A. V. and M. Swiontkowski (1999). Bone-graft substitutes. *The Lancet 353, Supplement 1*(0), S28 – S29.

Heng, B. C., T. Cao, L. W. Stanton, P. Robson, and B. Olsen (2004). Strategies for directing the differentiation of stem cells into the osteogenic lineage in vitro. *Journal of Bone and Mineral Research 19*(9), 1379–1394.

Hennessy, K. M., B. E. Pollot, W. C. Clem, M. C. Phipps, A. A. Sawyer, B. K. Culpepper, and S. L. Bellis (2009). The effect of collagen i mimetic peptides on mesenchymal stem cell adhesion and differentiation, and on bone formation at hydroxyapatite surfaces. *Biomaterials 30*(10), 1898 – 1909.

Hernandez, C., R. Majeska, and M. Schaffler (2004). Osteocyte density in woven bone. *Bone 35*(5), 1095 – 1099.

Hessle, L., K. A. Johnson, H. C. Anderson, S. Narisawa, A. Sali, J. W. Goding, R. Terkeltaub, and J. L. Milln (2002). Tissue-nonspecific alkaline phosphatase and plasma cell membrane glycoprotein-1 are central antagonistic regulators of bone mineralization. *Proceedings of the National Academy of Sciences 99*(14), 9445–9449.

Hing, K. A. (2004). Bone repair in the twenty-first century: biology, chemistry or engineering. *Philosophical Transactions of the Royal Society 362*, 2821–2850ba.

Hodde, J. (2002). Naturally occurring scaffolds for soft tissue repair and regeneration. *Tissue Engineering 8*, 295–308. 10.1089/107632702753725058.

Hoemann, C., H. El-Gabalawy, and M. McKee (2009). In vitro osteogenesis assays: Influence of the primary cell source on alkaline phosphatase activity and mineralization. *Pathologie Biologie 57*(4), 318 – 323.

Holguin, N., J. Muir, C. Rubin, and S. Judex (2009). Short applications of very low-magnitude vibrations attenuate expansion of the intervertebral disc during extended bed rest. *The Spine Journal 9*(6), 470 – 477.

Hsiong, S. X. and D. J. Mooney (2006). Regeneration of vascularized bone. *Periodontology 2000 41*(1), 109–122.

Huang, A. H., B. M. Baker, G. A. Ateshian, and R. L. Mauck (2012). Sliding contact loading enhances the tensile properties of mesenchymal stem cell-seeded hydrogels. *European Cells and Materials 24*, 29–45.

Huang, J., L. D. Silvio, M. Wang, I. Rehman, C. Ohtsuki, and W. Bonfield (1997). Evaluation of in vitro bioactivity and biocompatibility of bioglass-reinforced polyethylene composite. *Journal of Materials Science: Materials in Medicine 8*, 809–813. 10.1023/A:1018581100400.

Hutmacher, D. W. (2000). Scaffolds in tissue engineering bone and cartilage. *Biomaterials 21*(24), 2529 – 2543. Orthopaedic Polymeric Biomaterials: Applications of Biodegradables.

Ichinohe, N., T. Takamoto, and Y. Tabata (2008, Jan). Proliferation, osteogenic differentiation, and distribution of rat bone marrow stromal cells in nonwoven fabrics by different culture methods. *Tissue Engineering Part A 14*(1), 107–16.

Ilan, D. I. and A. L. Ladd (2002). Bone graft substitutes. *Operative Techniques in Plastic and Reconstructive Surgery 9*(4), 151 – 160. Hand Surgery.

Ingham, E. and J. Fisher (2005). The role of macrophages in osteolysis of total joint replacement. *Biomaterials 26*(11), 1271 – 1286.

Ingram, J. H., S. Korossis, G. Howling, J. Fisher, and E. Ingham (2007). The use of ultrasonication to aid recellularization of acellular natural tissue scaffolds for use in anterior cruciate ligament reconstruction. *Tissue Engineering 13(7)*, 1561–1572.

Isaksson, H., O. Comas, C. C. van Donkelaar, J. Mediavilla, W. Wilson, R. Huiskes, and K. Ito (2007). Bone regeneration during distraction osteogenesis: Mechano-regulation by shear strain and fluid velocity. *Journal of Biomechanics 40*(9), 2002 – 2011.

Jaasma, M. J. and F. J. O'Brien (2008). Mechanical stimulation of osteoblasts using steady and dynamic fluid flow. *Tissue Engineering:Part A 14(7)*, 1213–1223.

Jaasma, M. J., N. A. Plunkett, and F. J. OBrien (2008). Design and validation of a dynamic flow perfusion bioreactor for use with compliant tissue engineering scaffolds. *Journal of Biotechnology 133*(4), 490 – 496.

Jacobs, C. R., S. Temiyasathit, and A. B. Castillo (2010). Osteocyte mechanobiology and pericellular mechanics. *Annual Review of Biomedical Engineering 12*(1), 369–400.

Jozwiak, A. B., C. M. Kielty, and R. A. Black (2008). Surface functionalization of polyurethane for the immobilization of bioactive moieties on tissue scaffolds. *Journal of Materials Chemistry 18*, 2240–2248.

Judex, S., S. Boyd, Y.-X. Qin, S. Turner, K. Ye, R. Mller, and C. Rubin (2003). Adaptations of trabecular bone to low magnitude vibrations result in more uniform stress and strain under load. *Annals of Biomedical Engineering 31*, 12–20. 10.1114/1.1535414.

Judex, S., X. Lei, D. Han, and C. Rubin (2007). Low-magnitude mechanical signals that stimulate bone formation in the ovariectomized rat are dependent on the applied frequency but not on the strain magnitude. *Journal of Biomechanics 40*(6), 1333 – 1339.

Judex, S., N. Zhong, M. E. Squire, K. Ye, L.-R. Donahue, M. Hadjiargyrou, and C. T. Rubin (2005). Mechanical modulation of molecular signals which regulate anabolic and catabolic activity in bone tissue. *Journal of Cellular Biochemistry 94*(5), 982–994.

Jungreuthmayer, C., S. Donahue, M. Jaasma, A. Al-Munajjed, J. Zanghellini, D. Kelly, and F. O'Brien (2009). A comparative study of shear stresses in collagen-glycosaminoglycan and calcium phosphate scaffolds in bone tissue-engineering bioreactors. *Tissue Engineering: Part A 15(5)*, 1141–9.

Karlsson, C., K. Emanuelsson, F. Wessberg, K. Kajic, M. Z. Axell, P. S. Eriksson, A. Lindahl, J. Hyllner, and R. Strehl (2009). Human embryonic stem cell-derived mesenchymal progenitorspotential in regenerative medicine. *Stem Cell Research 3*(1), 39 – 50.

Keogh, M. B., F. J. OBrien, and J. S. Daly (2010). Substrate stiffness and contractile behaviour modulate the functional maturation of osteoblasts on a collagengag scaffold. *Acta Biomaterialia 6*(11), 4305 – 4313.

Khan, A. S., M. S. Aziz, D. Paul, F. Wong, and I. U. Rehman (2008). Synthesis and in-vitro analysis of degradative resistance of a novel bioactive composite. *Journal of Bionanoscience 2*(2), 75–88.

Kiiski, J., A. Heinonen, T. L. Jrvinen, P. Kannus, and H. Sievnen (2008). Transmission of vertical whole body vibration to the human body. *Journal*

of Bone and Mineral Research 23(8), 1318–1325.

Kim, H. K., W. S. Shim, S. E. Kim, K.-H. Lee, E. Kang, J.-H. Kim, K. Kim, I. C. Kwon, and D. S. Lee (2009). Injectable in situ-forming ph/thermo-sensitive hydrogel for bone tissue engineering. *Tissue Engineering: Part A 15(4)*, 923–933.

Kimelman, N., G. Pelled, G. A. Helm, J. Huard, E. M. Schwarz, and D. Gazit (2007). Review: Gene- and stem cell-based therapeutics for bone regeneration and repair. *Tissue Engineering 13(6)*, 1135–1150.

Klein-Nulend, J., R. Bacabac, and M. Mullender (2005). Mechanobiology of bone tissue. *Pathologie Biologie 53*(10), 576 – 580.

Klein-Nulend, J., R. Bacabac, J. Veldhuijzen, and J. V. Loon (2003). Microgravity and bone cell mechanosensitivity. *Advances in Space Research 32* (8), 1551 – 1559. Space Life Sciences: Gravitational Biology: 2002.

Knight, R. L., H. E. Wilcox, S. A. Korossis, J. Fisher, and E. Ingham (2008). The use of acellular matrices for the tissue engineering of cardiac valves. *Proceedings of the Institution of Mechanical Engineers, Part H: Journal of Engineering in Medicine 222*(1), 129–143.

Korossis, S., F. Bolland, J. Kearney, J. Fisher, and E. Ingham (2006). *Topics in Tissue Engineering*, Volume 2, Chapter Chapter 8 Bioreactors in Tissue Engineering.

Lamba, N. M., K. A. Woodhouse, and S. L. Cooper. (1998). *Polyurethanes in biomedical applications*. Boca Raton : CRC Press.

Lange, C., F. Cakiroglu, A.-N. Spiess, H. Cappallo-Obermann, J. Dierlamm, and A. R. Zander (2007). Accelerated and safe expansion of human mesenchymal stromal cells in animal serum-free medium for transplantation and regenerative medicine. *Journal of Cellular Physiology 213*(1), 18–26.

Lau, E., S. Al-Dujaili, A. Guenther, D. Liu, L. Wang, and L. You (2010). Effect of low-magnitude, high-frequency vibration on osteocytes in the regulation of osteoclasts. *Bone 46*(6), 1508 – 1515.

Lau, E., W. D. Lee, J. Li, A. Xiao, J. E. Davies, Q. Wu, L. Wang, and L. You (2011). Effect of low-magnitude, high-frequency vibration on osteogenic differentiation of rat mesenchymal stromal cells. *Journal of Orthopaedic Research 29*(7), 1075–1080.

Lee, O. K., T. K. Kuo, W.-M. Chen, K.-D. Lee, S.-L. Hsieh, and T.-H. Chen (2004). Isolation of multipotent mesenchymal stem cells from umbilical cord blood. *Blood 103*(5), 1669–1675.

Lee, T. C., T. L. Arthur, L. J. Gibson, and W. C. Hayes (2000). Sequential labelling of microdamage in bone using chelating agents. *Journal of Orthopaedic Research 18*(2), 322–325.

Lennon, D. P., S. E. Haynesworth, R. G. Young, J. E. Dennis, and A. I. Caplan (1995). A chemically defined medium supports in vitro proliferation and maintains the osteochondral potential of rat marrow-derived mesenchymal stem cells. *Experimental Cell Research 219*(1), 211 – 222.

Leung, K. S., H. F. Shi, W. H. Cheung, L. Qin, W. K. Ng, K. F. Tam, and N. Tang (2009). Low-magnitude high-frequency vibration accelerates callus formation, mineralization, and fracture healing in rats. *Journal of Orthopaedic Research 27*(4), 458–465.

Li, J. P., P. Habibovic, M. van den Doel, C. E. Wilson, J. R. de Wijn, C. A. van Blitterswijk, and K. de Groot (2007). Bone ingrowth in porous titanium implants produced by 3d fiber deposition. *Biomaterials 28*(18), 2810 – 2820.

Li, W.-J., R. Tuli, X. Huang, P. Laquerriere, and R. S. Tuan (2005). Multilineage differentiation of human mesenchymal stem cells in a three-dimensional nanofibrous scaffold. *Biomaterials 26*(25), 5158 – 5166.

Liedert, A., D. Kaspar, R. Blakytny, L. Claes, and A. Ignatius (2006). Signal transduction pathways involved in mechanotransduction in bone cells. *Biochemical and Biophysical Research Communications 349*(1), 1 – 5.

Liu, G., C. Shu, L. Cui, W. Liu, and Y. Cao (2008). Tissue-engineered bone formation with cryopreserved human bone marrow mesenchymal stem cells. *Cryobiology 56*(3), 209 – 215.

Lohmann, C. H., Z. Schwartz, Y. Liu, Z. Li, B. J. Simon, V. L. Sylvia, D. D. Dean, L. F. Bonewald, H. J. Donahue, and B. D. Boyan (2003). Pulsed electromagnetic fields affect phenotype and connexin 43 protein expression in mlo-y4 osteocyte-like cells and ros 17/2.8 osteoblast-like cells. *Journal of Orthopaedic Research 21*(2), 326–334.

Long, M. W., J. A. Robinson, E. A. Ashcraft, and K. G. Mann. Regulation of human bone marrow-derived osteoprogenitor cells by osteogenic growth factors.

Maggio, N. D., E. Piccinini, M. Jaworski, A. Trumpp, D. J. Wendt, and I. Martin (2011). Toward modeling the bone marrow niche using scaffold-based 3d culture systems. *Biomaterials 32*(2), 321 – 329.

Mannello, F. and G. A. Tonti (2007). Concise review: No breakthroughs for human mesenchymal and embryonic stem cell culture: Conditioned medium, feeder layer, or feeder-free; medium with fetal calf serum, human serum, or enriched plasma; serum-free, serum replacement nonconditioned medium, or ad hoc formula? all that glitters is not gold! *STEM CELLS 25*(7), 1603–1609.

Mao, J., W. Giannobile, J. Helms, S. Hollister, P. Krebsbach, M. Longaker, and S. Shi (2006). Craniofacial tissue engineering by stem cells. *Journal of Dental Research 85*(11), 966–979.

Marion, N. W., W. Liang, W. Liang, G. C. Reilly, D. E. Day, M. N. Rahaman, and J. J. Mao (2005). Borate glass supports the in vitro osteogenic differentiation of human mesenchymal stem cells. *Mechanics of Advanced Materials and Structures 12*(3), 239–246.

Martin, I., D. Wendt, and M. Heberer (2004). The role of bioreactors in tissue engineering. *Trends in Biotechnology 22*(2), 80 – 86.

Mauney, J., S. Sjostorm, J. Blumberg, R. Horan, J. O'Leary, G. Vunjak-Novakovic, V. Volloch, and D. Kaplan (2004). Mechanical stimulation promotes osteogenic differentiation of human bone marrow stromal cells on 3-d partially demineralized bone scaffolds in vitro. *Calcified Tissue International 74*, 458–468. 10.1007/s00223-003-0104-7.

Mauney, J. R., J. Blumberg, M. Pirun, V. Volloch, G. Vunjak-Novakovic, and D. L. Kaplan (2004). Osteogenic differentiaion of human bone marrow stromal cells on partially demineralized bone scaffolds in vitro. *Tissue Engineering 10(1/2)*, 81–92.

Mauney, J. R., V. Volloch, and D. L. Caplan (2005). Role of adult mesenchymal stem cells in bone tissue-engineering applications: Current status and future prospects. *Tissue Engineering 11(5/6)*, Joshua.

Melchels, F. P., A. M. Barradas, C. A. van Blitterswijk, J. de Boer, J. Feijen, and D. W. Grijpma (2010). Effects of the architecture of tissue engineering scaffolds on cell seeding and culturing. *Acta Biomaterialia 6*(11), 4208 – 4217.

Meyer, U., U. Joos, and H. Wiesmann (2004). Biological and biophysical principles in extracorporal bone tissue engineering: Part i. *International Journal of Oral and Maxillofacial Surgery 33*(4), 325 – 332.

Montjovent, M.-O., L. Mathieu, H. Schmoekel, S. Mark, P.-E. Bourban, P.-Y. Zambelli, L. A. Laurent-Applegate, and D. P. Pioletti (2007). Repair of critical size defects in the rat cranium using ceramic-reinforced pla scaffolds obtained by supercritical gas foaming. *Journal of Biomedical Materials Research Part A 83A*(1), 41–51.

Morris, H. L., C. I. Reed, J. W. Haycock, and G. C. Reilly (2010). Mechanisms of fluid-flow-induced matrix production in bone tissue engineering. *Proceedings of the Institution of Mechanical Engineers, Part H: Journal of Engineering in Medicine 224*(12), 1509–1521.

Moursi, A. M., C. H. Damsky, J. Lull, D. Zimmerman, S. B. Doty, S. ichi Aota, and R. K. Globus (1996). Fibronectin regulates calvarial osteoblast differentiation. *Journal of Cell Science 109*, 1369–1380.

Moursi, A. M., R. K. Globus, and C. H. Damsky (1997). Interactions between integrin receptors and fibronectin are required for calvarial osteoblast differentiation in vitro. *Journal of Cell Science 110*, 2187–2196.

Mullender, M., A. El Haj, Y. Yang, M. van Duin, E. Burger, and J. Klein-Nulend (2004). Mechanotransduction of bone cells in vitro: Mechanobiology of bone tissue. *Medical and Biological Engineering and Computing 42*, 14–21. 10.1007/BF02351006.

Murfee, W. L., L. A. Hammett, C. Evans, L. Xie, M. Squire, C. Rubin, S. Judex, and T. C. Skalak (2005). High-frequency, low-magnitude vibrations suppress the number of blood vessels per muscle fiber in mouse soleus muscle. *Journal of Applied Physiology 98*(6), 2376–2380.

Murphy, C. M., M. G. Haugh, and F. J. O'Brien (2010). The effect of mean pore size on cell attachment, proliferation and migration in collagen-glycosaminoglycan scaffolds for bone tissue engineering. *Biomaterials 31*(3), 461 – 466.

Murphy, W. L., S. Hsiong, T. P. Richardson, C. A. Simmons, and D. J. Mooney (2005). Effects of a bone-like mineral film on phenotype of adult human mesenchymal stem cells in vitro. *Biomaterials 26*(3), 303 – 310.

Murray-Dunning, C., S. L. McArthur, T. Sun, R. McKean, A. J. Ryan, and J. W. Haycock (2011). Three-dimensional alignment of schwann cells using hydrolysable microfiber scaffolds: Strategies for peripheral nerve repair. In J. W. Haycock (Ed.), *3D Cell Culture*, Volume 695 of *Methods in Molecular Biology*, pp. 155–166. Humana Press.

Ng, K. W., D. T. Leong, and D. W. Hutmacher (2005). The challenge to measure cell proliferation in two and three dimensions. *Tissue Engi 11(1/2)*, 182–191.

Ngiam, M., S. Liao, A. J. Patil, Z. Cheng, C. K. Chan, and S. Ramakrishna (2009). The fabrication of nano-hydroxyapatite on plga and plga/collagen nanofibrous composite scaffolds and their effects in osteoblastic behavior for bone tissue engineering. *Bone 45*(1), 4 – 16.

Nguyen, H., D. Morgan, and M. Forwood (2007). Sterilization of allograft bone: effects of gamma irradiation on allograft biology and biomechanics. *Cell and Tissue Banking 8*, 93–105. 10.1007/s10561-006-9020-1.

Nguyen, T. D., R. Liang, S. L.-Y. Woo, S. D. Burton, C. Wu, A. Almarza, M. S. Sacks, and S. Abramowitch (2009). Effects of cell seeding and cyclic stretch on the fiber remodeling in an extracellular matrixderived bioscaffold. *Tissue Engineering: Part A 15(4)*, 957–963.

Nicholson, J. W. (2012). *The Chemistry of Polymers* (4th Edition ed.). RSC Publishing.

Nirmalanandhan, V., J. Shearn, N. Juncosa-Melvin, M. Rao, C. Gooch, A. Jain, G. Bradica, and D. Butler (2008). Improving linear stiffness of the cell-seeded collagen sponge constructs by varying the components of the mechanical stimulus. *Tissue Engineering Part A 14(11)*, 1883–91.

Nth, U., A. M. Osyczka, R. Tuli, N. J. Hickok, K. G. Danielson, and R. S. Tuan (2002). Multilineage mesenchymal differentiation potential of human trabecular bone-derived cells. *Journal of Orthopaedic Research 20*(5), 1060–1069.

O'Brien, F., B. Harley, I. Yannas, and L. Gibson (2005). The effect of pore size on cell adhesion in collagen-gag scaffolds. *Biomaterials 26*(4), 433 – 441.

O'Brien, F. J., B. A. Harley, M. A. Waller, I. V. Yannas, L. J. Gibson, and P. J. Prendergast (2007, January). The effect of pore size on permeability and

cell attachment in collagen scaffolds for tissue engineering. *Technol. Health Care 15*(1), 3–17.

O'Brien, F. J., D. Taylor, and T. Lee (2002). An improved labelling technique for monitoring microcrack growth in compact bone. *Journal of Biomechanics 35*(4), 523 – 526.

Ogura, N., M. Kawada, W.-J. Chang, Q. Zhang, S.-Y. Lee, T. Kondoh, and Y. Abiko (2004). Differentiation of the human mesenchymal stem cells derived from bone marrow and enhancement of cell attachment by fibronectin. *Journal of Oral Science 46(4)*, 207–213.

Ollivere, B., J. A. Wimhurst, I. M. Clark, and S. T. Donell (2012). Current concepts in osteolysis. *Journal of Bone & Joint Surgery, British Volume 94-B*(1), 10–15.

Osyczka, A., D. Diefenderfer, G. Bhargave, and P. Leboy (2004). Different effects of bmp-2 on marrow stromal cells from human and rat bone. *Cells Tissues Organs 176*, 109–119.

Osyczka, A., U. Noth, J. O'Connor, E. Caterson, K. Yoon, K. Danielson, and R. Tuan (2002). Multilineage differentiation of adult human bone marrow progenitor cells transduced with human papilloma virus type 16 e6/e7 genes. *Calcified Tissue International 71*, 447–458. 10.1007/s00223-001-1090-2.

Osyczka, A. M., M. Damek-Poprawa, A. Wojtowicz, and S. O. Akintoye (2009). Age and skeletal sites affect bmp-2 responsiveness of human bone marrow stromal cells. *Connective Tissue Research 50*(4), 270–277.

Osyczka, A. M. and P. S. Leboy (2005). Bone morphogenetic protein regulation of early osteoblast genes in human marrow stromal cells is mediated by extracellular signal-regulated kinase and phosphatidylinositol 3-kinase signaling. *Endocrinology 146*(8), 3428–3437.

Owan, I., D. B. Burr, C. H. Turner, J. Qiu, Y. Tu, J. E. Onyia, and R. L. Duncan (1997). Mechanotransduction in bone: osteoblasts are more responsive to fluid forces than mechanical strain. *American Journal of Physiology - Cell Physiology 273*(3), C810–C815.

Oxlund, B., G. rtoft, T. Andreassen, and H. Oxlund (2003). Low-intensity, high-frequency vibration appears to prevent the decrease in strength of the femur and tibia associated with ovariectomy of adult rats. *Bone 32*(1), 69 – 77.

Pamula, E., J. Kokoszka, K. Cholewa-Kowalska, M. Laczka, L. Kantor, L. Niedzwiedzki, G. Reilly, J. Filipowska, W. Madej, M. Kolodziejczyk, G. Tylko, and A. Osyczka (2011). Degradation, bioactivity, and osteogenic potential of composites made of plga and two different sol-gel bioactive glasses. *Annals of Biomedical Engineering 39*, 2114–2129. 10.1007/s10439-011-0307-4.

Papachroni, K. K., D. N. Karatzas, K. A. Papavassiliou, E. K. Basdra, and A. G. Papavassiliou (2009). Mechanotransduction in osteoblast regulation and bone disease. *Trends in Molecular Medicine 15*(5), 208 – 216.

Partap, S., A. Muthutantri, I. Rehman, G. Davis, and J. Darr (2007). Preparation and characterisation of controlled porosity alginate hydrogels made via a simultaneous micelle templating and internal gelation process. *Journal of Materials Science 42*, 3502–3507. 10.1007/s10853-007-1533-x.

Partap, S., I. Rehman, J. Jones, and J. Darr (2006). "supercritical carbon dioxide in water" emulsion-templated synthesis of porous calcium alginate hydrogels. *Advanced Materials 18*(4), 501–504.

PD-USGov (2012a). Cortical and cancellouw bone structure image.

PD-USGov (2012b). Long bone illustration.

Peake, M. A., L. M. Cooling, J. L. Magnay, P. B. M. Thomas, and A. J. El Haj (2000). Selected contribution: Regulatory pathways involved in mechanical induction of c-fos gene expression in bone cells. *Journal of Applied Physiology 89*(6), 2498–2507.

Pedersen, J. and M. Swartz (2005). Mechanobiology in the third dimension. *Annals of Biomedical Engineering 33*, 1469–1490. 10.1007/s10439-005-8159-4.

Pittenger, M., G. Mbalaviele, M. Black, J. Mosca, and D. Marshak (2002). Mesenchymal stem cells. In M. R. Koller, B. O. Palsson, and J. R. Masters (Eds.), *Human Cell Culture*, Volume 5 of *Human Cell Culture*, pp. 189–207. Springer Netherlands.

Porter, J. R., T. T. Ruckh, and K. C. Popat (2009). Bone tissue engineering: A review in bone biomimetics and drug delivery strategies. *Biotechnology Progress 25*(6), 1539–1560.

Porter, R. M., W. R. Huckle, and A. S. Goldstein (2003). Effect of dexamethasone withdrawal on osteoblastic differentiation of bone marrow stromal cells. *Journal of Cellular Biochemistry 90*(1), 13–22.

Pre, D., G. Ceccarelli, M. G. C. Angelis, and G. Magenes (2010). High frequency mechanical vibrations stimulate the bone matrix formation in hbmscs (human bone marrow stromal cells). In P. D. Bamidis, N. Pallikarakis, and R. Magjarevic (Eds.), *XII Mediterranean Conference on Medical and Biological Engineering and Computing 2010*, Volume 29 of *IFMBE Proceedings*, pp. 494–497. Springer Berlin Heidelberg.

Pre, D., G. Ceccarelli, L. Benedetti, G. Magenes, and M. Cusella De Angelis (2009). Effects of low-amplitude, high-frequency vibrations on proliferation and differentiation of saos-2 human osteogenic cell line. *Tissue Engineering 15*(4), 669–79.

Pre, D., G. Ceccarelli, G. Gastaldi, A. Asti, E. Saino, L. Visai, F. Benazzo, M. C. D. Angelis, and G. Magenes (2011). The differentiation of human adipose-derived stem cells (hascs) into osteoblasts is promoted by low amplitude, high frequency vibration treatment. *Bone 49*(2), 295 – 303.

Puppi, D., N. Detta, A. M. Piras, F. Chiellini, D. A. Clarke, G. C. Reilly, and E. Chiellini (2010). Development of electrospun three-arm star poly(-caprolactone) meshes for tissue engineering applications. *Macromolecular Bioscience 10*(8), 887–897.

Pytlk, R., D. Stehlk, T. Soukup, M. Kalbov, F. Rypek, T. Tr, K. Mulinkov, P. Michnov, L. Kideryov, J. ivn, P. K. Jr., R. Vesel, and M. T. P. Klener (2009). The cultivation of human multipotent mesenchymal stromal cells in clinical grade medium for bone tissue engineering. *Biomaterials 30*(20), 3415 – 3427.

Rada, T., R. L. Reis, and M. E. Gomes (2009). Adipose tissue-derived stem cells and their application in bone and cartilage tissue engineering. *Tissue Engineering: Part B 15(2)*, 113–125.

Ramrattan, N. N., R. G. Heijkants, T. G. V. Tienen, A. J. Schouten, R. P. Veth, and P. Buma (2005). Assessment of tissue ingrowth rates in polyurethane scaffolds for tissue engineering. *Tissue Engineering 11(7/8)*, 1212–1223.

Reilly, G. and J. Currey (1999). The development of microcracking and failure in bone depends on the loading mode to which it is adapted. *Journal of*

Experimental Biology 202(5), 543–552.

Reilly, G. C. and A. J. Engler (2010). Intrinsic extracellular matrix properties regulate stem cell differentiation. *Journal of Biomechanics 43*(1), 55 – 62. ¡ce:title¿Special Issue on Cell Mechanobiology¡/ce:title¿.

Reilly, G. C., T. R. Haut, C. E. Yellowley, H. J. Donahue, and C. R. Jacobs (2003). Fluid flow induced pge2 release by bone cells is reduced by glycocalyx degradation whereas calcium signals are not. *Biorheology 40*, 591–603.

Reilly, G. C., S. Radin, A. T. Chen, and P. Ducheyne (2007). Differential alkaline phosphatase responses of rat and human bone marrow derived mesenchymal stem cells to 45s5 bioactive glass. *Biomaterials 28*(28), 4091 – 4097.

Richards, S., D. Leavesley, G. Topping, and Z. Upton (2008). Development of defined media for the serum-free expansion of primary human keratinocytes and human embryonic stem cells. *Tissue Engineering: Part C 14(3)*, 221–232.

Rickard, D., T. Sullivan, B. Shenker, P. Leboy, and I. Kazhdan (1994). Induction of rapid osteoblast differentiation in rat bone marrow stromal cell cultures by dexamethasone and bmp-2. *Developmental Biology 161*(1), 218 – 228.

Rittweger, J., G. Beller, G. Armbrecht, E. Mulder, B. Buehring, U. Gast, F. Dimeo, H. Schubert, A. de Haan, D. F. Stegeman, H. Schiessl, and D. Felsenberg (2010). Prevention of bone loss during 56 days of strict bed rest by side-alternating resistive vibration exercise. *Bone 46*, 137–147.

Rosario, D. J., G. C. Reilly, E. A. Salah, M. Glover, A. J. Bullock, and S. MacNeil (2008). Decellularisation and sterilisation of porcine urinary bladder matrix for tissue engineering in the lower urinary tract. *Regenerative Medicine 3(2)*, 145–156.

Rose, F. R., L. A. Cyster, D. M. Grant, C. A. Scotchford, S. M. Howdle, and K. M. Shakesheff (2004). In vitro assessment of cell penetration into porous hydroxyapatite scaffolds with a central aligned channel. *Biomaterials 25*(24), 5507 – 5514.

Rubin, C., S. Judex, and Y.-X. Qin (2006). Low-level mechanical signals and their potential as a non-pharmacological intervention for osteoporosis. *Age and Ageing 35*(suppl 2), ii32–ii36.

Rubin, C., M. Pope, J. Fritton, M. Magnusson, T. Hansson, and K. McLeod (2003). Transmissibility of 15-hertz to 35-hertz vibrations to the human

hip and lumbar spine: determining the physiologic feasibility of delivering low-level anabolic mechanical stimuli to skeletal regions at greatest risk of fracture because of osteoporosis. *Spine (Phila Pa 1976) 28(23)*, 2621–2627.

Rubin, C., R. Recker, D. Cullen, J. Ryaby, J. McCabe, and K. McLeod (2004). Prevention of postmenopausal bone loss by a low-magnitude, high-frequency mechanical stimuli: A clinical trial assessing compliance, efficacy, and safety. *Journal of Bone and Mineral Research 19*(3), 343–351.

Rubin, C. and J. Rubin (2006). *Primer on the Metabolic Bone Diseases and Disorders of Mineral Metabolism* (Sixth Edition ed.)., Chapter Biomechanics and Mechanobiology of Bone, pp. 36–42. ASBMR (American Society for Bone and Mineral Research).

Rubin, C., A. Turner, C. Mallinckrodt, C. Jerome, K. Mcleod, and S. Bain (2002). Mechanical strain, induced noninvasively in the high-frequency domain, is anabolic to cancellous bone, but not cortical bone. *Bone 30*(3), 445 – 452.

Rubin, C., A. S. Turner, R. Mller, E. Mittra, K. McLeod, W. Lin, and Y.-X. Qin (2002). Quantity and quality of trabecular bone in the femur are enhanced by a strongly anabolic, noninvasive mechanical intervention. *Journal of Bone and Mineral Research 17*(2), 349–357.

Rubin, C., G. Xu, and S. Judex (2001). The anabolic activity of bone tissue, suppressed by disuse, is normalized by brief exposure to extremely low-magnitude mechanical stimuli. *The FASEB Journal 15*(12), 2225–2229.

Rubin, C. T., D. W. Sommerfeldt, S. Judex, and Y.-X. Qin (2001). Inhibition of osteopenia by low magnitude, high-frequency mechanical stimuli. *Drug Discovery Today 6*(16), 848 – 858.

Rubin, J., C. Rubin, and C. R. Jacobs (2006). Molecular pathways mediating mechanical signaling in bone. *Gene 367*(0), 1 – 16.

Rubinacci, A., M. Marenzana, F. Cavani, F. Colasante, I. Villa, J. Willnecker, G. Moro, L. Spreafico, M. Ferretti, F. Guidobono, and G. Marotti (2008). Ovariectomy sensitizes rat cortical bone to whole-body vibration. *Calcified Tissue International 82*, 316–326. 10.1007/s00223-008-9115-8.

Sachlos, E. and J. Czernuszka (2003). Making tissue engineering scaffolds work. review on the application of solid freeform fabrication technology to the production of tissue engineering scaffolds. *European Cells and Materials 5*, 29–40.

Salgado, A. J., O. P. Coutinho, and R. L. Reis (2004). Bone tissue engineering: State of the art and future trends. *Macromolecular Bioscience 4* (8), 743–765.

Sandhu, E., J. D. Miles, L. E. Dahners, B. V. Keller, and P. S. Weinhold (2011). Whole body vibration increases area and stiffness of the flexor carpi ulnaris tendon in the rat. *Journal of Biomechanics 44*, 1189–1191.

Santis, G. D., A. Lennon, F. Boschetti, B. Verhegghe, P. Verdonck, and P. Prendergast (2011). How can cells sense the elasticity of a substrate? an analysis using a cell tensegrity model. *European Cells and Materials 22*, 202–213.

Sawyer, A., K. Hennessy, and S. Bellis (2005). Regulation of mesenchymal stem cell attachment and spreading on hydroxyapatite by rgd peptides and adsorbed serum proteins. *Biomaterials 26*(13), 1467 – 1475.

Scheffler, S., J. Gonnermann, J. Kamp, D. Przybilla, and A. Pruss (2008). Remodeling of acl allografts is inhibited by peracetic acid sterilization. *Clinical Orthopaedics and Related Research 466*(8), 1810–1818.

Schmidt, T., A. Hoburg, C. Broziat, M. Smith, U. Gohs, A. Pruss, and S. Scheffler (2012). Sterilization with electron beam irradiation influences the biomechanical properties and the early remodeling of tendon allografts for reconstruction of the anterior cruciate ligament (acl). *Cell and Tissue Banking 13*(3), 387–400.

Schwartz, J. (2007). *Skeleton keys: an introduction to human skeletal morphology, development, and analysis*. Oxford University Press.

Sehmisch, S., R. Galal, L. Kolios, M. Tezval, C. Dullin, S. Zimmer, K. Stuermer, and E. Stuermer (2009). Effects of low-magnitude, high-frequency mechanical stimulation in the rat osteopenia model. *Osteoporosis International 20*, 1999–2008. 10.1007/s00198-009-0892-3.

Shahdadfar, A., K. Frnsdal, T. Haug, F. P. Reinholt, and J. E. Brinchmann (2005). In vitro expansion of human mesenchymal stem cells: Choice of serum is a determinant of cell proliferation, differentiation, gene expression, and transcriptome stability. *STEM CELLS 23*(9), 1357–1366.

Shen, H., X. Hu, F. Yang, J. Bei, and S. Wang (2009). The bioactivity of rhbmp-2 immobilized poly(lactide-co-glycolide) scaffolds. *Biomaterials 30*(18), 3150 – 3157.

Shi, H.-F., W.-H. Cheung, L. Qin, A. H.-C. Leung, and K.-S. Leung (2010). Low-magnitude high-frequency vibration treatment augments fracture healing in ovariectomy-induced osteoporotic bone. *Bone 46*(5), 1299 – 1305.

Shikata, T., T. Shiraishi, S. Morishita, R. Takeuchi, and T. Saito (2008). Effects of amplitude and frequency of mechanical vibration stimulation on cultured osteoblasts. *Journal of System Design and Dynamics 2*(1), 382–388.

Silva, M., L. Cyster, J. Barry, X. Yang, R. Oreffo, D. Grant, C. Scotchford, S. Howdle, K. Shakesheff, and F. Rose (2006). The effect of anisotropic architecture on cell and tissue infiltration into tissue engineering scaffolds. *Biomaterials 27*(35), 5909 – 5917.

Sittichockechaiwut, A., A. M. Scutt, A. J. Ryan, L. F. Bonewald, and G. C. Reilly (2009). Use of rapidly mineralising osteoblasts and short periods of mechanical loading to accelerate matrix maturation in 3d scaffolds. *Bone 44*(5), 822 – 829.

Sittichokechaiwut, A., J. Edwards, A. Scutt, and G. Reilly (2010). Short bouts of mechanical loading are as effective as dexamethasone at inducing matrix production by human bone marrow mesenchymal stem cells. *European Cells and Materials 20*, 45–57.

Skerry, T. M. (2008). The response of bone to mechanical loading and disuse: Fundamental principles and influences on osteoblast/osteocyte homeostasis. *Archives of Biochemistry and Biophysics 473*(2), 117 – 123. Highlight Issue: Bone Remodeling: Facts and Perspectives.

Sommerfeldt and Rubin (2001). Biology of bone and how it orchestrates the form and function of the skeleton. *European Spine Journal 10*, S86–S95. 10.1007/s005860100283.

St. Pierre, C. A., M. Chan, Y. Iwakura, D. C. Ayers, E. A. Kurt-Jones, and R. W. Finberg (2010). Periprosthetic osteolysis: Characterizing the innate immune response to titanium wear-particles. *Journal of Orthopaedic Research 28*(11), 1418–1424.

Stevens, A., A. Stevens, and J. Lowe (2005). *Human histology*. Human Histology. Elsevier/Mosby.

Stevens, M. M. and J. H. George (2005). Exploring and engineering the cell surface interface. *Science 310*(5751), 1135–1138.

Strehl, R., K. Scumacher, U. de Vries, and W. W. Minuth (2002). Proliferating cells versus differentiated cells in tissue engineering. *Tissue Engineering 8(1)*, 37–42.

Sun, T., S. Jackson, J. W. Haycock, and S. MacNeil (2006). Culture of skin cells in 3d rather than 2d improves their ability to survive exposure to cytotoxic agents. *Journal of Biotechnology 122*(3), 372 – 381.

Sun, X., Y. Gan, T. Tang, X. Zhang, and K. Dai (2008). In vitro proliferation and differentiation of human mesenchymal stem cells cultured in autologous plasma derived from bone marrow. *Tissue Engineering: Part A 14(3)*, 391–400.

Suzuki, N., K. Kitamura, T. Nemoto, N. Shimizu, S. Wada, T. Kondo, M. Tabata, F. Sodeyama, K. Ijiri, and A. Hattori (2007). Effect of vibration on osteoblastic and osteoclastic activities: Analysis of bone metabolism using goldfish scale as a model for bone. *Advances in Space Research 40* (11), 1711 – 1721.

Swartz, M. A. and M. E. Fleury (2007). Interstitial flow and its effects in soft tissues. *Annual Review of Biomedical Engineering 9*(1), 229–256.

Takagishi, Y. (2006). Bone-like tissue formation by three-dimensional culture of mg63 osteosarcoma cells in gelatin hydrogels using calcium-enriched medium. *Tissue Eng. 12*, 927–937.

Tanaka, S. M., J. Li, R. L. Duncan, H. Yokota, D. B. Burr, and C. H. Turner (2003). Effects of broad frequency vibration on cultured osteoblasts. *Journal of Biomechanics 36*(1), 73 – 80.

Tang, H., Z. Xu, X. Qin, B. Wu, L. Wu, X. Zhao, and Y. Li (2009). Chest wall reconstruction in a canine model using polydioxanone mesh, demineralized bone matrix and bone marrow stromal cells. *Biomaterials 30*(19), 3224 – 3233.

Tang, L., Z. Lin, and Y. ming Li (2006). Effects of different magnitudes of mechanical strain on osteoblasts in vitro. *Biochemical and Biophysical Research Communications 344*(1), 122 – 128.

TE (2012). Tissue engineering schematic.

Thi, M. M., J. M. Tarbell, S. Weinbaum, and D. C. Spray (2004). The role of the glycocalyx in reorganization of the actin cytoskeleton under fluid

shear stress: A "bumper-car" model. *Proceedings of the National Academy of Sciences of the United States of America 101*(47), 16483–16488.

Thomas, G. and A. El Haj (1996). Bone marrow stromal cells are load responsive in vitro. *Calcified Tissue International 58*, 101–108. 10.1007/BF02529731.

Thompson, A. D., M. W. Betz, D. M. Yoon, and J. P. Fisher (2009). Osteogenic differentiation of bone marrow stromal cells induced by coculture with chondrocytes encapsulated in 3-dimensional matrices. *Tissue Engineering: Part A 15(5)*, 1181–1190.

Tischer, T., S. Aryee, G. Wexel, E. Steinhauser, C. Adamczyk, S. Eichhorn, S. Milz, V. Martinek, B. Gnsbacher, A. Imhoff, and S. Vogt (2010). Tissue engineering of the anterior cruciate ligament-sodium dodecyl sulfate-acellularized and revitalized tendons are inferior to native tendons. *Tissue engineering. Part A 16(3)*, 1031–40.

Tjandrawinata, R. R., V. L. Vincent, and M. Hughes-Fulford (1997). Vibrational force alters mrna expression in osteoblasts. *The FASEB Journal 11*(6), 493–7.

Tong, W. Y., W. Shen, C. W. Yeung, Y. Zhao, S. H. Cheng, P. K. Chu, D. Chan, G. C. Chan, K. M. Cheung, K. W. Yeung, and Y. W. Lam (2012). Functional replication of the tendon tissue microenvironment by a bioimprinted substrate and the support of tenocytic differentiation of mesenchymal stem cells. *Biomaterials 33*(31), 7686 – 7698.

Torvinen, S., P. Kannus, H. Sievnen, T. A. Jrvinen, M. Pasanen, S. Kontulainen, A. Nenonen, T. L. Jrvinen, T. Paakkala, M. Jrvinen, and I. Vuori (2003). Effect of 8-month vertical whole body vibration on bone, muscle performance, and body balance: A randomized controlled study. *Journal of Bone and Mineral Research 18*(5), 876–884.

Tsigkou, O., J. R. Jones, J. M. Polak, and M. M. Stevens (2009). Differentiation of fetal osteoblasts and formation of mineralized bone nodules by 45s5 bioglass conditioned medium in the absence of osteogenic supplements. *Biomaterials 30*(21), 3542 – 3550.

Tuan, R., G. Boland, and R. Tuli (2002). Adult mesenchymal stem cells and cell-based tissue engineering. *Arthritis Research & Therapy 5*, 1–14. 10.1186/ar614.

Tullberg-Reinert, H. and G. Jundt (1999). In situ measurement of collagen synthesis by human bone cells with a sirius red-based colorimetric microassay: effects of transforming growth factor 2 and ascorbic acid 2-phosphate. *Histochemistry and Cell Biology 112*, 271–276. 10.1007/s004180050447.

Uzer, G., S. Manske, M. Chan, F.-P. Chiang, C. Rubin, M. Frame, and S. Judex (2012). Separating fluid shear stress from acceleration during vibrations in vitro: Identification of mechanical signals modulating the cellular response. *Cellular and Molecular Bioengineering 5*, 266–276. 10.1007/s12195-012-0231-1.

van der Laan, L. J. W., C. Lockey, B. C. Griffeth, F. S. Frasier, C. A. Wilson, D. E. Onions, B. J. Hering, Z. Long, E. Otto, B. E. Torbett, and D. R. Salomon (2000). Infection by porcine endogenous retrovirus after islet xenotransplantation in scid mice. *Nature 407*(6800), 90–94. 10.1038/35024089.

Viswanathan, P., S. Chirasatitsin, K. Ngamkham, A. J. Engler, and G. Battaglia (2012). Cell instructive microporous scaffolds through interface engineering. *Journal of the American Chemical Society 134*(49), 20103–20109.

von Stengel, S., W. Kemmler, K. Engelke, and W. Kalender (2011). Effects of whole body vibration on bone mineral density and falls: results of the randomized controlled elvis study with postmenopausal women. *Osteoporosis International 22*, 317–325. 10.1007/s00198-010-1215-4.

Wang, J., L. Wang, X. Li, and C. Mao (2013). Virus activated artificial ecm induces the osteoblastic differentiation of mesenchymal stem cells without osteogenic supplements. *Scientific Reports 3*, 1242.

Ward, K., C. Alsop, J. Caulton, C. Rubin, J. Adams, and Z. Mughal (2004). Low magnitude mechanical loading is osteogenic in children with disabling conditions. *Journal of Bone and Mineral Research 19*(3), 360–369.

Weiner, S., W. Traub, and H. Wagner (1999). Lamellar bone: Structure and function relations. *Journal of Structural Biology 126* (3), 241 – 255. need to find a copy.

Weiner, S. and H. D. Wagner (1998). The material bone: Structure-mechanical function relations. *Annual Review of Materials Science 28* (1), 271–298. hardcopy only.

Wenger, K. H., J. D. Freeman, S. Fulzele, D. M. Immel, B. D. Powell, P. Molitor, Y. J. Chao, H.-S. Gao, M. Elsalanty, M. W. Hamrick, C. M. Isales, and J. C.

Yu (2010). Effect of whole-body vibration on bone properties in aging mice. *Bone 47*, 746–755.

Wiesmann, H., U. Joos, and U. Meyer (2004). Biological and biophysical principles in extracorporal bone tissue engineering: Part ii. *International Journal of Oral and Maxillofacial Surgery 33*(6), 523 – 530.

Williamson, M. R., R. Black, and C. Kielty (2006). Pcl-pu composite vascular scaffold production for vascular tissue engineering: Attachment, proliferation and bioactivity of human vascular endothelial cells. *Biomaterials 27*(19), 3608 – 3616.

Wood, M., Y. Yang, E. Baas, D. Meredith, R. Richards, J. Kuiper, and A. El Haj (2008). Correlating cell morphology and osteoid mineralization relative to strain profile for bone tissue engineering applications. *Journal of The Royal Society Interface 5*(25), 899–907.

Xie, L., J. M. Jacobson, E. S. Choi, B. Busa, L. R. Donahue, L. M. Miller, C. T. Rubin, and S. Judex (2006). Low-level mechanical vibrations can influence bone resorption and bone formation in the growing skeleton. *Bone 39*(5), 1059 – 1066.

Xie, L., C. Rubin, and S. Judex (April 2008). Enhancement of the adolescent murine musculoskeletal system using low-level mechanical vibrations. *Journal of Applied Physiology 104*(4), 1056–1062.

Xin, X., M. Hussain, and J. J. Mao (2007). Continuing differentiation of human mesenchymal stem cells and induced chondrogenic and osteogenic lineages in electrospun plga nanofiber scaffold. *Biomaterials 28*(2), 316 – 325. Cellular and Molecular Biology Techniques for Biomaterials Evaluation.

Yang, H., S. Yang, X. Chi, and J. R. G. Evans (2006). Fine ceramic lattices prepared by extrusion freeforming. *Journal of Biomedical Materials Research Part B: Applied Biomaterials 79B*(1), 116–121.

Yang, X., H. Roach, N. Clarke, S. Howdle, R. Quirk, K. Shakesheff, and R. Oreffo (2001). Human osteoprogenitor growth and differentiation on synthetic biodegradable structures after surface modification. *Bone 29(6)*, 523–531.

Yaszemski, M. J., R. G. Payne, W. C. Hayes, R. Langer, and A. G. Mikos (1996). Evolution of bone transplantation: molecular, cellular and tissue

strategies to engineer human bone. *Biomaterials 17*(2), 175 – 185. Polymer Scaffolding and Hard Tissue Engineering.

Yellowley, C. E., Z. Li, Z. Zhou, C. R. Jacobs, and H. J. Donahue (2000). Functional gap junctions between osteocytic and osteoblastic cells. *Journal of Bone and Mineral Research 15*(2), 209–217.

You, J., G. C. Reilly, X. Zhen, C. E. Yellowley, Q. Chen, H. J. Donahue, and C. R. Jacobs (2001). Osteopontin gene regulation by oscillatory fluid flow via intracellular calcium mobilization and activation of mitogen-activated protein kinase in mc3t3-e1 osteoblasts. *Journal of Biological Chemistry 276*(16), 13365–13371.

Yuge, L., A. Okubo, T. Miyashita, T. Kumagai, T. Nikawa, S. Takeda, M. Kanno, Y. Urabe, M. Sugiyama, and K. Kataoka (2003). Physical stress by magnetic force accelerates differentiation of human osteoblasts. *Biochemical and Biophysical Research Communications 311*(1), 32 – 38.

Zanetta, M., N. Quirici, F. Demarosi, M. Tanzi, L. Rimondini, and S. Far (2009). Ability of polyurethane foams to support cell proliferation and the differentiation of mscs into osteoblasts. *Acta Biomaterialia 5*(4), 1126 – 1136.

Zhang, C., J. Li, L. Zhang, Y. Zhou, W. Hou, H. Quan, X. Li, Y. Chen, and H. Yu (2012). Effects of mechanical vibration on proliferation and osteogenic differentiation of human periodontal ligament stem cells. *Archives of Oral Biology* (0), –.

Zhang, Y., D. Khan, J. Delling, and E. Tobiasch (2012a). Mechanisms underlying the osteo- and adipo-differentiation of humanmesenchymal stem cells. *The Scientific World Journal 2012*.

Zhao, L., Z. Wu, and Y. Zhang (2009). Low-magnitude mechanical vibration may be applied clinically to promote dental implant osseointegration. *Medical Hypotheses 72*(4), 451 – 452.